

UNCLASSIFIED

AD NUMBER

AD831887

LIMITATION CHANGES

TO:

Approved for public release; distribution is unlimited.

FROM:

Distribution authorized to U.S. Gov't. agencies and their contractors; Critical Technology; MAR 1968. Other requests shall be referred to Air Force Materials Laboratory, Wright-Patterson AFB, OH 45433. This document contains export-controlled technical data.

AUTHORITY

USAFSC ltr, 22 May 1972

THIS PAGE IS UNCLASSIFIED

**Best Available
Copy
for all Pictures**

SOLID STATE DIFFUSION BONDED
TANTALUM ALLOY HONEYCOMB PANELS

D. B. Hugill
J. Shabarack

Northrop Norsair
Division of Northrop Corp.

TECHNICAL REPORT APML-TR-68-42

March 1968

Project No. S-214

This document is subject to special export controls and each transmittal to foreign governments or foreign nationals may be made only with prior approval of the Advanced Fabrication Techniques Branch, Manufacturing Technology Division, Air Force Materials Laboratory, Wright-Patterson Air Force Base, Ohio 45433

Air Force Materials Laboratory
Air Force Systems Command
Wright-Patterson Air Force Base, Ohio

DN
MAY 15 1968



AFML-TR-68-42

SOLID STATE DIFFUSION BONDED
TANTALUM ALLOY HONEYCOMB PANELS

D. B. Hugill
J. Shabarack

Northrop Norair
Division of Northrop Corp.

TECHNICAL REPORT AFML-TR-68-42
March 1968

Project No. 8-214

This document is subject to special export controls and each transmittal to foreign governments or foreign nationals may be made only with prior approval of the Advanced Fabrication Techniques Branch, Manufacturing Technology Division, Air Force Materials Laboratory, Wright-Patterson Air Force Base, Ohio 45433

Air Force Materials Laboratory
Air Force Systems Command
Wright-Patterson Air Force Base, Ohio

FOREWORD

This Final Technical Report covers all work performed under Contract AF 33(615)-2777 from 1 June 1965 to 30 November 1967. The manuscript was released by the authors on 1 January 1968 for publication as an AFML Technical Report.

This contract with Northrop Norair, a Division of Northrop Corporation, Hawthorne, California, was initiated under AFML Project 8-214, "Solid State Diffusion Bonded Tantalum Alloy Honeycomb Panels". It was accomplished under the technical direction of Mr. Carl A. Tobin and Mr. Frederick R. Miller, both of the Advanced Fabrication Techniques Branch (MATF), Manufacturing Technology Division, Air Force Materials Laboratory, Wright-Patterson AFB, Ohio.

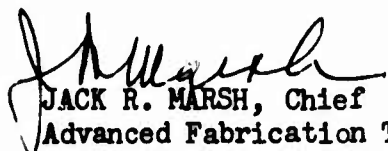
Mr. D.B. Hugill was Program Director and Mr. J. Shabarack was the Principal Engineer. Major contributions to the effort were made by:

Manufacturing: R. Bridwell, E. Kohlhoff, T. Gilmore, R. Giguere
Metallurgy: R.R. Wells, T. Krinke
Structures: W. Rehm, R. Evers
Stress Analysis: J. Preston
Welding: R.S. Collins, P. Adams

This project has been accomplished as part of the Air Force Manufacturing Methods Program, the primary objective of which is to develop, on a timely basis, manufacturing processes, techniques and equipment for use in economical production of USAF materials and components.

Norair has assigned Report No. NOR 67-292 for internal control.

This technical report has been reviewed and is approved.



JACK R. MARSH, Chief
Advanced Fabrication Techniques Branch
Manufacturing Technology Division
Air Force Materials Laboratory

ABSTRACT

A program is described for the development of solid state diffusion bonding technology for production of tantalum alloy (T111) honeycomb panels suitable for either hot structural or heat shield applications in aerospace environments. The investigation and selection of appropriate intermediate materials to effect joining at relatively low temperatures and pressures suitable to the panel configurations is discussed. Emphasis was placed on methods suitable for reasonably low-cost processing.

A method for determining optimum bonding parameters for a given binary alloy system is described. This technique was implemented in the current program to establish bonding parameters conducive to the fabrication of tantalum honeycomb panels. Selection of bonding parameters was further complicated by the manufacturing problems arising when bonding at the times and temperatures required to obtain a satisfactory bond of tantalum honeycomb structures. Consideration of these manufacturing problems and possible remedies are discussed.

Program materials, equipment, and tooling utilized in panel manufacture, as well as processing procedures are described. Specific manufacturing problem areas encountered, such as forming, welding, and intermediate application, are discussed. Heating, atmosphere control, and pressure application requirements are described and actions taken to satisfy these requirements are reported.

A survey of oxidation protective coatings for tantalum alloys is presented with the actual coatings and procedures used in the program being discussed.

Structural testing techniques used in evaluating the integrity of the manufactured honeycomb panels are described. Standard analytical procedures employed in determining failure modes and predicted failure stresses are presented.

The distribution of this report is limited because the report contains technology identifiable with items on the strategic embargo lists.

BLANK PAGE

TABLE OF CONTENTS

	<u>PAGE</u>
I INTRODUCTION	1
II SUMMARY	3
III PROGRAM MATERIALS	5
FACE SHEETS	5
HONEYCOMB CORE	5
IV TECHNICAL DISCUSSION	17
SOLID STATE DIFFUSION BONDING	17
SELECTION OF INTERMEDIATE MATERIALS	18
RECRYSTALLIZATION STUDY	28
BONDING PRESSURE TOLERANCE ON CORE	28
BONDING PARAMETER STUDY	28
BONDING PARAMETER SELECTION	49
V PANEL DESIGN	52
STRUCTURAL PANELS	52
HEAT SHIELD PANELS	52
VI MANUFACTURING PROCESSING TECHNOLOGY	58
TOOLING AND PARTS FABRICATION	58
ASSEMBLY AND PREPARATION OF PANEL AND TOOLING FOR BONDING	65
MODE OF OPERATION FOR PANEL BONDING	72
INTERMEDIATE APPLICATION BY VAPOR DEPOSITION STUDY	78
VII PHASE I TEST PANEL FABRICATION	84
PANELS 1 AND 2	84
PANEL 3	87
PANELS 4 AND 5	87
PANEL 6	88
PANELS 7 AND 8	88
PANEL 9	89
SUMMARY OF PANELS 3 THROUGH 9	89
PANEL 10	90
PANEL 11	90
PANEL 12	92
PANEL 13	94
PANELS 14 AND 15	94
ANALYSIS OF PHASE I TEST PANEL FABRICATION	95

TABLE OF CONTENTS (Continued)

	<u>PAGE</u>
VIII PHASE II TANTALUM HONEYCOMB PANEL FABRICATION	97
STRUCTURAL PANELS	97
HEAT SHIELD PANELS	105
IX OXIDATION PROTECTIVE COATING SELECTION AND APPLICATION . . .	119
MOLYBDENUM AND TUNGSTEN DISILICIDE COATINGS	120
X STRUCTURAL TESTING AND ANALYSIS	130
STRUCTURAL AND SPECIMEN TESTING PROCEDURE	130
PANEL SPECIMEN TEST RESULTS AND DISCUSSION	142
EDGEWISE COMPRESSION STRUCTURAL TEST RESULTS	158
EDGEWISE SHEAR STRUCTURAL TEST RESULTS	172
PANEL STRUCTURAL ANALYSIS	177
XI CONCLUSIONS AND RECOMMENDATIONS	198
REFERENCES	200
DISTRIBUTION LIST	201

LIST OF ILLUSTRATIONS

<u>FIGURE</u>		<u>PAGE</u>
1	DIFFUSION BONDED NODAL JOINT AS PRODUCED IN CORE MANUFACTURING PROCESS. Ta-10W-Cb INTERFACE- (DARK MARGIN AT INTERFACE RESULTED FROM SPECIMEN ETCHING) 100X MAGNIFICATION	12
2	TITANIUM EMBRITTLEMENT OF Ta-10W FOIL	19
3	EFFECT OF TITANIUM VAPOR ON Ta-10W FOIL	19
4	EFFECT OF DIFFUSION BONDING TEMPERATURE ON LAP-SHEAR STRENGTH AT 2800F. (BONDING TIME = 120 MIN., BONDING PRESSURE = 1000 psi)	21
5	EFFECT OF TEST TEMPERATURE OF LAP-SHEAR STRENGTH. LAP-SHEAR SPECIMENS DIFFUSION BONDED AT 2600F FOR 120 MIN. UNDER 1000 psi.	22
6	MICROSTRUCTURE OF DIFFUSION BONDED LAP-SHEAR SPECIMENS	25
7	MICROHARDNESS PROFILES FOR DIFFUSION BONDED LAP-SHEAR JOINTS	26
8	MICROSTRUCTURE AND MICROHARDNESS FOR DIFFUSION BONDED LAP-SHEAR JOINT USING MOLYBDENUM INTERMEDIATE WITH Ta-10W BASE ALLOY. ETCHANT: 10 gms NaOH, 30 gms $K_3Fe(CN)_6$, 100 ml H_2O ; MAG: 1000X. LAP-SHEAR SPECIMEN BONDED AT 2600F FOR 120 MINUTES UNDER 1000 psi	27
9	SKETCHES SHOWING TYPICAL COMPOSITION PROFILES ACROSS DIFFUSION BONDED JOINTS OF Ta-10W	33
10	SCHEMATICS SHOWING METHOD OF COMPUTING D FOR EXTENSIVE DIFFUSION, THIN-FILM METHOD, AND FOR LIMITED DIFFUSION, MATANO METHOD	34
11	LOG D VS 1/T FOR DIFFUSION ON Ti AND Cb INTO Ta-10W	35
12	LOG D VS T(°F) FOR DIFFUSION OF Ti AND Cb INTO Ta-10W	36
13	SKETCH OF EFFECT OF TIME AT TEMPERATURE ON CONCENTRATION GRADIENT IN A DIFFUSION BONDED JOINT	38

<u>FIGURE</u>		<u>PAGE</u>
14	RELATIONSHIP BETWEEN TIME AND DIFFUSION COEFFICIENT FOR DIFFUSION BONDING Ta-10W WITH Ti OR Cb INTER- MEDIATE, 0.0005 INCH THICKNESS	40
15	CONCENTRATION CURVES AS A FUNCTION OF TIME AND TEMPERATURE FOR 0.0005 INCH THICK Ti-75A INTER- MEDIATE	41
16	CONCENTRATION CURVES AS A FUNCTION OF TIME AND TEMPERATURE FOR 0.0010 INCH THICK Ti-75A INTER- MEDIATE	42
17	CONCENTRATION CURVES AS A FUNCTION OF TIME AND TEMPERATURE FOR 0.0015 INCH THICK Ti-75A INTER- MEDIATE	43
18	CONCENTRATION CURVES AS A FUNCTION OF TIME AND TEMPERATURE FOR 0.0020 INCH THICK Ti-75A INTER- MEDIATE	44
19	CONCENTRATION CURVES AS A FUNCTION OF TIME AND TEMPERATURE FOR 0.0005 INCH THICK Cb INTERMEDIATE . . .	45
20	CONCENTRATION CURVES AS A FUNCTION OF TIME AND TEMPERATURE FOR 0.0010 INCH THICK Cb INTERMEDIATE . . .	46
21	CONCENTRATION CURVES AS A FUNCTION OF TIME AND TEMPERATURE FOR 0.0015 INCH THICK Cb INTERMEDIATE . . .	47
22	CONCENTRATION CURVES AS A FUNCTION OF TIME AND TEMPERATURE FOR 0.0020 INCH THICK Cb INTERMEDIATE . . .	48
23	TANTALUM - FLAT STRUCTURAL PANEL DESIGN	53
24	TANTALUM - CURVED STRUCTURAL PANEL DESIGN	54
25	TANTALUM - FLAT HEATSHIELD PANEL	55
26	TANTALUM - CURVED HEATSHIELD PANEL	56
27	TANTALUM - HEATSHIELD PANEL MOUNTING ASSEMBLY	57
28	FLAT AND CURVED STRUCTURAL EDGEMEMBER TOOLING AND PARTS FORMED FROM .025" T111 SHEET ON A VERSION WHEELON HYDRO PRESS AND HUFFORD STRETCH PRESS	59
29	FORM DIES FOR OUTER SKIN FLAT HEAT SHIELD	59

<u>FIGURE</u>		<u>PAGE</u>
30	ROLL FORM DIE WITH FORMED FLAT AND CURVED .008 INCH T111 OUTER HEAT SHIELD PANEL SKINS	60
31	FORM DIE FOR INNER SKIN FLAT HEAT SHIELD	60
32	DIES, FILLER AND WIPER RINGS USED IN FORMING WELD MELT DOWN FLANGE ON FLAT (LEFT) AND CURVED (RIGHT) HEAT SHIELD PANEL INNER SKINS	62
33	BEND-STRENGTH FIXTURE SPECIALLY DESIGNED FOR CONTOURING THE CURVED HEAT SHIELD INNER SKINS HELD IN TOOLING READY FOR FORMING ON PRESS BRAKE	62
34	STARTING SKIN (RIGHT) AND RESULTANT CONTOURED SKIN (LEFT) AFTER FORMING ON PRESS BRAKE	63
35	HEAT SHIELD PANEL ATTACH CLIPS FABRICATED FROM .040" T111 SHEET WITH FORM BLOCK	64
36	INNER (RIGHT) AND OUTER (LEFT) FORMED HEAT SHIELD SKINS WITH CORE, WASHERS, AND PANEL ATTACH CLIPS	64
37	ENVELOPE FORM BLOCKS AND INCONEL 600 .C25 INCH ENVELOPE HALVES	66
38	CURVED ENVELOPE FORM BLOCK WITH TOP AND BOTTOM ENVELOPE HALVES	66
39	ALIGNMENT OF EDGEMEMBERS FOR WELDING (CURVED)	67
40	TIG WELDING OF EDGEMEMBERS IN ATMOSPHERE CONTROL CHAMBER (CURVED)	67
41	CORE FITTED AND SPOT TACKED TO EDGEMEMBER FRAME (CURVED)	68
42	TEST PANEL 3 BONDED AT 2300F FOR 2.5 HOURS ILLUSTRATING THE PACKAGE COMPONENTS AND THEIR AVAILABILITY FOR SUBSEQUENT PANEL FABRICATION	68
43	PANEL 11, THE FIRST 12X12 INCH PANEL MANUFACTURED, WAS DIFFUSION BONDED AT 2250F FOR 3.5 HOURS UTILIZING .0015 INCH T1-55A FOIL AS INTERMEDIATE. A PANEL STRESS OF 2,000 PSI WAS OBTAINED ON 2X2 INCH FLATWISE TENSION SPECIMENS	70

<u>FIGURE</u>		<u>PAGE</u>
44	ARRANGEMENT OF PANEL AND TOOLING WITHIN THE ENVELOPE (CURVED)	70
45	CROSS-SECTION SCHEMATIC OF HEAT SHIELD PACKAGING PROCEDURE	71
46	ALUMEL-CHROMEL THERMOCOUPLES SPOT WELDED TO SEALED ENVELOPE. ENVELOPE IS COATED WITH EVERLUBE T-50	73
47	COUNTER VACUUM CHAMBER EMPLOYED FOR PURGING OF PACKAGE	73
48	PURGING OF PACKAGE IN COUNTER-VACUUM CHAMBER WITH AUTOMATIC PURGE CYCLING SYSTEM	75
49	ORIENTATION OF PACKAGE IN HEATING FIXTURE	75
50	QUARTZ LAMP RADIANT HEATER IN OPERATION DURING THE BONDING OF A STRUCTURAL PANEL AT 2250F	76
51	POWER CONTROL PANELS	76
52	SOLID STATE TEMPERATURE CONTROLLERS AND RECORDERS EMPLOYED FOR BONDING OF TANTALUM PANELS	77
53	T111 CORE VAPOR DEPOSITED WITH T1-35 INTERMEDIATE. ARROWS DESIGNATE DEMARCATION BETWEEN INFERIOR DE- POSIT (RIGHT) AND SATISFACTORY DEPOSIT (LEFT). PHOTOMICROGRAPHIC INSERTS ILLUSTRATE THIS DIFFERENCE IN QUALITY OF DEPOSIT	80
54	PHOTOMICROGRAPH SHOWING VAPOR DEPOSITED TITANIUM ON EDGE OF HONEYCOMB CORE	81
55	TYPICAL TEE JOINT FORMED BY CORE CELL WALL AND FACE SHEET WITH .0005 INCH TITANIUM FOIL	86
56	ULTRASONIC TRACE OF 12X12 INCH PANEL 11. DOTTED LINES REPRESENT EDGE OF PANEL AT EDGEMEMBERS	91
57	FLATWISE TENSION SPECIMEN FIXTURED AND READY FOR TESTING AT 2800F	93
58	FAILED SURFACE OF TENSION TEST SPECIMENS SHOWING THAT MUCH OF THE FAILURE OCCURRED THROUGH THE CORE INSTEAD OF AT THE BOND INTERFACE	93

<u>FIGURE</u>		<u>PAGE</u>
59	TYPICAL FLAT STRUCTURAL PANEL BONDED AT 2250F FOR 3.5 HOURS EMPLOYING .0015 INCH T1-55A FOIL AS INTERMEDIATE	98
60	TYPICAL CURVED STRUCTURAL PANEL BONDED AT 2250F FOR 3.5 HOURS EMPLOYING .0015 INCH T1-55A FOIL AS INTERMEDIATE	99
61	FLAT STRUCTURAL PANEL AFTER POST BOND PROCESSING. EDGES ARE WELDED WITH WELD AND SHARP CORNERS RADIUSSED BY SANDING. THE PANEL IS THEN VACUUM BLASTED	100
62	TYPICAL ULTRASONIC TRACE OBTAINED ON FLAT STRUCTURAL PANELS. BLACK LINES REPRESENT EDGE OF PANEL	102
63	A CURVED PANEL MATCHED TO MACHINED DIE ILLUSTRATING CLOSE CONFORMANCE TO DESIGN RADIUS OF CURVATURE	104
64	INNER SKIN SURFACE OF BONDED FLAT HEAT SHIELD PANEL . . .	106
65	OUTER SKIN SURFACE OF BONDED FLAT HEAT SHIELD PANEL . . .	106
66	INNER SKIN SURFACE OF CURVED HEAT SHIELD PANEL	107
67	OUTER SKIN SURFACE OF CURVED HEAT SHIELD PANEL	107
68	HEAT SHIELD PANEL SHOWING WELDING REQUIREMENTS AND LOCATION	109
69	CROSS SECTIONAL SCHEMATICS OF WELDING LOCATIONS SHOWN IN FIGURE 68	110
70	PHOTOMICROGRAPH OF CROSS SECTION OF TIG WELDED TANTALUM SHEET	112
71	PHOTOMICROGRAPH OF CROSS SECTION OF LASER WELDED TANTALUM SHEET. NOTE LACK OF MELT DOWN OF SHEETS AND THE RESULTANT LACK OF FUSION	112
72	A COMPARISON OF BEAD APPEARANCE OF LASER (TOP) AND TIG (BOTTOM) WELDS IN TANTALUM SHEET. HIGH- LIGHTED AREAS REPRESENT DISTORTION OF THE SHEET DURING WELDING	113
73	SIMULATED WELD JOINT TO DETERMINE EFFECT OF TITANIUM ONLY ON TANTALUM WELDS	115

<u>FIGURE</u>		<u>PAGE</u>
74	USE OF FILLER STRIP IN JOINT TO EFFECT METAL-TO-METAL CONTACT AND TO PROVIDE EASIER INITIATION OF MELTDOWN	115
75	SIMULATED SPECIMEN USED TO DETERMINE THE EFFECTS OF ENTRAPPED AIR, PUMP DOWN TIME, AND VACUUM LEVEL ON TANTALUM PANEL WELDABILITY. T111 SHEET WAS USED TO SIMULATE HONEYCOMB CORE BAFFLE EFFECT	115
76	FOUR FLAT STRUCTURAL PANELS COATED WITH SYLVANIA R505F AL-Sn-Mo COATING	121
77	FOUR CURVED STRUCTURAL PANELS COATED WITH SYLVANIA R505F Al-Sn-Mo OXIDATION PREVENTATIVE COATING	122
78	CLOSE-UP OF COATED PANEL EDGE SHOWING CRACKS IN Al-Sn-Mo COATING	123
79	CLOSE-UP OF COATED PANEL CORNER SHOWING CRACKING AND CHIPPING OF Al-Sn-Mo COATING	123
80	CLOSE-UP OF FLAT HEAT SHIELD PANEL COATED WITH MoSi ₂ (TNV-12) SHOWING CRACKS IN COATING	126
81	DOWNSIDE OF HEAT SHIELD PANELS COATED WITH WS ₁₂ (LEFT) AND MoSi ₂ (RIGHT) SHOWING MOTTLED APPEARANCE OF COATING. INCLUDED ARE COLUMBIUM (D36) BOLTS COATED WITH WS ₁₂ TO BE USED FOR ATTACHMENT OF PANEL TO TEST FIXTURE	126
82	UPSIDE OF HEAT SHIELD PANELS COATED WITH WS ₁₂ (LEFT) AND MoSi ₂ (RIGHT) SHOWING A SOMEWHAT IMPROVED SURFACE APPEARANCE WS ₁₂ . COATED COLUMBIUM ATTACH BOLTS ARE SHOWN IN FOREGROUND	127
83	MODES OF LOADING USED IN DETERMINING THE STRUCTURAL INTEGRITY OF TANTALUM HONEYCOMB PANELS	131
84	TEST SETUP FOR ROOM TEMPERATURE EDGEWISE COMPRESSION TESTING OF CURVED STRUCTURAL PANEL	132
85	CURVED PANEL EDGEMEMBER WITH STAINLESS STEEL SHIMS TO PREVENT COLLAPSE OF THIS AREA DURING LOADING	132
86	TEST SETUP OF PANEL AND QUARTZ LAMP RADIANT HEATING FIXTURE FOR EDGEWISE COMPRESSION TESTING OF CURVED STRUCTURAL PANEL AT ELEVATED TEMPERATURES	133

<u>FIGURE</u>		<u>PAGE</u>
87	TEST SETUP OF PANEL AND HEATING UNIT FOR EDGEWISE SHEAR TESTING OF FLAT STRUCTURAL PANEL AT ELEVATED TEMPERATURES	133
88	TEST SETUP FOR ROOM TEMPERATURE EDGEWISE SHEAR TESTING OF FLAT STRUCTURAL PANELS	135
89	THERMOCOUPLE INSTALLATION TECHNIQUE	136
90	COMPARISON OF TEMPERATURE MEASUREMENTS BETWEEN PLATINUM-RHODIUM THERMOCOUPLES WITH BORON NITRIDE CAPS AND CHROMEL-ALUMEL THERMOCOUPLES	138
91	TEMPERATURE COMPATIBILITY CURVE USED TO ALLOW FOR THE DIFFERENCE IN THERMAL EXPANSION BETWEEN THE TANTALUM PANEL AND L605 TEST FIXTURE DURING TESTING . . .	139
92	CONFIGURATIONS FOR HONEYCOMB SPECIMEN TESTING	141
93	EDGEWISE COMPRESSION TEST SET-UP	143
94	FLATWISE TENSION TEST SET-UP	143
95	FACE SHEET TENSILE PROPERTIES AS A FUNCTION OF TEMPERATURE	144
96	MODULUS OF ELASTICITY OF FACE SHEET MATERIAL AS A FUNCTION OF TEMPERATURE	146
97	STRESS-STRAIN AND TANGENT MODULUS CURVES AT ROOM TEMPERATURE AND 2800F	147
98	BEARING STRESS-STRAIN CURVE OF THE FACING MATERIAL ($e/D = 2.0$)	148
99	FLATWISE COMPRESSION STRENGTH AT ROOM AND ELEVATED TEMPERATURES FROM SPECIMENS TAKEN FROM PANEL 11	150
100	FLATWISE COMPRESSIVE MODULUS OF ELASTICITY OF THE CORE AT ROOM AND ELEVATED TEMPERATURES	151
101	FLATWISE COMPRESSION STRESS-STRAIN CURVE AT ROOM TEMPERATURE AND 2800F	152
102	FLATWISE TENSION STRENGTH OF SPECIMENS TAKEN FROM AS FABRICATED AND STRUCTURALLY TESTED PANELS AT ROOM AND ELEVATED TEMPERATURES	154

<u>FIGURE</u>		<u>PAGE</u>
103	EDGEWISE COMPRESSION STRENGTH AS A FUNCTION OF TEMPERATURE OF SPECIMENS TAKEN FROM AS-FABRICATED AND STRUCTURALLY TESTED PANELS. FULL SIZE PANEL EDGEWISE COMPRESSION TEST RESULTS ARE INCLUDED FOR CORRELATIVE PURPOSES	155
104	FAILURE MODE OF EDGEWISE COMPRESSION SPECIMENS. INTERCELL DIMPLING WAS ALSO EVIDENT ON THE SPECIMENS	156
105	MICROSTRUCTURE OF TYPICAL HONEYCOMB/FACESHEET JOINTS	159
106	PHOTOMICROGRAPH SHOWING DEFORMATION ABSORBED BY A HONEYCOMB/FACESHEET JOINT	160
107	LOAD CYCLE AND DEFLECTION OF PANEL 1 TESTED IN EDGEWISE COMPRESSION AT ROOM TEMPERATURE	163
108	LOAD CYCLE AND DEFLECTION OF PANEL 4 TESTED IN EDGEWISE COMPRESSION AT ROOM TEMPERATURE	164
109	MODE OF FAILURE OF PANEL 1 TESTED IN EDGEWISE COMPRESSION AT ROOM TEMPERATURE. FAILURE WAS MAINLY AT THE EDGEMEMBER - CORE TRANSITION PLANE	165
110	MODE OF FAILURE OF PANEL 4 TESTED IN EDGEWISE COMPRESSION AT ROOM TEMPERATURE. FAILURE WAS SHEAR CRIMPING AT THE EDGEMEMBER - CORE TRANSITION PLANE	165
111	VARIATION OF TEMPERATURE ON CONVEX SIDE OF PANEL 2 TESTED IN EDGEWISE COMPRESSION AT 2800F	166
112	LOAD AND TEMPERATURE CYCLE FOR PANEL 2 TESTED IN EDGEWISE COMPRESSION AT 2800F	167
113	PANEL 2 TESTED IN EDGEWISE COMPRESSION AT 2800F SHOWING MODE OF FAILURE. NOTE SAGGING OF COATING AT BOTTOM OF PANEL DUE TO TIN RUNOFF. WHITE SPOTS ON PANEL ARE THERMOCOUPLE CONTACT POINTS	168
114	LOAD-DEFLECTION CURVE FOR PANEL 2 TESTED IN EDGEWISE COMPRESSION AT 2800F	168
115	TEMPERATURE DISTRIBUTION OF BOTH SIDES OF PANEL 3 TESTED IN EDGEWISE COMPRESSION AT 2900F	169

<u>FIGURE</u>		<u>PAGE</u>
116	LOAD-TEMPERATURE CYCLE FOR PANEL 3 TESTED IN EDGEWISE COMPRESSION AT 2900F	170
117	PANEL 3 FAILURE MODE AT 2900F. NOTE MOST OF FAILURE ON ONE SIDE AND THE OVERLAP OF FAILED SKIN SURFACES	171
118	PANEL 3 AFTER 2900F STRUCTURAL TEST WITH FACE SHEET PULLED AWAY. NOTE HEAVY WHITE AREAS OF TANTALUM OXIDE. ARROW DESIGNATES PROBABLE START OF FAILURE AS CORE WAS COMPLETELY OXIDIZED IN THIS AREA	171
119	ELECTRON BACKSCATTER MICROGRAPHS OBTAINED FOR COATING ANALYSIS USING ELECTRON MICROPROBE TECHNIQUE	173
120	PHOTOMICROGRAPHS OF SPECIMENS OBTAINED FROM PANELS FAILED IN EDGEWISE COMPRESSION AT 2800F	174
121	LOAD CYCLE AND LOAD-DEFLECTION CURVES FOR PANEL 7 TESTED IN EDGEWISE SHEAR AT ROOM TEMPERATURE	175
122	LOAD CYCLE AND LOAD-DEFLECTION CURVES FOR PANEL 8 TESTED IN EDGEWISE SHEAR AT ROOM TEMPERATURE	176
123	PANEL 7 TESTED IN EDGEWISE SHEAR AT ROOM TEMPERATURE. CRACK AROUND PERIPHERY OF THE PANEL AT THE LOAD HOLES IS IN COATING ONLY	178
124	PANEL 8 TESTED IN EDGEWISE SHEAR AT ROOM TEMPERATURE	178
125	CLOSE UP OF FAILURE AT CORNER OF PANEL 8. CRACK- ING WAS ASSOCIATED WITH COATING ONLY AS PANEL EXHIBITED A DUCTILE TYPE FAILURE	179
126	TEMPERATURE DISTRIBUTION ON PANEL 9 TESTED IN EDGEWISE SHEAR AT 2100F	180
127	LOAD CYCLE AND LOAD-DEFLECTION CURVES FOR PANEL 9 TESTED IN EDGEWISE SHEAR AT 2100F	181
128	TEMPERATURE DISTRIBUTION ON PANEL 10 TESTED IN EDGEWISE SHEAR AT 2650F	182
129	LOAD CYCLE AND LOAD-DEFLECTION CURVES FOR PANEL 10 TESTED IN EDGEWISE SHEAR AT 2650F	183

<u>FIGURE</u>		<u>PAGE</u>
130	PANEL 9 TESTED IN EDGEWISE SHEAR AT 2100F	184
131	PANEL 10 TESTED IN EDGEWISE SHEAR AT 2650F	184
132	STRENGTH OF SHEAR PANELS AT ROOM AND ELEVATED TEMPERATURES	185
133	BUCKLING PARAMETER FOR TANTALUM T-111 SANDWICH PANELS	188
134	CORE SHEAR PARAMETER FOR DETERMINING THE BUCKLING STRENGTH OF TANTALUM HONEYCOMB PANELS	189
135	CHART FOR DETERMINING THE INTERCELL DIMPLING STRENGTH OF TANTALUM HONEYCOMB PANELS	190
136	POSSIBLE MODES OF FAILURE OF SANDWICH COMPOSITE UNDER EDGEWISE LOADS: GENERAL BUCKLING, SHEAR CRIMPING, DIMPLING OF FACINGS, AND WRINKLING OF FACINGS EITHER AWAY FROM OR INTO THE CORE. (REFERENCE 12)	191
137	CHART FOR DETERMINING THE SHEAR CRIMPING STRENGTH OF TANTALUM T-111 HONEYCOMB PANELS	192
138	GRAPH OF FORMULA FOR THE WRINKLING STRESS OF FACINGS OF HONEYCOMB SANDWICH PANELS (REFERENCE 11) . . .	194
139	SHEAR BUCKLING CURVE FOR TANTALUM T-111 HONEY- COMB PANELS	195

LIST OF TABLES

<u>TABLE</u>		<u>PAGE</u>
I	FACE SHEET MATERIAL CERTIFICATION (NRC)	6
II	FACE SHEET MATERIAL CERTIFICATION (Wah Chang)	6
III	CHEMICAL ANALYSES (AS ROLLED) TANTALUM ALLOY FOIL . . .	7
IV	FLAT BEND TEST TANTALUM ALLOY FOIL	7
V	TENSILE PROPERTIES OF .002 INCH TANTALUM ALLOY FOIL AT ROOM TEMPERATURE	9
VI	TENSILE PROPERTIES OF .002 INCH TANTALUM ALLOY FOIL AT 2800F	10
VII	CENTER-OF-NODE MICROHARDNESS FOR DIFFUSION BONDED Ta-10W HONEYCOMB CORE (TITANIUM INTERMEDIATE) AFTER VARIOUS THERMAL EXPOSURES	12
VIII	INSPECTION ANALYSIS OF PHASE I TANTALUM HONEYCOMB CORE	13
IX	INSPECTION ANALYSIS OF PHASE II TANTALUM HONEYCOMB CORE	14
X	EDGEMEMBER MATERIAL CERTIFICATION	16
XI	LAP SHEAR STRENGTH DATA OBTAINED FOR Ta-10W AND Ti-11 BASE ALLOYS USING Cb, Hf, and Ti-75A INTERMEDIATES	23
XII	DIFFUSION COEFFICIENTS FOR VARIOUS DIFFUSION BONDING CONDITIONS. BASE ALLOY: Ta-10W	30
XIII	DATA SUMMARY FOR 6X6 INCH PHASE I TEST PANELS	96
XIV	DIMENSIONAL VARIATIONS OF STRUCTURAL PANELS	103
XV	DIMENSIONAL VARIATIONS OF FLAT HEAT SHIELD PANELS . . .	105
XVI	SUMMARY OF VERY HIGH TEMPERATURE TESTING ON SOLAR WS ₁₂ COATING	125
XVII	SUMMARY OF PANEL CONFIGURATIONS AND VARIOUS CONDITIONS ANALYZED	140
XVIII	SPECIMEN FLATWISE COMPRESSION TEST RESULTS	150

LIST OF TABLES (Continued)

<u>TABLE</u>		<u>PAGE</u>
XIX	SPECIMEN FLATWISE TENSION TEST RESULTS	153
XX	SPECIMEN EDGEWISE COMPRESSION TEST RESULTS	157
XXI	TYPICAL MECHANICAL PROPERTIES OF THE TANTALUM SANDWICH CONSTRUCTION COMPONENTS	161
XXII	SUMMARY OF RESULTS OBTAINED ON TANTALUM T111 HONEYCOMB PANELS	196

LIST OF SYMBOLS

b	panel length, in.
\bar{c}	column fixity coefficient
E	modulus of elasticity, psi
E'	effective modulus of elasticity, psi
F_{su}	ultimate shear stress, psi
F_{bry}	yield bearing strength, psi
F_{cr}	critical facing stress, psi
F_{bru}	ultimate bearing strength, psi
F_{fc}	flatwise compressive strength of the core, psi
F_{ft}	flatwise tension strength of the core, psi
F_s	shear buckling stress, psi
F_{ty}	yield tensile strength, psi
F_{tu}	ultimate tensile strength, psi
F_w	facing wrinkling stress, psi
G	modulus of rigidity, psi
I	moment of inertia, in ³ .
L	length, in.
P_{cr}	critical load, lbs.
P_E	Euler column load, lbs
t	thickness, in.
δ	initial deflection of facing waviness, in.
λ	$1 - u^2$ where u is Poisson's ratio of the facings

τ	shear stress, psi
s	cell size, in.
N	distributed load, lbs/in.
ρ	radius of gyration, in.

Subscripts:

c	core or compression
f	facing
t	tangent

I INTRODUCTION

The inherently high melting point of tantalum (5400F) has in recent years magnified its potential for aerospace applications where high temperatures and heating rates are to be encountered. It is one of a group of refractory alloys in which extensive investigations are being conducted to determine its ability to meet requirements for hypersonic and re-entry vehicles. Coupled with its high operational temperature regime (2000F-4000F), tantalum exhibits excellent fabricability, good weldability, excellent ductility at cryogenic temperatures, and general corrosion resistance second to none among metallic structural materials. However, tantalum does have two major adverse characteristics: namely, a very high density (.601 lbs/in³), and very poor oxidation resistance at normal service temperatures. Nonetheless, tantalum, with columbium, will continue to be the foremost metallic materials for high temperature structural stability in aerospace vehicles.

In order to realize the full potential of tantalum for hot structural and thermal protective applications, joining techniques must be developed to provide composite structures to meet required load carrying capabilities. Conventional joining processes thus far have not proven to be efficient in accomplishing this aim. Solid state diffusion bonding, an age-old technique which has with the advent of the nuclear industry gained considerable attention on a more scientific basis, exhibits certain features which circumvent some of the undesirable characteristics associated with more conventional processes such as fusion welding and high temperature brazing. Diffusion bonding can be accomplished at lower temperatures than brazing or welding allowing the use of more conventional manufacturing methods and equipment. In addition, a higher joint remelt temperature is effected increasing service temperature limits.

Whether through the utilization of intermediaries or by direct metal-to-metal contact, this technique provides the ideal method for joining metals insofar as approaching base metal properties in a bonded joint. The diffusion process itself is basic to the metallurgical community as it represents the single most important phenomenon of metallurgy, since virtually all changes in metal structures and consequently in metal properties result from this process. The diffusion bonding process as applied in the current program consists essentially of effecting a transfer of atoms between two metal surfaces by the thermal excitation of the respective metal atoms.

The purpose of this program was to establish the design, and to develop manufacturing methods, processes, fabrication techniques and testing procedures for the manufacture and evaluation of solid state diffusion bonded tantalum alloy honeycomb panels capable of service temperatures of 2800F or higher. Two types of panels were fabricated for application to aerospace vehicles as either hot structure or heat shield. Each type panel, in turn, was fabricated in two configurations, flat and curved.

These panels were solid state diffusion bonded at relatively low pressure. The pressure cycle takes advantage of the differential attainable between

atmospheric pressure and an evacuated protective envelope. Since the actual surface area of the honeycomb core represents only a small percentage of the surface area of the panel, a multiplication of the 14.7 psi atmospheric pressure is effected yielding an actual unit bonding pressure between honeycomb and face sheet of approximately 1000 psi.

In order to maintain bonding parameters within practical manufacturing limits, as well as to provide improved bond surface area contact, commercially pure titanium was employed as intermediate.

Tantalum alloy foil for honeycomb core fabrication was supplied by the Air Force Materials Laboratory (MATB). The honeycomb was manufactured by diffusion bonding strips of foil in flat packs using a columbium intermediate, and then expanding the pack to yield the required honeycomb configuration.

In evaluating the band of the basic parameters for diffusion bonding tantalum alloys, and considering the state-of-art of applying and controlling heat, the quartz lamp radiant heating method was chosen as being the most suitable for this project. By using radiant heating, temperature cycles were accurately maintained, contamination was held to a minimum, and precise zone control allowed uniformity of temperature on all portions of the packaged panel. A company-funded radiant heating fixture was designed and manufactured to specifically meet the needs of the program.

The program was performed in three phases, during the first of which panel design, bonding parameters, and manufacturing techniques (including honeycomb core fabrication) were established and verified by bonding 6 x 6 inch honeycomb panel specimens. In subsequent phases, 12 x 12 inch panels were fabricated, tested, and test data evaluated to determine panel strength, thermal characteristics, dimensional stability, and manufacturing reliability.

II SUMMARY

The system employed in fabricating tantalum honeycomb panels utilized a sealed, thin metal envelope containing the panel and tooling details, with the bonding temperature being obtained by quartz lamp radiant heating. The function of the envelope was to shield the assembly from atmospheric contact, and through evacuation, to exert a controlled compressive force on the panel assembly during the bond cycle.

During Phase I, bonding parameters and manufacturing procedures were established with the fabrication of 14 6x6 inch and one 12x12 inch panels. Titanium foil was used as an intermediate material to provide for improved fitup of bond surfaces and to render bonding parameters within practical manufacturing limits. Attempts to utilize vapor deposited titanium rather than foil titanium met with only partial success. While a uniform, contaminant free titanium layer could be applied to the core edges and not flake or chip off during subsequent core processing, the thickness of the deposited layer proved to be inadequate to effect satisfactory bonding.

The bonding parameters selected for use in fabricating the Phase II 12x12 inch structural and heat shield panels were as follows:

Temperature	- 2250F
Time	- 3.5 hours
Pressure	- 1000 psi
Intermediate-	.0015 inch Ti55 (structural panels)
	- .0005 inch Ti75 (heat shield panels)

With these bonding parameters, 13 - 12x12 inch structural panels (9 flat, 4 curved) and 7 - 12x12 inch heat shield panels (5 flat, 2 curved) were manufactured during Phase II.

No major difficulties were encountered with the manufacturing procedures and techniques employed in fabricating these panels. Quartz lamp heating with closed loop feed back control provided exceptional uniformity of temperature on all portions of the panel during the bond cycle.

Welding of the panels proved to be the most difficult avenue of processing in the program. Attempts to weld extensions to the structural panel edges for load fixture attachment resulted in excessive weld cracking and warpage of the extensions. These extensions were subsequently eliminated and attachment of the load fixtures for structural testing was made directly to the panel edgemembers. The heat shield panels were to be hermetically sealed after bonding by welding around the panel edge and around the panel access holes. Weld and parent metal cracking occurred on all of the panels to varying degrees. TIG, laser, and electron beam welding techniques were all attempted without success. The majority of welding was accomplished with electron beam since this process proved superior to the other techniques. Contamination was the chief suspect for the cracking which occurred, although it seemed more apparent that a combination of factors contributed to the lack of weldability experienced on the panels.

To provide protection of the panels from oxidation during testing, the structural panels were coated with Al-Sn-Mo by Sylvania Electric Products, Hicksville, N.Y., while the heat shield panels were coated with MoSi₂ and WSi₂ by Solar Division of International Harvester, San Diego, California. Except for one panel which apparently failed prematurely due to coating failure during edgewise compression testing at 2800F, the Al-Sn-Mo provided adequate protection for the 10-15 minute test loading interval at temperatures to 2800F. The heat shield panels designed for service above 2800F required a more durable coating at these higher temperatures. One panel was coated with MoSi₂ and three panels were coated with WSi₂. No problems were encountered during the application of the WSi₂ coating. However, application of the MoSi₂ coating was not successful as numerous cracks in the coating were experienced.

Structural analysis consisted of edgewise compression testing of the curved structural panels and edgewise shear testing of the flat structural panels. Tests were performed at room and elevated temperatures. Due to problems encountered during the manufacture and coating of the heat shield panels, no testing was accomplished on these panels. The curved structural panels exhibited failure stresses of 91,700 psi and 71,600 psi at room temperature. At 2800F and 2900F, failure stresses of 17,200 psi and 5,200 psi, respectively, were obtained. The results of the 2900F test were not considered a true representation of panel integrity as coating failure appeared to initiate the fracture. Edgewise shear tests revealed panel failure stresses of 74,500 psi and 81,500 psi at room temperature. At 2100F, panel failure occurred at 33,400 psi while at 2650F failure occurred at 13,400 psi.

III PROGRAM MATERIALS

FACE SHEETS

The face sheet materials used in fabricating the structural and heat shield panels were .012 inch and .008 inch thick T111 (Ta-8W-2Hf) respectively. These sheets were procured from the National Research Corporation, Newton, Massachusetts and Wah Chang Corporation, Albany, Oregon. The need for a second source became apparent when considerable delays in material shipments were experienced. These delays, which resulted in program rescheduling, were caused by processing difficulties experienced at the mill with the T111 alloy. Some of these production problems included poor surface finish, excessive carbon content, splitting of the ingot along its longitudinal axis during swage forging, and the lack of facilities for producing .008 inch T111 sheet in widths greater than 12 inches. Consequently, low yields of acceptable material were experienced. The material which was finally considered acceptable for use in this program still contained many sheets with small, isolated surface defects. Mechanical properties and chemical analyses of the acceptable sheet material are given in Tables I and II.

HONEYCOMB CORE

Material

The tantalum alloy foil for fabrication of the honeycomb core used in this program was furnished by the Air Force Materials Laboratory, and was produced under Air Force Contract AF 33(657)-8912 (Reference 1). Three tantalum alloys were reduced to foil gages (one to five mil thickness) in the rolling program: Ta-10W; T111, and T222 (Ta-9.5W-2.5Hf). The Ta-10W and T111 foils were rolled into twelve inch wide strips and twenty-four inch wide, 2 mil thick strips, were rolled from T111 and T222 alloys and subsequently coiled.

The materials received for program use were:

Ta-10W	- 12 inch wide, 2 mil thick (4 coils)
T111	- 12 inch wide, 2 mil thick (4 coils)
T111	- 24 inch wide, 2 mil thick (1 coil)
T222	- 24 inch wide, 2 mil thick (1 coil)

Tables III and IV show the results of tests conducted by the foil roller for the chemistry and bend ductility of the materials.

Visual examination of the foil was made as received with the assistance of unwind-rewind reels. Foil thickness and surface condition were found to be generally in good agreement with those reported in AFML-TR-65-43 (Reference 2).

TABLE I

FACE SHEET MATERIAL CERTIFICATION (NRC)

Source: National Research Corporation, Newton, Mass.

Material: Ta-8W-2Hf (T111)

- 1) .008 x 15 x 15 Heat No. 5146
 2) .012 x 12 x 12 Heat No. 3057

Material Condition: Cold worked 90 percent and then 100 percent recrystallized at 2800F for one hour

Chemistry: (Sheet-ppm)

	<u>O</u>	<u>N</u>	<u>C</u>	<u>Al</u>	<u>Cr</u>	<u>Cu</u>	<u>Fe</u>
Heat No. 5146	25	14	29	< 25	< 5	< 1	20
Heat No. 3057	112	15	88	< 25	< 5		25

	<u>Mo</u>	<u>Cb</u>	<u>Ni</u>	<u>Si</u>	<u>Ti</u>	<u>W</u>	<u>Hf</u>
Heat No. 5146	20	200	< 5	17	< 10	8.0%	2.08%
Heat No. 3057	10	200	< 5		< 5	7.8%	2.01%

Tensile Properties:

	<u>Ultimate Strength (psi)</u>	<u>Yield Strength (psi) (.2% Offset)</u>	<u>Elongation in 2 inches (%)</u>
Heat No. 5146	106,800	85,500	24
Heat No. 3057	91,200	77,800	25

TABLE II

FACE SHEET MATERIAL CERTIFICATION

(Wah Chang)

Source: Wah Change Corporation, Albany, Oregon

Material: Ta-8W-2Hf (T111)

.012 x 12 x 12 Heat No. 65079-T111

Material Condition: Cold worked 90 percent and then 100 percent recrystallized at 2800F for one hour

Chemistry: (Ingot-ppm)

	<u>O</u>	<u>N</u>	<u>C</u>	<u>Al</u>	<u>Cr</u>	<u>Cu</u>	<u>Fe</u>	<u>Mo</u>	<u>Cb</u>
Top (ppm)	100	< 5	40	10	10	< 20	< 20	15	760
Bottom	100	< 5	40	10	10	< 20	< 20	15	800

	<u>Ni</u>	<u>Si</u>	<u>Ti</u>	<u>Co</u>	<u>H</u>	<u>V</u>	<u>Zr</u>	<u>W</u>	<u>Hf</u>
Top	< 10	< 20	-	< 5	3	< 10	< 1000	8.75%	2.00%
Bottom	< 10	< 20	-	< 5	3	< 10	< 1000	8.65%	1.80%

Tensile Properties:
(sheet)

	<u>Ultimate Strength (psi)</u>	<u>Yield Strength (psi) (.2% offset)</u>	<u>Elongation in 1/2 inch (%)</u>
	99,900	83,500	33.0

TABLE III

CHEMICAL ANALYSES (AS ROLLED) TANTALUM ALLOY FOIL

Alloy	Width	O ppm	N ppm	C ppm	H ppm	W %	Hf %
Ta-10W-1	12	193	31	39	2	10.4	-
Ta-10W-3	12		not measured				
T111-2	12	187	29	469	14	8.2	1.8
T111	24	182	48	61	11	7.9	1.8
XT222	24	182	14	178	14	9.5	2.5

TABLE IV

FLAT BEND TEST TANTALUM ALLOY FOIL

Alloy	Width	Condition	Longitudinal	Transverse
Ta-10W-1	12	as rolled	180°-OK	180°-OK
Ta-10W-3	12	as rolled	180°-OK	180°-OK
T111-2	12	as rolled	180°-OK	180°-OK
T111	24	as rolled	180°-OK	180°-OK
		recrystallized	180°-OK	180°-OK
XT222	24	as rolled	180°-OK	180°-OK
		recrystallized	180°-OK	180°-OK

The Tantalum alloy foil selected for the fabrication of the honeycomb core for Phase I consisted of:

Ta-10W

.003 x 12"
.002 x 12"

T111

.003 x 12"
.0021 x 12"

The honeycomb core was fabricated as .250 inch square cell, .500 inch x 6 inches x 6 inches.

In the Phase II honeycomb core fabrication, the tantalum alloys used were:

T222

.0022 x 24"

T111

.0022 x 24"

The honeycomb for the flat and curved heat shield panels was fabricated as .250 inch square cell x .375 inch x 12 inches x 12 inches. The honeycomb core for the flat and curved structural panels was fabricated as .250 inch square cell x .500 inch x 12 inches x 12 inches.

Table V lists the results of room temperature tensile tests of 2 mil foil rolled from each alloy; elevated temperature properties of the 2 mil foil are shown in Table VI. (Data from same source as Table I and Table II)

Fabrication

The primary consideration in fabrication of tantalum honeycomb core is production of a strong node joint with minimum embrittlement of the base metal. To accomplish this aim, fabrication of the honeycomb core was sub-contracted to Hexcel Products, Inc., Dublin, California. The "ASTROWELD" process developed by Hexcel is a method of core manufacture by solid state diffusion bonding, which achieves a joint with properties which approach the base metal properties of the materials being fabricated. This method was selected for its advantages over the alternate methods available.

- 1) Unlike resistance or electron beam welding, diffusion joining temperatures are far below the liquidus temperature of the base metal. Embrittlement is therefore reduced to a minimum.
- 2) The joint is continuous, in contrast to a spot welded joint consisting of a series of separate or overlapping welds.
- 3) The width of the joined area is greater than that achievable with electron beam welding, enhancing the columnar strength of the node joint.

Prior to manufacture of the honeycomb core for use in actual panel fabrication, samples of diffusion bonded (titanium intermediate) Ta-10W were obtained from Hexcel. Specimens of the core were exposed to temperatures of

TABLE V
TENSILE PROPERTIES OF .002 INCH TANTALUM
ALLOY FOIL AT ROOM TEMPERATURE

Alloy	Width In.	Condition	Direction*	Ultimate Strength ksi	Yield Strength (.2% Offset) ksi	% Elongation in 2"
Ta-10W-1	12	as rolled	L	184.7	175.5	1.8
			T	201.5	184.3	1.3
Ta-10W-3	12	as rolled	L	-	-	-
			T	-	-	-
T-111-2	12	as rolled	L	175.4	164.5	2.3
			T	191.4	172.5	2.0
T-111	24	as rolled	L	126.2	-	4.0
			T	149.5	-	13.0
T-222	24	as rolled	L	163.6	-	14.0
			T	185.7	-	6.0
T-111	24	recrystallized	L	128.9	107.7	15.8
			T	128.0	104.8	14.4
XT-222	24	recrystallized	L	141.1	126.0	13.7
			T	137.5	116.8	8.4

Specimen Width: .25"

Strain rate: .005"/in/min to yield; .05"/in/min to failure

*L - longitudinal

T - transverse

TABLE VI
TENSILE PROPERTIES OF .002 INCH
TANTALUM ALLOY FOIL AT 2800F

Alloy	Width In	Test Temp °F	Condition	*Direction	Ultimate Strength ksi	Yield Strength (.2% Off- set)ksi	% Elongation in 2"
Ta-10W-1	12	2800	recrystallized	L	15.7	13.6	27
				T	19.3	18.6	20
Ta-10W-3	12	2800	recrystallized	L	-	-	-
				T	-	-	-
T-111-2	12	2800	recrystallized	L	24.6	20.8	45
				T	24.2	20.8	64
T-111	24	2800	recrystallized	L	26.0	22.2	26.6
				T	20.8	24.4	4.3
XT-222	24	2800	recrystallized	L	33.3	24.8	17.6
				T	25.1	31.5	18.4

Specimen width: .25"

Strain rate: .05"/in/min

Specimens at temperature 15 minutes prior to loading

*L - longitudinal

T - transverse

2800F, 3000F, and 3500F for one hour. Microstructure studies showed widening of the diffusion zone with increasing temperature from a relatively negligible amount at 2800F to an extensive zone at 3500F (some grains were found to cover up to 80 percent of the node thickness). Microhardness traverses were conducted for each condition. The center-of-node hardnesses are given in Table VII. Honeycomb core produced by this method received extensive evaluation as past experience has indicated a tendency toward embrittlement of tantalum alloys when exposed to titanium at high temperatures. No embrittlement was noted in these solid state diffusion bonded joints. Samples of diffusion bonded Ta-10W honeycomb core using a columbium intermediate were also produced. Metallographic examination of the nodes revealed joints of good quality, based on similar joints produced in an earlier Northrop Norair program (Reference 3). Tear tests conducted on several nodes resulted in failure in the base alloy, further evidence of good joint integrity. A photomicrograph of a bonded node is shown in Figure 1.

The actual honeycomb core employed in the manufacture of honeycomb panels in this program was produced by assembling into a flat pack sheets of foil which had regularly spaced strips of columbium intermediate metal applied to the surface. The spacing and width of the strips determined the cell size and shape of the honeycomb since the bond takes place only at the areas covered by the intermediate metal. In laying up the pack, each succeeding sheet was placed with its strip of intermediate metal midway between the strips on the sheet below. The pack was then placed under a protective atmosphere where temperature and pressure were applied to produce the required bonded node.

The finished pack resembles a piece of solid metal referred to as HOBE* (Honeycomb Before Expansion). Being in a near solid or compact assembly allows the HOBE to be easily sliced to any desired thickness, ground to exceptionally close tolerances (an extremely important factor in subsequent face sheet to core fit-up), and expanded mechanically into honeycomb. The core produced for this program was bonded in double widths of .0022 inch thick foil followed by the slicing of each hobe to produce two pieces of core. Each piece of core was then ground to the final thickness dimensions of .375 inch or .500 inch and expanded.

Hexcel reported no problems encountered in bonding the T111 and T222 core. All bonding was successful with a 100 percent yield of foil into core being accomplished. However, problems did arise during the manufacture of the Ta-10W honeycomb resulting in only a 50 percent yield of honeycomb core from this alloy. The Ta-10W foil required a higher temperature and pressure to bond. The bond strength was lower and there was a tendency for the foil to become brittle. The reason for this difference in the bonding characteristics between the T111 and T222 alloys and that of the Ta-10W alloy during honeycomb core manufacture was not readily apparent, as all previous studies appeared to show little if any difference in bonding between all three alloys. As a result, no Ta-10W panels were produced in the Phase II portion of the program.

All pieces of honeycomb core were inspected for overall dimensions and possible core defects. The results of this inspection are shown in Tables VIII and IX.

*Trademark of Hexcel Corp.

TABLE VII

CENTER-OF-NODE MICROHARDNESS FOR DIFFUSION BONDED
Ta-10W HONEYCOMB CORE (TITANIUM INTERMEDIATE)
AFTER VARIOUS THERMAL EXPOSURES

EXPOSURE TEMP. F	EXPOSURE TIME-MIN	CENTER-OF-NODE HARDNESS-KNOOP (100 gm.)
As-Received	--	340
2800	60	420
3000	60	440
3500	60	360

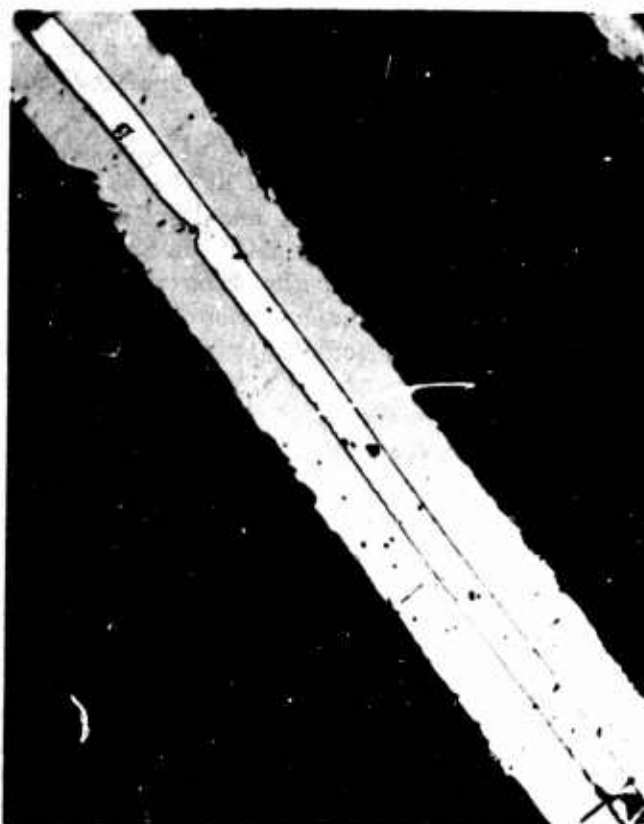


FIGURE 1 DIFFUSION BONDED NODE JOINT AS PRODUCED IN
CORE MANUFACTURING PROCESS. Ta10W-Cb
INTERFACE-(DARK MARGIN AT INTERFACE RESULTED
FROM SPECIMEN ETCHING) 100X MAGNIFICATION

TABLE VIII

INSPECTION ANALYSIS OF PHASE I TANTALUM HONEYCOMB CORE

HOBE NO.	SLICE NO.	ROLL NO.	PIECES 6"x6"	RIBBONS WIDE	CELLS LONG	CELL SEPARATIONS	RIBBONS SEVERED	REMARKS
1		1	1					Expanded
2		3	1					Expanded
3		4	4	76	33	0	0	No apparent defects
4	1	2	2	54	33	1	5	Severed ribbons were trimmed off as excess; cell separation was not
4	2	2	1	62	21	0	6	Four ribbons severed and were trimmed off as excess; two were not
5		1	1	40	16	0	0	No apparent defects
6	1	3	4	80	33	0	0	No apparent defects
6	2	3	4	80	33	0	0	No apparent defects
7	1	1	2	80	16	0	1	One piece contained a broken ribbon
7	2	1	2	82	18	1	3	All defects were trimmed off as excess
8		1	2	69	32	2	3	Ribbons 49-69 were deformed; both pieces contained either severed ribbons or separated cells

NOTES: Rolls 1 and 2 - Ta-10W
Rolls 3 and 4 - T111

TABLE IX

INSPECTION ANALYSIS OF PHASE II TANTALUM HONEYCOMB CORE

Core No.	Hobe No.	Slide No.	Alloy	Nominal Thickness (inch)	Ribbons Wide	Cells Long	Cell Separations	Ribbons Saved
1	4	2	T111	1/2	94	33	0	0
2	5	1	T111	1/2	96	33	0	0
3	5	2	T111	1/2	96	33	0	0
4	6	1	T111	1/2	94	33	0	0
5	6	2	T111	1/2	94	33	0	0
6	7	1	T111	1/2	94	33	0	0
7	7	2	T111	1/2	94	33	0	0
8		1	T111	1/2	94	33	0	0
9		2	T111	1/2	94	33	0	0
10	8	1	T111	1/2	94	33	0	0
11	9	2	T111	1/2	94	33	0	0
12	14	1	T111	1/2	94	33	0	0
13	10	1	T222	1/2	91	33	0	0
14	10	2	T222	1/2	91	33	0	0
15	11	1	T222	1/2	92	33	0	0
16	11	2	T222	1/2	92	33	0	0
17	1	1	T111	3/8	92	33	0	0
18	2	1	T111	3/8	94	33	0	0
19	2	2	T111	3/8	94	33	0	0
20	3	1	T111	3/8	95	33	0	0
21	3	2	T111	3/8	95	33	0	0
22	4	1	T111	3/8	94	33	0	0
23	12	1	T222	3/8	92	33	0	2
24	12	2	T222	3/8	92	33	0	1
25	13	1	T222	3/8	94	33	0	0
26	13	2	T222	3/8	94	33	0	0

NOTE: Each hobe was expanded to approximately 12" x 12"

It may be seen in Table VIII that all of the defects noted occurred in core fabricated from the Ta-10W alloy. However, it was possible to trim away most of the defects thus excluding them from actual panels. Of the 26 pieces of core manufactured for the Phase II panels, only two exhibited defects. It may be noted that both pieces were produced from the same hobe. The defects consisted of one and two severed ribbons, which did not hamper their use in producing satisfactory test panels.

Edgemembers

Edgemembers for the flat and curved structural panels were fabricated from .025 inch x 2 inch x 13 inch and .025 inch x 2 inch x 18 inch T111 annealed sheet procured from the National Research Corporation. Chemistry and mechanical properties of this material are shown in Table X.

Envelope Material

Inconel 600 sheet, .025 inch thickness was procured for the envelope material. The selection of Inconel 600 was based on previous experience with the material (Reference 4). Inconel 600 has the ability to withstand the long term cycles demanded in the program. A previous consideration of Hastelloy X was discounted due to excessive warpage and embrittlement during similar test cycles.

TABLE X

EDGE MEMBER MATERIAL CERTIFICATION

Source: National Research Corp., Newton, Mass

Material: Ta-8W-2Hf

1) .025" x 2 x 13 Heat No. 3352

2) .025" x 2 x 18 Heat No. 5100

Condition: Annealed and flat

Chemistry: (ppm)	<u>O</u>	<u>N</u>	<u>C</u>	<u>Al</u>	<u>Cr</u>	<u>Cu</u>	<u>Fe</u>
Heat 3352	19	28	63	10	5	5	10
Heat 5100	37	27	28	25	5	10	10

	<u>Mo</u>	<u>Cb</u>	<u>Ni</u>	<u>Ti</u>	<u>W</u>	<u>Hf</u>
Heat 3352		80	5	5	8.0%	2.1%
Heat 5100	10	150	10	5	7.8%	2.32%

Tensile Properties:	Ultimate Strength (psi)	Yield Strength (psi) (.2% offset)	Elongation in 2 inches(%)
Heat 3352	96,500	81,000	26
Heat 5100	104,000	86,500	22.5

Strain Rate - .02 in/in/min

IV TECHNICAL DISCUSSION

SOLID STATE DIFFUSION BONDING

Factors which control solid state diffusion bonding are the time, temperature, and pressure of the bonding operation, and the surface cleanliness and surface finish of the materials to be bonded. Assuming that a clean surface (one relatively free of oxides and hydrocarbons) can be provided with relative ease, the effects of these other factors are the major concern:

1. Surface roughness, projections, and general asperity hold the two surfaces of the bond joint apart. This controls the extent of contact between the two surfaces, and hence the amount of surface area available for diffusion to occur. Since the joint or bond strength is dependent upon the amount of metal diffusion, which in turn is dependent upon the amount of surface in contact, the degree of actual surface contact is a critical controlling factor in joint strength.
2. Temperature affects the amount of surface contact by reducing the yield and creep strength of the material providing improved fit-up or contact between surfaces. Even more important, however, is the fact that temperature is the prime mover of the interchange of atoms between the metal surfaces to be bonded. The rate of diffusion or atom migration is logarithmically dependent on temperature.
3. Pressure plastically deforms the surface projections, causing greater area of contact of the surfaces and hence increased bond strength. Increases in pressure increase bond strength until the joint is virtually void-free. Further pressure increases add little to the strength of the bond.
4. Time has a direct effect on the amount of diffusion and creep which occurs between surface asperities. In general, longer bonding time increases surface contact and atomic diffusion across the interface.

Diffusion bonding of honeycomb core to face sheets can be accomplished without intermediates; however, two problems exist:

1. The node is twice the thickness of the cell walls and gains additional rigidity from the X-like shape of the surrounding walls. The effects mean that, in most bondments, the cell wall buckles and does not bond, while the node area supports the pressure and bonds.
2. Fit-up between the cell edges and the face sheet is extremely critical for the reasons previously mentioned. With commercial tolerances, many voids may remain.

The use of a soft intermediate for diffusion bonding minimizes both of the above effects resulting in nearly complete bonds. In addition, the intermediate buildup around the core walls form a type of fillet which is believed to enhance acoustic fatigue strength.

SELECTION OF INTERMEDIATE MATERIALS

Diffusion rates have been shown to be directly related to the melting point and the crystal structure of the alloy being diffusion bonded. Consequently, refractory alloys, due to their high melting points (especially tantalum-5400F) usually require lower melting point intermediate materials to effect satisfactory bonding within practical time, temperature limitations. In addition, close tolerance fit-up between bond surfaces can be greatly enhanced by an intermediate material. The selection of a suitable intermediate for diffusion bonding tantalum honeycomb panels revolves around three basic concepts:

1. A diffusion bonded tantalum alloy joint must possess high temperature strength; therefore, the intermediate material must form a high-melting-temperature alloy with tantalum.
2. The intermediate must be metallurgically compatible with tantalum in order to retain joint and base metal ductility.
3. The intermediate should effect satisfactory diffusion within practical time and temperature limitations.

Titanium is a readily available foil which possesses a low yield strength in the bonding range, is metallurgically compatible with tantalum, and will form a joint with a melting point satisfactory for service applications using practical bonding times and temperatures. However, one problem exists with the use of titanium foil as the intermediate. The excess foil which is not directly used in forming the actual bond is free to evaporate during bonding or service conditions if the required evaporation temperatures are achieved.

Titanium evaporation during brazing, diffusion treating, and simulated service exposure for up to one hour at 3500F with closed cell titanium brazed Ta-10W panels has been shown to cause serious embrittlement of the core (References 5 and 6). Figure 2 illustrates this effect by showing the maximum times at temperature to which a Ta-10W honeycomb panel may be subjected without serious core embrittlement from titanium vapors. In addition, this data reveals that although titanium can be successfully used for Ta-10W bonding with up to 800 hours life in the 2200F range, service exposures above 3000F must be limited to one hour or less to inhibit core embrittlement. Core embrittlement at these service temperatures and durations will result in a non-reusable structure. While the exact mode of titanium embrittlement has not been determined, it is believed to be associated with grain boundary diffusion of atoms from the titanium vapor along the large recrystallized tantalum grains. An example of the result of this phenomenon is illustrated in Figure 3 showing Ta-10W foil exposed to titanium vapor at 2850F for 24 hours.

Other intermediates such as vanadium, columbium and hafnium were considered for heat shield applications (3000 to 3500F). The characteristics of these elements were compared with tantalum and titanium and are tabulated as follows:

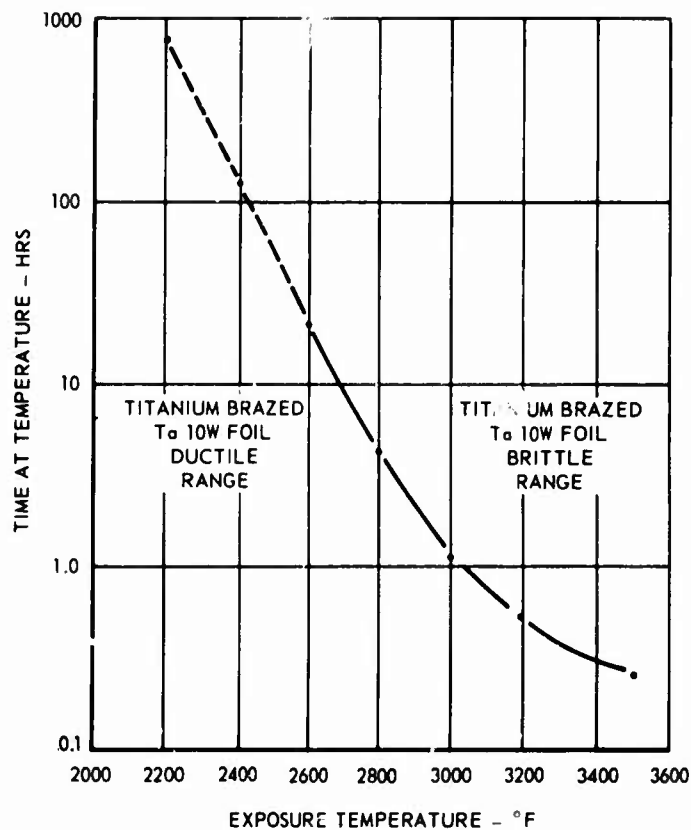
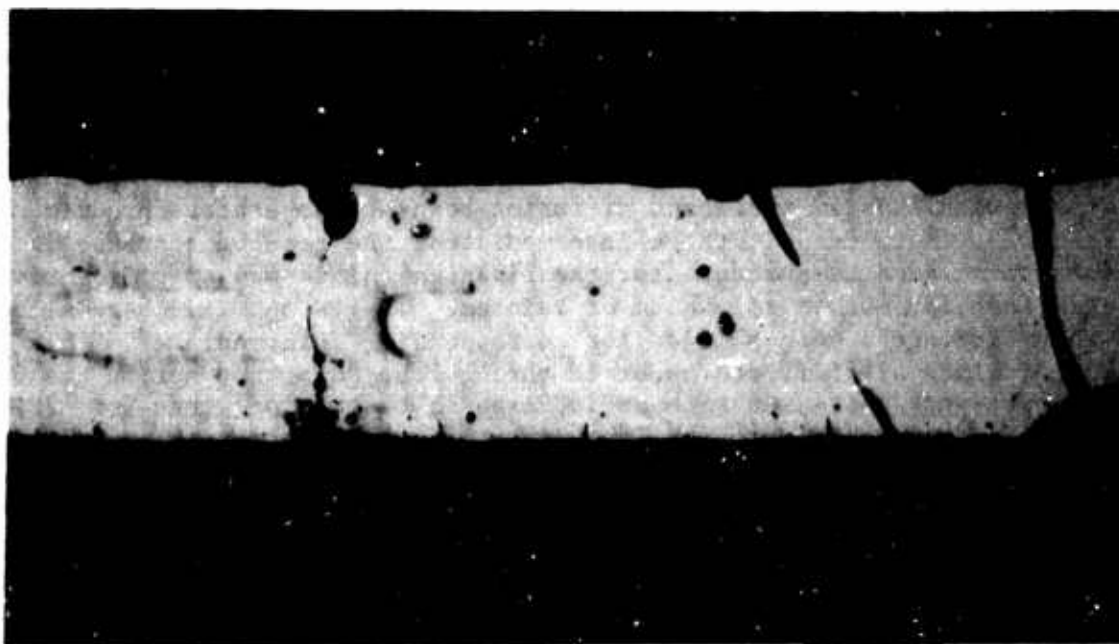


FIGURE 2 TITANIUM EMBRITTLEMENT OF Ta 10W FOIL



MAG = 500X
ETCH FREEDMAN'S

Ta 10W FOIL EXPOSED
FOR 24 HOURS AT
2850F IN PRESENCE OF
TITANIUM VAPOR

FIGURE 3 EFFECT OF TITANIUM VAPOR ON Ta-10W FOIL

	Ta	Ti	V	Zr	Hf	Cb
Melting Point	5425F	3050F	3450F	3360F	4028F	4379F
Atomic Size Goldschmidt Radii	1.47	1.47	1.36	1.60	1.59	1.47
Solubility in Ta at 2200F	-	complete	forms TaV ₂	5%	15%	complete
Density GMS/CC	16.6	4.51	6.1	6.49	13.1	8.57
Vapor Pressure Torr at 3000F	5×10^{-11}	2×10^{-2}	2×10^{-4}	5×10^{-5}	1×10^{-8}	4×10^{-10}

Based on the above, vanadium was eliminated for use with tantalum due to the formation of brittle TaV₂. Zirconium with a low solubility in tantalum and a relatively high vapor pressure would limit its usefulness. Hafnium has a somewhat low solubility in tantalum but has proven useful in tantalum braze alloys. Columbium appeared to be the most promising of the possible intermediates for 3000 to 3500F service.

The diffusion bonding characteristics of Ta-10W and Ti-75A were studied using Ti-75A, pure columbium, and pure hafnium foils as intermediate materials. This study consisted of fabricating and testing lap shear specimens, metallographic analyses, microhardness determinations, and microprobe scans to derive appropriate diffusion coefficients for each binary alloy system, that is, Ta-Ti, Ta-Cb, and Ta-Hf.

Figure 4 graphically represents the affect of bond temperature on lap shear strength. While increased diffusion bonding temperature produced high lap shear strength for all three intermediates, the rate of increase in strength with bond temperature for the titanium joints was significantly greater than for either columbium or hafnium. Ta-10W and Ti-75A base-alloy lap-shear strengths were similar for corresponding intermediates. This was expected, since all failures occurred through the joint and not in the base alloy. Strength decreases with an increase in test temperature from 2800F to 3500F as shown in Figure 5. The highest lap-shear strength was exhibited by the Ti-75A joints; Hf joints had intermediate strength and Cb joints had the lowest strength.

Lower strength Cb joints were expected since Cb possesses the highest yield strength and, therefore, cannot deform to compensate for fit-up disparities as readily as either Ti-75A or Hf for equivalent bonding parameters. All strength data are summarized in Table XI.

Improvement of the lap shear strength of the Hf and Cb intermediate specimens was attempted by decreasing the intermediate thickness. Columbium foil, .001 inch thick, was chemically milled to a thickness of .0005 inch. Hafnium foil, .002 inch thick, was chemically milled to a thickness of .001 inch. Lap shear specimens were fabricated (2600F for 120 minutes at 1000 psi) using these foils as intermediates. Three specimens of each thickness of Cb

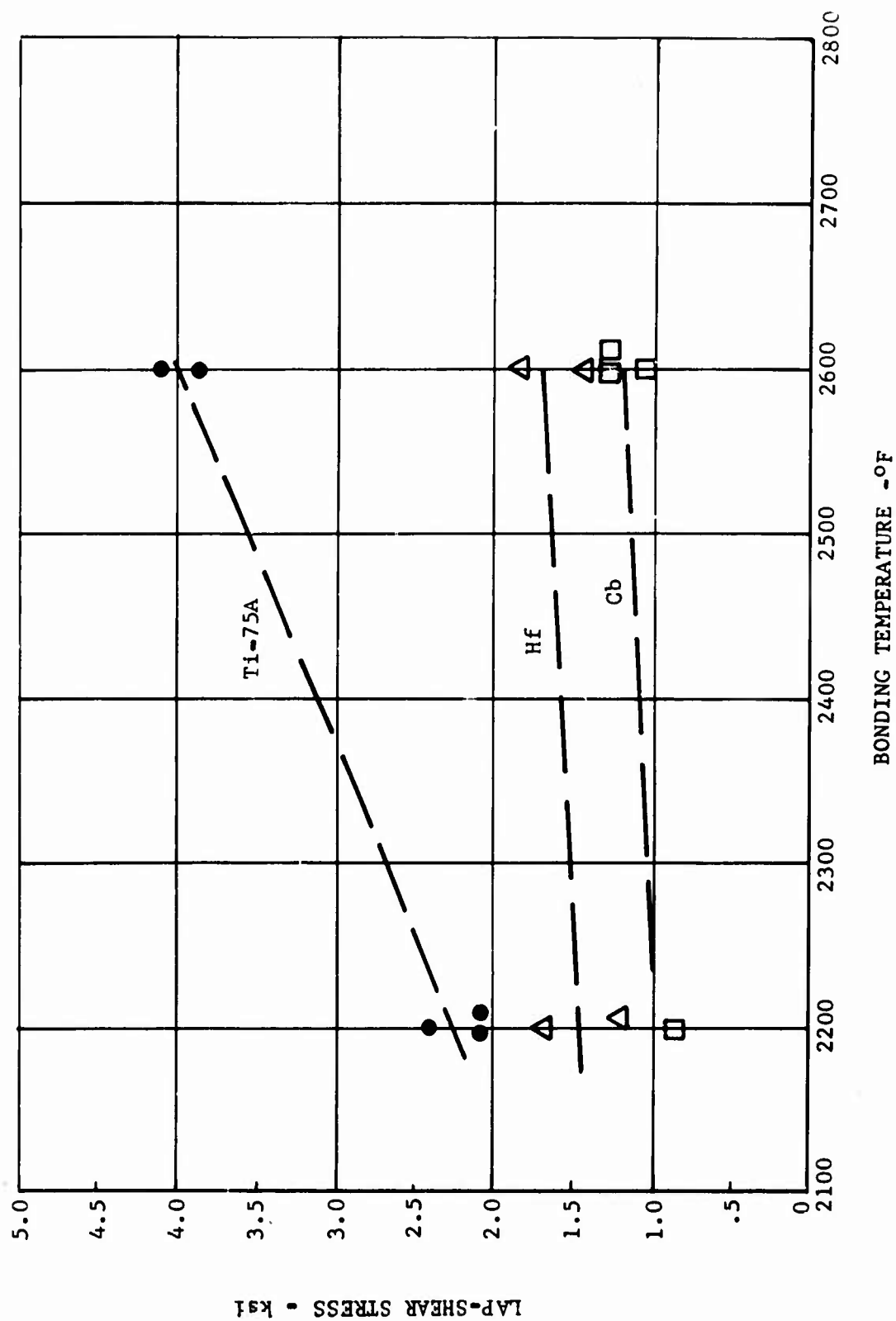


FIGURE 4 EFFECT OF DIFFUSION BONDING TEMPERATURE ON LAP-SHEAR STRENGTH AT 2800F. (BONDING TIME = 120 MINUTES, BONDING PRESSURE = 1000 psi)

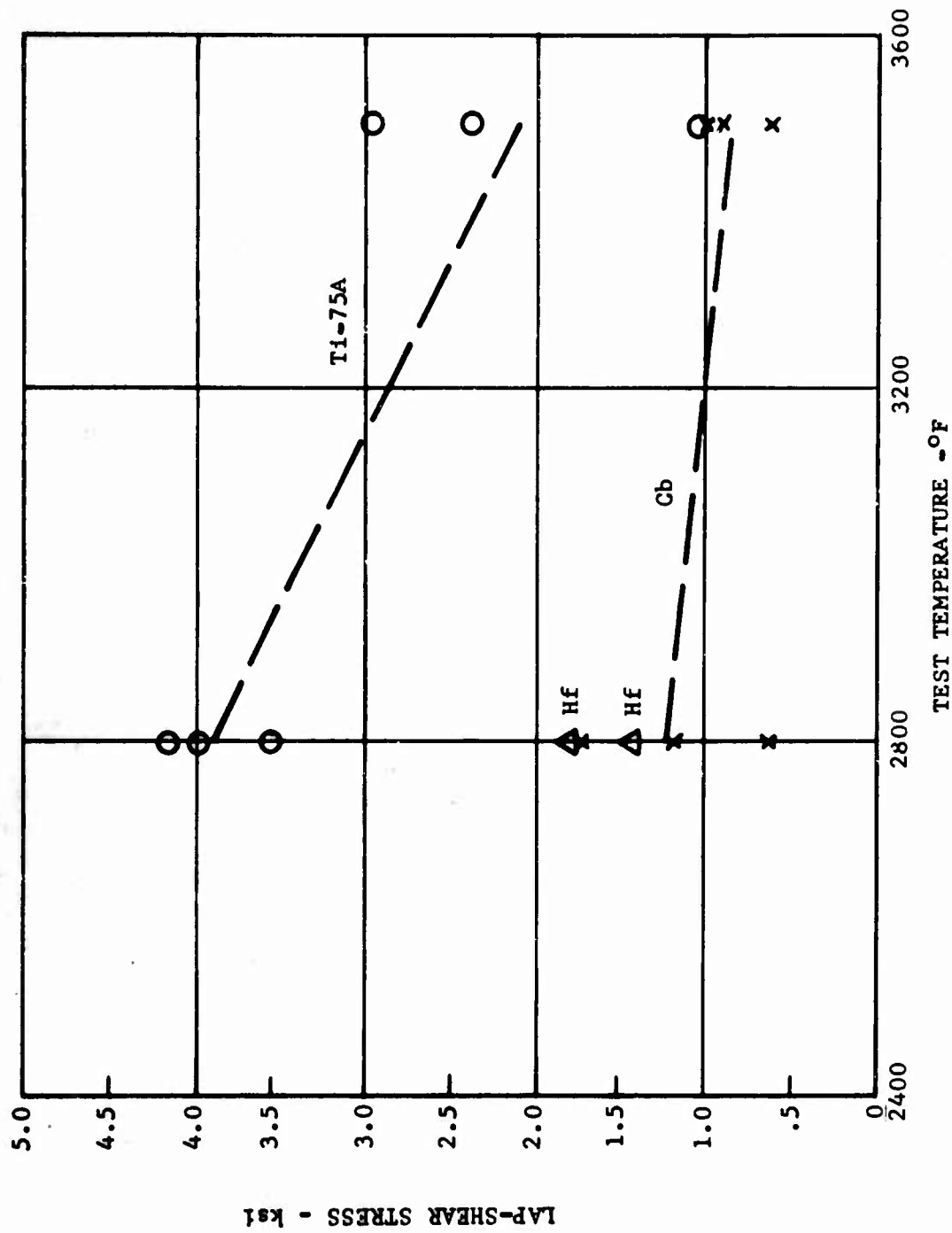


FIGURE 5 EFFECT OF TEST TEMPERATURE OF LAP-SHEAR STRENGTH.
LAP-SHEAR SPECIMENS DIFFUSION BONDED AT 2600°F FOR
120 MINUTES UNDER 1000 psi

TABLE XI

LAP-SHEAR STRENGTH DATA OBTAINED FOR Ta-10W AND T-111 BASE ALLOYS
USING Cb, Hf, AND Ti-75A INTERMEDIATES

BASE ALLOY	INTERMEDIATE & THICKNESS	DIFF. BONDING PARAM TEMP. F	TIME-MIN.	TEST TEMP. F	LAP-SHEAR STRENGTH-psi
Ta-10W	Ti-75A .0015"	2200	70	2800	2480
					1280
		2600	150	2800	2729
					2440
			150	2800	2068
					2061
T-111	Ti-75A .0015"	2600	52	2800	3821
					4080
		2600	150	2800	4645
					3135
			150	2800	2638
					3992
Ta-10W	Cb .001"	2200	120	2800	4127
					3518
		2600	120	2800	2945
					1032
			120	3500	2362
					884
T-111	Cb .001"	2600	120	2800	1280
					1032
		2600	120	2800	1275
					1409
			120	2800	984
					652
Ta-10W	Hf .002"	2200	120	2800	1739
					1161
		2600	120	2800	952
					600
			120	3500	1040
					1680
T-111	Hf .002"	2600	120	2800	1345
					1431
		2600	120	2800	1882
					3132
			120	2800	2480
					2209
Ta-10W	Mo .001"	2400	120	2800	3347
					2209
		2600	120	3500	3427
					1480
			120	3500	1660
					1000
					1040
					1040

were tested in tension at 2800F and 3500F. The Hf specimens were tested in tension at 2800F. Results indicated little effect of intermediate thickness on the strength of Cb joints, while the Hf joints exhibited a 40 percent increase in strength for a 50 percent reduction in intermediate thickness.

The characteristic microstructures of diffusion-bonded joints of Ta-10W using Ti-75A, Cb, and Hf intermediates are shown in Figure 6. The Ti11 joint microstructures are similar in appearance. The microhardness traverses corresponding to Figure 6 are shown in Figure 7. Since titanium alloys are inherently harder than Cb or Hf, the higher microhardness profile exhibited by the titanium joint was expected.

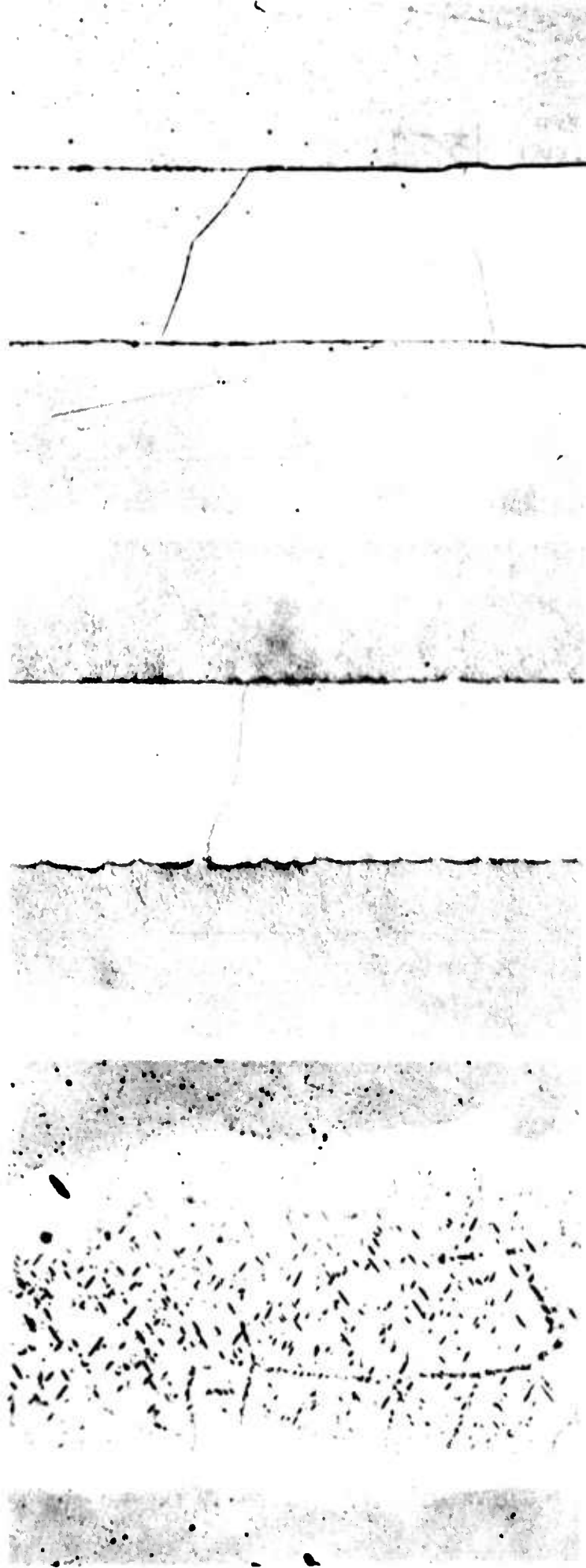
As an additional effort to further improve on the lap-shear strength of diffusion-bonded refractory intermediate joints, pure molybdenum, .001 inch thick, was used to produce seven lap shear specimens. The resultant lap shear strengths are given in Table XI. Figure 8 shows the microstructure and attendant microhardness profile for the Mo intermediate specimen bonded at 2600F for 120 minutes. Comparison of these properties with those of Cb lead to the conclusion that no advantage is to be gained by using molybdenum.

Due to its limited availability, its similarity to Cb, and cost considerations, Hf was ruled out as a potential intermediate material for this program. The chief objection to the use of columbium as intermediate was the excessively long bonding times required at the temperatures to be employed. From a manufacturing standpoint, 2350F was considered the maximum safe bonding temperature when considering the temperature limitations of the tooling materials to be employed for panel bonding, particularly the Inconel 600 protective envelopes which have a reported melting temperature range of 2450-2600F.

Titanium was therefore selected as the intermediate to be used in the fabrication of all panels to be manufactured in the program for the following reasons:

1. Higher strength joints
2. Shorter times and lower temperatures to effect satisfactory bonds.
3. Lower yield and creep strength at the bonding temperature providing better fit-up and thus greater surface contact area.

The embrittlement problem encountered with titanium as previously discussed would be prevented in the structural panels since service temperatures are designed for 2800F maximum. The heat shield panels could tolerate mild embrittlement since this type panel was designed to withstand high heat fluxes only, as this panel is not required to withstand stresses other than those resulting from normal aerodynamic surface loading. In addition, the feasibility of applying the titanium intermediate directly to the core edges by vapor deposition was investigated. This would result in no excess titanium within the panel thus minimizing titanium embrittlement of the panel at all service temperatures. This investigation is described in detail in a later section of the report entitled, "INTERMEDIATE APPLICATION BY VAPOR DEPOSITION".



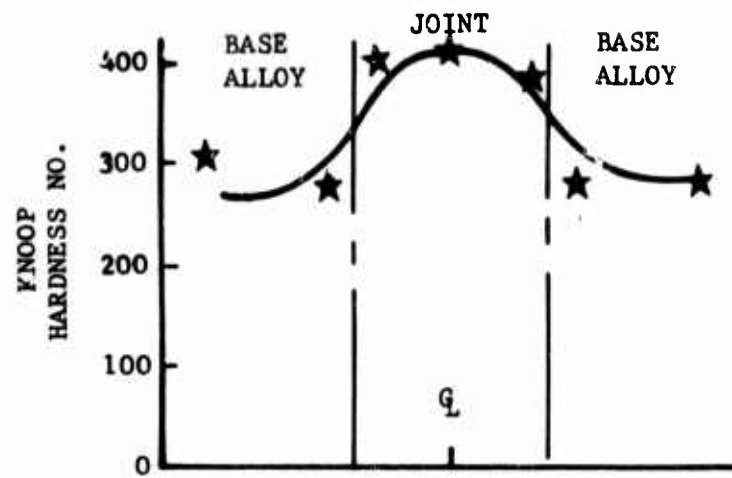
(a) Ti-75A, Etchant: Kroll's
Mag: 1000X

(b) Columbium
Etchant:
50% Hf
12.5% H_2SO_4
12.5% HNO_3
50% H_2O
Magnification: 1000X

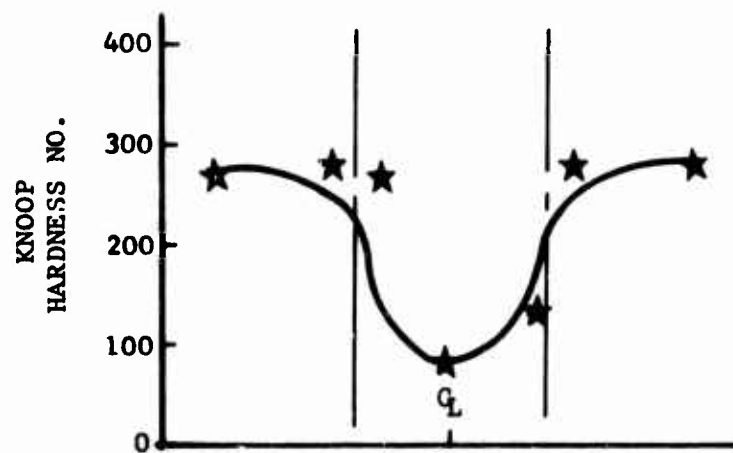
(c) Hafnium, Etchant: Kroll's
Mag: 1000X

NOTE: All specimens tested at 2600F for
120 minutes under 1000 psi

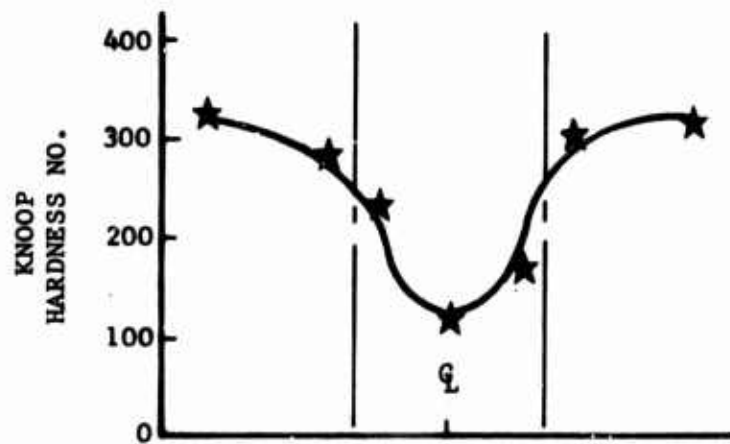
FIGURE 6 MICROSTRUCTURE OF DIFFUSION BONDED LAP-SHEAR SPECIMENS



(a) Ti-75A INTERMEDIATE

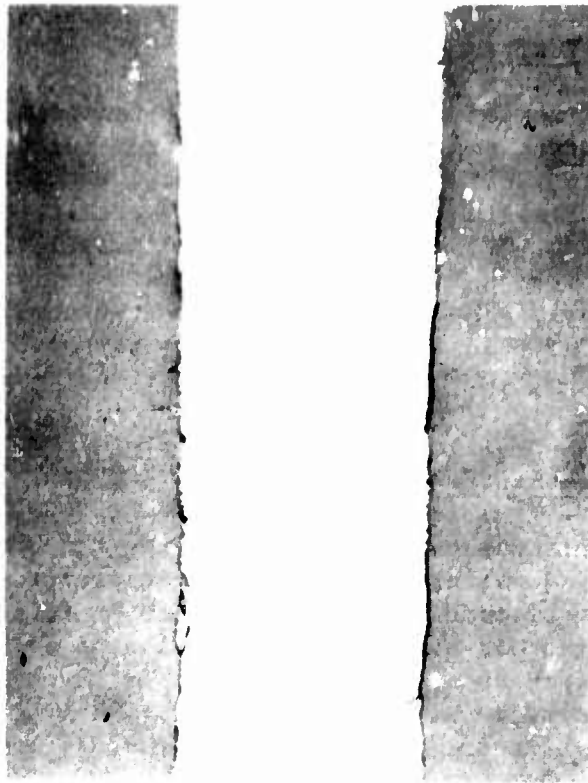


(b) Hf INTERMEDIATE



(c) Cb INTERMEDIATE

FIGURE 7 MICROHARDNESS PROFILES FOR DIFFUSION BONDED LAP-SHEAR JOINTS



ETCHANT: 10 gms NaOH MAG: 1000X
 30 gms $K_3Fe(CN)_6$
 100 ml H_2O

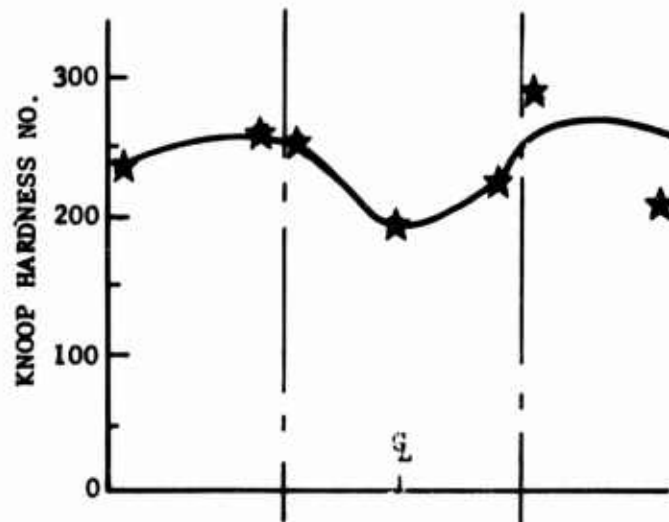


FIGURE 8 MICROSTRUCTURE AND MICROHARDNESS FOR DIFFUSION BONDED LAP-SHEAR JOINT USING MOLYBDENUM INTERMEDIATE WITH Ta-10W BASE ALLOY. LAP SHEAR SPECIMEN BONDED AT 2600F FOR 120 MINUTES UNDER 1000 PSI

RECRYSTALLIZATION STUDY

The recrystallization characteristics of tantalum alloys are sensitive to interstitial content and may vary widely from ingot to ingot. It was therefore desired to verify the quality of Ta-10W and T111 foils based on a metallographic study of the recrystallization characteristics of each alloy. Both Ta-10W and T-111 foils were found to recrystallize after one hour exposure at 2800F, which is in good agreement with the published recrystallization data for these alloys. The T-222 foils exhibited complete recrystallization after one hour at 2800F instead of 3000F as reported in Reference 7. One hour exposures at 2900F, 3000F, and 3500F resulted in progressive grain growth in each foil.

BONDING PRESSURE TOLERANCE ON CORE

The maximum pressure available for bonding the honeycomb panels in this program, was the 14.7 psi atmospheric pressure exerted on the panel enclosed within an evacuated protective envelope, which in turn is magnified to 1000 psi when consideration is given to the actual area of bond surface between the honeycomb and face sheets. Since it was highly desirable to utilize as much pressure for bonding as was available, the ability of the tantalum honeycomb to resist crushing during the bond cycle under a stress of 1000 psi was investigated.

A half-inch square of electron beam welded Ta-10W honeycomb core containing 12 cells (3/16 inch cell size) was subjected to 15 psi face sheet stress at 3000F in an Abar cold-wall vacuum furnace under a vacuum of 10^{-5} Torr. Pressure on the core was obtained by placing tungsten weights directly on the sample. The test was terminated after one hour (at least equal in severity to the time, temperature bond cycle of 3.5 hours at 2250F). Subsequent examination revealed no crushing of the core. Consequently, the maximum pressure available for bonding was deemed to have no effect on the mechanical stability of the core.

BONDING PARAMETER STUDY

Method of Determining Bond Parameters

If the diffusion constants are known for a specific diffusion bonding system, it is possible to calculate the final composition of a joint. When these calculations are made for various joint compositions, an array of time and temperature curves can be constructed. If various joint compositions are produced and tested at several service temperatures, it is possible to predict the service strength from these curves. When D values are lacking for the diffusion system of interest, diffusion couples must be made at several temperatures. Electron microprobe analyses of these diffusion couples then provides the information needed to solve for the D values.

Electron microprobe analysis was used to determine the variation in chemical composition with distance across the joint. This data lends itself to the calculation of the diffusion coefficient for each intermediate material at the particular temperature studied. Results of these calculations for the various materials and temperatures studied are summarized in Table XII. Calculation of a sufficient number of "D" values for a particular intermediate material permits construction of time-temperature curves, the use of which allows prediction of high temperature strength and consequently, diffusion bonding parameters.

Curves for the diffusion of columbium and titanium in Ta-10W were constructed. Diffusion curves for T111 were not constructed since previous studies revealed no significant differences between the diffusion characteristics of Ta-10W and those of T111 with columbium and titanium.

A computer program was utilized to obtain several time-temperature-concentration relationships for the diffusion of Cb and Ti into tantalum alloy Ta-10W. The product of the computer analysis was a set of log time versus diffusion coefficient curves for .0005, .0010, .0015, and .0020 inch thicknesses of each intermediate material. These curves show the final intermediate concentration at the center of the joint ranging from 10 to 100 percent of the original concentration. These curves were then converted to log time versus temperature in degrees fahrenheit for each thickness of intermediate and final center-of-joint concentration.

The value of such a set of curves is that they may be used to obtain a reasonable estimate of the time required at a given temperature to achieve the desired center-of-joint concentration. Knowledge of the final concentration for a given intermediate thickness then allows prediction of joint strength to be made.

The following discussion is presented to describe the technique utilized in arriving at the curves employed for selecting the optimum solid state diffusion bonding parameters in this program.

Study of Diffusion of Titanium and Columbium Into Ta-10W

The diffusion of titanium and columbium into tantalum alloy Ta-10W was studied. Diffusion-bonded lap shear specimens, using Ti-75A and Cb intermediates, were fabricated at various times and temperatures. Several of these specimens were then sectioned and mounted for electron microprobe analysis of the chemical gradients in the diffusion-bonded zone.

Analysis of the electron microprobe data required a rather lengthy manipulation of mathematical equations to determine the proper corrections. Therefore, a Norair-developed computer program, devised to perform these calculations on microprobe data, was used. The results of the computer program are traces of the relative intensity versus the corrected concentration of a given element. Curves of corrected concentration versus distance across the diffusion-bonded zone are plotted from the computer data.

TABLE XII

DIFFUSION COEFFICIENTS FOR VARIOUS DIFFUSION BONDING CONDITIONS
BASE ALLOY: Ta-10W

INTERMEDIATE	DIFF. BONDING TEMPERATURE, F	DIFF. BONDING TIME-MIN.	DIFFUSION D^* COEFFICIENT-Cm ² /Sec
Ti-75A	2200	70	4.89×10^{-10}
	2200	150	6.46×10^{-10}
	2200	480	1.125×10^{-10}
	2800	30	28.6×10^{-10}
Cb	2400	120	2.73×10^{-12}
	2600	120	11.22×10^{-12}
Hf	2400	120	6.32×10^{-12}

*NOTE: These are the calculated values. Due to the scatter in experimental results, the probable diffusion coefficients are:

Ti-75A	2200F	4×10^{-10} cm ² /sec
Ti-75A	2800F	3×10^{-9} cm ² /sec
Cb	2400	3×10^{-12} cm ² /sec
Cb	2600F	1×10^{-11} cm ² /sec
Hf	2400F	6×10^{-12} cm ² /sec

The diffusion coefficient for a specific temperature is then obtained from these curves. Calculation of the diffusion coefficient from several such curves for different temperatures allows the construction of a plot of the logarithm of the diffusion coefficient versus temperature. Finally, another computer program was used to obtain joint concentration as a function of the logarithm of time and temperature.

The joint concentration curves yield an accurate estimate of the time required to promote a specified amount of diffusion for a given intermediate, intermediate thickness, and temperature. If the lap shear strength has been determined for a given chemical composition in the joint, these curves may further be applied to obtain an estimate of the diffusion bonding parameters required to produce a desired lap shear strength.

Electron Microprobe Computer Program

The electron microprobe is essentially an electron source whose beam is collimated by an electromagnetic lens which focuses the beam to diameter of a few microns. When the beam is focused on an area of a specimen whose composition is to be determined, the atoms of the matrix located within the beam become excited and release radiation whose wave length is characteristic of the element irradiated. The characteristic radiation is separated into individual wavelengths by a crystal.

It is then received by a detector situated at a specific angle, as required by the elements under analysis, with reference to the crystal. Different elements will be detected at different angles.

The intensity of the wavelength characteristic of the element under analysis is then compared with the intensity of a beam received from a pure sample of the element. Relative intensities are recorded continuously and may be interpreted as the percent of the specified element present within the area (diffusion zone) covered by the electron beam. It should be noted that the entire diffusion zone is traversed in one micron increments.

Data obtained by the electron microprobe technique contains inherent inaccuracies which may yield values too high or too low relative to the actual percentage of the element analyzed within the matrix. The method used herein for correcting these inherent inaccuracies is based on an analysis by L. S. Birks⁸ of the U.S. Naval Research Laboratory in Washington D.C. The equations suggested by Birks were programmed into an IBM 7090 computer using the Fortran IV system.

Action and reaction of a beam of electrons focused on a sample is described in terms of mutual excitation, absorption, and fluorescence. Essentially, the electron beam is focused indiscriminately upon the atoms of the matrix and excites characteristic wavelengths of radiation as described above. Prior to leaving the matrix, however, these excited wavelengths may be absorbed, to some degree, by the heavier elements of the matrix in proportion to the concentration of these elements and their relative atomic number. As a result, the relative intensities obtained from the electron microprobe may be somewhat low.

In addition to absorption, the effects of fluorescence must be accounted for. Due to the relatively high energy of the x-rays from atoms whose concentration is to be measured, adjacent atoms are excited such that the relative intensities recorded will tend to be higher than the intensities indicative of the actual composition. Thus, the effects of fluorescence tend to cancel the effects of absorption. However, both must be considered.

The equation cited below represents the generalized form of the analysis programmed into the computer.

$$I_A / I_{A100} = \frac{F_A W_A (1-K_F)}{F_{A100}}$$

where

I_A = actual x-ray intensity of unknown

I_{A100} = actual x-ray intensity of pure element

F_A = absorption correction of unknown

F_{A100} = absorption correction of pure element

K_F = fluorescence correction

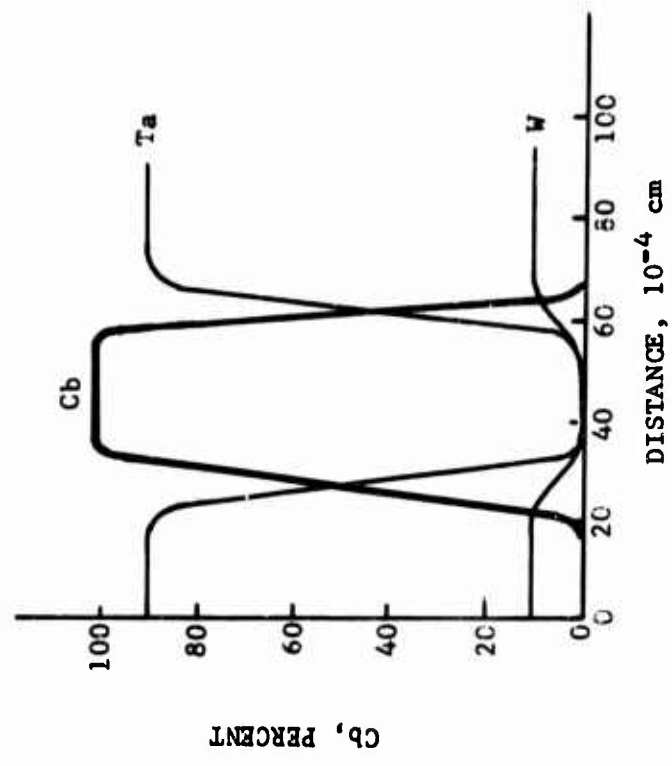
W_A = weight fraction of unknown

A standard curve of relative intensity, or I_A / I_{A100} , is plotted against the actual weight fraction of the element. The relative intensity data, as obtained from the electron microprobe, is then compared to the relative intensity axis I_A / I_{A100} and the corrected concentration is determined. The corrected concentration is then plotted as a function of the diffusion distance.

Construction of Diffusion Coefficient Versus Temperature Curves

The electron microprobe data as reduced by the computer program yields curves of the variation in concentration with distance across the joint. Sketches of these curves are shown in Figure 9. By applying the appropriate method of solution, the diffusion coefficients (D) for each intermediate and each diffusion temperature, may be calculated. Figure 10 illustrates the two methods used for this work. The thin-film analysis was used for the titanium since titanium behaves as a thin film; that is diffusion occurs across the entire diffusion zone during diffusion bonding, whereas the Matano analysis was used for Cb because it is applicable to situations involving limited diffusion. After a sufficient number of D values have been calculated, a curve of the logarithm of the diffusion coefficient (log D) versus the reciprocal of the absolute temperature (1/T) is constructed as shown in Figure 11. This is readily converted to the more useful form found in Figure 12. The curves in Figure 12 show the temperature range of interest for the intermediate materials used in this diffusion bonding program, thus establishing the range for log D.

Cb FOIL INTERMEDIATE -
 0.0010 INCH THICK
 DIFFUSION BONDING PARAMETERS -
 120 MINUTES AT 2400F



T1 - 75A FOIL INTERMEDIATE -
 0.0015 INCH THICK
 DIFFUSION BONDING PARAMETERS -
 52 MINUTES AT 2600F

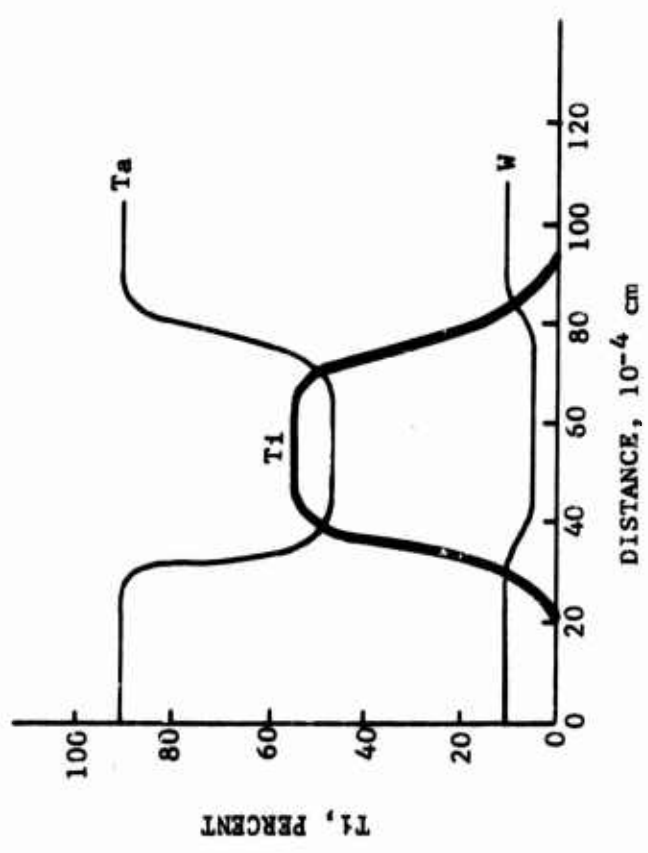
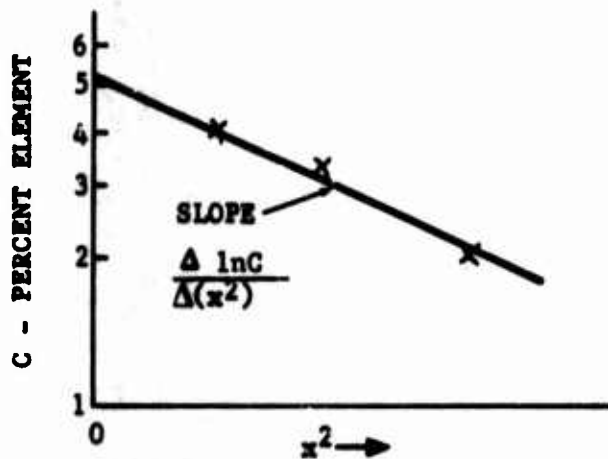
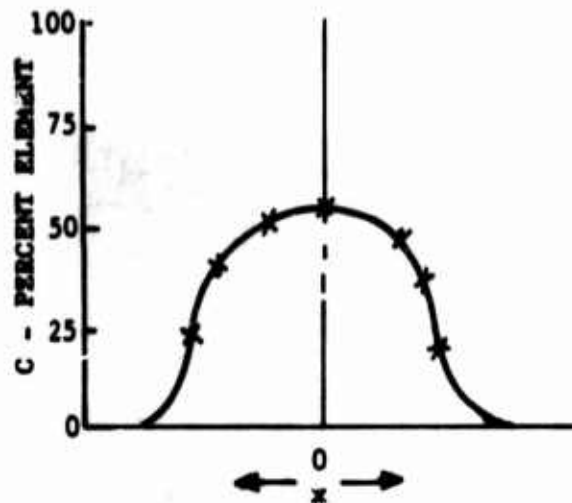


FIGURE 9 SKETCHES SHOWING TYPICAL COMPOSITION PROFILES
 ACROSS DIFFUSION BONDED JOINTS OF Ta-W

THIN-FILM METHOD

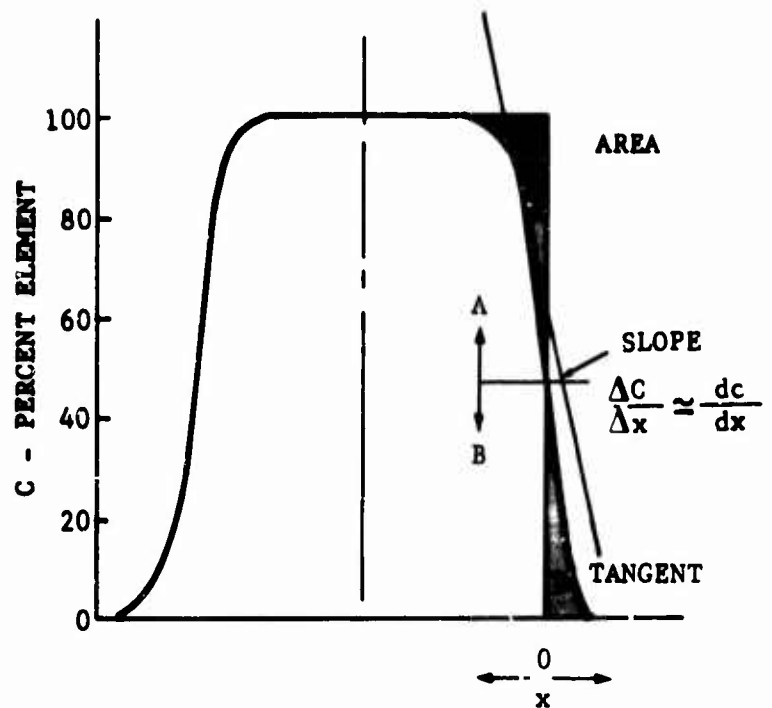


$$D = \frac{\Delta(x^2)}{4t (\Delta \ln C)}$$

t = DIFFUSION BONDING TIME
IN SECONDS

RESULT: DIFFUSION COEFFICIENT, D,
FOR TEMPERATURE, T

MATANO METHOD



AREA OBTAINED GRAPHICALLY SUCH
THAT IT MAY BE SUBSTITUTED FOR
 $\int x dC$ IN THE EQUATION BELOW.

BOUNDARIES FOR AREA MUST BE
SELECTED SUCH THAT A = B.
POINT OF CONTACT OF TANGENT
TO CURVE DETERMINES LOWER BOUNDARY
FOR AREA

$$D = \frac{1}{2t} \frac{dx}{dc} \int x dC$$

t = DIFFUSION BONDING TIME
IN SECONDS

$\frac{dx}{dc}$ = RECIPROCAL OF SLOPE

RESULT: DIFFUSION COEFFICIENT, D FOR
TEMPERATURE, T

FIGURE 10 SCHEMATICS SHOWING METHOD OF COMPUTING D FOR
EXTENSIVE DIFFUSION, THIN-FILM METHOD, AND
FOR LIMITED DIFFUSION, MATANO METHOD

DIFFUSION COEFFICIENT - TITANIUM

$D - \text{cm}^2/\text{sec}$

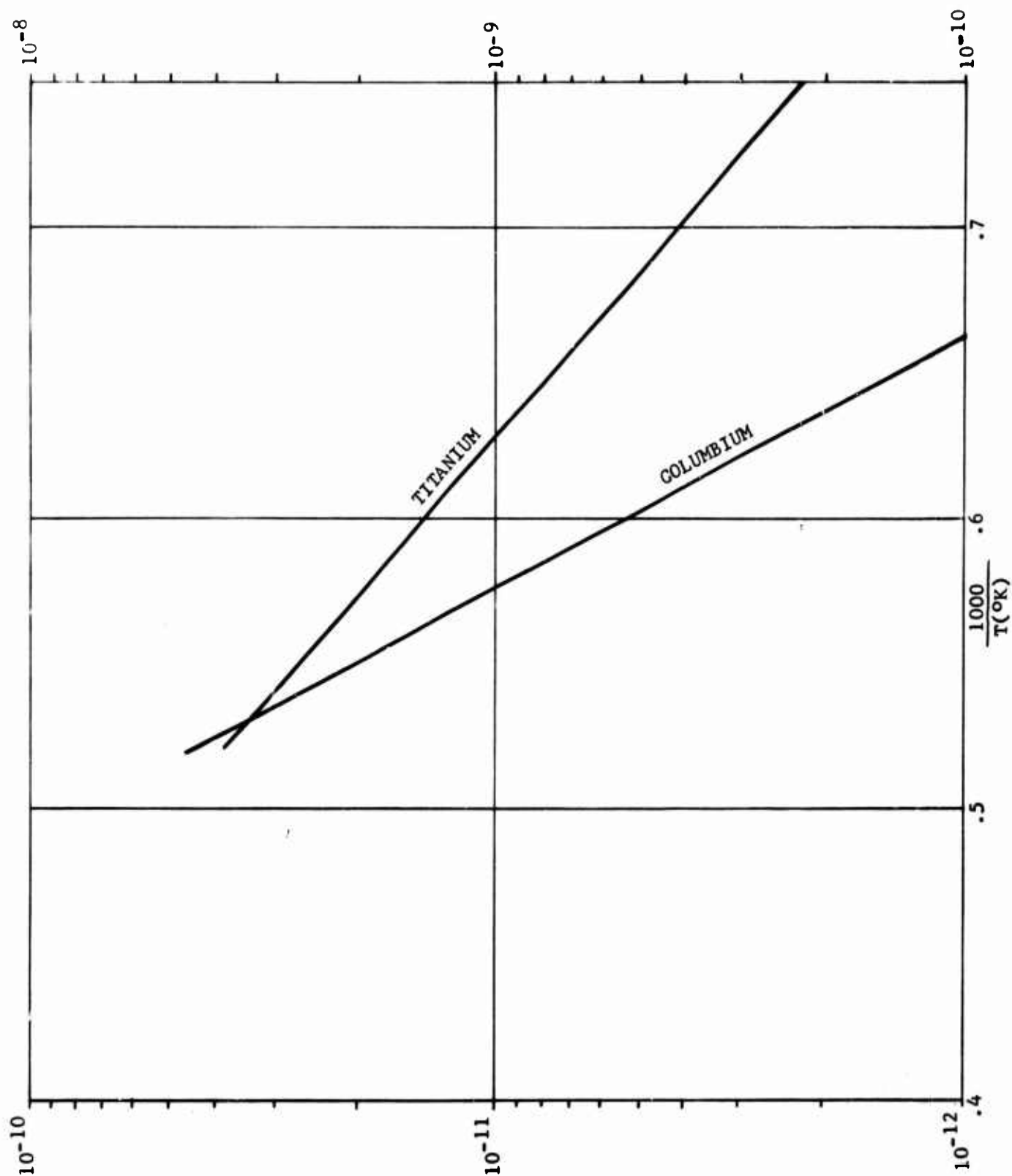


FIGURE 11 LOG D VS 1/T FOR DIFFUSION OF Ti AND Cb INTO Ta-10W

DIFFUSION COEFFICIENT - COLUMBIUM
 $D - \text{cm}^2/\text{sec}$

DIFFUSION COEFFICIENT - TITANIUM

$D - \text{cm}^2/\text{sec}$

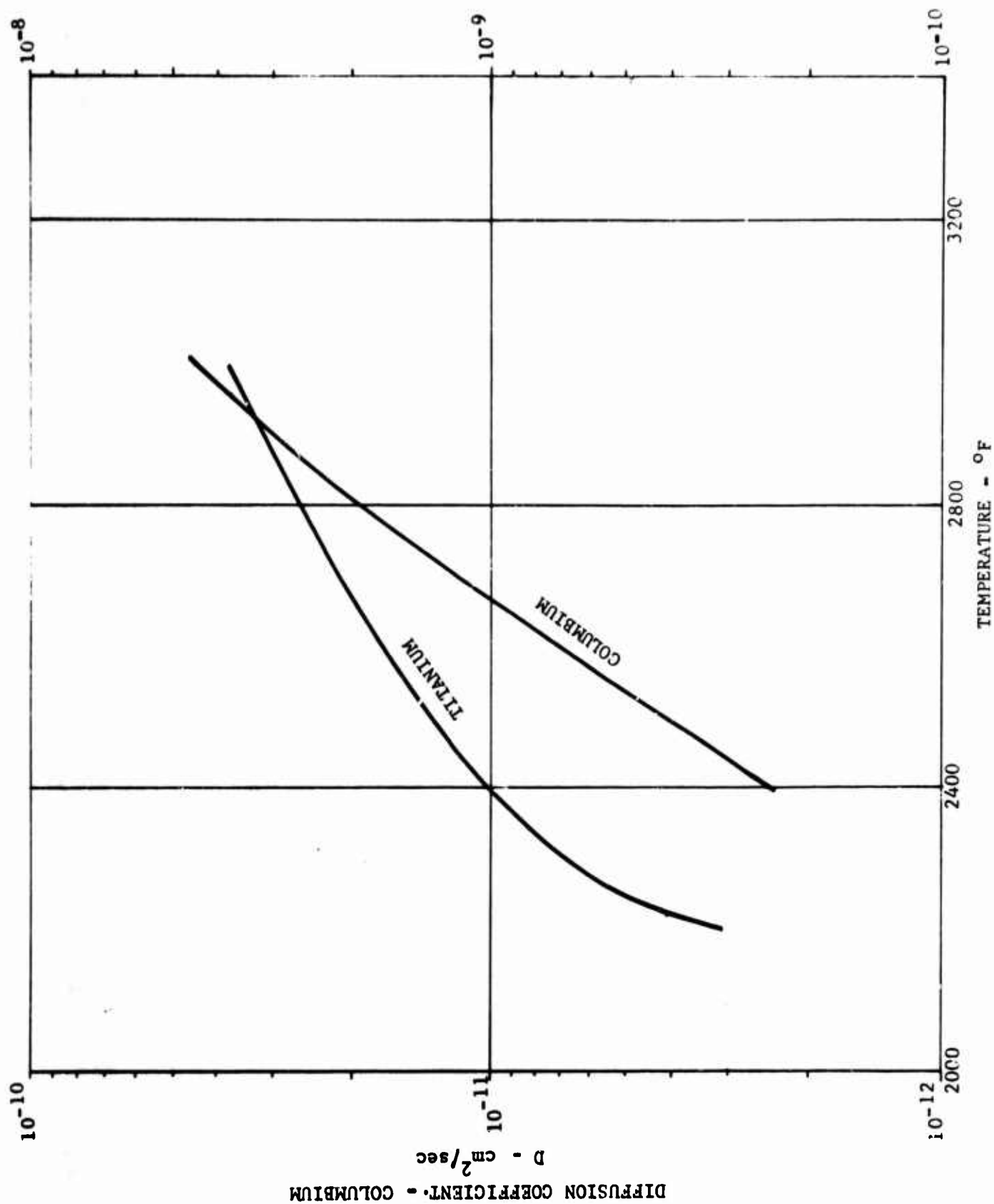


FIGURE 12 LOG D VS T(°F) FOR DIFFUSION OF Ti AND Cb INTO Ta-10W

With the desired range of log D established for Ti and Cb, it was possible to determine the effects of time and temperature on the concentration at the center of the joint for various thicknesses of the intermediate. This normally tedious, time-consuming task was readily accomplished through use of a computer program developed under this contract.

Computer Analysis of Time and Temperature Effects

The product of the computer program used was a set of concentration curves as a function of the logarithm of the diffusion time, log T, plotted against log D. Computation of the data points for the curves was based on the following equation:

$$C = \frac{d_I C_I}{2 \sqrt{\pi D t}} \exp \frac{(-x^2)}{4 D t} \quad (1)$$

where

C = final concentration at the center of the joint

d_I = initial intermediate thickness

C_I = initial concentration difference for the diffusing element
expressed in convenient units; e.g., percent

x = distance from the center of the joint

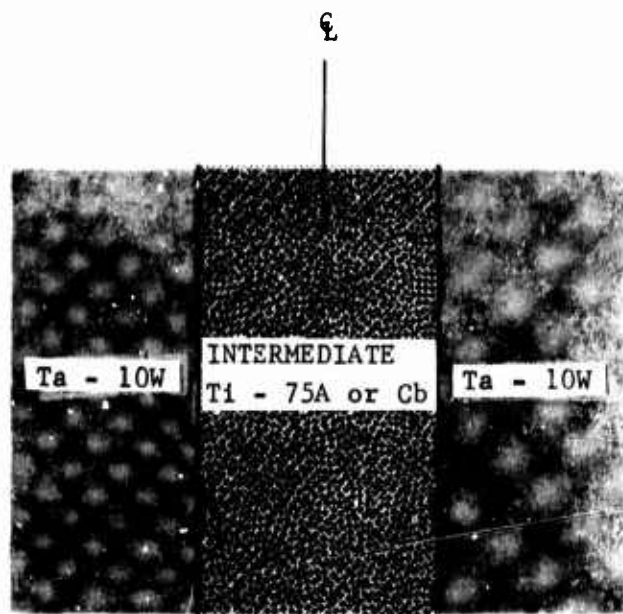
D = Diffusion coefficient

t = diffusion time; i.e., time at a given temperature

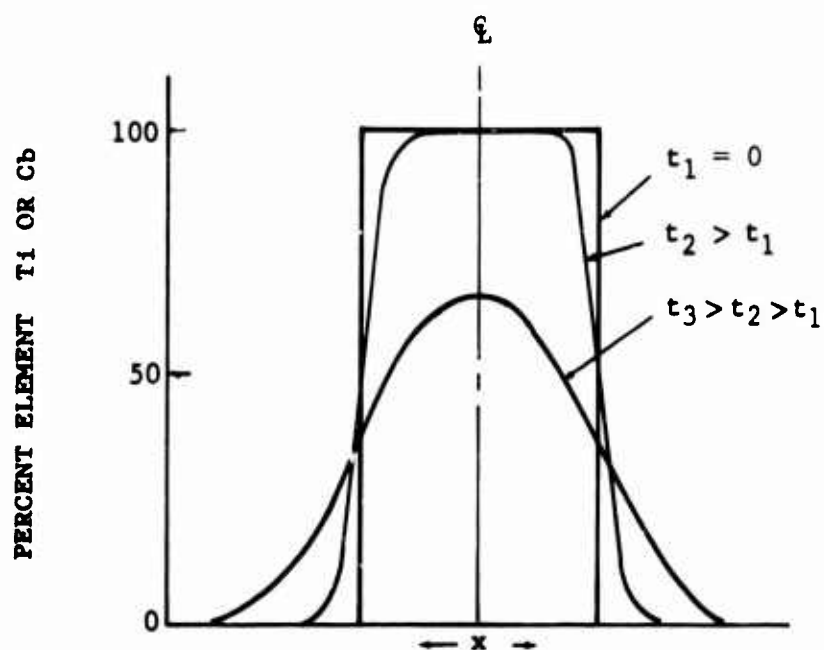
The equation may be greatly simplified by judicious selection of the boundary conditions involved with its application. Figure 13 is a sketch of the theoretical situation. During thermal exposure, diffusion occurs as a mutual reaction between the intermediate material and the base alloy for two reasons: (1) thermal excitation and (2) concentration gradients. Because of these driving forces, tantalum diffuses into the intermediate material and titanium or columbium, which are of primary interest here, diffuse into the base alloy. At a given temperature, the thermal energy remains essentially constant while the effect of the concentration gradient decreases as the diffusion process progresses. Since diffusion of Ti and Cb takes place in both directions, Figure 13, the concentration at the center of the joint becomes a rate-controlling factor for the diffusion process. Logically then, the highest concentration of intermediate elements is found at the center of the joint or center of the thickness of the intermediate material. This midpoint is chosen to be $X = 0$. Set X equal to zero in equation (1) and obtain:

$$C = \frac{d_I C_I}{2 \sqrt{\pi D t}} \exp = \frac{(0)^2}{4 D t} \quad (2)$$

$$C = \frac{d_I C_I}{2 \sqrt{\pi D t}}$$



MODEL OF DIFFUSION BONDED JOINT
BEFORE THERMAL EXPOSURE



CONCENTRATION GRADIENTS AFTER
VARIOUS THERMAL EXPOSURE, OR,
DIFFUSION BONDING TIMES

FIGURE 13 SKETCH OF EFFECT OF TIME AT TEMPERATURE
ON CONCENTRATION GRADIENT IN A DIFFUSION
BONDED JOINT

Solving equation (2) for time, t , obtains:

$$t = \frac{d_I^2 C_I^2}{4 \pi D C^2} \quad (3)$$

Examination of this equation shows that it is applicable to a pair of diffusing materials for any temperature, initial concentration difference, and initial intermediate thickness. It is easily utilized in a computer program by merely selecting the desired values for d_I , C_I , and C .

In this analysis, the initial intermediate thicknesses (d_I) of interest were .0005, .0010, .0015, and .0020 inch; the initial concentration difference (C_I) was 100 percent in all cases; the final concentrations (C) were selected in increments of ten from 10 to 100 percent; and a range of diffusion coefficients (D) was selected from Figure 12 such that it included values for both Ti-75A and Cb, thereby reducing the number of $\log t$ versus $\log D$ curves by a factor of two. A set of values for $\log t$ was obtained by varying D over the given range for each thickness and final concentration resulting in an accurate set of $\log t$ versus $\log D$ curves, an example of which is shown in Figure 14. Conversion of these curves to $\log t$ versus T is a simple matter when compared to the calculations performed by the computer. Temperatures corresponding to D for a given $\log t$ are found in Figure 12 and plotted against $\log t$. The final results are shown in Figures 15 through 22.

Implementation of these curves on an application basis may be shown by citing a few examples:

- Example 1: Given: Titanium intermediate, .0020 inch thick;
 diffusion bonding temperature is to be 2200F;
 and a final concentration at the center of the
 joint of 40 percent titanium is desired.
- Find: Required diffusion bonding time to satisfy
 the above conditions
- Solution: (See Figure 18) From 2200F on the temperature
 scale, go up to the curve for 40 percent final
 concentration, then over to the time scale and
 find that 680 minutes is the time required to
 produce the desired joint.
- Example 2: Given: Diffusion bonded joints were produced with
 an .0010 inch thick foil of titanium at
 2600F for 110 minutes.
- Find: Final center-of-joint concentration and the
 diffusion bonding times required to produce
 an equivalent joint at the following temper-
 atures: 2200F, 2400F, and 2800F.

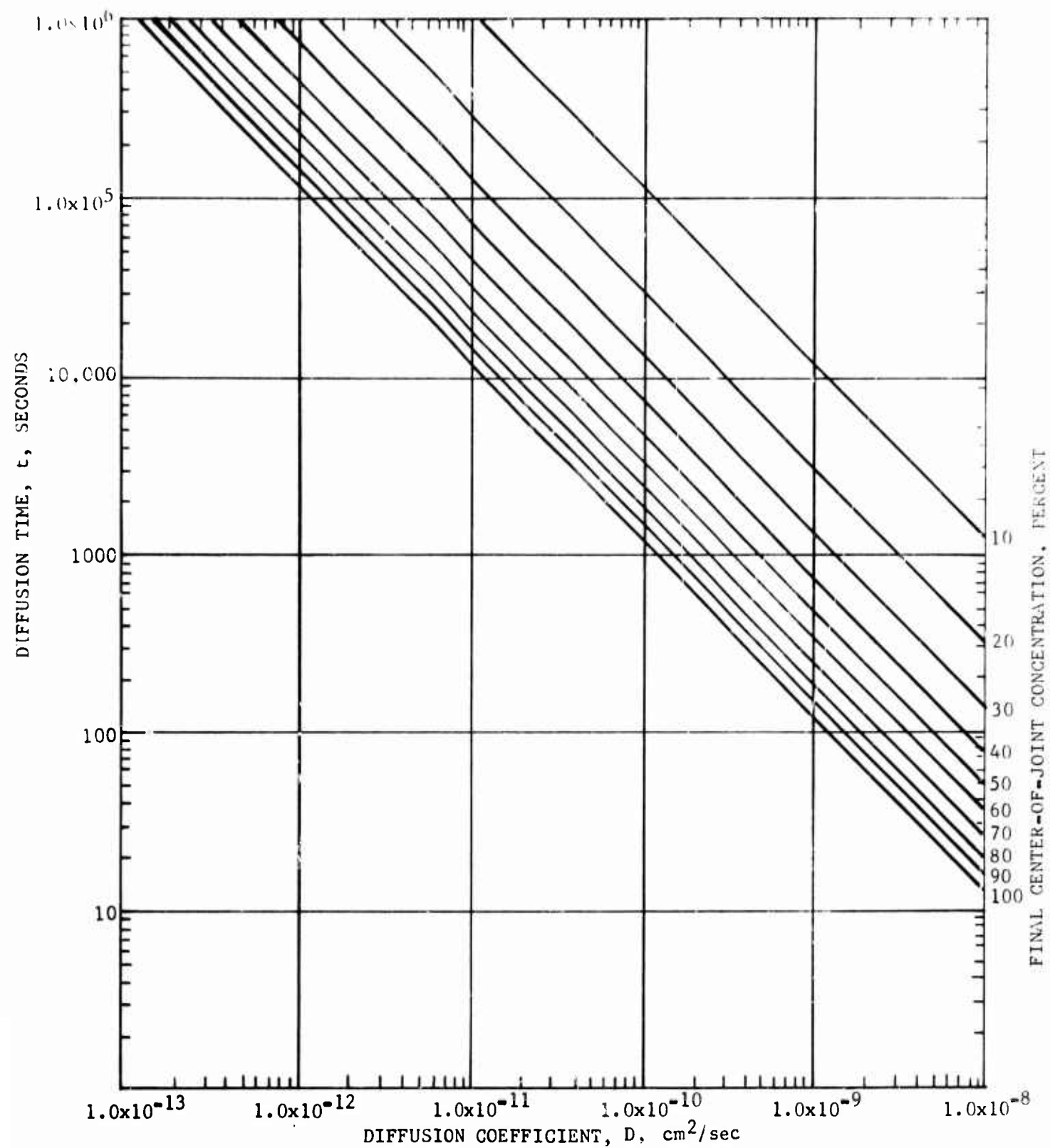


FIGURE 14 RELATIONSHIP BETWEEN TIME AND DIFFUSION COEFFICIENT FOR DIFFUSION BONDING Ta-10W WITH Ti OR Cb INTERMEDIATE, .0005 INCH THICKNESS

Ti-75A AND Ta-10W FOIL THICKNESS - .0005 INCH

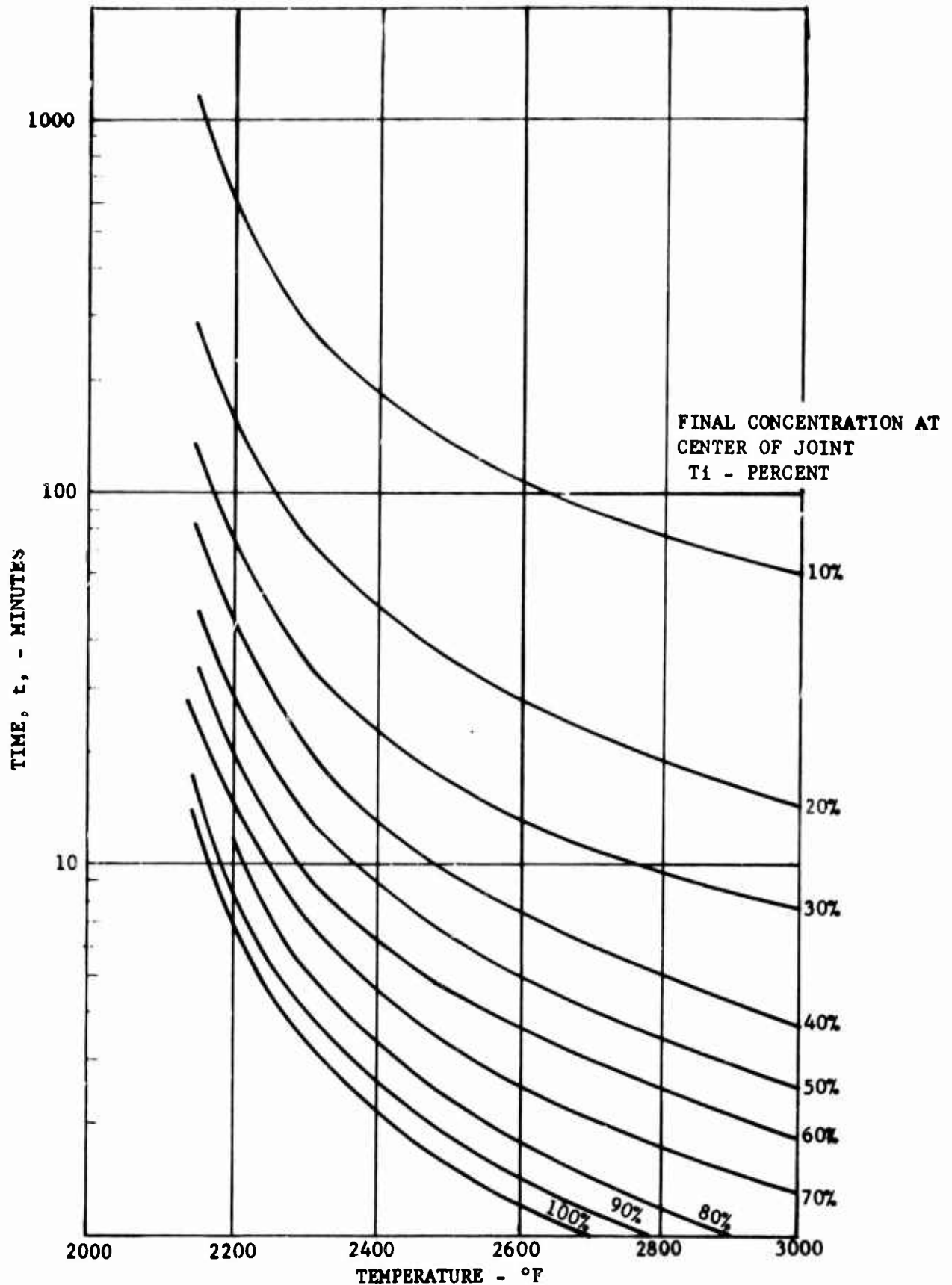


FIGURE 15 CONCENTRATION CURVES AS A FUNCTION OF TIME AND TEMPERATURE FOR .0005 INCH THICK Ti-75A INTERMEDIATE

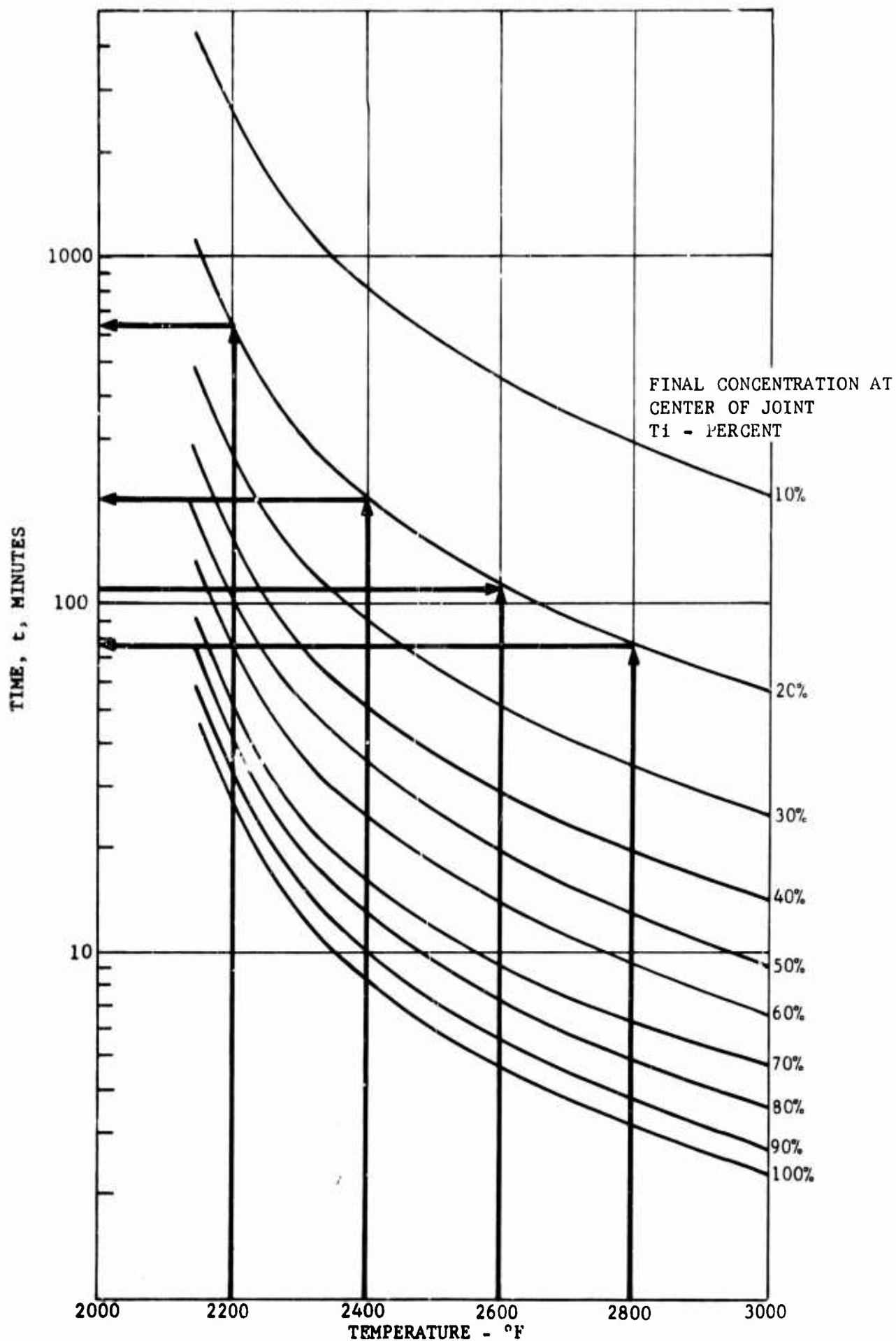


FIGURE 16 CONCENTRATION CURVES AS A FUNCTION OF TIME AND TEMPERATURE FOR .0010 INCH THICK Ti - 75A INTERMEDIATE

Ti-75A AND Ta-10W FOIL THICKNESS .0015 INCH

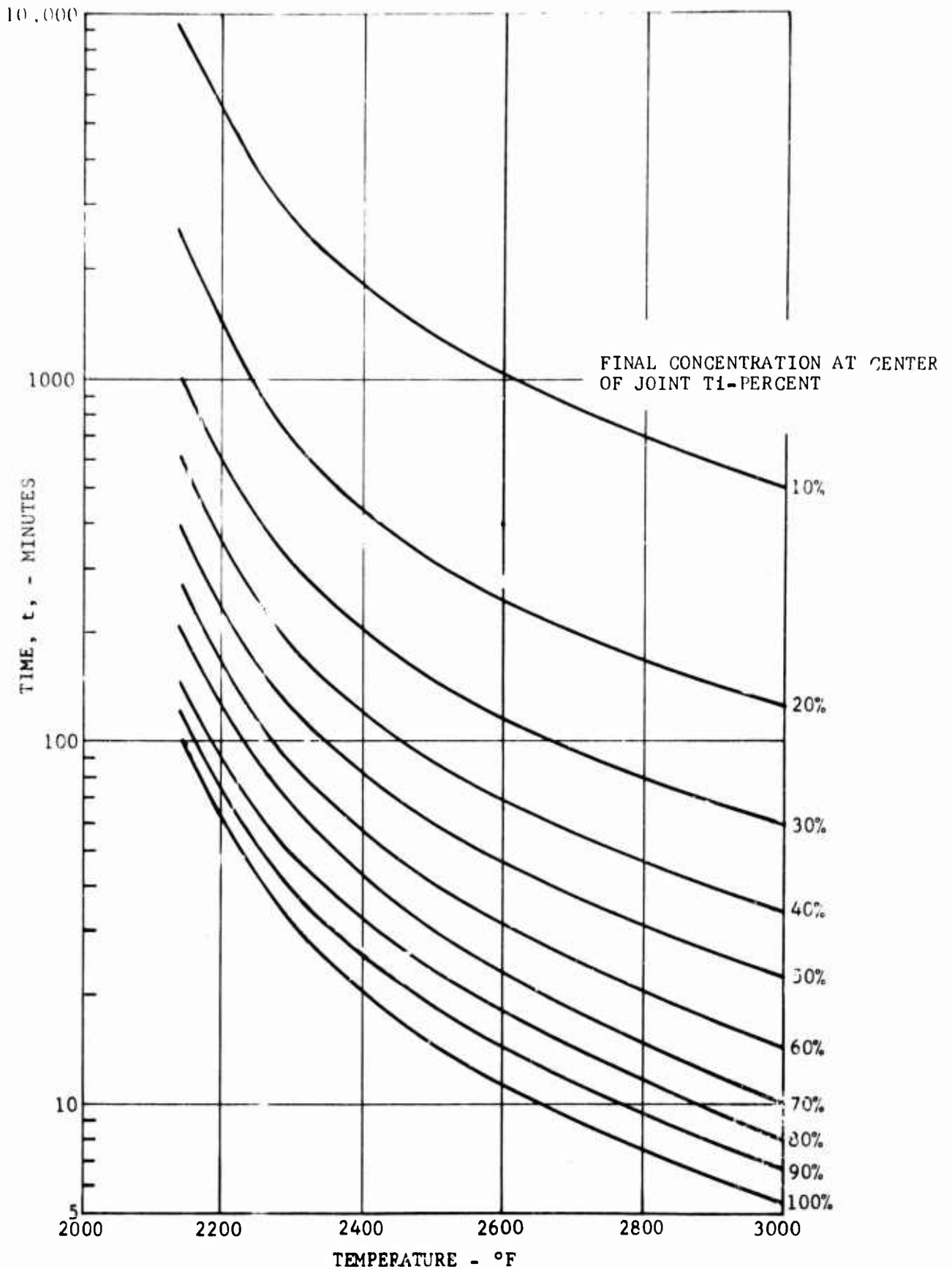


FIGURE 17 CONCENTRATION CURVES AS A FUNCTION OF TIME AND TEMPERATURE FOR .0015 INCH THICK Ti-75A INTERMEDIATE

Ti-75A AND Ta-10W FOIL THICKNESS = .0020 INCH

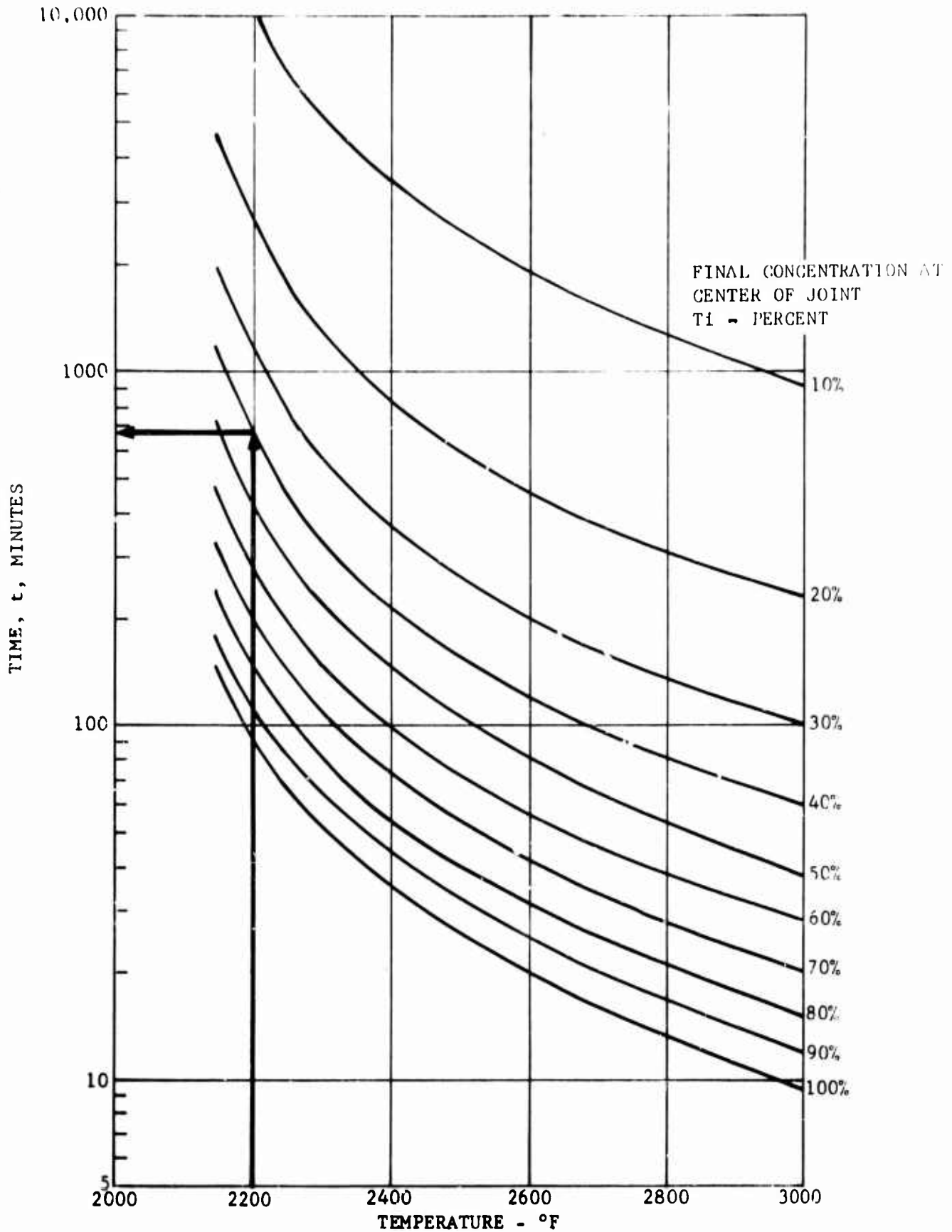


FIGURE 18 CONCENTRATION CURVES AS A FUNCTION OF TIME AND TEMPERATURE FOR .0020 INCH THICK Ti-75A INTERMEDIATE

CB AND Ta-10W FOIL THICKNESS - .0005 INCH

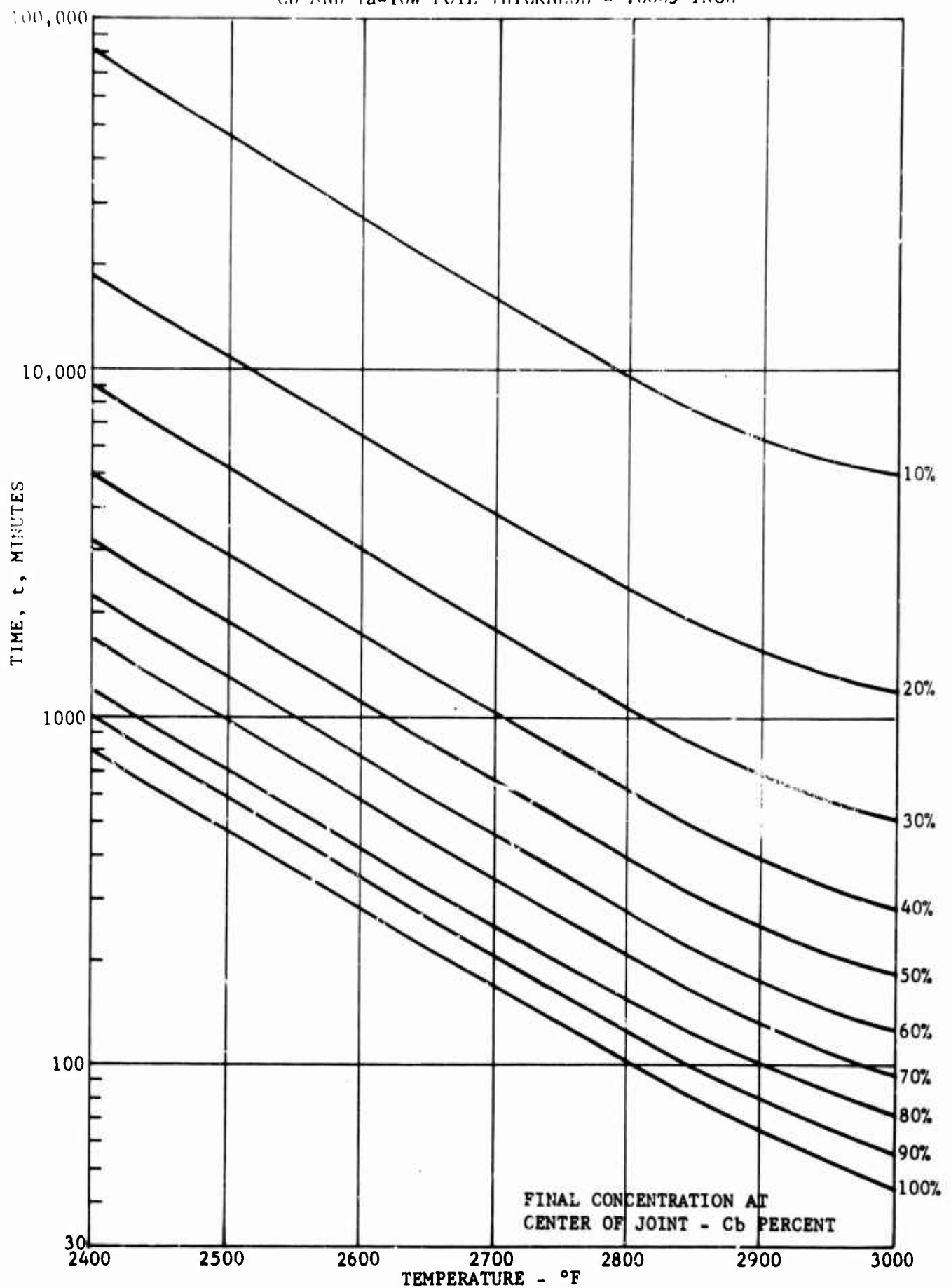


FIGURE 19 CONCENTRATION CURVES AS A FUNCTION OF TIME AND TEMPERATURE FOR .0005 INCH THICK Cb INTERMEDIATE

CB AND Ta-TiO₂ FOLLY THICKNESS = .0010 INCH

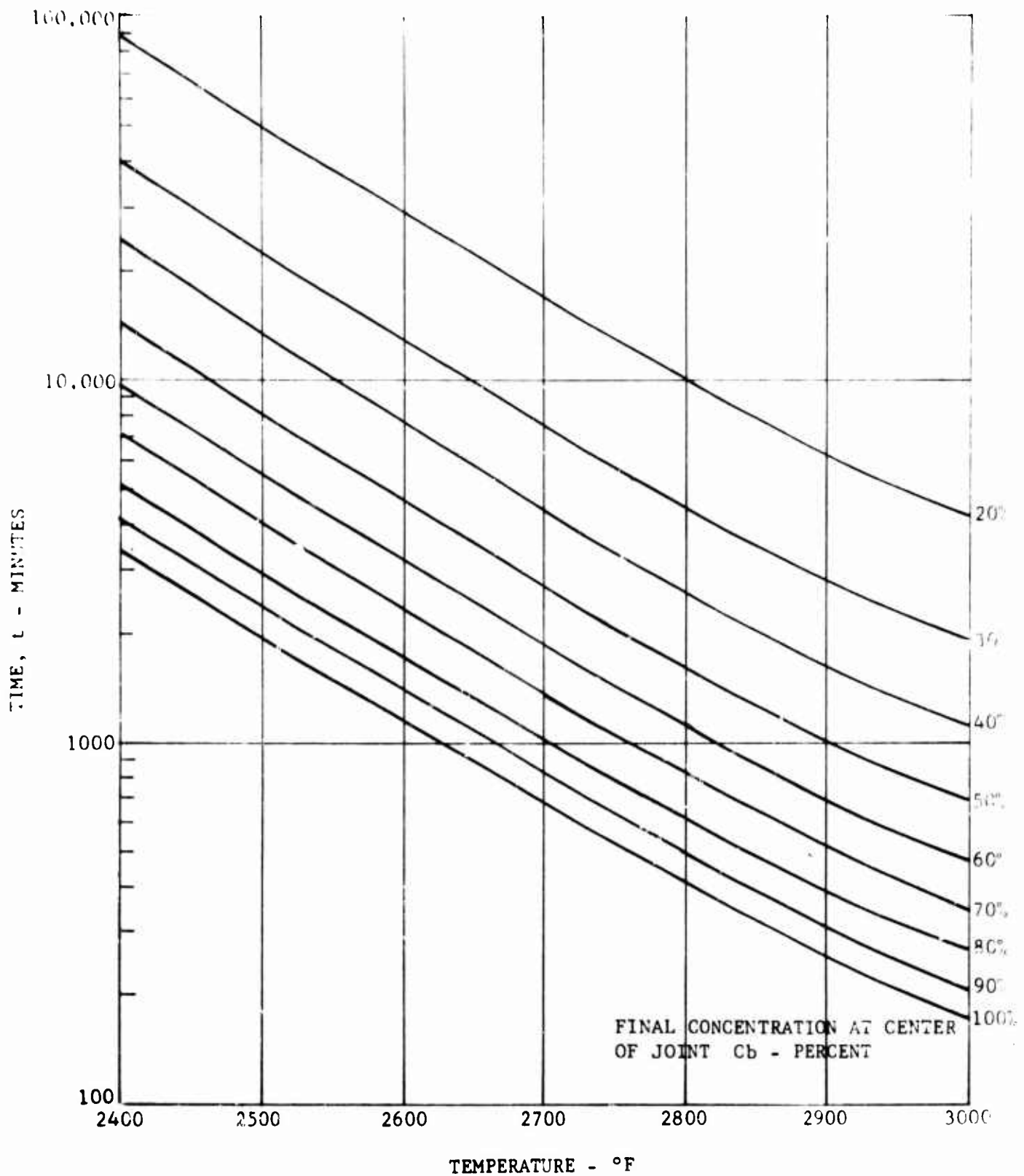


FIGURE 20 CONCENTRATION CURVES AS A FUNCTION OF TIME AND TEMPERATURE FOR .0010 INCH THICK Cb INTERMEDIATE

Cb AND Ta-10W FOIL THICKNESS - .0015 INCH

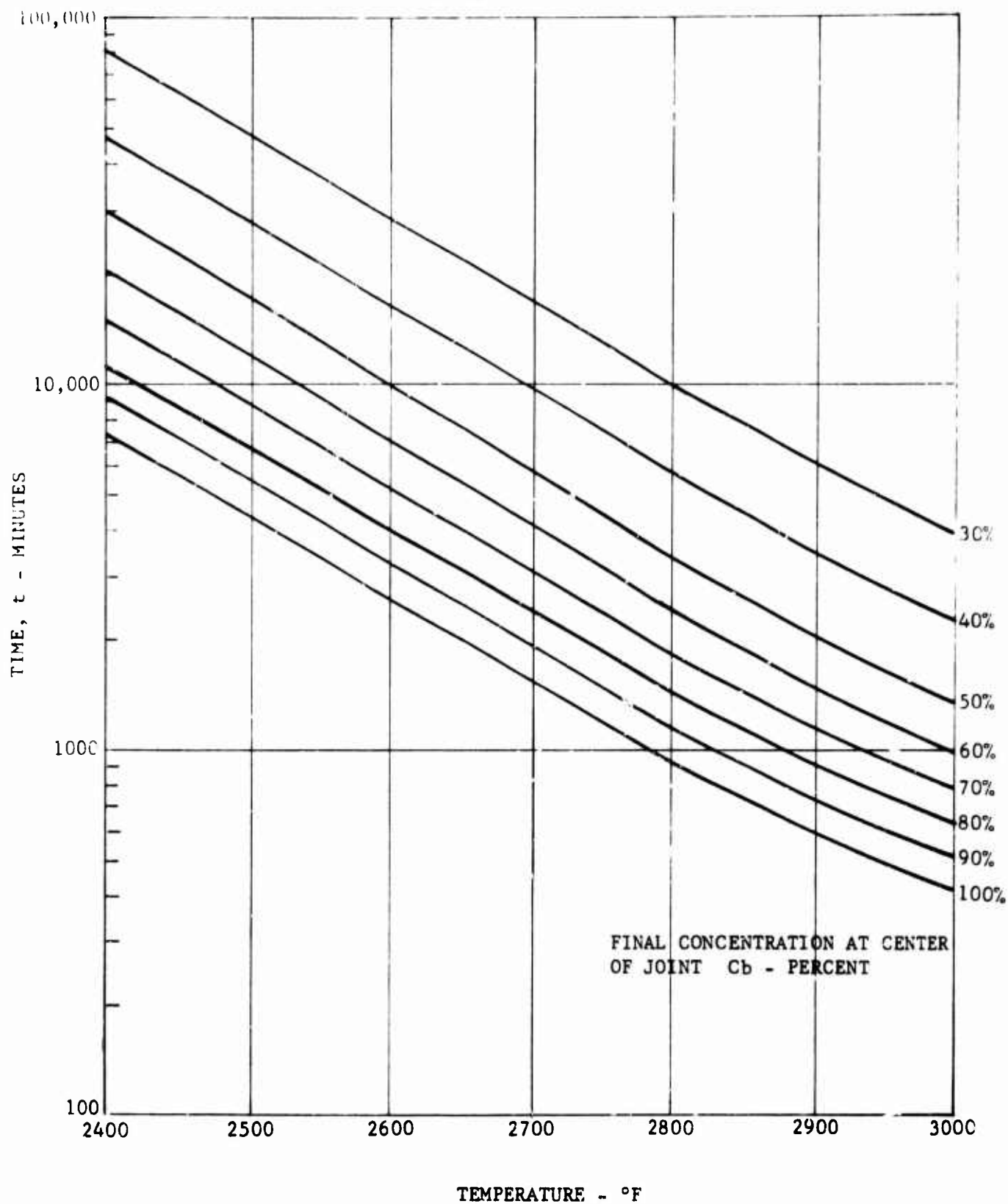


FIGURE 21 CONCENTRATION CURVES AS A FUNCTION OF TIME
AND TEMPERATURE FOR .0015 INCH THICK Cb
INTERMEDIATE

Cb AND Ta - 10W FOIL THICKNESS - .0020 INCH

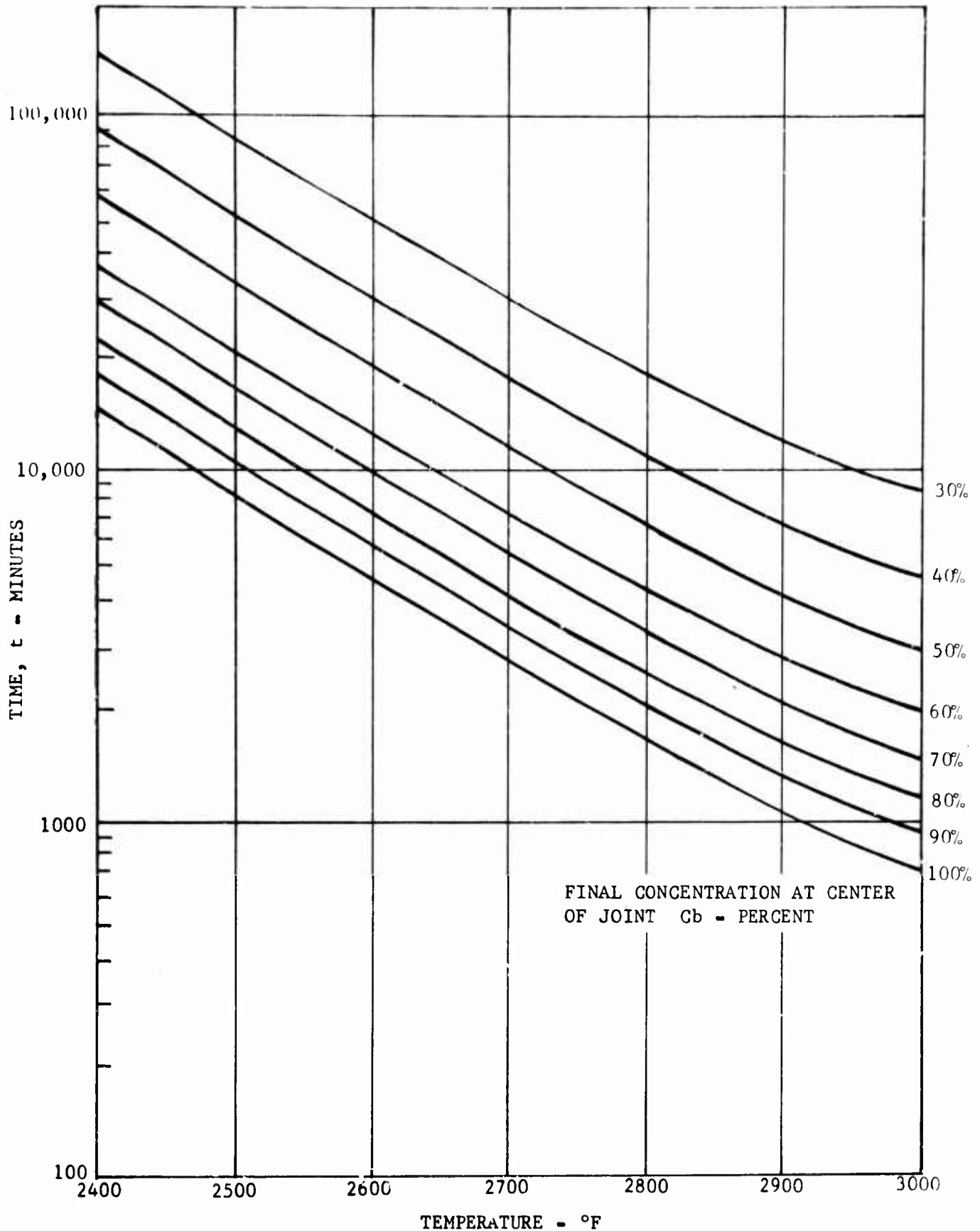


FIGURE 22 CONCENTRATION CURVES AS A FUNCTION OF TIME AND TEMPERATURE FOR .0020 INCH THICK Cb INTERMEDIATE

Solution: (See Figure 16) Find 2600F and 110 minutes on the set of curves for .0010 inch thick titanium intermediate. The final concentration is found to be 20 percent. The times to form equivalent joints; i.e., 20 percent final concentration for .0010 inch thick titanium intermediate, are found as in Example 1 and are as follows:
2200F-640 minutes
2400F-200 minutes
2800F-76 minutes

Example 3: Given: Diffusion bonded joints were produced with a final concentration of 20 percent at the joint center when using diffusion bonding parameters of 110 minutes at 2600F and 200 minutes at 2400F with a .0010 inch thick titanium intermediate.

Find: The diffusion bonding times for 2400F and 2600F using a .0005 inch thick titanium intermediate to obtain a 20 percent concentration of titanium at the joint center.

Solution: (See Figure 15) Using the set of curves for a .0005 inch thick titanium intermediate, find the intersection of 2400F and 2600F with the 20 percent curve and read on the log t scale times of 49 minutes for 2400F and 28 minutes for 2600F.

For the above typical applications, the time-temperature-concentration relationships established in this study are of great value, since a final center-of-joint concentration may be achieved within ± 10 percent by merely selecting from the curves the appropriate diffusion bonding parameters for a given intermediate thickness. Further, it has been demonstrated that a strong correlation exists between the lap shear strength and final center-of-joint concentration for diffusion bonded joints, since the high temperature properties are dependent upon the maximum concentration of intermediate element. (These curves could also be used to determine the metallurgical condition of flight hardware after flights causing temperatures of 2200F and above. This could be done if the temperature were monitored during flight since the diffusion which occurs is additive).

BONDING PARAMETER SELECTION

The bonding parameters (temperature, time) employed in effecting satisfactory fabrication of tantalum honeycomb panels was dependent on two factors:

1. The center-of-joint concentration desired, which in turn is a measure of joint strength, and operational temperature properties.
2. The elevated temperature limitations of the tooling materials and equipment employed in fabricating the tantalum honeycomb panels.

The tooling materials and equipment used in this program to fabricate the tantalum honeycomb panels decidedly affected the choice of bonding parameters. The Inconel 600 envelopes which would contain each panel have a reported melting temperature range of 2500-2600F. Since chromel-alumel thermocouples were utilized for temperature measurements, temperatures in the bonding range were critical insofar as oxidation and diffusion effects on accurate temperature measurements and the subsequent possibilities of opening or severing of the thermocouple wires. Chromel-alumel type thermocouples are reportedly accurate to a maximum of 2400F, above which temperature recordings become erratic and inconsistent. The effects of the relatively long times required for bonding tantalum at the bond temperatures under consideration on the quartz lamp heating fixture components was also a factor to be reckoned with in selection bonding parameters. As a result of these factors, it was decided that bonding temperatures would be limited to a maximum 2400F. From the diffusion study conducted and discussed in the previous section, it was determined that due to the logarithmic variation of bonding time with temperature, bonding temperatures of 2200F and below would result in excessively long bonding times. Consequently, from a manufacturing standpoint, bonding of the tantalum panel had to be limited to a temperature range of 2200F to 2400F. Employing a columbium intermediate in this temperature range would have resulted in completely unrealistic bonding times.

The selection of a specific bonding temperature to be employed was made by an examination of Figure 12 which relates temperature to diffusion coefficient. It was determined that the greatest percentage increase in diffusion coefficient occurred at 2250F. Therefore, 2250F was selected as the optimum temperature for bonding.

Originally, an intermediate thickness of .0005 inch was chosen for use in diffusion bonding the tantalum panels in this program. However, during the manufacture of the structural panels, this thickness of intermediate was found to be inadequate for producing a sufficiently strong bond. It was determined empirically that an intermediate thickness of .0015 was required to develop satisfactory bonding. This aspect of intermediate thickness selection is discussed in detail in a later section of the report entitled, "Phase I Test Panel Fabrication". With the use of a .0015 inch thick intermediate and a bonding temperature of 2250F, a bonding time of 3.5 hours was selected to effect a center-of-joint composition of approximately 60Ta-40Ti, as predicted in Figure 17. While this joint chemistry was a compromise from that originally proposed (80Ta-20Ti), it did produce a strong bond with a remelt temperature of approximately 3650F, which is 850F above the design limiting temperature of 2800F for the structural panels.

A .0005 inch thick intermediate was employed in fabricating the heat shield panels since a higher remelt temperature was of prime concern, as this type panel was designed for service temperatures to 3500F. In addition, a bond strength lower than that required in the structural panels could be tolerated, since the heat shield panels were not designed to sustain the loads required of the structural panels. The thinner intermediate would also reduce the tendency toward deterioration of the heat shield panels by titanium embrittlement at the higher service temperature.

The optimum bonding parameters selected for the manufacture of tantalum honeycomb panels were as follows:

Temperature:	2250F
Time:	3.5 hours
Intermediate Thickness:	.0015 inch Ti-55 (structural panels) .0005 inch Ti-75 (heat shield panels)
Pressure:	1000 psi

V PANEL DESIGN

STRUCTURAL PANELS

Two types of honeycomb panels were designed for fabrication during the course of this program, structural and heat shield. Basically, the philosophy involved in designing solid-state diffusion-bonded tantalum structural panels is to separate the two thin load-carrying facings by a low density core to obtain high strength and stiffness-to-weight ratios. The facings are designed to provide resistance to edgewise loads and bending moments, and the core and core-facing bond is designed to resist shearing loads. This arrangement allows the integrated elements to resist a combination of loading modes as a composite assembly with a high degree of structural efficiency.

The design of the tantalum structural panels, both flat (Figure 23) and curved (Figure 24), incorporated fastener-type edge enclosures to duplicate the actual fixity of an aerospace vehicle hot structure. For this program the core design was developed around a nonperforated .0022 inch foil and a square cell size of .250 inch. Facing thickness for these panels was .012 inch with an overall panel size of .524 x 12 x 12 inches. The tantalum alloy utilized in the fabrication of the structural panels was Ta-8W-2Hf (T111)

HEAT SHIELD PANELS

The second type of panel manufactured during the course of this program was a heat shield panel designed for service to 3500F. The configurations of these panels, both flat and curved, are shown in Figures 25 and 26, respectively. The heat shield panels do not incorporate channeled edgemembers as do the structural panels, but possess a stepped edge to allow for the fitting together of several such panels.

Core design was developed around a .0022 inch foil and a square cell size of .250 inch. The heat shield panels employed core 3/8-inch thick and .008 inch T111 face skins. All of the design variations of the heat shield panels from those of the structural panels result from the proposed service use of the heat shield panels. These panels are intended to be employed in those locations of a hypersonic cruise or re-entry vehicle which will encounter high heat fluxes, and to be supported so that no stresses other than aerodynamic surface loading are imposed. The heat shield panels utilized Ta-8W-2Hf (T111) and Ta-9.5W-2.5Hf (T222). The use of the T222 alloy was limited to the core on some panels. T111 was employed for all facing sheets, and the core for the majority of the panels. Allowance was made for incorporating into the manufacture of the heat shield panels mounting brackets as shown in Figure 27.

The structural and heat-shield panel designs were consistent with the manufacturing and testing requirements of the program and were such that the data derived could be correlated with similar projects and test data evolved from prior contracts.

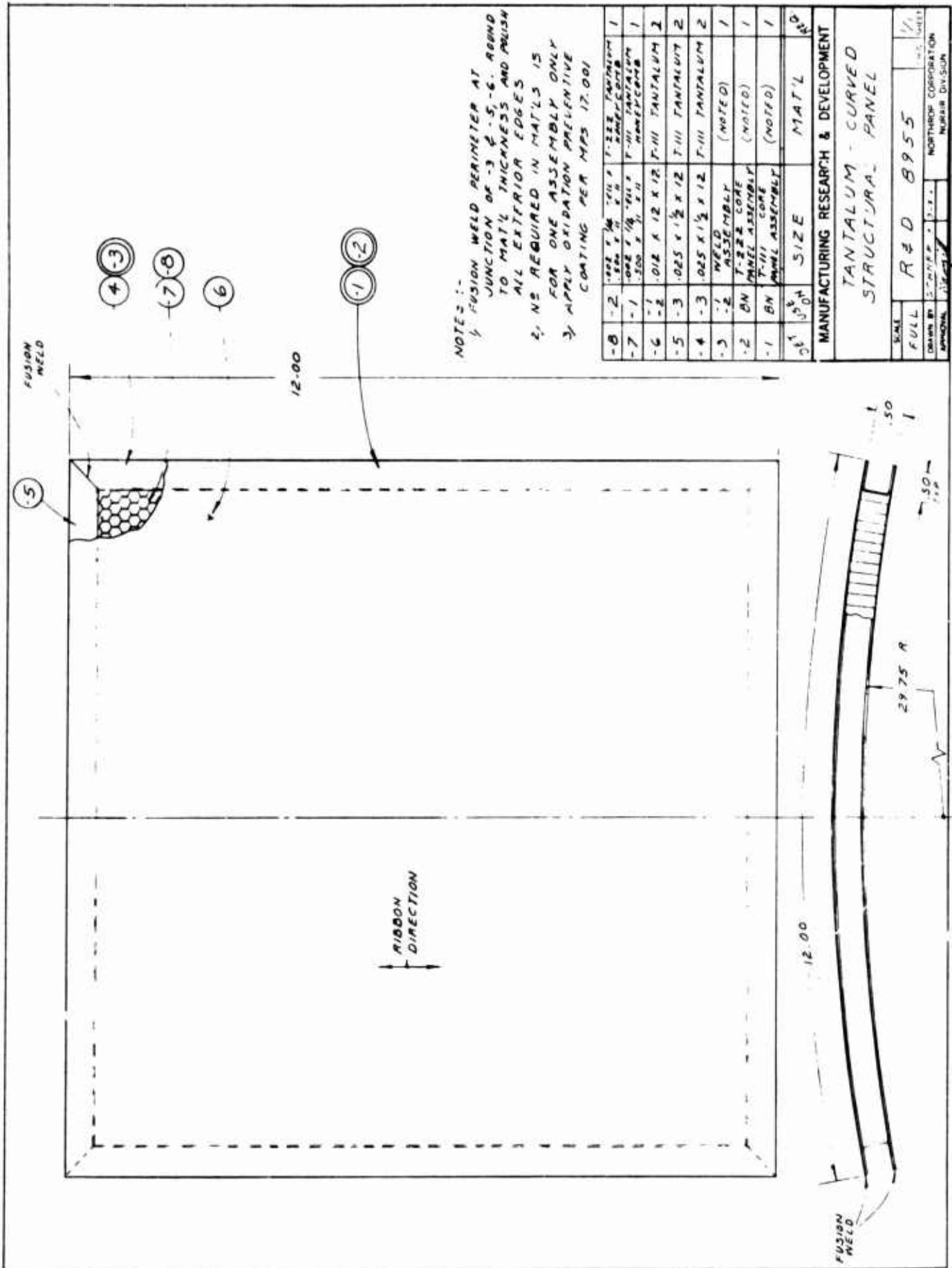


FIGURE 24 TANTALUM - CURVED STRUCTURAL PANEL DESIGN

VI MANUFACTURING PROCESSING TECHNOLOGY

TOOLING AND PARTS FABRICATION

Edgemembers

The channeled edgemembers for the flat structural panels were formed from .025 inch T111 sheet on a Verson-Wheelon Hydropress. The straight channel edgemembers were then contoured on a Hufford Stretch Press for use in fabricating the curved structural panels. Flat and curved edgemember tooling and formed parts are shown in Figure 28. Some difficulties did arise initially in forming the edgemember components. The straight edgemembers exhibited heavy "orange peel" on the formed radii and excessive springback of the sides. The curved edgemembers displayed undercutting of the channel and an excessive radius of curvature. The "orange peel" was indicative of a large material grainsize. An increase in bend radius was adopted to reduce any cracking tendencies due to this "orange peel" during subsequent forming. The springback tendencies of both the straight and curved edgemembers were compensated for by reworking the hydroform and stretch-form blocks to allow for an additional amount of springback over that originally contemplated. The undercutting of the channel was remedied by reducing stretch forming pressures.

Heat Shield Skins

The outer flat heat shield skins were formed on a Watson-Stillman Double-Action Draw Press. The forming consisted of drawing the edges of the sheet 90 degrees to produce a flange which overlaps the flange of the inner skins to obtain the stepped edge design and a weld melt-down flange for hermetically sealing the panels. The curved outer heat shield skins were fabricated by roll forming to the required radius of curvature a previously formed flat skin. The dies for forming the flat outer skins are shown in Figure 29, and the roll-form die with formed flat and curved outer heat-shield skins are shown in Figure 30. The panel access holes with .020 inch weld melt-down flange were produced by first drilling a small pilot hole in the sheet and then using a small punch-form tool to obtain the required 1/4 inch hole and .020 inch weld flange in one operation.

No problems were encountered in forming either the flat or curved outer heat shield skins.

The flat inner skins were formed on a Watson-Stillman Press and Lake Erie and Verson-Wheelon Hydropresses. The stepped edge and skin dimples were first formed on the Watson-Stillman Press with the dies shown in Figure 31. The weld melt-down flange was then formed using the wiper, filler rings, and dies shown in the left of Figure 32 on the Lake Erie and Verson-Wheelon Hydropresses. Three "hits" were required to form the weld flange. The first hit was with the filler ring and die on the Lake Erie Press to initiate the bending of the flange. The second and third hits were made on the Verson-Wheelon Press, first without a filler or wiper ring in place on the die, and

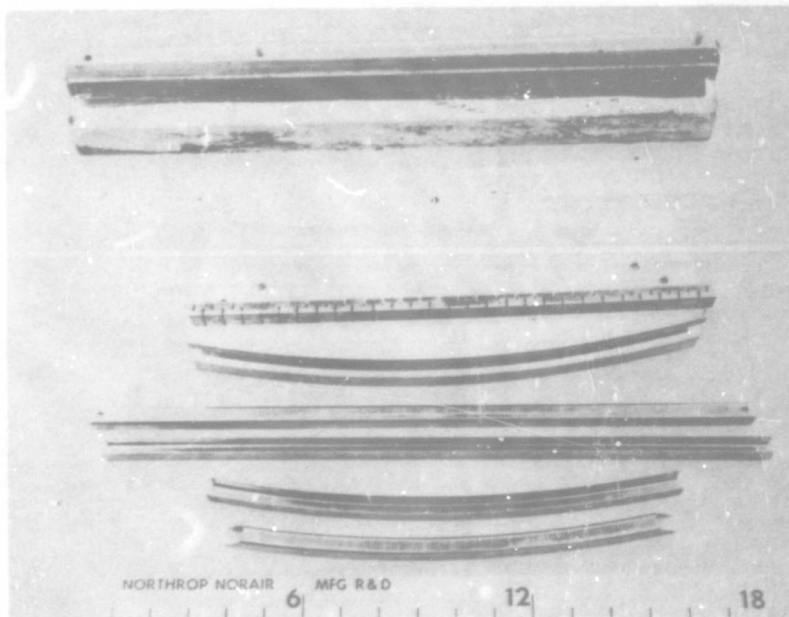


FIGURE 28 FLAT AND CURVED STRUCTURAL EDGEMEMBER TOOLING AND PARTS FORMED FROM .025" T111 SHEET ON A VERSION WHEELON HYDROPRESS AND HUFFORD STRETCH PRESS

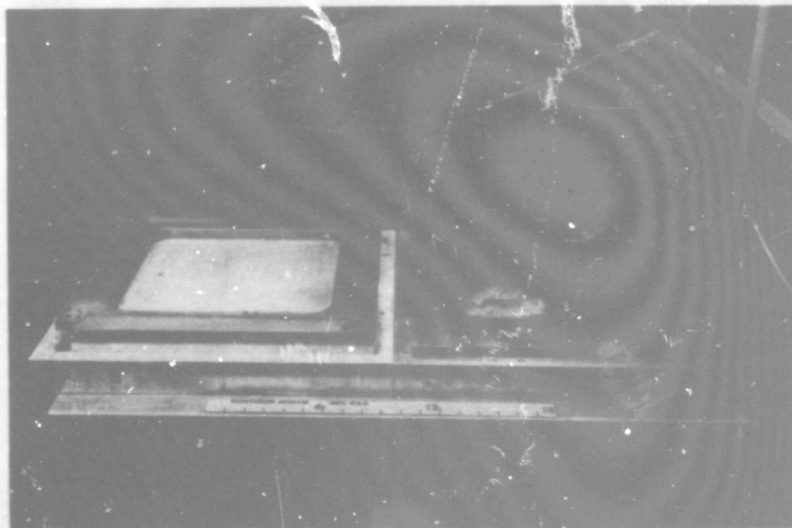


FIGURE 29 FORM DIES FOR OUTER SKIN FLAT HEAT SHIELD

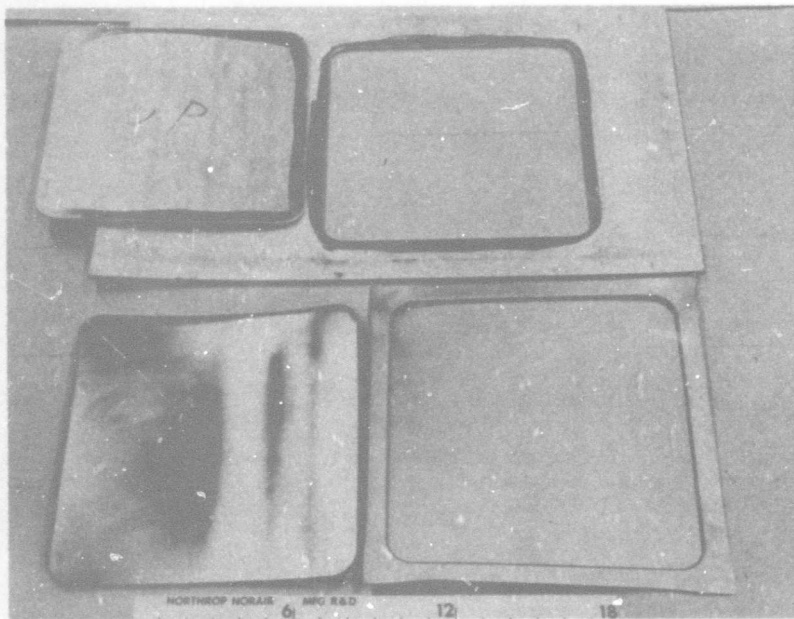


FIGURE 30 ROLL FORM DIE WITH FORMED FLAT AND CURVED .008 INCH T111 OUTER HEAT SHIELD PANEL SKINS

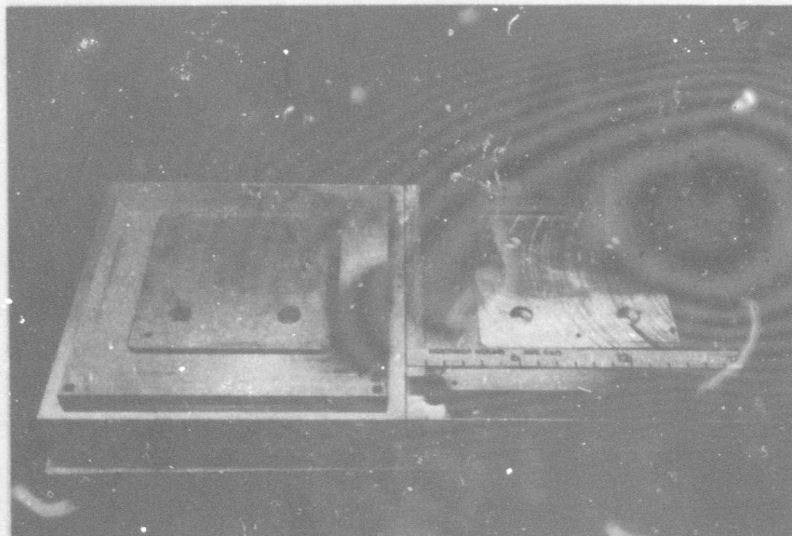


FIGURE 31 FORM DIE FOR INNER SKIN FLAT HEAT SHIELD

then with the wiper ring in place. This technique was used to minimize cracking and to obtain a complete 90 degree flange.

The forming of the curved inner skins was initiated similar to the flat skins on the Watson-Stillman Press except that the dimples were not formed in this operation due to the misalignment which would occur during subsequent contouring of the skins. Forming of the required radius of curvature of the inner skins was initially attempted with a curved die on a Verson-Wheelon Hydropress. This technique, however, proved inadequate as the hydropress forming action placed the inner skin surface in compression while the previously formed stepped edge surface was in tension since these two surfaces lay on opposite sides of the bending centroid. This resulted in excessive compression wrinkling of the inner skin adjacent to the stepped edge. The problem was remedied by fabricating the special bending fixture shown in Figure 33. This fixture was arranged so that all surfaces of the skin are contained and that tension can be applied during bending. The tool is so proportioned that the centroid of the combination of tool and skin clamped therein is located beyond the tantalum skin, closer to the required radius center. Brake forming of this combination results in tensile forces being applied to all surfaces of the skin during bending, much the same as in a stretch press operation in conventional section forming. This technique proved successful in contouring the inner heat shield skins with Figure 34 showing skins before and after contouring. The curved skin is then placed on the curved die shown in the right of Figure 32, and "hit" on Lake Erie and Verson Wheelon Hydropresses to form the weld melt-down flange and skin dimples using the filler and wiper rings and hard rubber inserts shown. This final operation is identical in procedure to that used on the flat inner skins for forming the weld-flange. Two additional problems were encountered, in forming the inner skins. The first consisted of cracking in the corner radii. This difficulty was remedied by using an increased bend radius and by eliminating as much of the trim as possible prior to forming. The second problem was the formation of compression wrinkles on the stepped-edge surface at the corners. While rework of the wrinkled surface did reduce the amount of wrinkling evident after forming, it was not possible to eliminate it entirely.

Panel Attach Clips

The panel attach clips of the heat-shield mounting-bracket assembly were fabricated from .040 inch T111 sheet on a Verson-Wheelon Hydropress. Final forming of the side flanges had to be performed by hand due to the shortness of the flange. The formed clips and form block are shown in Figure 35.

Final parts fabrication consisted of machining and drilling the heat-shield mounting bracket washers and clips to finished configurations. The mounting bracket washers are .040 inch thick, 1-1/4 inch in diameter with a 15 degree machined bevel around the circumference. These washers, with skins, clips, and core are shown in Figure 36. The skins, clips, and washers contained a 1/4 inch hole to accommodate a 1/4 inch tube which ran from the end of the clip through the panel to the outer surface of the heat shield skin. The purpose of the tubing was to effect added rigidity when the panel was mounted for testing.

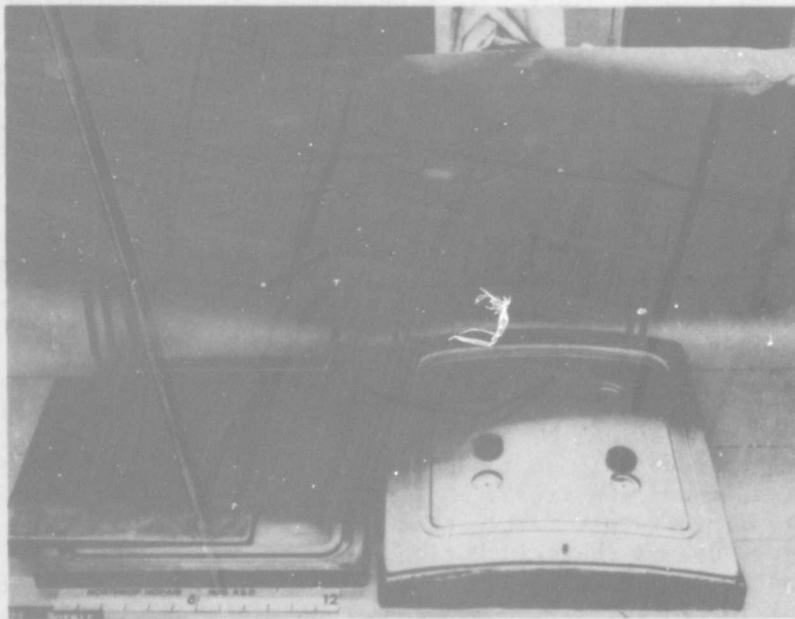


FIGURE 32 DIES, FILLER AND WIPER RINGS USED IN FORMING WELD MELT DOWN FLANGE ON FLAT (LEFT) AND CURVED (RIGHT) HEAT SHIELD PANEL INNER SKINS

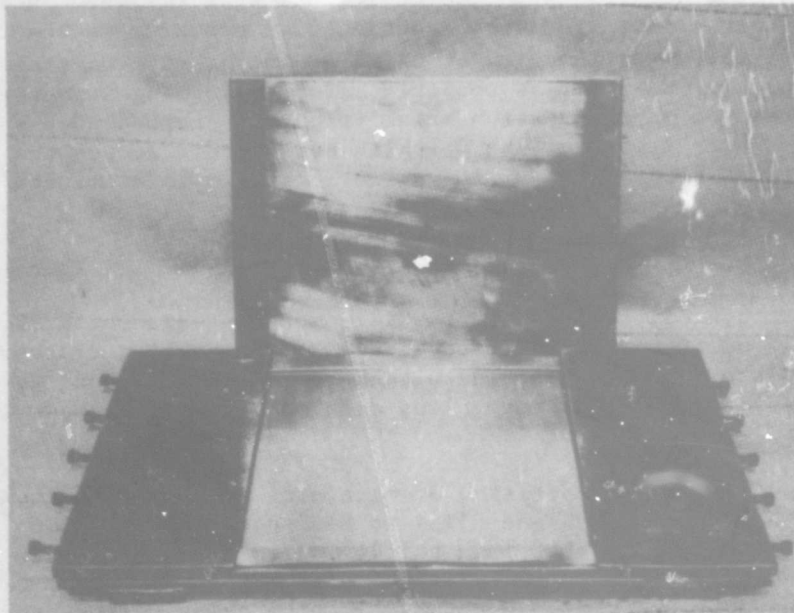


FIGURE 33 BEND-STRETCH FIXTURE SPECIALLY DESIGNED FOR CONTOURING THE CURVED HEATSHIELD INNER SKINS HELD IN TOOLING READY FOR FORMING ON PRESS BRAKE

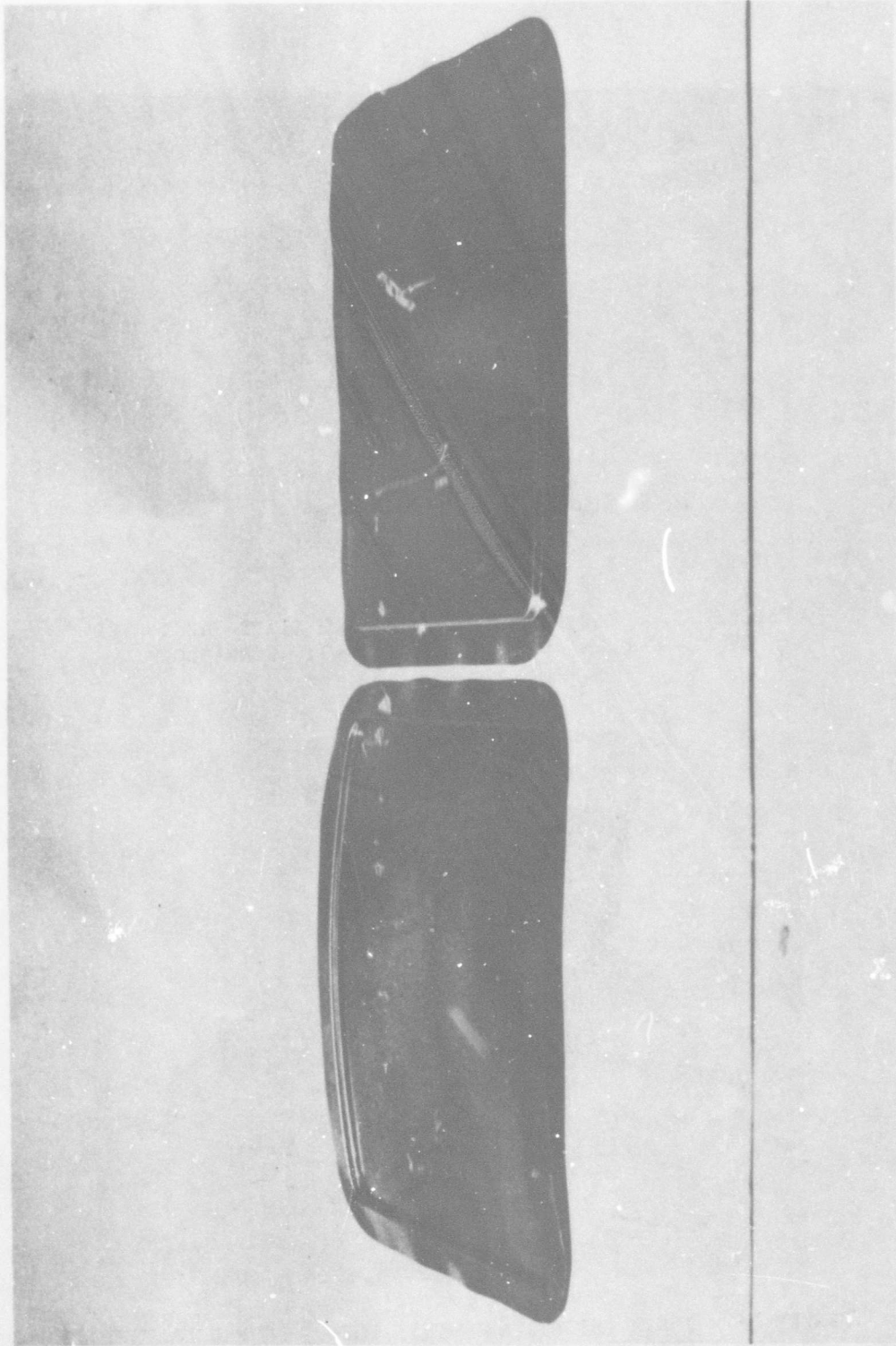


FIGURE 34 STARTING SKIN (RIGHT) AND RESULTANT
CONTOURED SKIN (LEFT) AFTER FORMING
ON PRESS BRAKE

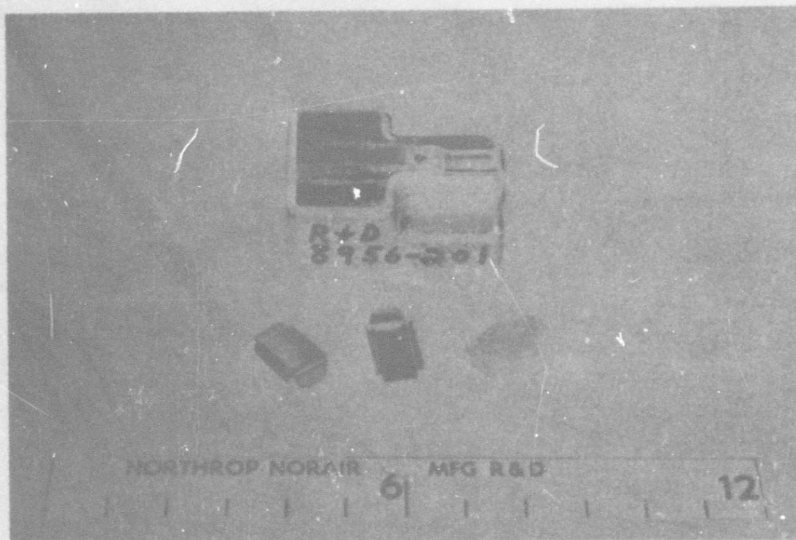


FIGURE 35 HEAT SHIELD PANEL ATTACH CLIPS FABRICATED FROM .040" T111 SHEET WITH FORM BLOCK

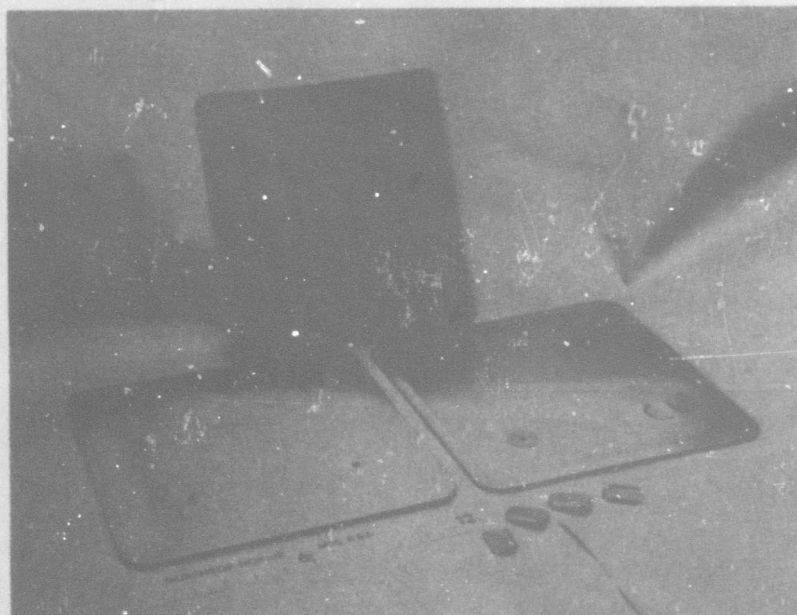


FIGURE 36 INNER (RIGHT) AND OUTER (LEFT) FORMED HEATSHIELD SKINS WITH CORE, WASHERS, AND PANEL ATTACH CLIPS

Envelopes

Envelope halves for sealing the assembled panels for bonding, were formed from .025 inch Inconel 600 on a Verson-Wheelon Hydropress. The form blocks and envelope halves, both flat and curved, are shown in Figures 37 and 38 respectively.

ASSEMBLY AND PREPARATION OF PANEL AND TOOLING FOR BONDING

Structural and Phase I Test Panels

Panel Assembly

Assembly of the panel was initiated by TIG welding the edgemember components into a "picture frame" configuration. Ends of the edgemembers were sawed to a 45 degree angle, fitted together, and held in place by clamping as shown in Figure 39. The assembly was then welded in an argon-filled atmosphere control chamber shown in Figure 40. Weld buildup was ground flush to the edgemember surface to allow for proper fit-up with the facing sheets. A section of core was cut to size and fitted to the edgemember "picture frame". Face sheets, which were cut to size at the mill, edgemembers, and core were then cleaned employing the following sequence:

1. Alkaline clean - 6-10 oz/gal Wyandotte
Nuvat solution at 180F \pm 10F for 5 minutes.
2. Cold water rinse
3. Acid pickle (2 minutes at room temperature)
12.5 vol. % HF (49%)
25 vol. % HNO₃ (70%)
62.5 vol. % H₂SO₄ (98%)
4. Cold Water Rinse
5. Alcohol dip
6. Air Dry

After cleaning, all further handling was performed with clean white gloves. The core was then spot-tacked to the edgemember frame utilizing .0005 inch titanium foil as intermediate to facilitate spot welding as shown in Figure 41. The .0015 inch titanium intermediate used to facilitate bonding between the face sheet and core was cut to size, alkaline cleaned in a Wyandotte Nuvat solution, lightly abraded, and spot tacked to the tantalum face sheets. Face sheets were then placed on the core and edgemember assembly and held in place by means of tantalum foil edge straps.

Tool Assembly

Tooling consisted essentially of columbium filler core, molybdenum cover sheets, and edgemember supports. The molybdenum sheets served to prevent contact between the columbium filler core, tantalum panel, and Inconel 600 envelope. No interactions were experienced between the molybdenum sheets and

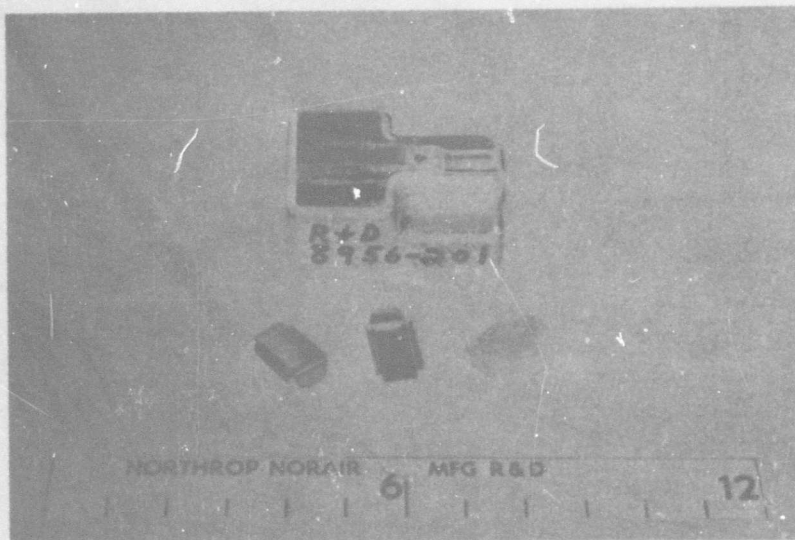


FIGURE 35 HEAT SHIELD PANEL ATTACH CLIPS FABRICATED FROM .040" T111 SHEET WITH FORM BLOCK



FIGURE 36 INNER (RIGHT) AND OUTER (LEFT) FORMED HEATSHIELD SKINS WITH CORE, WASHERS, AND PANEL ATTACH CLIPS

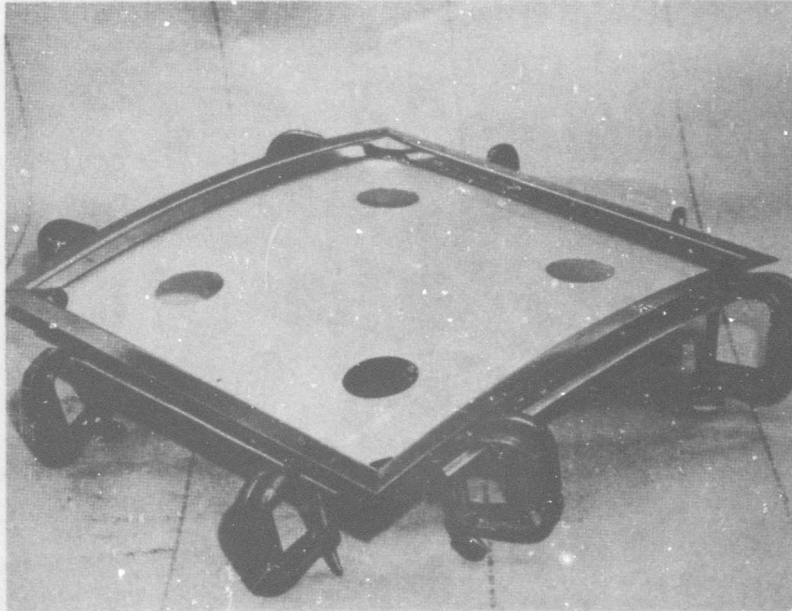


FIGURE 39 ALIGNMENT OF EDGEMEMBERS FOR WELDING (CURVED)

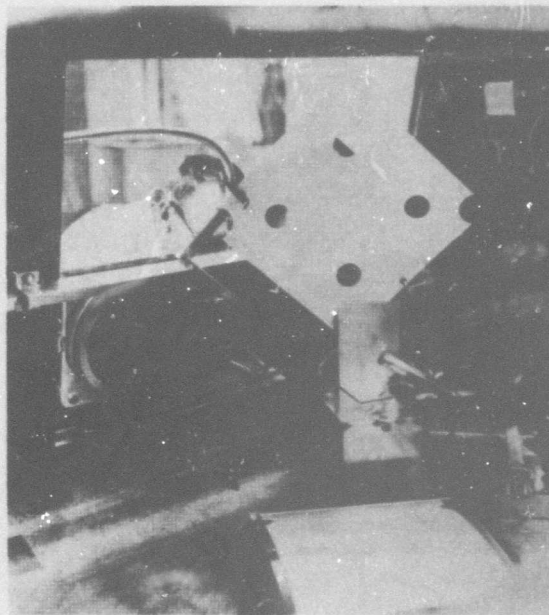


FIGURE 40 TIG WELDING OF EDGEMEMBERS IN
ATMOSPHERE CONTROL CHAMBER (CURVED)

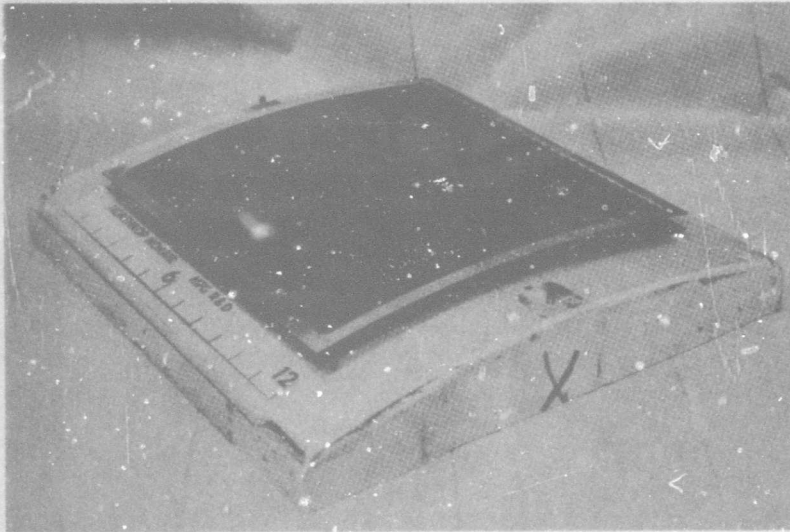


FIGURE 41 CORE FITTED AND SPOT TACKED TO
EDGEMEMBER FRAME (CURVED)

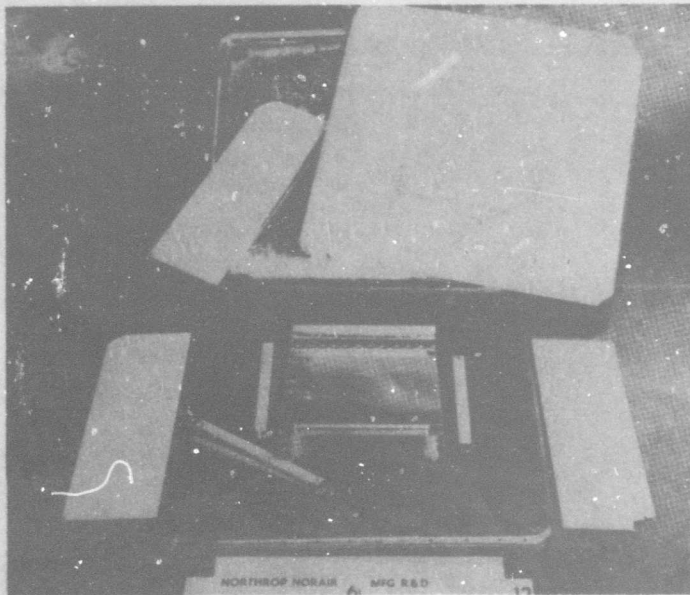


FIGURE 42 TEST PANEL 3 BONDED AT 2300F FOR 2.5 HOURS
ILLUSTRATING THE PACKAGE COMPONENTS AND
THEIR AVAILABILITY FOR SUBSEQUENT PANEL
FABRICATION

the tantalum or columbium components. However, an interaction can occur between molybdenum and Inconel 600 which deteriorates both materials. To prevent this, zirconium oxide was sprayed on all surfaces of the molybdenum sheets which came into contact with the Inconel 600 envelope. The edgemember supports consisted of columbium core with molybdenum cover sheets, and were wedged into the channeled edgemembers to prevent their collapse during the bond cycle.

Tooling materials referred to here were columbium and molybdenum items salvaged from a prior ASD refractory honeycomb panel program. The practicability of application of these normally costly materials was proven by the re-use of all materials inside of the protective envelope for multiple cycles. The filler core and details shown in Figure 2 were used for the complete Phase I series and were still usable on completion of Phase I.

The techniques and tooling design used in the assembly of panel and tooling for bonding as discussed above, were essentially the same for the Phase I 6x6 inch test panels and the Phase II 12x12 inch flat and curved structural panels.

Packaging arrangement of the three types of panels are shown in Figures 42, 43, and 44. As may be seen, the Phase I panels, being smaller in size, required more filler core than the Phase II panels. The difference in tooling design between the flat and curved Phase II panels was in the contouring of the tooling to fit the curvature requirements of the panel. This tooling design proved very effective in that reuse of the tooling components resulted in efficient panel fabrication. The molybdenum sheets became embrittled after several bonding runs due to recrystallization and had to be replaced periodically.

Heat Shield Panels

Packaging procedures and tooling varied somewhat from those employed on the structural panels reflecting the difference in design of the two types of panels. Tooling materials remained the same. A cross section of the heat shield package as it was assembled is shown in Figure 45. As may be seen, columbium filler core with molybdenum cover sheets were employed around the outside of the panel. Core, machined to .179 inch thickness, was employed within the stepped portion of the panel and spot welded to the .375 inch thick major core. Spot welding was used with a Ti interleaf to hold the assembly until the diffusion process added to joint strength. Solid molybdenum tooling comprised the remainder of the package to an extent sufficient to transmit pressure to all the surfaces to be bonded. In the case of the curved heat shield panels, the tooling components were formed to the desired contour by rolling.

The titanium intermediate thickness used in bonding the heat shield panels was reduced to .0005 inch from the .0015 inch used in fabricating the structural panels. However, .001 inch titanium foil was used to bond the stepped edge portion of the heat shield panels due to the more critical fit-up required in this area. This reduction in intermediate thickness, while not producing as strong a bond as the .0015 inch foil in the structural panels was necessary to reduce the tendency toward embrittlement due to an excess of titanium within the panel at temperatures exceeding 2800F. All other procedures

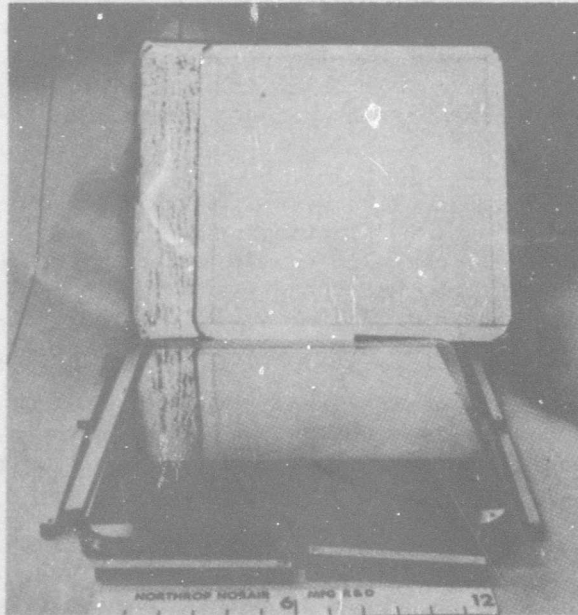


FIGURE 43 PANEL 11, THE FIRST 12X12 INCH PANEL MANUFACTURED, WAS DIFFUSION BONDED AT 2250F FOR 3.5 HOURS UTILIZING .0015 INCH Ti-55A FOIL AS INTERMEDIATE. A PANEL STRESS OF 2,000 PSI WAS OBTAINED ON 2X2 INCH FLATWISE TENSION SPECIMENS

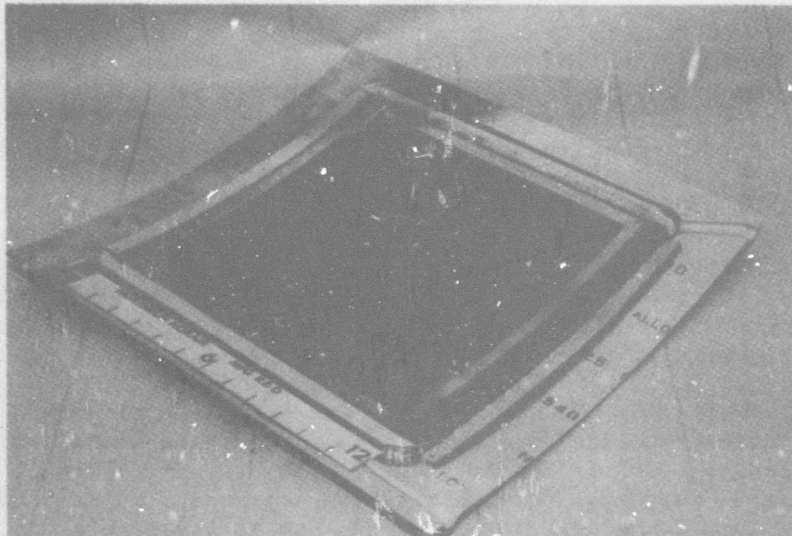
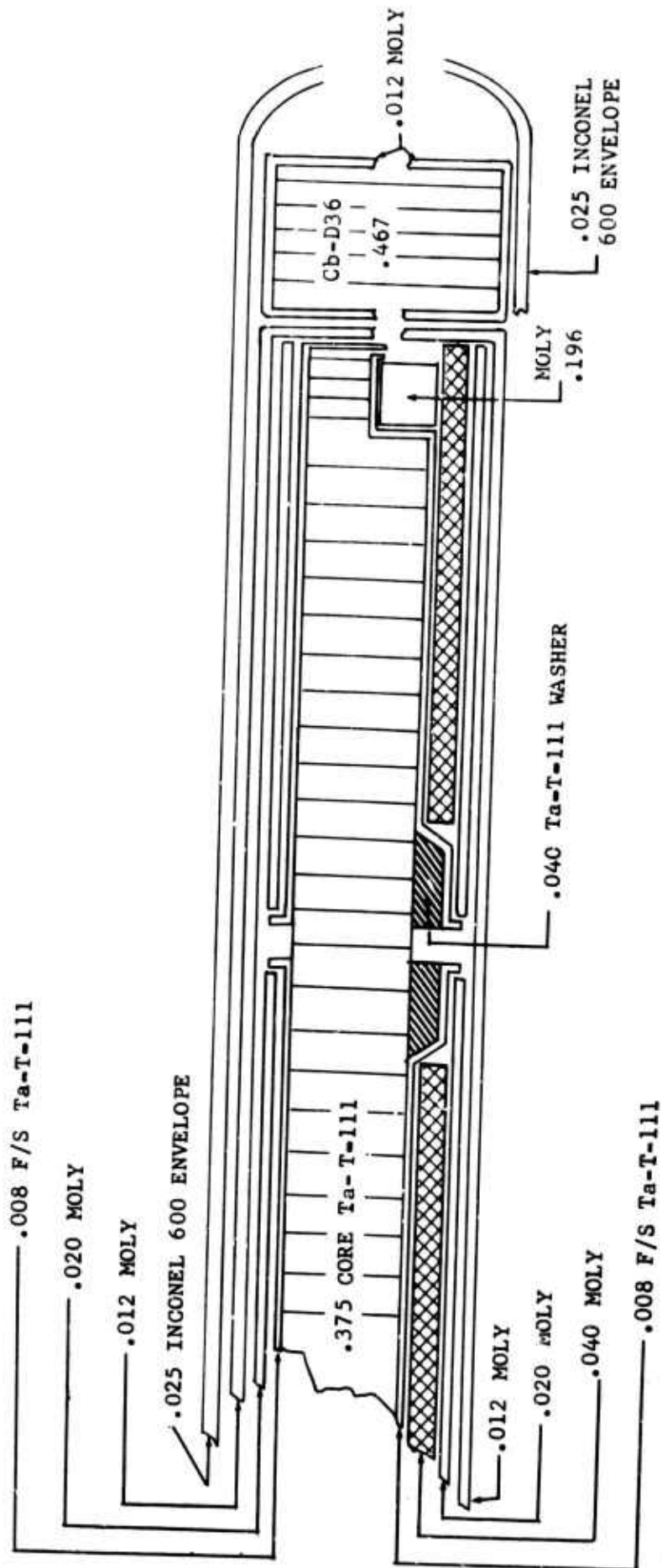


FIGURE 44 ARRANGEMENT OF PANEL AND TOOLING WITHIN THE ENVELOPE (CURVED)



.495 TOTAL PACKAGE THICKNESS

FIGURE 45 CROSS-SECTION SCHEMATIC OF HEATSHIELD PACKAGING PROCEDURE

employed in fabricating the heat shield panels remained essentially the same as those used in fabricating the structural panels.

Enveloping and Thermocouple Attachment

Upon completion of panel and tooling fit-up and assembly, initial sealing of the envelope halves was accomplished by seam welding along the edge flange of the envelope. Vacuum and argon lines were placed in the formed channels of the envelope and final sealing was performed by TIG welding. The envelopes employed in fabricating the heat shield panels were identical to those used for structural panel fabrication, except that the depth of the recess was shallower to accommodate the thinner heat shield panel.

Four 30-gage chromel-alumel thermocouples were spot welded to each side of the envelopes. The envelope was then coated with Everlube T-50 for oxidation protection and to afford a black body for the infrared radiation of the quartz lamp heating unit. A completed package is shown in Figure 46. The additional thermocouples shown (one side thermocouple and the corner thermocouple) were employed for monitoring on this particular run only.

Purging of Package

To allow bonding of the panel in an inert-gas atmosphere, the package was purged prior to the bonding cycle. To prevent clamping of the envelope on the panel during purging, thus closing off the inner portions of the panel in the core area, the package was placed in the counter vacuum chamber shown in Figure 47.

Purging was then accomplished by evacuating the package followed shortly thereafter with evacuation of the chamber. Evacuation of the package was maintained for a minimum of 30 minutes after which time both chamber and package were back-filled with high purity argon, package following chamber. This sequence of operations was repeated a minimum of four cycles for each package. The purging of the package was accomplished with an automatic pre-programmed purge-cycling vacuum system. The vacuum system with counter vacuum chamber is shown in Figure 48 during the purging of one of the packages.

MODE OF OPERATION FOR PANEL BONDING

Heating Method

Quartz-Lamp radiant-heating was employed in the program to obtain the required bonding temperatures for fabricating the honeycomb panels. This method was selected for its unique advantages over other types of heating techniques:

1. Independent zone control during heating and cooling cycles to match the heat sinks in the parts to be bonded, thus eliminating panel distortion.
2. Easy adaptability to closed-loop feedback operation providing excellent temperature control during the bond cycle.

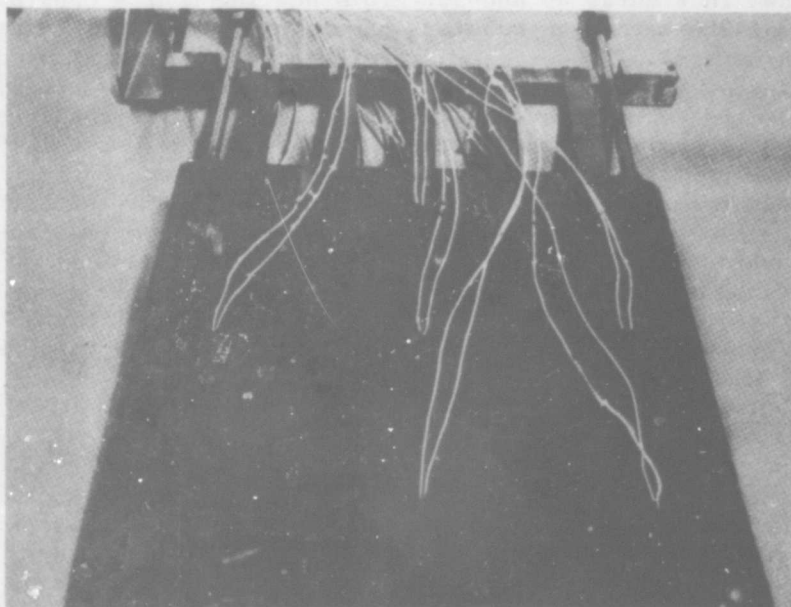


FIGURE 46 ALUMEL-CHROMEL THERMOCOUPLES SPOT WELDED TO SEALED ENVELOPE. ENVELOPE IS COATED WITH EVERLUBE T-50

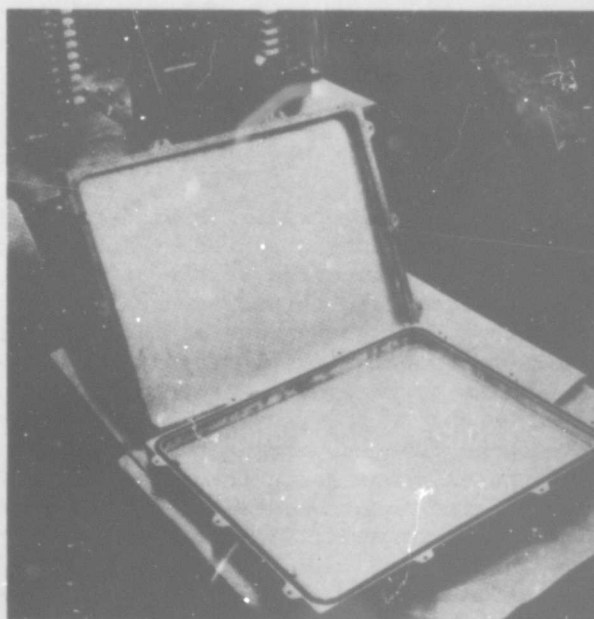


FIGURE 47 COUNTER VACUUM CHAMBER EMPLOYED FOR PURGING OF PACKAGE

To meet the needs of the program for attaining bonding temperatures, a specially-designed quartz lamp radiant heating unit was manufactured. The fixture is shown in Figures 49 and 50. This heating source consisted of opposed banks of 200 watt/inch tubular quartz lamps mounted in water-cooled, gold-fired reflectors. Air was circulated through the electrical conduits to allow cooling of the lamp end-seals. Vycor plate windows positioned between the lamps and working zone allowed the creation of a cooling air plenum which effectively eliminated the tendency of the quartz in the lamps to sag during sustained periods where part temperatures exceeded 2000F. In addition, the translucent vycor windows diffused the infrared radiation sufficiently to allow a more even distribution of heat. The quartz-lamp radiant-heating fixture as shown and described proved to be highly efficient in providing the necessary bonding temperatures for panel fabrication. In meeting the needs of the current program, the fixture logged in excess of 120 hours at a temperature of 2250F with only minor maintenance being required.

Temperature Control

Eight independent zones of operation were incorporated into the quartz lamp heating fixture, the output of each being controlled by a thermocouple attached to the package operating in a closed-loop feed-back system. Heating and cooling rates were controlled by two Data-Trak function generators with holding times at temperature maintained by the "set-point" mode of operation on eight Research Incorporated solid-state temperature controllers. Power was supplied by eight Ignitron power controllers wired to permit their operation as individual controllers or as paired master-slave units for four channel control (Figure 51). Transformer-facilities for 480 or 660 volt operation provided available power up to 2000 KVA at 600V continuous operation. Five dual-point Bristol stripchart recorders were utilized in recording temperature cycles. The temperature controller and recorders are shown in Figure 52. This mode of operation allowed exceptional uniformity of temperature on all portions of the package. Normal indicated variations in temperature during all panel bonding runs was $\pm 5F$.

Bond Pressure Application

The system developed by Northrop Norair for high-temperature diffusion-bonding of sandwich assemblies utilizes a sealed, thin metal envelope containing the assembly details. The function of the envelope is to shield the assembly from atmospheric contact, and through evacuation, exert a controlled compressive force on the panel during the bonding cycle. Consequently, the maximum available pressure for bonding was atmospheric pressure. However, in the case of bonding face-skins to honeycomb core, a multiplication of the bonding pressure is affected due to the very small area of actual bond interface between the skin and honeycomb supporting the total atmospheric force on the panel. Dividing this total atmospheric force by the actual supporting surface area contact at the bond interface results in pressures of approximately 1000 psi. This technique very conveniently eliminates the necessity for expensive and bulky pressure plates, dies, autoclaves, etc. In addition, uniformity of pressure can be attained easily on all portions of the panel.

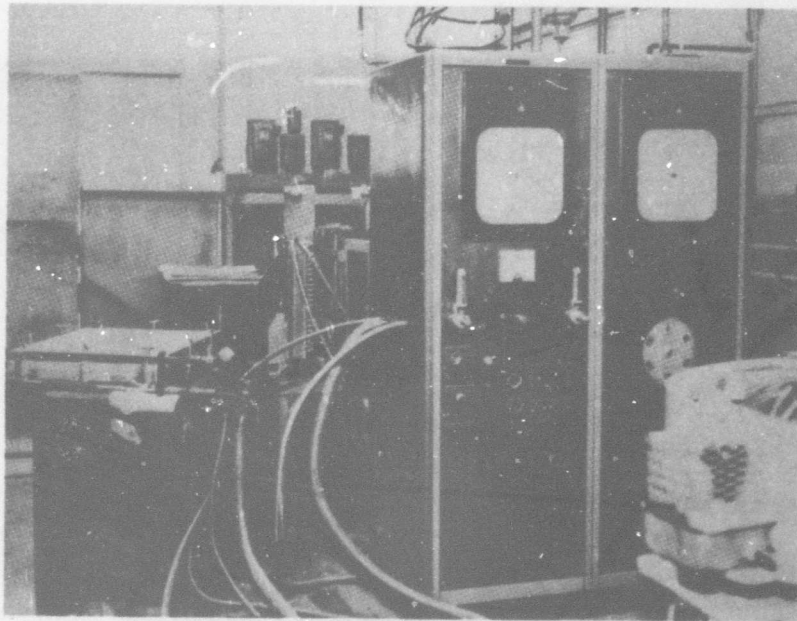


FIGURE 48 PURGING OF PACKAGE IN COUNTER-VACUUM CHAMBER
WITH AUTOMATIC PURGE CYCLING SYSTEM

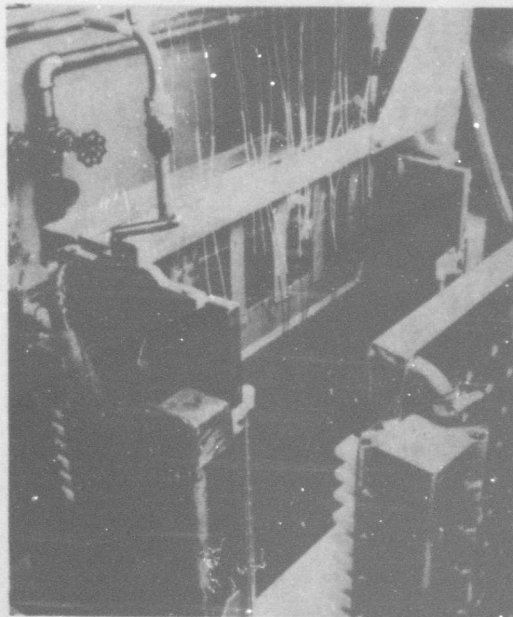


FIGURE 49 ORIENTATION OF PACKAGE IN HEATING FIXTURE

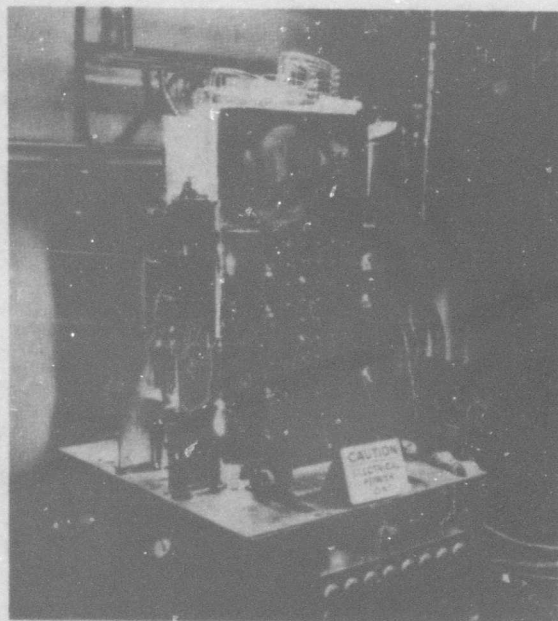


FIGURE 50 QUARTZ LAMP RADIANT HEATER IN OPERATION DURING THE BONDING OF A STRUCTURAL PANEL AT 2250F

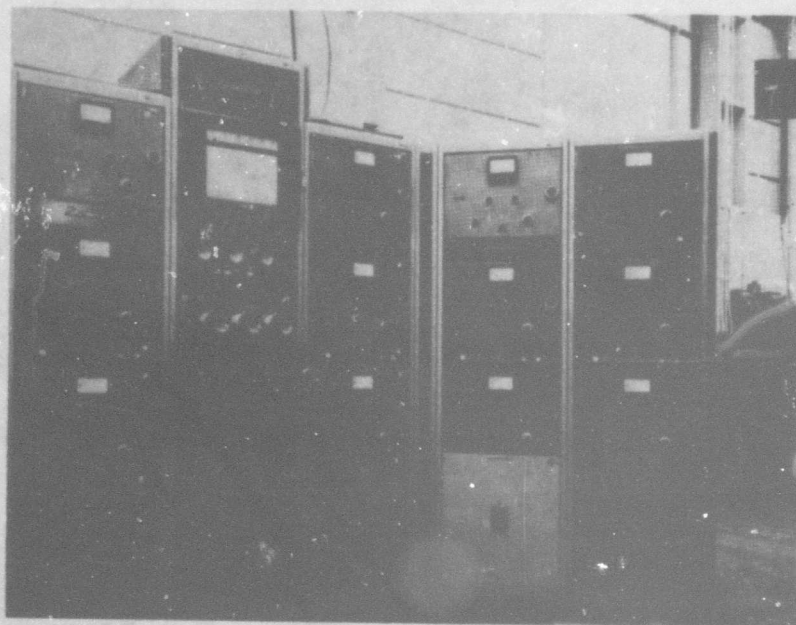


FIGURE 51 POWER CONTROL PANELS

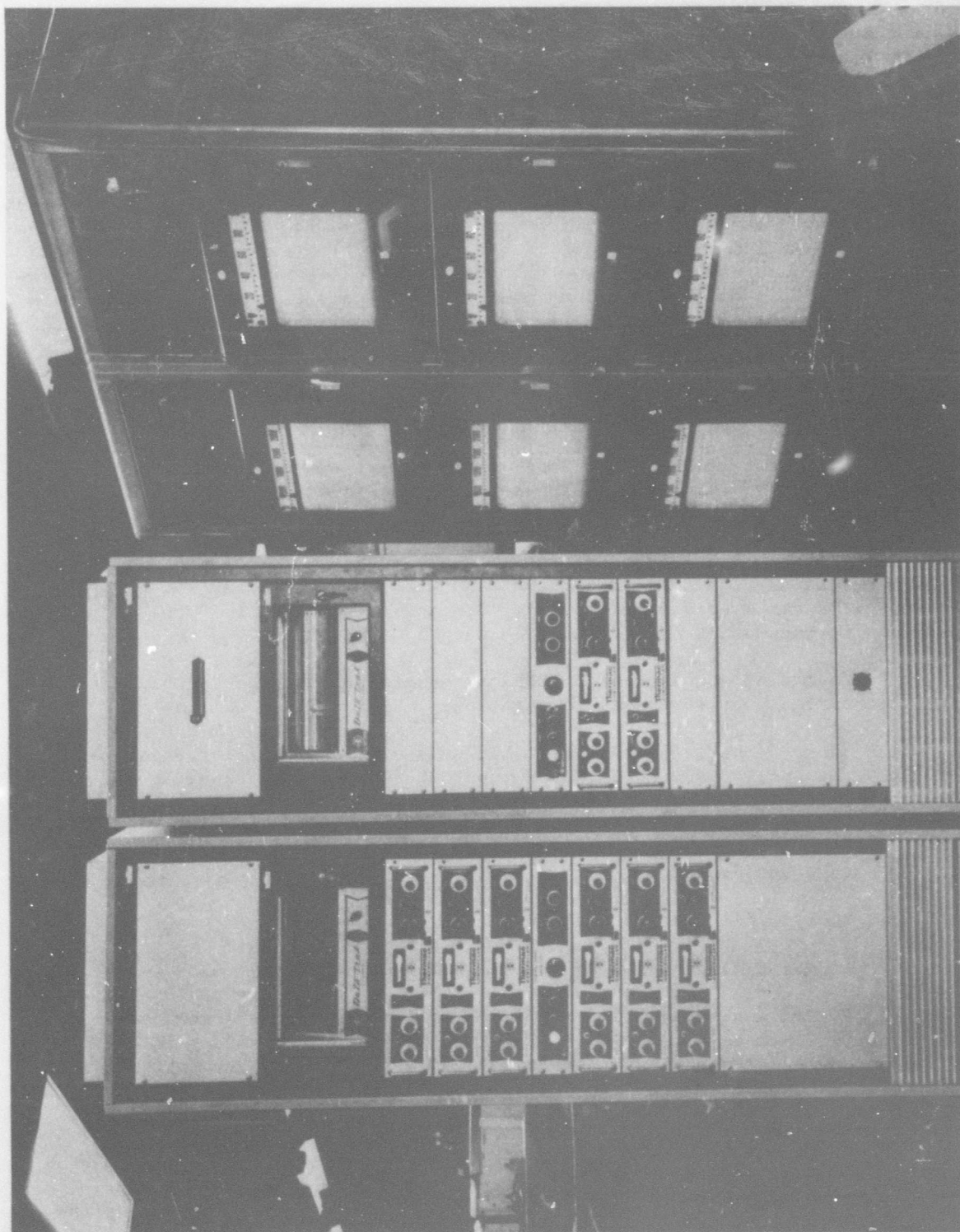


FIGURE 52 SOLID STATE TEMPERATURE CONTROLLERS AND RECORDERS
EMPLOYED FOR BONDING OF TANTALUM PANELS

With the equipment described in a preceding section ("Purging of Package") bonding pressures could be controlled between 100 and 1000 psi by regulating the internal pressure of the envelope. In the case of tantalum honeycomb core, the maximum pressure of 1000 psi was actually used for the full length of the bond cycle since previous studies had shown no core crushing employing this pressure with the bonding parameters selected for panel fabrication. This technique of bonding pressure application proved to be very satisfactory during subsequent honeycomb panel manufacture.

INTERMEDIATE APPLICATION BY VAPOR DEPOSITION STUDY

Previous investigations have shown tantalum honeycomb core to be seriously embrittled when exposed to titanium vapors above 2800F. The use of a titanium intermediate in foil form results in the presence of a considerable excess of titanium which is not involved in the actual diffusion process within a honeycomb panel. This excess titanium subsequently vaporizes above 2800F and diffuses into the tantalum core walls resulting in core embrittlement. No such embrittlement occurs with titanium solid-state diffusion in tantalum. While the exact nature of this embrittling tendency of tantalum by titanium is yet unknown, it appears to be related to the selective diffusion of titanium atoms along the tantalum grain boundaries. Consequently, as a supplement to the current program, an investigation of vapor deposition techniques was conducted to determine the feasibility of applying the exact amount of titanium on the core edges, thus eliminating the presence of excess titanium within the honeycomb panel.

Since this process required special equipment, the vapor deposition study was conducted as a joint effort between Northrop and qualified vendors. Two sources were employed for this study: Temescal Metallurgical Corp., Berkeley, California; and Curtis Associates, San Diego, California.

The following sequence of operations was to be employed in obtaining the vapor deposited core for panel fabrication:

1. Vapor deposit the required thickness of titanium intermediate on the honeycomb core edges in the HOBE (unexpanded) condition.
2. Diffusion heat-treat in a vacuum at 2200F for 1 hour to effect limited diffusion of the deposit into the core to form a more adherent deposit.
3. Mechanically expand the core.
4. Alkaline clean prior to panel assembly.

An 18-inch length by 2.5 inch width section of T111 honeycomb core HOBE was sent to Temescal for the initial attempt at vapor depositing titanium on the core edges. Temescal had performed similar studies in the past and had subsequently established procedures for this technique.

The core was preheated to 1200F prior to deposition with a radiant heating lamp. The deposition of titanium on a substrate of tantalum which is at a temperature less than approximately one-third the melting point of titanium results in an inferior deposit. In addition, the heat reduces the surface oxide of the tantalum to a lower oxidation state which readily combines with the titanium leaving the tantalum surface free for subsequent diffusion of titanium. Insufficient preheat usually results in a dark-appearing deposit which has been found to be of inferior quality.

The Ti-75A grade of commercially pure titanium was originally stipulated as the depositing material. However, Ti-35 was actually employed. Due to the lower iron content of the Ti-35 and the higher vapor pressure of iron over titanium, the calculated resultant deposit contained the same iron content as that of Ti-75A before deposition. An excessive iron content of the deposit would have resulted had Ti-75A been used as the depositing material.

The titanium was placed in a 3 inch diameter by 2 inch deep water-cooled copper crucible situated 8 to 10 inches below the core and melted with a 30KW electron gun with an electron beam magnetically deflected 270 degrees. A vacuum of approximately 3×10^{-5} torr was obtained by two mechanical pumps and a 32 inch oil diffusion pump with a water-cooled baffle. No liquid nitrogen trap was employed. A titanium deposition rate of .001 inch/minute was obtained with this set-up.

The quality of the deposit is dependent on the ratio of titanium atoms to oxygen atoms impinging on the substrate surface. Since the rate of oxygen atoms impinging on the substrate does not vary appreciably, a more rapid rate of deposition of the titanium increases this ratio thus producing a higher quality deposit.

Proper masking of the core was a necessity since an angle of deposition greater than 30 degrees from the normal would produce an inferior deposit. The mask used contained an opening equal to the width of the hole times a length equal to the width through which the vapors were allowed to pass and be deposited on the core. The core was then moved over this opening at a constant rate of speed.

Figure 53 is an illustration of the core after vapor deposition, diffusion heat treatment, and expansion. Most of the core except for certain areas around the sides appeared to possess a good quality deposit. The deposit exhibited no discoloration, was light in appearance, and possessed a smooth, even surface. The deposit also exhibited good adherence to the surface as was evidenced by bend tests on several pieces of foil. Figure 54 shows the thickness of the deposit which was determined to be .0005 inch. The periphery of the core, however, exhibited a darkened deposit, which under the microscope appeared to be very granular, porous, and uneven. One side of the core exhibited this effect more extensively than any of the other sides. This area is designated by the arrows in Figure 54. The photomicrographic inserts depict the appearance of the deposit in the two areas discussed. The brittleness of this inferior deposit was evident during bend testing and especially after the diffusion heat treating cycle as spalling occurred. The explanation put forth by Temescal for this darkened deposit was that the ends of the core received an insufficient amount of preheat.

Some titanium had also deposited on the sidewalls of the honeycomb core. The appearance of the side walls ranged from a brown to blue-black. Alkaline cleaning removed much of this sidewall deposit. This core-wall deposit did affect the ductility of the core material as subsequent tests revealed some embrittlement had occurred. Two pieces of the core, however, each measuring 6x6 inches were obtained for test panel fabrication to determine the bonding capabilities of the deposit.

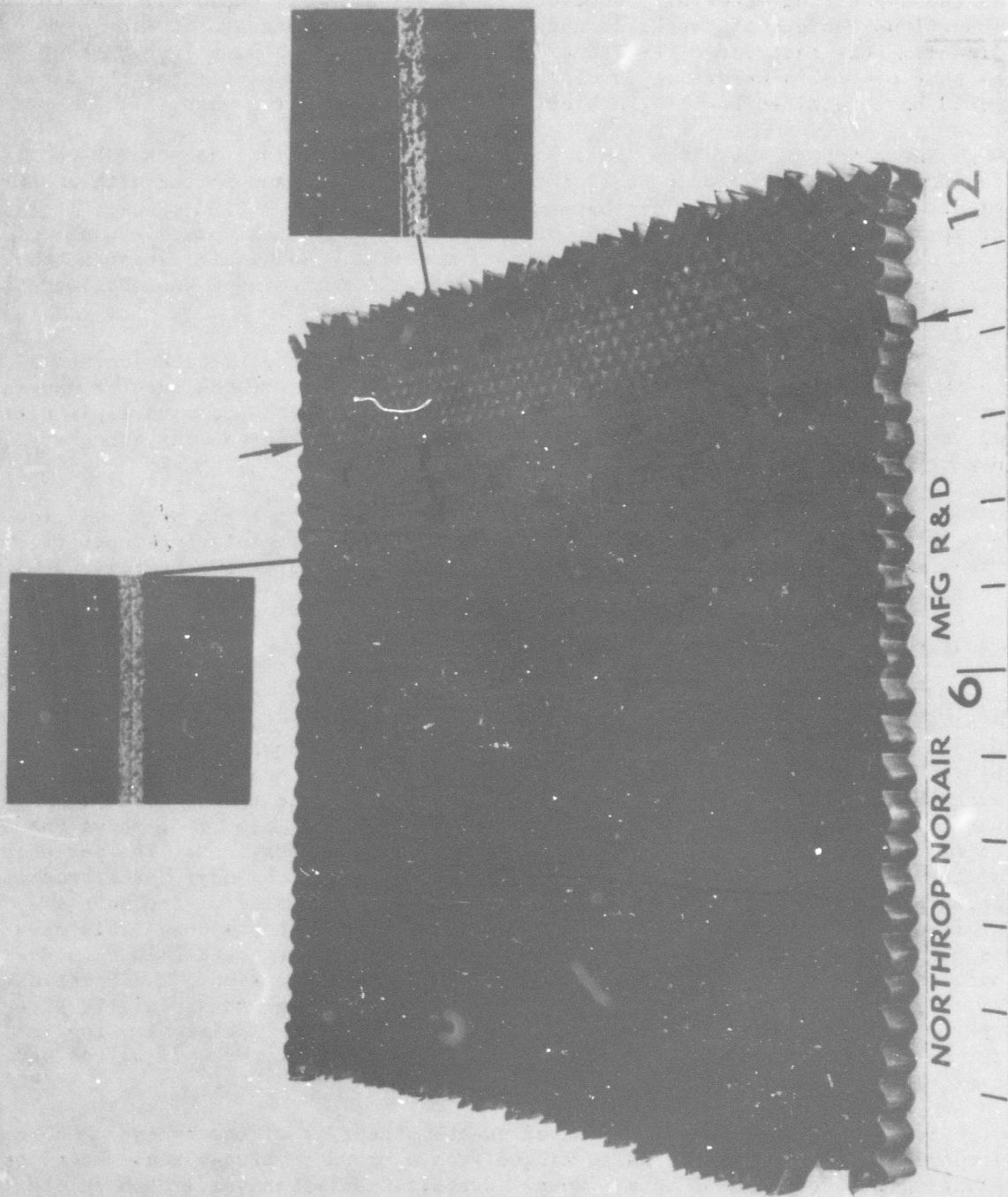


FIGURE 53 T111 CORE VAPOR DEPOSITED WITH T1-35 INTERMEDIATE. ARROWS DESIGNATE DEMAR-
CATION BETWEEN INFERIOR DEPOSIT (RIGHT) AND SATISFACTORY DEPOSIT (LEFT).
PHOTOMICROGRAPHIC INSERTS ILLUSTRATE THIS DIFFERENCE IN QUALITY OF DEPOSIT

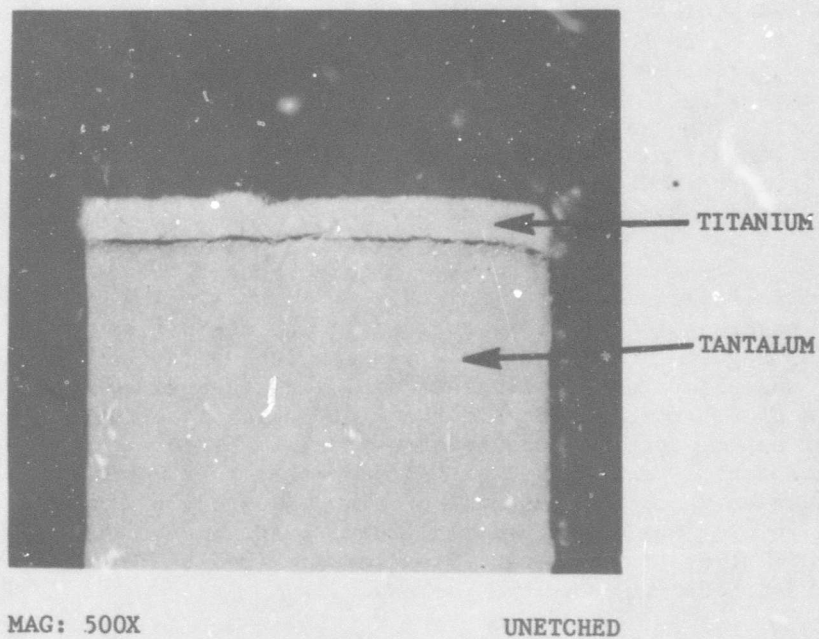


FIGURE 54 PHOTOMICROGRAPH SHOWING VAPOR DEPOSITED TITANIUM
ON EDGE OF HONEYCOMB CORE

Further investigations of the vapor deposition process for applying the titanium intermediate to the honeycomb core edges were performed utilizing the facilities of Curtis Associates. Curtis accomplished the deposition by means of electron beam melting of titanium in a water-cooled copper crucible located below a track and transport system which held and moved the honeycomb core at a specified rate of speed over the titanium source. The system was contained within a cylindrical, transparent vacuum chamber. The HOBE was clamped into a holder and resistance heated to 1200F while the chamber pressure was reduced to 2×10^{-5} torr. The HOBE was then moved at a specified rate over the opening of a mask placed between the honeycomb and the titanium source. Prior to the actual deposition of titanium on a piece of honeycomb, several sample test strips of tantalum (.012x.5x6 inches) were employed by Curtis to evaluate the system as well as to develop deposition parameters; i.e., current, voltage, vacuum, deposition rate, and preheat temperature of substrate. The chief problems encountered during deposition was the maintenance of proper focus of the electron beam on the titanium and the rapid depletion rate of the titanium source.

The first side of the honeycomb core exposed to titanium deposition was moved in increments of 1/2-inch every 90 seconds. The electron gun was at a fixed setting of 3500 volts at 150ma. The deposition angle was approximately 45 degrees. After the run was completed, inspection showed a dark area of the core near the finished end. It was surmised that this dark appearance of the core was due to the wide angle of deposition used. Consequently, before starting the reverse side of the core, the deposition angle was reduced to 30 degrees. The honeycomb was then moved at a steady rate of six minutes per pass for a total of six passes or 36 minutes of deposition. The gun setting was increased to 175ma. Inspection of the second side showed no discoloration of the core. The distance from the titanium source to the work during both runs was two inches.

The honeycomb core so deposited was analyzed as to deposit quality and thickness. An x-ray diffraction analysis of the core revealed no evidence of contamination of either the titanium deposit or the core. However, metallographic analysis revealed only .0003 inch of titanium to be present on the core edges which was less than the minimum .0005 inch thickness desired for bonding.

A second attempt at increasing the amount of titanium deposit resulted in an unusable contaminated core. A heavy bluish-black discoloration was evident on most of the core indicative of excessive oxygen being present during the deposition process.

A second section of honeycomb in the unexpanded condition was sent to Curtis. It was felt that many of the problems encountered during the initial deposition trials had been identified and could be remedied on the second honeycomb core. The deposition of titanium on this second honeycomb resulted in a completely contaminant-free deposit and core. The thickness of the deposit was found to be .0008 inch. Two 6x6 inch pieces were obtained after vacuum heating, and expanded for fabrication of Phase I 6x6 inch test panels.

The investigation conducted during this program on utilizing vapor deposition as a means of applying the intermediate material to the edges of the honeycomb core was very limited. However, it demonstrated the feasibility of this technique for fabrication of tantalum honeycomb panels. Contaminant-free deposits and core were obtained and no flaking off of the deposit occurred during subsequent fabrication. The expansion of the honeycomb core from the hobe condition, which does place considerable stress on the core, well illustrated the ductility of both core and deposit after deposition. The use of this technique for intermediate application would be far more desirable in fabricating tantalum honeycomb panels than the use of the titanium intermediate in foil form.

The embrittlement problem which is the chief deterrent to realizing the full potential of tantalum bonded components would be eliminated. The results obtained in utilizing the vapor deposited honeycomb for test panel fabrication is discussed in the succeeding section "PHASE I TEST PANEL FABRICATION". Due to the limited nature of the investigation, this technique could not be employed in the fabrication of the larger Phase II structural and heat shield panels.

VII PHASE I TEST PANEL FABRICATION

The initial portion of Phase I was characterized by the establishment of optimum bonding parameters and manufacturing techniques and procedures to be utilized in the manufacture of the Phase II structural and heat shield panels. Phase I was initiated with the utilization of a previously-established computer program to obtain several time-temperature-concentration relationships for the diffusion of Titanium into Tantalum. The value of these relationships was a set of curves yielding a reasonable estimate of the time required at a given temperature to achieve a desired center-of-joint concentration. This in turn would determine bond strengths and joint remelt temperatures. With these curves as a guide, a series of 6x6 inch test panels were manufactured to finalize bonding parameters and manufacturing procedures.

The manufacturing techniques and procedures, i.e., panel and tooling materials and assembly, pressure requirements for bonding, cleaning methods, and bonding parameter derivations have already been described in previous sections of the report. During this portion of Phase I, the actual application of these parameters to the manufacture of small size panels was accomplished with the fabrication of fourteen 6x6 inch panels and one 12x12 inch panel for analysis. Four of these panels utilized core in which the titanium intermediate was applied by vapor deposition.

During the course of fabricating these panels, difficulties were encountered in effecting a satisfactory diffusion-bonded joint. While the initial panels manufactured appeared to offer some reliability and integrity in bonding, subsequent panels deteriorated in quality. In order to improve the bonding capabilities of the system certain manufacturing and bonding procedures were altered in later panels in an attempt to obtain improved bonds. For this reason, more panels than were originally planned for had to be fabricated.

Since the Phase I portion of the program was concerned mainly with the fabrication of a satisfactory diffusion-bonded joint, panel testing was limited to flatwise tension tests and metallographic analysis. Tests were performed at room temperature and 2800F. These tests were deemed adequate for the intended purpose of the Phase I portion of the program as the larger Phase II 12x12 inch panels were subjected to a series of structural and high temperature tests to evaluate the suitability of tantalum honeycomb panels for aerospace environments. Ultrasonic inspection was performed on some of the panels. Microprobe analyses were also performed on several panels to correlate the actual extent of diffusion with predicted values obtained from the time-temperature-concentration curves derived for the tantalum-titanium binary system.

An analysis of each panels fabricated in Phase I follows:

PANELS 1 AND 2:

Fabrication

The first two panels were fabricated to determine the relative diffusion bonding characteristics of the Ta-10W and Ta-8W-2Hf (T111) alloys, since it

had been reported during core manufacture that the T111 alloy had exhibited superior diffusion bonding characteristics compared to Ta-10W. Panel 1 was fabricated from Ta-10W while Panel 2 utilized T111 components. Both panels were bonded at 2250F for 2.5 hours with .0005 inch Ti-75A foil as intermediate. Pressure for bonding was applied by maintaining a hard vacuum within the envelope for the initial 30 minutes of the run and then converting to a regulated pressure of 500mm absolute of Hg for the remaining two hours of the run.

Hard vacuum at the start of each run consisted of an envelope pressure of 20-30 microns, increasing to approximately 1000 microns during heat-up and decreasing to approximately 90 microns prior to converting to regulated pressure after 30 minutes. Pressure requirements in diffusion bonding are most critical during the initial phase of bonding since intimate contact must be maintained between the surfaces to be bonded to provide for maximum contact area by plastic deformation of the intermediate. Once diffusion has commenced, the process becomes time, temperature dependent only, with further pressure increases adding little to the strength of the bond as further plastic deformation of the intermediate is unnecessary. Hence, a full vacuum for the entire run was not considered necessary in evaluating bonding capabilities. This also reduced envelope stresses during the remaining two hours of the run.

Evaluation

Flatwise tension tests were performed on Panels 1 and 2. Two specimens from each panel, approximately 2x2 inches square were adhesively bonded to test blocks and loaded in tension to failure at room temperature. Loads of 1350 and 1540 pounds were obtained on Panel 1 (Ta 10W) which are equivalent to face sheet stresses of 324 psi and 370 psi, respectively. Based on a ribbon length of 23.6 inches and a core foil thickness of .0025 inch, a core stress of 26,500 psi was developed with the 1540 pound load. The flatwise tension results on Panel 2 (T111) yielded loads at failure of 2000 and 2375 pounds and are equivalent to face sheet stresses of 474 psi and 560 psi, respectively. Core stresses obtained on Panel 2 were 34,500 psi and 41,000 psi.

Both panels were examined metallographically to determine the extent of bonding. Sections of core-to-facesheet and edgemember-to-facesheet were mounted, polished, and examined. A good metallurgical joint was obtained between the core and face sheet as shown in Figure 55. The joint was found to be typical of those examined on both panels. However, the edgemember-to-facesheet joint contained many voids. This was expected, since the edgemember-to-facesheet joint encompasses a far greater surface area than that existing between the core and facesheet. This results in greater chances of surface mismatch and lower unit bonding pressures. This effect was compensated for in the panel design by fusion welding the panel periphery after bonding.

To determine the validity of the time-temperature concentration curves developed earlier in the program for selection of bonding parameters, an electron microprobe analysis of a core-to-face sheet joint was conducted. A peak concentration of 31 percent titanium was observed, a good correlation with the earlier work, which predicted a maximum titanium concentration for the joining parameters used of 28 percent.

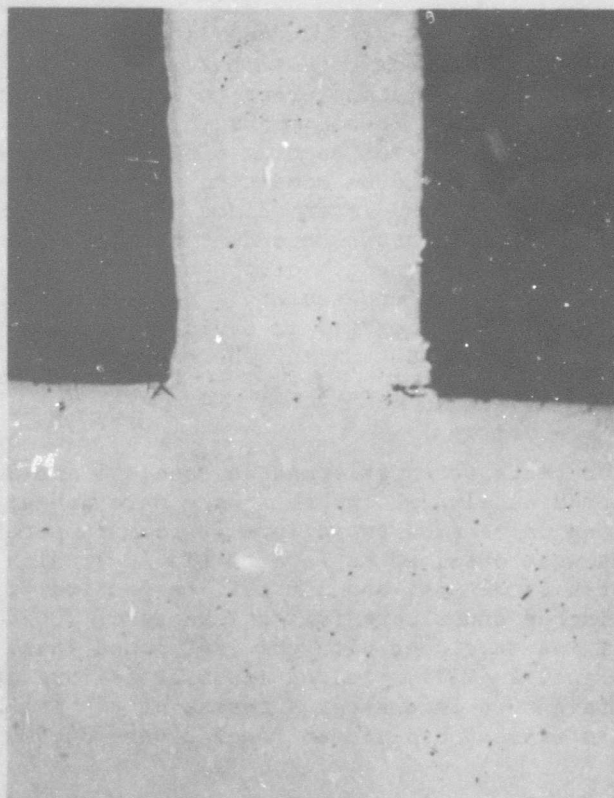


FIGURE 55 TYPICAL TEE JOINT FORMED BY CORE CELL WALL
AND FACE SHEET WITH .0005 INCH TITANIUM FOIL

While the results obtained on these two panels may not conclusively prove the superiority of T111 over Ta-10W in diffusion bonding capabilities, it was felt that satisfactory bonding could be more consistently obtained with the T111 alloy. In addition, the T111 alloy is superior to the Ta-10W in elevated temperature strength and weldability - both important factors in subsequent program work. As a result of the above factors and the limited amount of foil available for Phase II core manufacture, it was decided that the T111 alloy would be employed for the remainder of the program.

PANEL 3

Fabrication

Panel 3 was manufactured to determine the effect of an increase in temperature on bond strength. A temperature of 2300F was employed for this purpose with all other parameters and procedures remaining the same as those employed in the manufacture of Panels 1 and 2.

Evaluation

Flatwise tension tests could not be performed since most of the facesheet and core separated during sectioning of the panel. The reason for the inferior bonding of this panel was not readily apparent.

PANELS 4 AND 5

Fabrication

Both panels represent initial attempts at utilizing honeycomb core on which the titanium intermediate was vapor deposited. Both panels were bonded at 2300F for 2.5 hours with all other parameters remaining the same as those employed in fabricating the previous three panels. In addition to evaluating the vapor deposition method of applying the intermediate material, the effects of cleaning procedures on the deposited intermediate were also evaluated. It was previously felt that any attempt to clean the core after vapor depositing the titanium intermediate on the core edges would remove the deposit. However, due to excessive handling of the core after deposition as a result of vacuum heat treating, core expansion, and the fact that a thin deposit was formed on the sidewalls of the core during the deposition process, it was decided that the core might become embrittled during the bonding cycle. Consequently, Panel 4 contained core which had been alkaline and acid cleaned, while the core employed in Panel 5 was not cleaned and used in the as-received condition. Examination of the core after cleaning, prior to assembly, showed a completely continuous network of titanium on the core edges. However, no examination was made as to possible reduction of the intermediate thickness. The cleaning operation consisted essentially of that used on previous panels for the core except that the immersion time in the acid bath was reduced from 5 to 2 minutes.

The titanium deposit thickness as previously determined metallographically was .0005 inch so as to allow direct comparison with previous foil bonded panels.

Evaluation

Ultrasonic inspection performed on both panels indicated only a small percentage of each panel to be bonded. These indications were confirmed when the facesheets and core separated during sectioning of the panels for testing. It was concluded that whatever contamination was present either in the deposit or on the core prevented effective diffusion between the titanium and tantalum.

PANEL 6

Fabrication

Panel 6 was a second attempt to evaluate the effects of temperature on bonding and, in addition, to test the limits of the packaging system. A temperature of 2350F for 2.5 hours was employed. After 30 minutes at temperature, rupture of the envelope occurred. Examination of the package revealed melting occurred on the inner surface of the envelope. This was a result of contact between the Molybdenum slip sheet and the Inconel 600 envelope causing interdiffusion of the two materials, with the subsequent formation of a low melting point eutectic. It was evident on further examination that contact occurred because of an insufficient amount of zirconium oxide stopoff on both components.

Evaluation

As a result of envelope rupture, a portion of the panel was severely oxidized and no tests were attempted on the undamaged portion, due to possible contamination not readily apparent upon visual examination.

PANELS 7 AND 8

Fabrication

The effects of bonding pressure and diffusion time were to be examined with Panels 7 and 8. The previous six panels were all fabricated with a hard vacuum within the envelope for only the initial 30 minutes of the cycle. With Panels 7 and 8 the hard vacuum was maintained for the entire period of the bonding cycle. Bonding temperature was 2250F since it was concluded that this temperature gave the best results both from a bonding as well as a manufacturing standpoint. Bonding times for Panels 7 and 8 were 2.5 and 5 hours, respectively.

Evaluation

Ultrasonic inspection indicated that both panels were between 80 and 90 percent bonded. However, separation of facesheets and core occurred during the sectioning of Panel 7. Flatwise tension tests performed on Panel 8 yielded panel strengths of 251 and 188 psi. The reason for unsatisfactory joint strength was still not readily apparent, thus a thorough analysis was made of all manufacturing procedures used in packaging and bonding.

PANEL 9

Fabrication

Panel 9 was intended to duplicate the bond strengths attained in Panel 2, the strongest thus far manufactured. Panel 9 was bonded at 2250F for 2.5 hours with a hard vacuum within the envelope (1000 psi bond pressure) for the length of the cycle. Ti-40 foil was employed on one facesheet to joint surface, while Ti-75, the foil used on all previous panels, was used on the other facesheet to core interface. Both foil intermediates were .0005 inch in thickness. New cleaning solutions were used in cleaning all tooling and panel components. A counter-vacuum chamber was used for the first time to effect more efficient purging and evacuation of the package, especially within the panel itself.

Evaluation

Panel 9 exhibited some improvement in panel integrity in that no facesheet separations occurred. Both sides of the panel appeared to show a difference in flatwise-tension test results between the two grades of titanium intermediate. Although the Ti-40 side appeared weaker, these results were generated with four different specimens, each of which had one facesheet joined with Ti-40 and one with Ti-75. Thus, on two tests, the Ti-40 side failed indicating the Ti-75 bond was stronger while on the other two tests, the Ti-75 failed indicating the Ti-40 bond was stronger. The side bonded with the Ti-40 failed at 198 and 168 psi; while the side employing Ti-75 exhibited panel stresses of 262 and 206 psi. Therefore, there appeared to be little, if any, difference caused by the grade of titanium foil used. In addition, none of the other procedures used in fabrication of this panel appeared to offer any solution to the lack of bond strength encountered thus far.

SUMMARY OF PANELS THREE THROUGH NINE

Of the previous 7 panels, 3 through 9 represent attempts at improving the bonding capabilities of the system by varying certain manufacturing and bonding procedures. Cleaning methods, fit-up of tooling and panel components, grade of titanium intermediate, bond temperature, time, and pressure were all altered in an attempt to obtain improved bonds. Examination of these panels revealed two significant aspects of the problem:

1. Most of the titanium had diffused into the tantalum; that is, the original foil form was no longer discernible.
2. The core-to-facesheet mating surfaces revealed definite contact between both members as evidenced by a continuous core pattern on the facesheet.

From these observations, two possible reasons could be drawn for the lack of satisfactory bonding thus far encountered:

1. Adequate pressure application to the panel was not afforded to eliminate small voids at the bond interface and thus produce a strong, continuous bond.

2. The use of a .0005 inch-thick intermediate was inadequate to completely compensate for very minute core-to-facesheet mismatches.

Small scale laboratory tests have indicated that the pressure attained should be adequate; therefore, the second possibility was explored.

PANEL 10

Fabrication

Panel 10 was fabricated employing .0005 inch titanium intermediate on one side and .0015 inch titanium intermediate on the opposite side of the panel. The use of the thicker intermediate was the only new factor in panel processing over that of Panel 9.

Evaluation

Ultrasonic inspection of this panel indicated both faces to be nearly 100 percent bonded. Failure in flatwise tension tests occurred on the side bonded with the .0005 inch foil at panel stresses of 432 psi and 684 psi. Tests performed at 2800F also failed on the .0005 inch foil side at 90 psi and 122 psi.

Peel tests indicated that the side bonded with the .0015 inch foil was far stronger than that of the .0005 inch foil side of the panel. Core tearing was definitely indicated with the .0015 inch foil bond. These results were the best attained from any panel previously fabricated and were definitely indicative of the nature of solution of the problem.

PANEL 11

Fabrication

With the demonstration of Panel 10 to effect satisfactory bonding with a thicker intermediate, fabrication of the first 12x12 inch Phase II panel was accomplished. This panel was intended to reveal any unforeseen difficulties in fabricating these larger panels. Bonding was performed at 2250F for 3.5 hours employing .0015 inch Ti-55 foil as intermediate. The longer bonding time was used because the greater thickness of intermediate required longer diffusion time to produce a center-of-joint concentration commensurate with good strength and joint remelt temperature. A hard vacuum was maintained within the package for the length of the cycle. No critical problems were encountered during the fabrication of this panel.

Evaluation

An ultrasonic inspection trace of this panel is shown in Figure 56. A near 100 percent bond is indicated between facesheet and core. Some nonbonded areas indicated between the facesheets and edgemembers. Effecting a complete

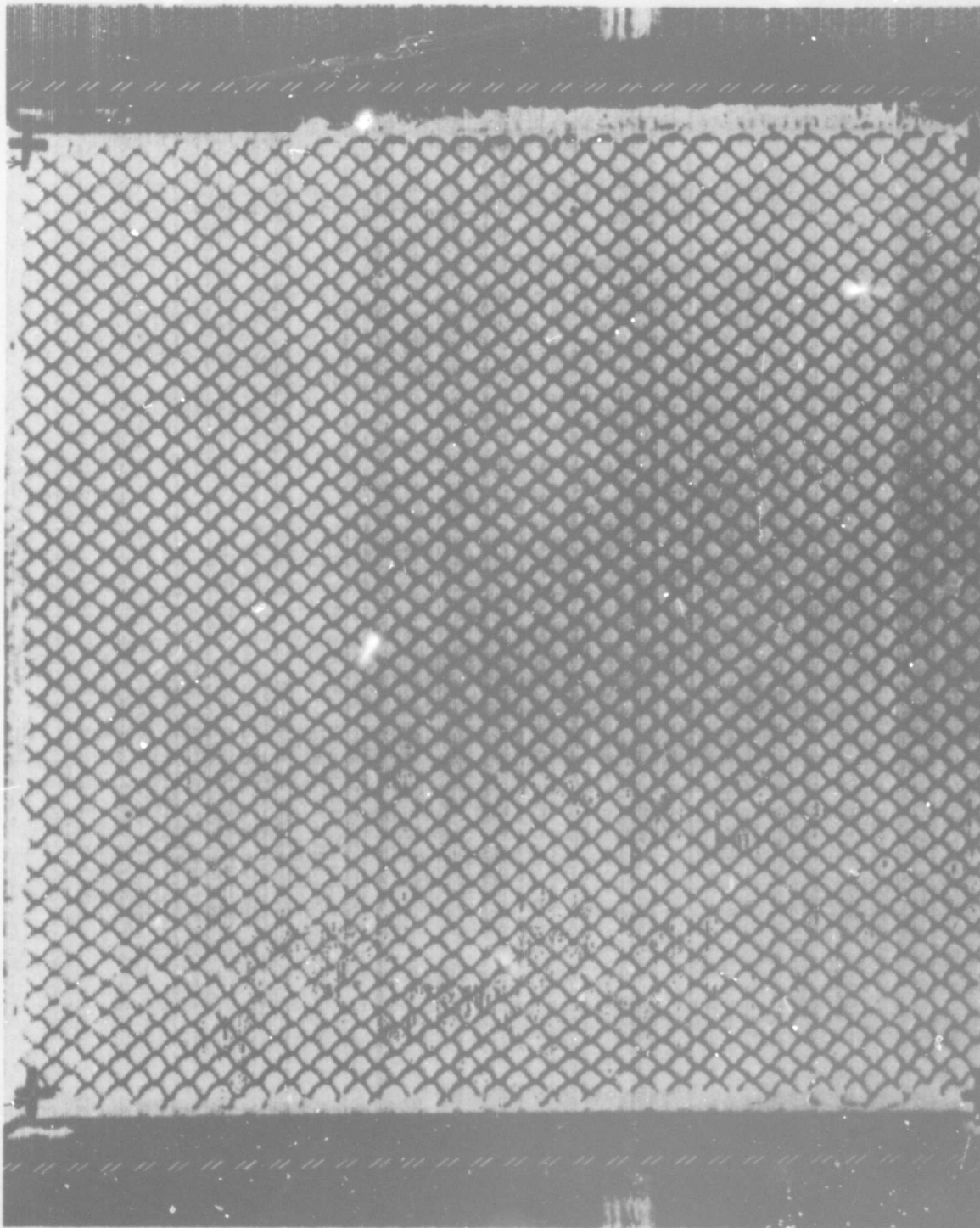


FIGURE 56 ULTRASONIC TRACE OF 12X12 INCH PANEL 11. DOTTED
LINES REPRESENT EDGE OF PANEL AT EDGEMEMBERS

bond between the facesheets and edgemembers was difficult since unit bonding pressures were significantly less than between facesheets and core. Flatness and thickness variation measurements on the panel revealed an out-of-flatness of .022 inch from edge-to-center and a maximum variation in thickness of .003 inch.

The maximum variation specified by the Air Force on these 12x12 inch panels for flatness and thickness was .022 inch and .005 inch, respectively.

Flatwise tension tests revealed panel strengths averaging 2000 pounds per square inch of panel surface at failure. These strength values were about 400 percent higher than any attained previously. Tests performed at 2800F showed panel strengths averaging 245 psi. The high temperature vacuum furnace and fixtures used in flatwise tension testing are shown in Figure 57. Failed surfaces of the room temperature specimens are shown in Figure 58. Much of the failure of these specimens occurred through the core rather than at the bond interface.

PANEL 12

Fabrication

It was noted earlier in this section that examination of the panels fabricated with .0005 inch foil revealed that all of the titanium foil intermediate diffused into the tantalum with no excess foil being present. It was reasoned that this situation might lend itself to the use of foil as an intermediate in the fabrication of the Phase II heat shield panels without experiencing the embrittlement problem (associated with titanium evaporation at temperatures of 2800F and above) discussed earlier in this report. In addition, the .008 inch facings employed on the heat-shield panels, exhibiting less stiffness than the .012 inch facings of the structural panels conformed more readily to the honeycomb surface resulting in better fit-up with the core, thus lessening the intermediate thickness requirement. Consequently, Panel 12 was fabricated to evaluate the possibility of utilizing .0005 inch foil as intermediate in fabricating the heat-shield panels and thus serve as a backup to the vapor deposition technique for intermediate application.

Evaluation

Sections of the panel were obtained after bonding and subjected to the following thermal cycles:

2100F 24 Hrs.

3400F 1 Hour

The core after the 2100F exposure exhibited no embrittlement. However, after the 3400F exposure mild embrittlement of the core had occurred. This reduction in ductility, it was felt, would not appreciably affect the performance of the heat-shield panels. This assumption was predicated on the

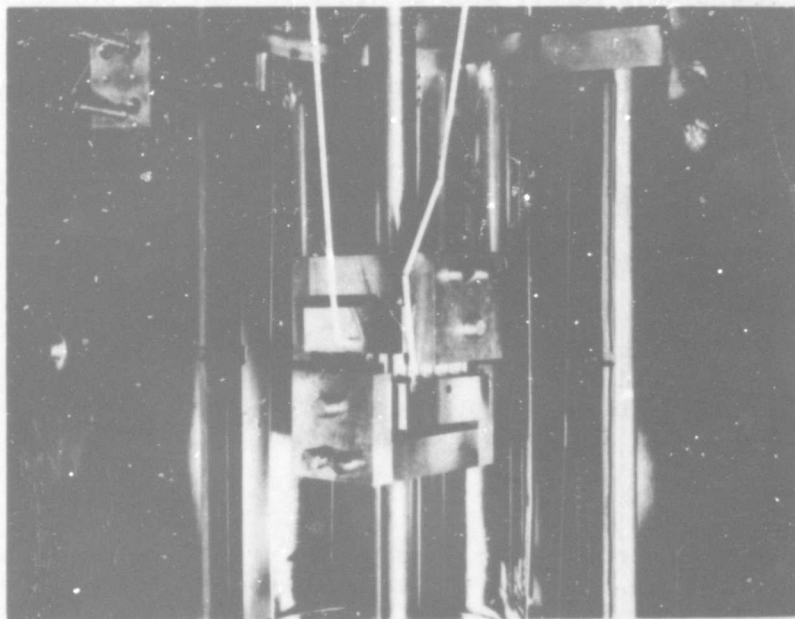


FIGURE 57 FLATWISE TENSION SPECIMEN FIXTURED
AND READY FOR TESTING AT 2800F

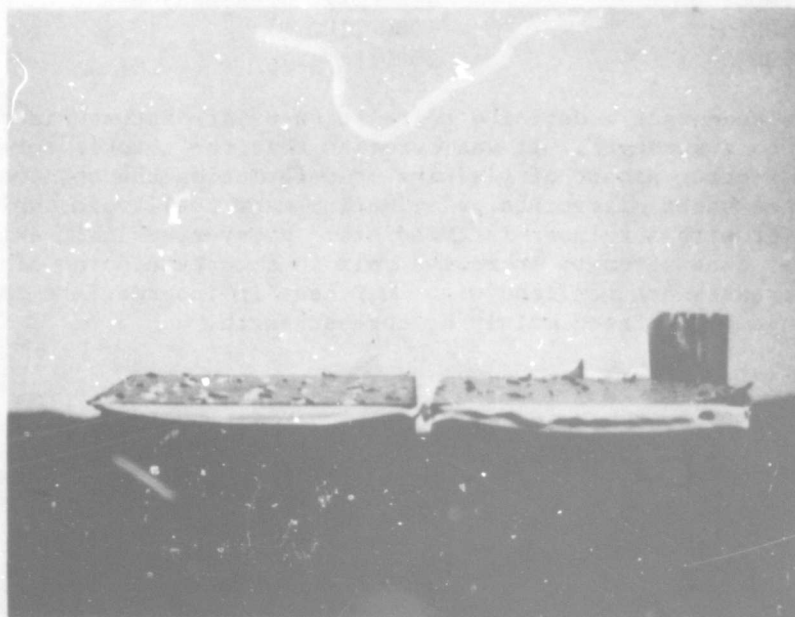


FIGURE 58 FAILED SURFACE OF TENSION TEST SPECIMENS SHOWING
THAT MUCH OF THE FAILURE OCCURRED THROUGH THE
CORE INSTEAD OF AT THE BOND INTERFACE

fact that the heat-shield panels were designed for thermal protection only with no loading other than normal aerodynamic stress being applied to the panel. Under these circumstances, some loss in ductility could be tolerated. However, this is not to imply that titanium foil is an equivalent substitute for vapor deposited titanium as the latter would produce a superior structure. It had been planned to use the foil only if vapor deposition techniques could not be developed in time for heat-shield panel fabrication.

PANEL 13

Fabrication

Panel 13 was fabricated to further investigate the effects of intermediate thickness on bond strength. The panel was fabricated using a .001 inch Ti-55 foil intermediate and .012 inch facings. Bonding parameters were 2250F for 3.5 hours with a bonding pressure of 1000 psi.

Evaluation

Flatwise tension tests at room temperature yielded panel stresses at failure of 1000-1100 psi. These results fell between those obtained on panels employing the .0005 inch foil and .0015 inch foil. These results are shown in the following tabulation:

<u>Intermediate Thickness (In.)</u>	<u>Flatwise Tension Test Strength (psi)</u>
.0005	684 (max. attained)
.0010	1000-1100
.0015	2000 (Ave.)

It may be seen that a definite correlation exists between intermediate thickness and bond strength. It was surmised that the thicker intermediate can undergo a greater amount of yielding or deformation thereby compensating for core-to-face sheet mismatches, eliminating many small voids which otherwise would exist with a thinner intermediate. However, a limit exists, of course, in that bond strength increases only to a certain point after which no further increases are realized with increases in intermediate thickness. This limit would be dictated mainly by core strength.

PANELS 14 AND 15

Fabrication

Both panels represent final attempts at using vapor deposited titanium in panel fabrication. The panels had been deposited with .0008 inch titanium although a minimum of .001 inch was specified based on the results previously discussed. Due to time limitations no further attempts at increasing this thickness could be made. Panel 14 was bonded at 2250F for 3.5 hours and Panel 15 was bonded at 2300F for 6 hours. Panel 15 was an attempt to compensate for the sub-specification intermediate thickness with increases in both temperature and time.

Both panels exhibited facesheet separations from the core during sectioning for examination. Further examination did reveal Panel 15 to exhibit a somewhat stronger bond than Panel 14 but not to any appreciable degree. Panel 15 did exhibit a continuous core mark-off on the facing; again revealing the inconsistency in bonding encountered with an intermediate less than .001 inch in thickness.

ANALYSIS OF PHASE I TEST PANEL FABRICATION

The Phase I portion of the program was completed with the establishment of the bonding parameters and manufacturing procedures to be utilized in fabricating the Phase II 12x12 inch panels. The difficulties encountered in Phase I were primarily in achievement of high strength bonds. This was attributed directly to intermediate thickness, as the tooling materials, panel and tooling assembly, temperature, time and pressure parameters used, proved to be satisfactory in providing the necessary controls in manufacturing tantalum honeycomb panels. Quartz-lamp radiant-heating operating in a closed-loop feedback automatic-temperature-control system proved to be adaptive in providing close control of bonding cycles.

The limited success experienced with fabricating panels using a titanium intermediate vapor-deposited onto the core edges was attributed to the thickness of the deposit rather than to any aspects of the deposition process itself. It has been shown that titanium can be deposited free of contamination on the core edges. The vapor deposited honeycomb core can then be vacuum heat-treated, expanded, and cleaned without experiencing any flaking or spalling of the deposit. It is felt that with the required amount of titanium deposited on the core edges, high strength bonds can be attained. Time limitations of the program have prevented this next step of depositing the required titanium on the core from being taken. However, this step is mandatory if the full potential of tantalum honeycomb structures is to be realized at temperatures of 2800F and above. The decision was made to use foil intermediate for all Phase II panels since program funding was not sufficient for a vapor deposition development project, and the necessary time involved for such an effort would result in prohibitive delays. The work performed during Phase I yielded the following bonding parameters which were to be employed during Phase II:

Temperature - 2250F
Time - 3.5 hours
Pressure - 1000 psi
Intermediate - .0015 inch Ti-55 foil (structural)
.0005 inch Ti-75-foil (heat shield)

An analysis of the panels fabricated in Phase I are summarized in Table XIII.

TABLE XIII

DATA SUMMARY FOR 6 x 6 INCH PHASE I TEST PANELS

PANEL NO.	ALLOY	BONDING TEMP °F	TIME-Hrs.	INTERMEDIATE	ROOM TEMPERATURE FLATWISE TENSION (psi)	2800F FLATWISE TENSION (psi)	ELECTRON MICRO- PROBE ANALYSIS
1	Ta-10W	2250	2.5	.0005" Ti-75A foil	324 and 370	None	Maximum Ti Content 31%
2	T111	2250	2.5	.0005" Ti-75A foil	474 and 560	114	---
3	T111	2300	2.5	.0005" Ti-75A foil		Poor Bonds - No Tests	---
4	T111	2300	2.5	Vapor Deposited Ti (.0005")		Poor Bonds - No Tests	---
5	T111	2300	2.5	Vapor Deposited Ti (.0005")		Poor Bonds - No Tests	---
6	T111	2350	2.5	.0005" Ti-75A foil		Envelope Rupture - No Tests	---
7	T111	2250	2.5	.0005" Ti-75A foil		Poor Bonds - No Tests	---
8	T111	2250	5.0	.0005" Ti-75A foil	251 and 188 - lost rest of panel face- sheet due to poor bond		---
9	T111	2250	2.5	.0005" Ti-40A foil .0005" Ti-75A foil	198 and 168 Ti-40 failures 262 and 206 Ti-75A failures	--	---
10	T111	2250	2.5	.0005" Ti-75A foil .0015" Ti-55A foil	432 and 684 Ti-75A failures 90 and 122 Ti-75A failures		---
11 *	T111	2250	3.5	.0015" Ti-55A foil	2,000	245	52%
12 (.008")	T111	2250	3.5	.0005" Ti-55A foil	Thermal Cycle-2100F, 24 Hrs -3400F, 1 Hr. Result - mild embrittlement of core		---
13	T111	2250	3.5	.001" Ti-55A foil	1000 & 1100	175	---
14	T111	2250	3.5	Vapor deposited Ti (.0008")		Poor Bonds - No Tests	---
15	T111	2300	6.0	Vapor deposited Ti (.0008")		Poor Bonds - No Tests	---

* 12 x 12 inch panel

VIII PHASE II - TANTALUM HONEYCOMB PANEL FABRICATION

STRUCTURAL PANELS

During Phase II, thirteen structural panels were fabricated; nine flat panels and four curved panels. Packaging and bonding procedures have already been described in previous sections of the report. No deviations from these procedures were necessary during Phase II panel fabrication, as all panels were successfully bonded. Figures 59 and 60 show typical examples of flat and curved panels after bonding. The panels exhibited no contamination or other visual defects after the bonding cycle. All panels showed a slight core pattern on the facing sheets.

Post Bonding Panel Processing

Processing of the panels after bonding consisted essentially of edge finishing and surface preparations for coating. The panels were initially checked for overall dimensions. The curved edges of the contoured panels were ground flat and parallel to allow for proper alignment of the panels during edgewise compression testing. The panel edges were then TIG welded to form a hermetically-sealed panel and to insure edgemember-facesheet joint integrity. All of the panels were ultrasonically inspected. All welds and sharp corners were radiused by sanding to facilitate coating. The panels were finally sand blasted to provide an adherent coating surface. A flat panel after processing is shown in Figure 61.

Welding

Weld requirements for the structural panels consisted essentially in providing a welded edge to hermetically seal the panels and produce added structure integrity. All welding was performed by the TIG welding process. No difficulties were encountered in welding the flat panels as evidenced by subsequent visual and dye penetrant inspection. Problems did arise during welding of the edges of the curved panels. These difficulties were intermittent as they did not occur on all of the curved panels. Two panels exhibited no weld defects while two panels showed small weld cracks and slight blistering of the facesheet in the vicinity of the weld. These defects occurred mainly on the curved edge of the two panels. The reason for the weld cracks on the one panel was probably due to insufficient cleaning of the edge in the cracked area. The cracks were subsequently repair welded and finished flush with the facesheet surface. The slight blistering was attributed to minute pockets of trapped argon in voids between the facesheet and edgemember, which expanded under the weld heat. These defects, however, were not present in the panels during testing, since later analysis of testing procedures dictated the reduction of the edgemember to a 1/4 inch width from the original 1/2 inch width. This eliminated all of the weld defects described above from the panels submitted for structural analysis.

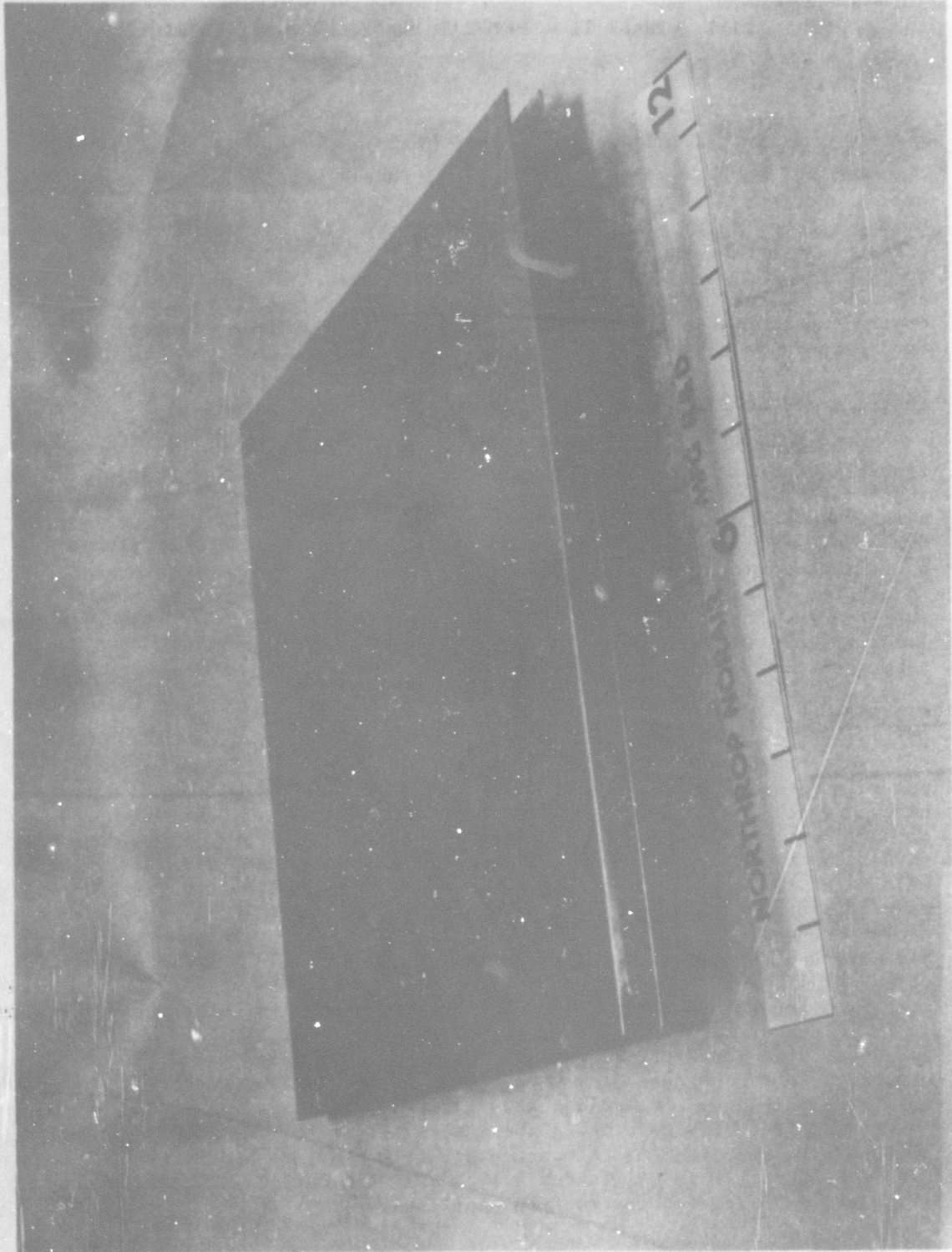


FIGURE 59 TYPICAL FLAT STRUCTURAL PANEL BONDED AT 2250F FOR 3.5 HOURS
EMPLOYING .0015 INCH T4-55A FOIL AS INTERMEDIATE

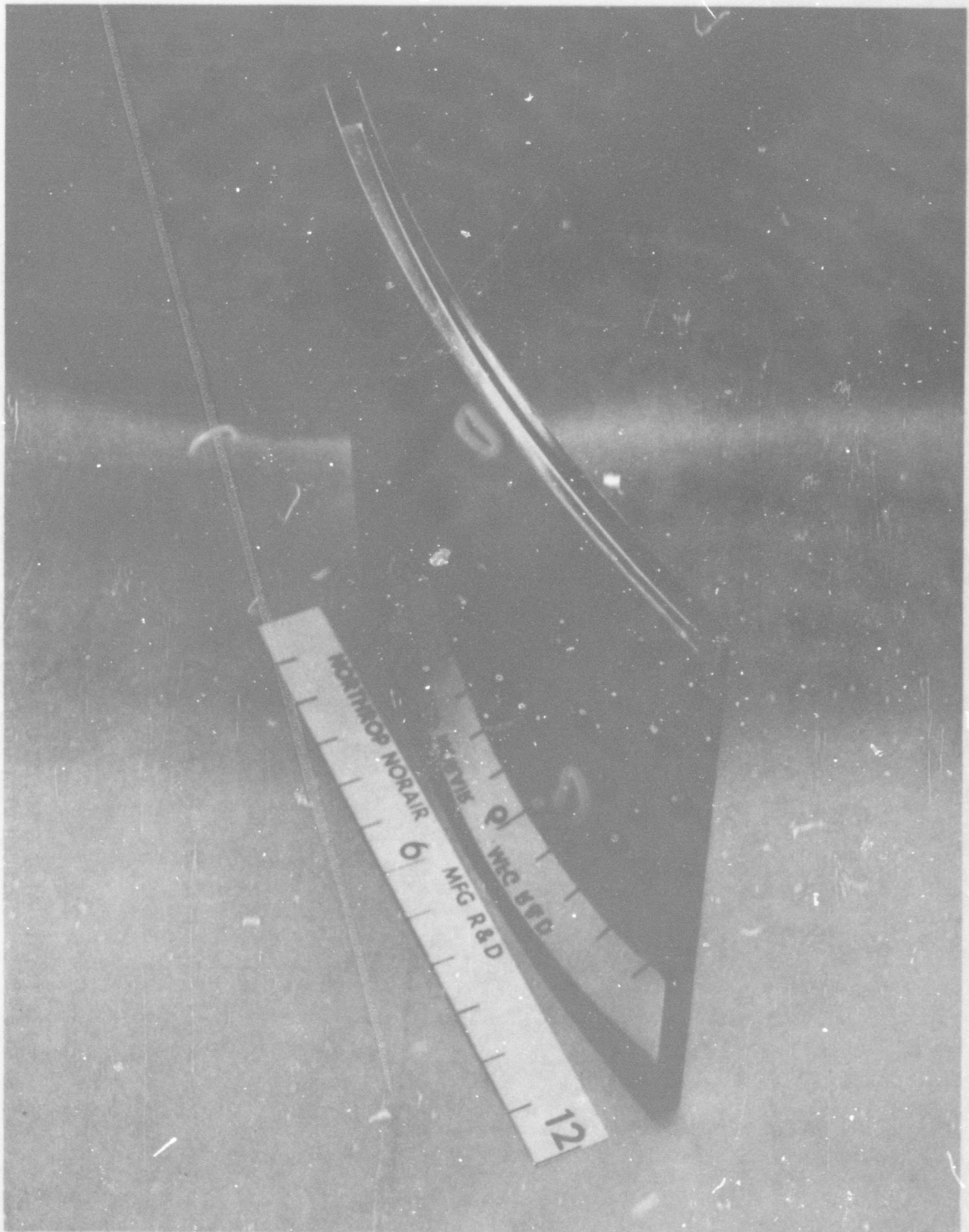


FIGURE 60 TYPICAL CURVED STRUCTURAL PANEL BONDED AT 2250F FOR 3.5 HOURS EMPLOYING .0015 INCH T1-55A FOIL AS INTERMEDIATE

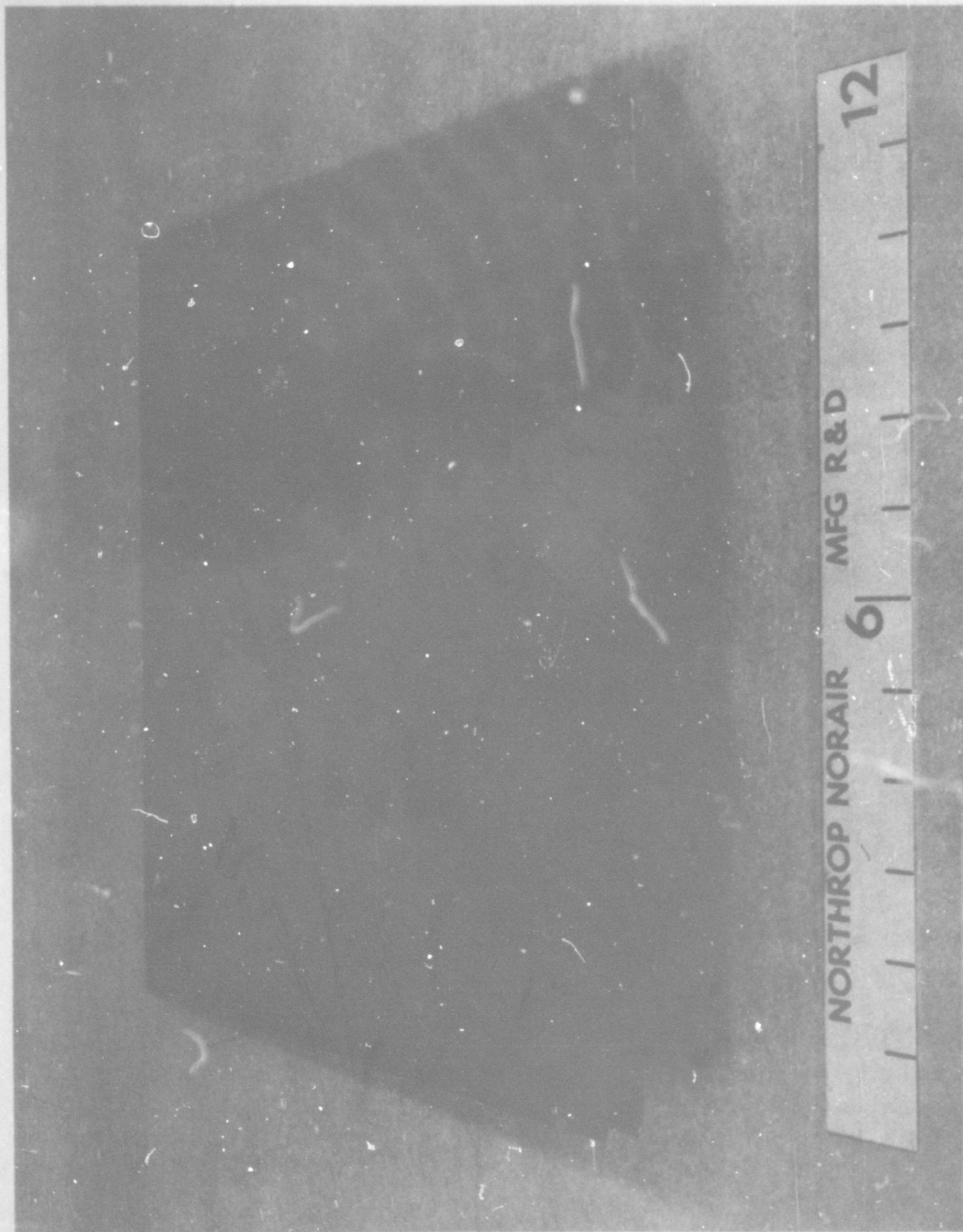


FIGURE 61 FLAT STRUCTURAL PANEL AFTER POST BOND PROCESSING. EDGES ARE
WELDED WITH WELD AND SHARP CORNERS RADIUSSED BY SANDING.
THE PANEL IS THEN VACUUM BLASTED

Joining one inch extensions to the flat structural panels for subsequent load fixture attachment during structural testing was originally contemplated. Both TIG and electron beam welding were tried in accomplishing this task. However, extensive weld cracking and warpage of the extensions were experienced. Fixtures were designed and fabricated in an attempt to remedy the problem.

While the fixture was effective in warpage control, the resultant welds still exhibited cracking. Attempts to repair weld only served to progress the cracks further into the panels. Consequently, the use of panel edge extension for testing purposes were eliminated. Attachments of the load fixtures were made directly to the edgemembers. Due to the severity of weld cracking in the weld of the extensions, two of the flat structural panels were not used for any further evaluations.

Ultrasonic Inspection

C-scan recordings of the structural panels were produced by standard ultrasonic pulse-echo ringing techniques, using an Automation Industries short-focus transducer transmitting and receiving at 15 MHz. Both flat and curved panels exhibited a near 100 percent bond between facesheet and core. As mentioned previously some unbonded areas did exist between the facesheets and edgemembers. However, a high percentage of bonding (80-90 percent) was effected between these two components and in conjunction with the welded edges provided a joint of high structural integrity. A typical ultrasonic trace of one of the panels is shown in Figure 62. Unfortunately as has been the case with ultrasonic inspection techniques in the past, no correlation could be made with joint bond strength.

Dimensional Stability

The structural panels were dimensionally checked and the results are tabulated in Table XIV. All of the panels were found to be within satisfactory dimensional tolerances except for Panel I which exhibited an out-of-flatness of .034 inch exceeding the target .022 inch maximum. This deviation, however, proved to be of little consequence to the structural integrity of the panel as revealed by subsequent structural tests. The length and width dimensions of the panels could be brought within closer tolerances by trimming the panel sides, but was not deemed necessary for the current program. The curvature of the curved panels was held to within 3 percent of nominal. The small deviation obtained in the radius of curvature is indicated in Figure 63 showing one of the panels matched to a machined form-tool used in the program.

Density

Weight measurements made on the flat panels ranged from 3.88 pounds to 4.13 pounds. The nominal dimensions of a flat panel were .524x12x12 inches. These values are equivalent to an average bulk density of approximately 96 lbs/ft³.

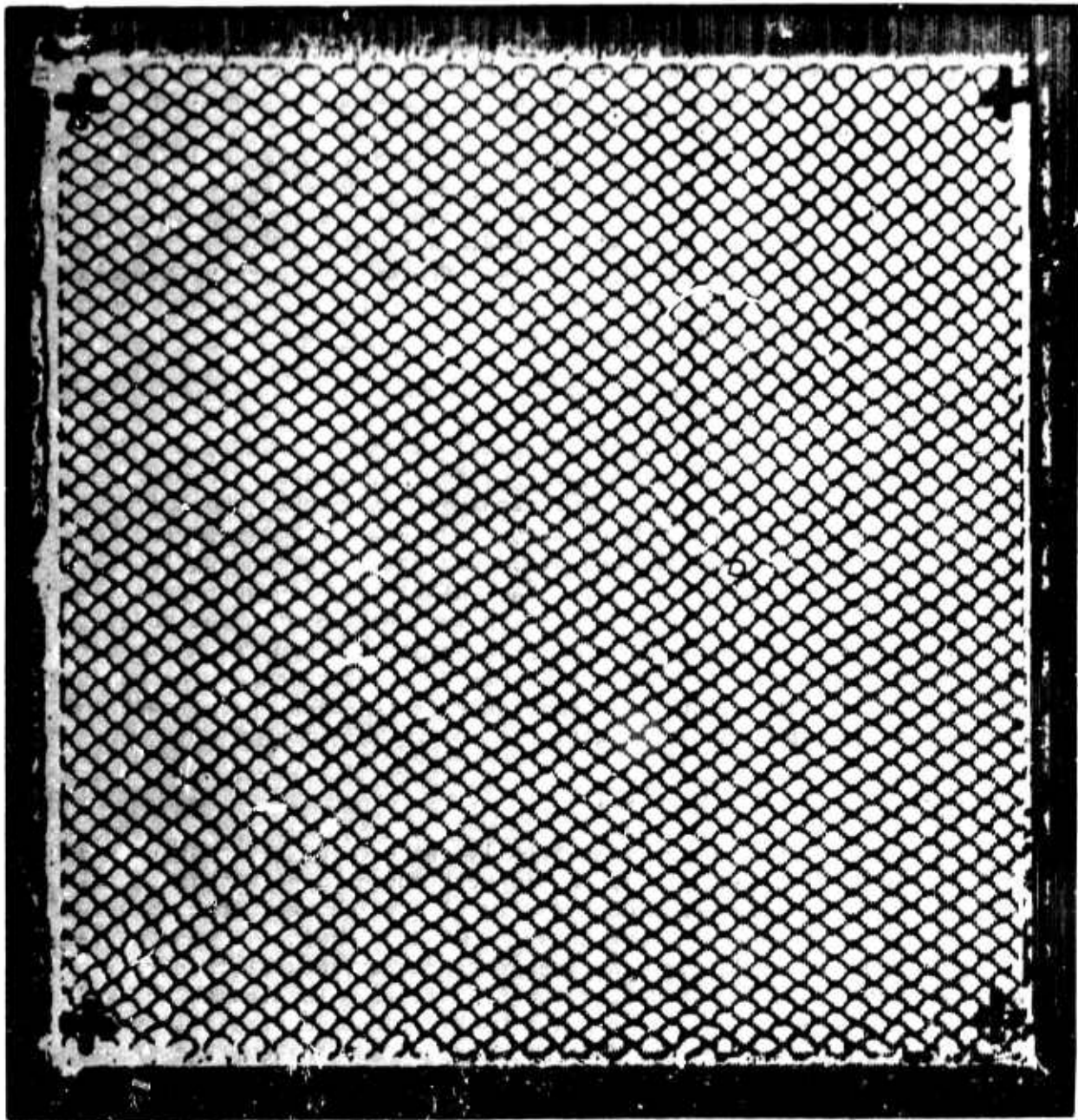


FIGURE 62 TYPICAL ULTRASONIC TRACE OBTAINED ON FLAT STRUCTURAL PANELS. BLACK LINES REPRESENT EDGE OF PANEL

TABLE XIV DIMENSIONAL VARIATIONS OF STRUCTURAL PANELS

Panel No.	Type	Length (In.)	Width (In.)	Width (In.) (Inner Skin)	Thickness (In.)	Flatness (In.)	Radius of Curvature (In.)	Weight (Lbs.)
1	Flat	+ .010	+ .025	-	+ .001	.034	-	4.00
2	Flat	+ .015	+ .025	-	+ .005	.020	-	4.13
3	Flat	+ .030	+ .033	-	+ .001	.016	-	3.91
4	Flat	+ .020	+ .035	-	+ .002	.014	-	3.99
5	Flat	+ .035	+ .035	-	+ .001	.012	-	4.10
6	Flat	+ .035	+ .030	-	+ .001	.018	-	3.95
7	Curved	+ .010	+ .015	+ .030	+ .001	-	+ .27	-
8	Curved	+ .020	+ .010	.000	+ .002	-	+ .88	-
9	Curved	.000	+ .020	.000	+ .002	-	+ .18	-
10	Curved	.000	+ .010	+ .020	+ .001	-	+ .35	-
	Nominal	12.000	12.000	11.800	.524	-	29.87	

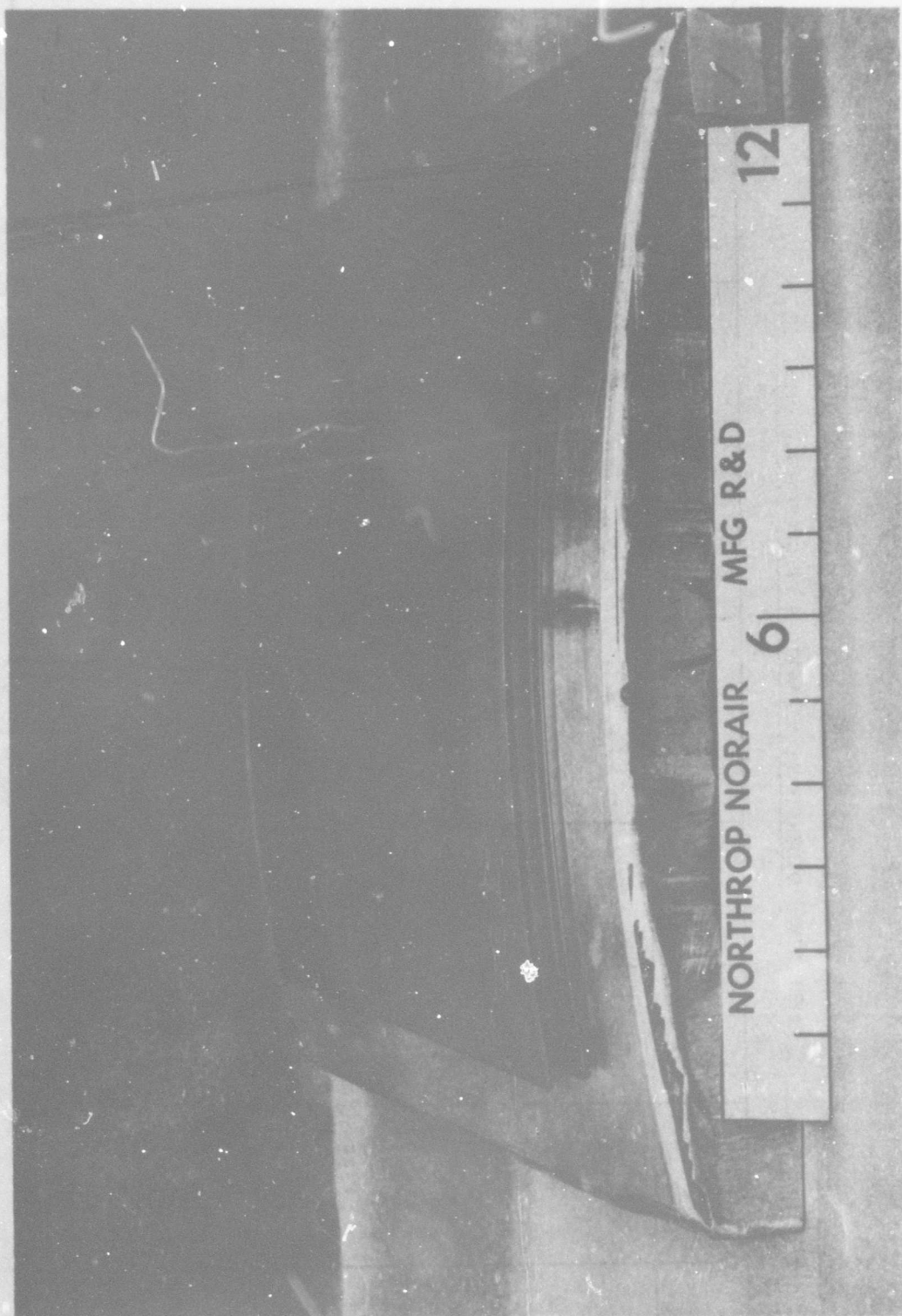


FIGURE 63 A CURVED PANEL MATCHED TO MACHINED DIE ILLUSTRATING
CLOSE CONFORMANCE TO DESIGN RADIUS OF CURVATURE

HEAT SHIELD PANELS

Eight heat shield panels were fabricated during Phase II; six flat and two curved. The inner and outer skin surfaces of a flat and curved panel are shown in Figures 64 thru 67. The bonding parameters employed in fabricating these panels remained the same as those used in the manufacture of the structural panels, 2250F for 3.5 hours. Ti-75A, .0005 inch foil, was utilized as intermediate except in the stepped edge portion of the panel where .001 inch foil was used. This was done since core-to-skin fitup proved to be more critical in this area than in other sections of the panel. Several problems developed during the course of manufacturing these panels, resulting in structures somewhat less than desirable for actual heat shield service usage. These problem areas were, 1) welding 2) dimensional stability, and 3) bond strength. Each of these difficulties are discussed individually in the following sections and should be remedied before the use of tantalum honeycomb panels for actual heat shield applications can be realized. Remedial action could not be fully accomplished within the time limitations of the current program. They can only be identified herein for future reference.

Dimensional Stability

The initial problem encountered in the manufacture of the heat shield panels was that of flatness. None of the flat panels exhibited out-of-flatness tolerances within the .020 inch maximum limit proposed in the program. This was due to 1) the out-of-flatness of the .040 inch molybdenum tooling sheets obtained from the mill, and 2) the lack of stiffness inherent in the heat shield panels as compared to the structural panels which employed channeled edgemembers. The .040 inch tooling sheet was later replaced with two .020 inch sheets of much improved flatness quality. The lack of stiffness inherent in the panel itself could only be compensated for by incorporating a suitable strongback within the tooling used for bonding. However, this could not be done within the span of time remaining in the program due to major changes involved in the existing tooling already manufactured. Consequently, flatness was compromised as it was felt no appreciable effects would be encountered by the dimensional "instability" of the panels during the proposed testing schedule. The dimensional tolerances of the two panels coated are given in Table XV. The out-of-flatness experienced on these panels would have to be remedied with the proposed strongback before the panels could be utilized in actual service.

TABLE XV

DIMENSIONAL VARIATIONS OF FLAT HEAT SHIELD PANELS

	<u>LENGTH (in.)</u>		<u>WIDTH (in.)</u>		<u>THICKNESS (in)</u>		<u>FLATNESS (in.)</u>
	<u>Inner Skin</u>	<u>Outer Skin</u>	<u>Inner Skin</u>	<u>Outer Skin</u>	<u>Panel</u>	<u>Stepped Edge</u>	
Panel 1	-.009	-.001	-.005	+.002	+.002	+.003	.035
Panel 2	-.008	-.010	-.007	-.008	+.002	+.003	.040
Nominal	11.000	12.000	11.000	12.000	.391	.195	.020 max.

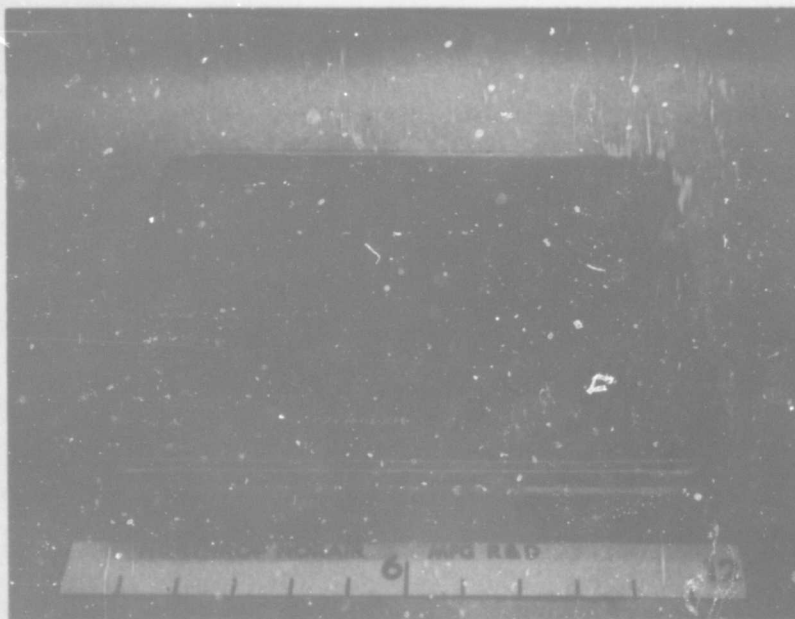


FIGURE 64 INNER SKIN SURFACE OF BONDED FLAT
HEAT SHIELD PANEL

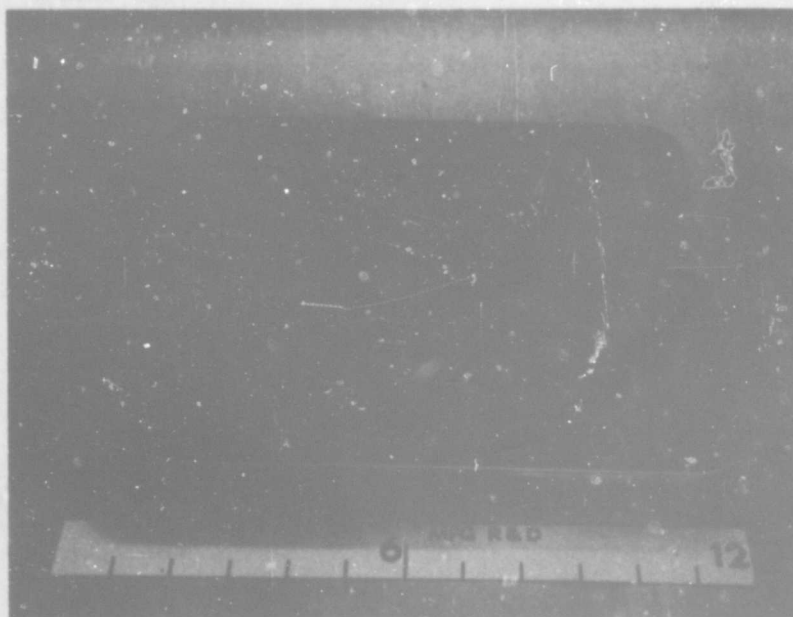


FIGURE 65 OUTER SKIN SURFACE OF BONDED FLAT
HEAT SHIELD PANEL



FIGURE 66 INNER SKIN SURFACE OF CURVED
HEAT SHIELD PANEL

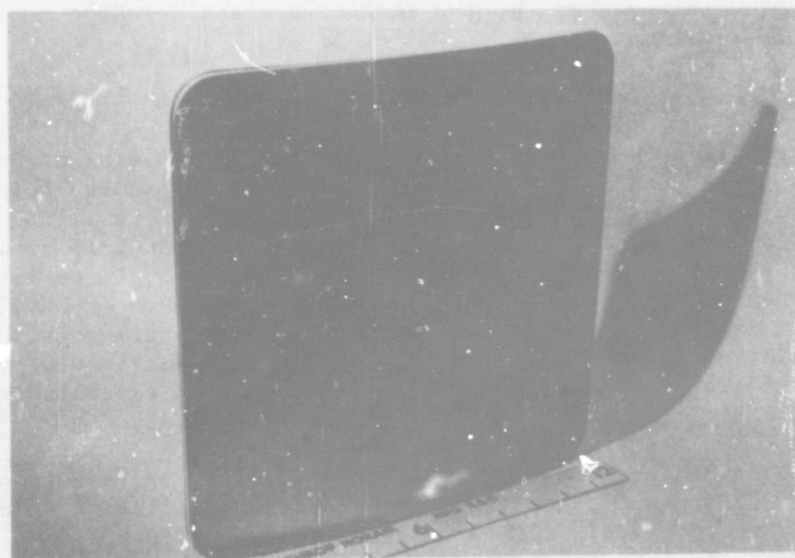


FIGURE 67 OUTER SKIN SURFACE OF CURVED
HEAT SHIELD PANEL

All other above dimensions were considered within reasonable limits although no tolerances were specified, except for thickness, where a maximum deviation of .005 inch was allowed. As may be seen actual maximum deviation in thickness of the panels was .003 inch. No face indentations into the core cells of any measurable magnitude were apparent on the panels, although a very slight core pattern could be seen on the facesheets. Due to the bow in the panels, accurate measurements of waviness were difficult to obtain. However, it was determined that any waviness of the panels was definitely well within the .031 inch maximum specified.

Bond Strength

The bonded joint strength within the heat shield panels was somewhat less than desired. In bonding the heat shield panels two phenomena came into conflict. As was determined in previous investigations in the program an intermediate thickness of .001 inch minimum, preferably .0015 inch, was required to obtain satisfactory bond strengths. On the other hand, an intermediate thickness in this range would have resulted in sufficient "free" titanium foil in the panel, not involved in the actual bond, to effect rapid embrittlement of the core at test and service temperatures. Since vapor deposition techniques could not be developed sufficiently to apply the exact amount of titanium on the core edges, thereby eliminating the presence of this excess titanium, bond strength had to be compromised to reduce the embrittlement tendencies of the titanium intermediate. While in theory these panels are not load supporting structures, in actual service the bond strength should be improved over that obtained with only an .0005 inch titanium intermediate thickness. With development of a technique such as vapor deposition the necessary .0015 inch thick intermediate could be applied to the honeycomb core edges yielding more than adequate bond strength and at the same time greatly reduce possible panel embrittlement in service.

Welding

Welding requirements for the heat shield panels consisted of hermetically sealing the panels around the perimeter and at the panel access holes. The location of the welding required to perform this function is illustrated in Figure 68 with a cross section of each location diagrammed in Figure 69. This aspect of the program proved to be very difficult. Although the Ta-8W-2Hf alloy is considered a weldable alloy, persistent cracking of the welds and adjacent base metal occurred on all panels. Weld tests were previously performed on simulated specimens with no unusual difficulties; however, it later became apparent, that, while welding parameters could be established on specimens, welding conditions could not be completely simulated.

Three welding processes were utilized; TIG, laser, and electron beam. Initially, TIG welding was attempted with no success, as severe weld cracking was immediately encountered. It was apparent that heat inputs were too great with this process and subsequent welding would have to be performed with either electron beam or laser welding techniques to significantly reduce the amount of heat energy applied during welding.

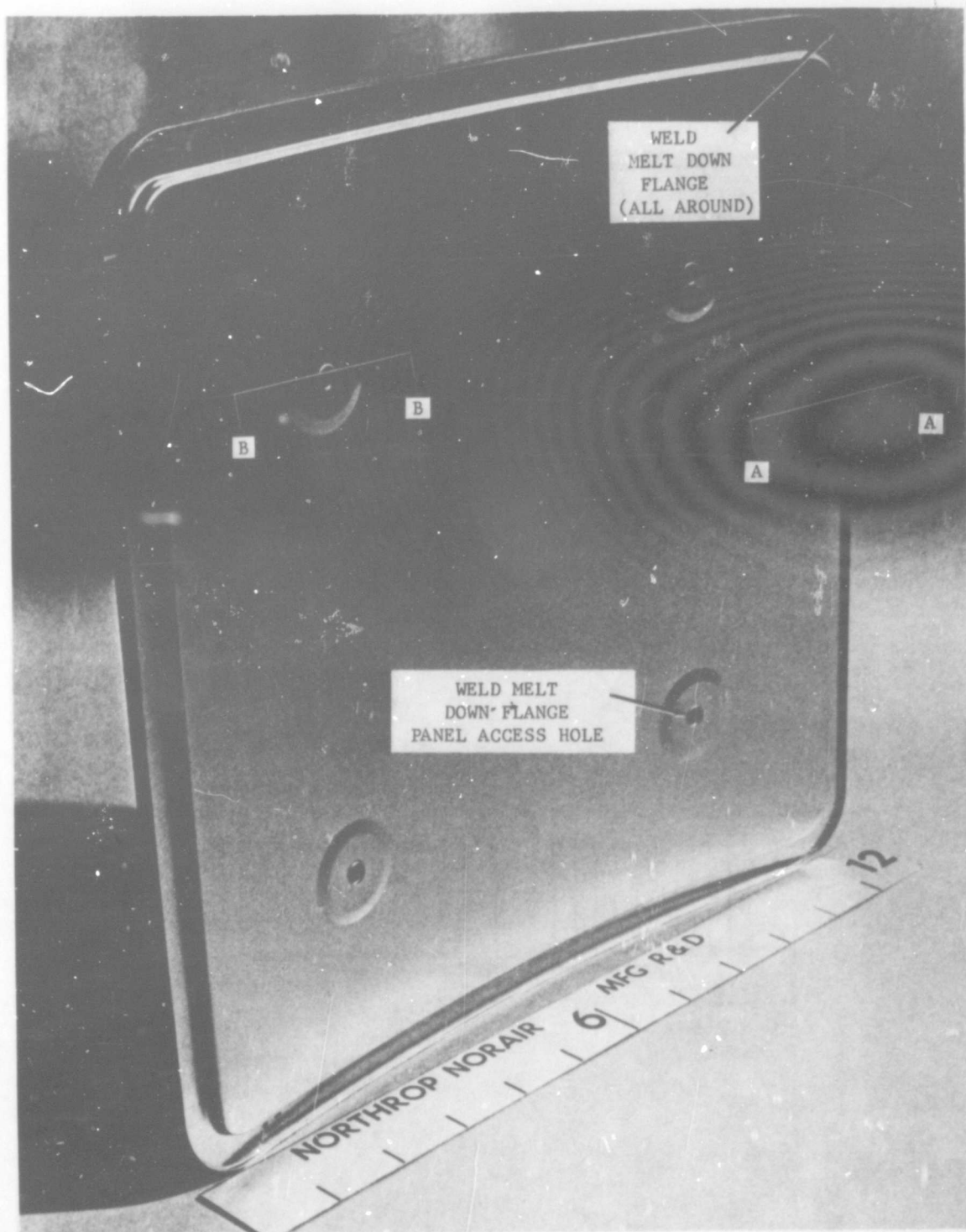
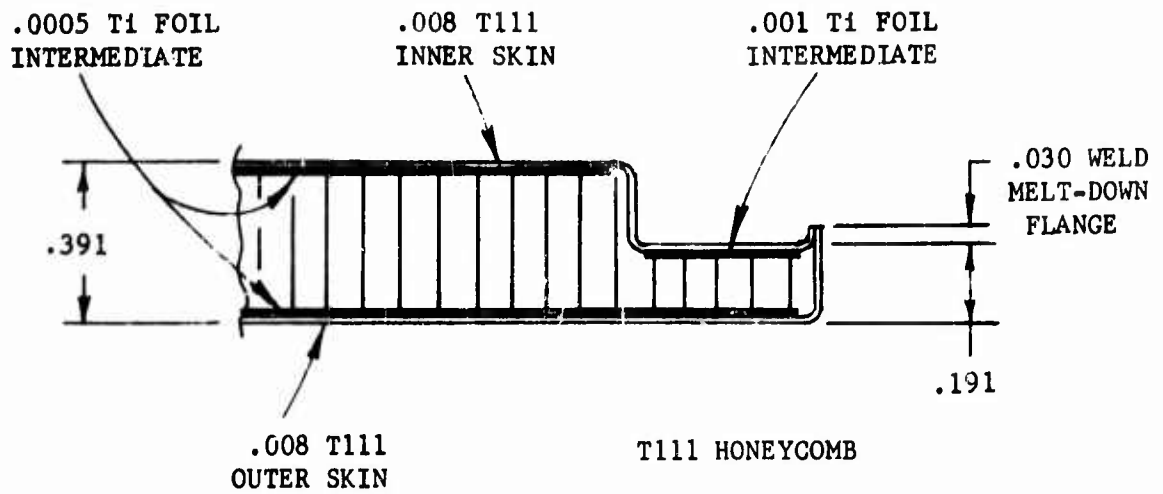
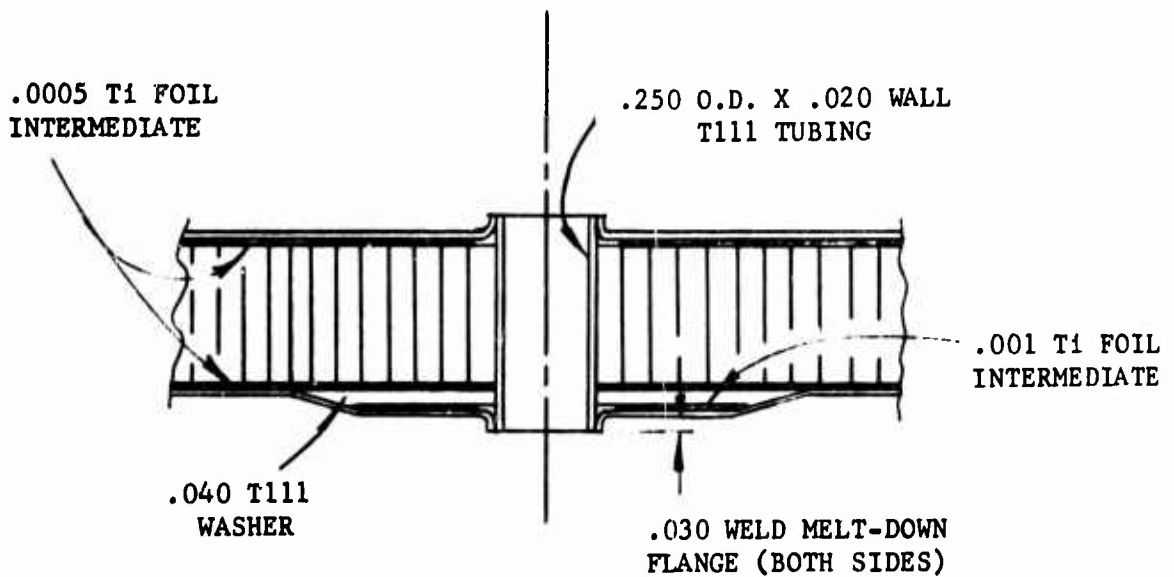


FIGURE 68 HEAT SHIELD PANEL SHOWING WELDING REQUIREMENTS AND LOCATION



SECTION A-A



SECTION B-B

FIGURE 69 CROSS SECTIONAL SCHEMATICS OF WELDING LOCATIONS SHOWN IN FIGURE 68

Laser Welding

Certain aspects of laser welding appeared attractive for welding refractory alloys. These included less warpage, the ability to generate beam power without a chamber, easier control of the beam with simple, stable optics, and the narrow zone of fusion which is effected. Consequently, this technique was investigated with the welding of several test specimens by Metals Joining Corp., Redondo Beach, California. The welding equipment employed for this study was a prototype, embodying several proprietary developments by the said firm. It utilized a pulsed ruby laser pumped by a xenon flash lamp, and an electrostatic energy storage system. The system provided a maximum pulse repetition rate of 22 pulses per second.

The laser welding head and control console were similar to that used with MIG/TIG welding.

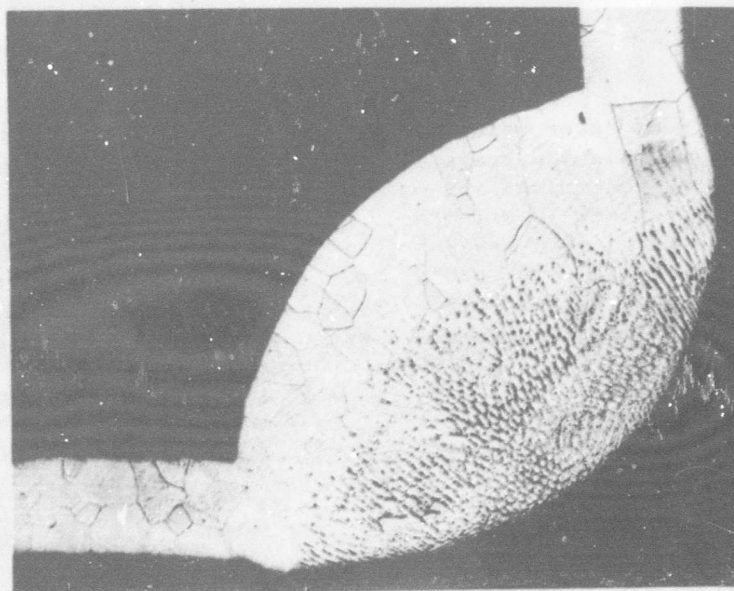
The laser unit used was rated at 47 joules, which is considered powerful for this type of equipment. However, due to the machine's inability to operate at full capacity, 32 joules was actually used. This proved to be inadequate to produce sufficient melting of an 0.030 inch melt down flange which would have been required on the actual panel.

Figures 70 and 71 show photomicrographs of TIG and laser welded joints, respectively. The laser weld exhibits little melt down of the flange with little or no fusion resulting, whereas, the TIG weld shows complete melt down and fusion of both members. The weld bead produced did contain some porosity and cracks. The bead was quite rough (Figure 72) which would have been an unfavorable factor during the coating of the panels. No further work was done with this technique.

Electron Beam Welding

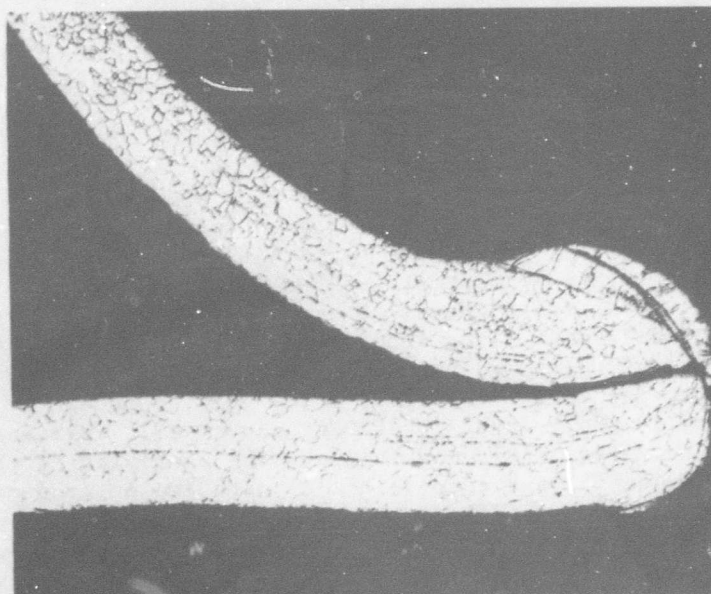
Electron beam welding appeared to be the most promising method of fulfilling the welding requirements of the heat shield panels. Although many variations in applying this welding process were attempted, all of the panels exhibited cracking to varying degrees. Cracking for the most part ran transverse to the weld and in most cases into the adjacent base metal. Complete melt down of the weld flanges was not accomplished because the additional heat input caused an increase in the degree of cracking. Consequently, the requirements on later panels were relaxed to effect only a seal, irrespective of final panel geometry. This would have allowed the panels to be coated and tested, but it would not have been possible to mate two or more panels for actual service usage, as a portion of the flange would have remained around the perimeter of the panel. Due to the difficulties encountered during welding, two panels were rendered unusable for testing and had to be scrapped. The goal which eventually was pursued was to minimize cracking in later panels in anticipation that the coating applied to the panels would flow over and effectively seal the panels for test purposes.

Several potential sources of this cracking problem were expounded and investigated to the extent possible with the limited quantity of specimens. These possible causes were:



MAG. 75X

FIGURE 70 PHOTOMICROGRAPH OF CROSS SECTION OF
TIG WELDED TANTALUM SHEET



MAG. 75X

FIGURE 71 PHOTOMICROGRAPH OF CROSS SECTION OF
LASER WELDED TANTALUM SHEET. NOTE
LACK OF MELT DOWN OF SHEETS AND THE
RESULTANT LACK OF FUSION

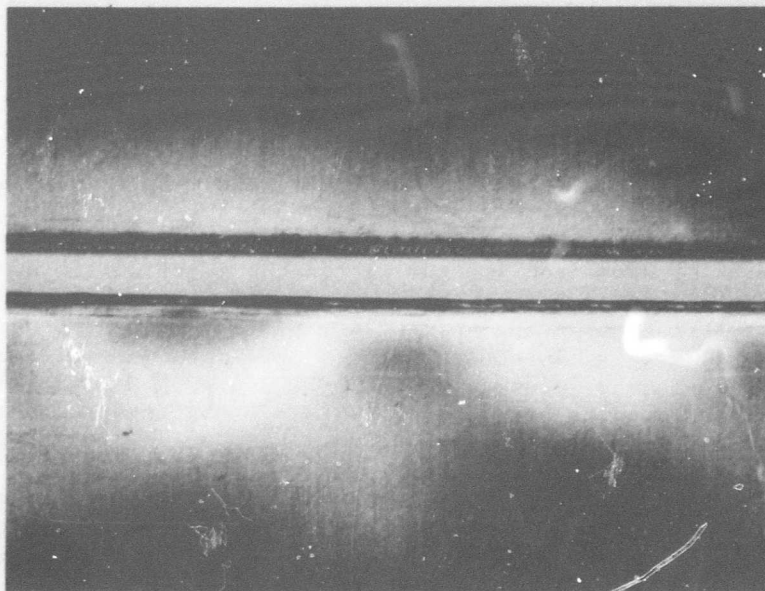


FIGURE 72 A COMPARISON OF BEAD APPEARANCE OF LASER (TOP) AND TIG (BOTTOM) WELDS IN TANTALUM SHEET. HIGHLIGHTED AREAS REPRESENT DISTORTION OF THE SHEET DURING WELDING.

1. Titanium contamination during welding from the intermediate used in bonding.
2. Reduction in weldability resulting from the solid state bonding operation.
3. Fit-up of the inner and outer skin flanges at the location of welding.
4. Possible contamination of the tantalum by interstitial gases entrapped inside the panel at the weld joint.
5. High residual stresses due to restraint resulting from panel design.
6. Weld flange height and surface finish.
7. Entrapment of extraneous matter within the joint during preparation.

The effect of titanium on the weldability of T111 proved to be far less detrimental than was originally contemplated. Specimens were welded with titanium foil placed in the joint as shown in Figure 73. No cracking occurred and the only difference noted between joints with and without titanium was the discoloration evident with the titanium joint.

However, for precautionary purposes the titanium intermediate was recessed 1/4 inch from all welded joints in the panel. It seemed apparent that titanium in itself will not cause cracking in T111 but may promote cracking with other factors present.

The effects of the bonding cycle on the T111 alloy were not readily apparent. From an analysis of this operation it did not appear that any deleterious effects to the material's weldability would have occurred. Bead on sheet tests showed no cracking either on the virgin or processed material. Hardness tests did show a slight increase in hardness after the bonding cycle, but it was not so significant as to cause the material to be overly crack-sensitive.

Fit-up, or mating, of the inner and outer skin weld flanges was considered a critical factor, as was joint preparation. A near perfect match between the two flanges was extremely difficult due to variations incurred during forming, especially at the panel corner radii. Gaps between the two mating flanges ranged from .001 inch to .010 inch. Since cracking occurred at the .001 inch as well as the .010 inch mismatch locations, it was felt that metal-to-metal contact would be necessary. Several panels were thus welded by wedging an .008 inch tantalum filler strip between the flanges as shown in Figure 74. In this manner only a single surface was available to melt down and effectively seal the panel. In addition, metal-to-metal contact between the flanges was attained for further melting if desired. This technique offered little improvement in performance as weld cracks still appeared.

The possibility of contamination by the interstitial gases, H_2 , O_2 , N_2 was considered to be the most probable cause of cracking. This contamination could have resulted during the EB welding operation, since no purging with an inert gas was possible. The chamber was merely pumped down to what was

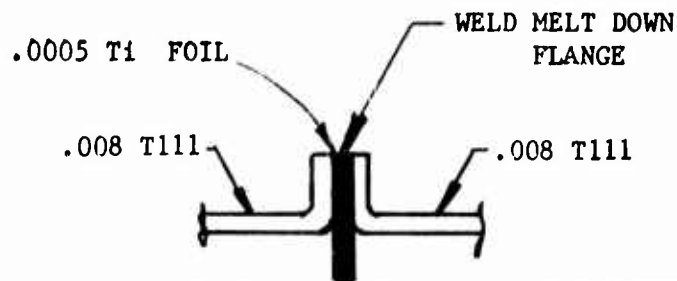


FIGURE 73 SIMULATED WELD JOINT TO DETERMINE EFFECT OF TITANIUM ONLY ON TANTALUM WELDS

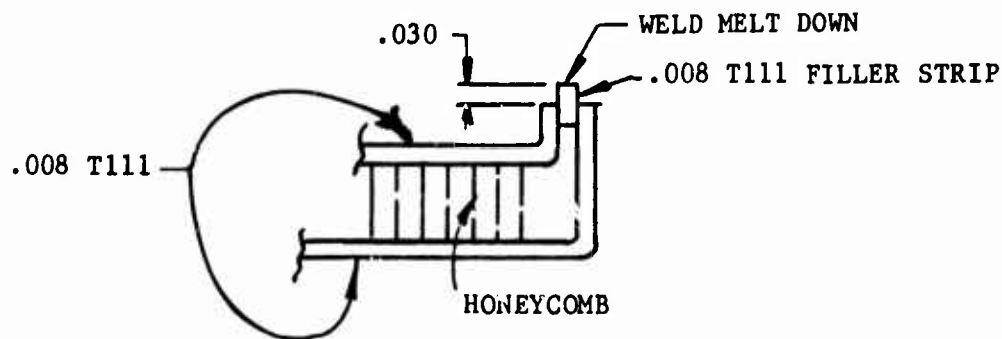


FIGURE 74 USE OF FILLER STRIP IN JOINT TO EFFECT METAL-TO-METAL CONTACT AND TO PROVIDE EASIER INITIATION OF MELTDOWN

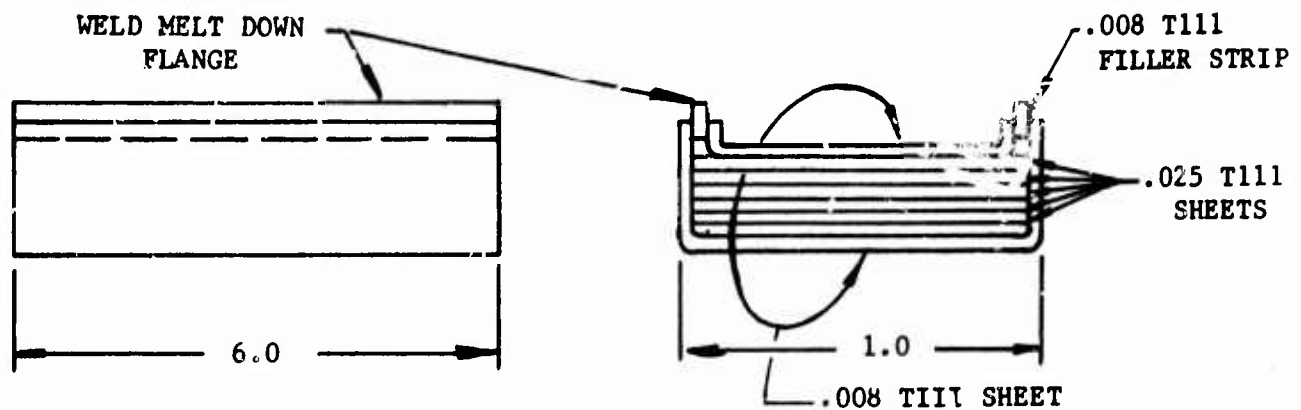


FIGURE 75 SIMULATED SPECIMEN USED TO DETERMINE THE EFFECTS OF ENTRAPPED AIR, PUMP DOWN TIME, AND VACUUM LEVEL ON TANTALUM PANEL WELDABILITY. T111 SHEET WAS USED TO SIMULATE HONEYCOMB CORE BAFFLE EFFECT

indicated as a safe operating level (2×10^{-4} to 8×10^{-5} mm Hg) with welding commencing shortly thereafter. The interstitial contamination during welding could have resulted from small quantities of air remaining in the chamber or from entrapped air within the panel adjacent to the weld joint. Microhardness tests could not be taken on the panel itself without destroying the panel. In an attempt to prove or disprove this theory, simulated panel specimens were fabricated as diagrammed in Figure 75. Tantalum strips were employed to simulate the honeycomb maze for entrapment of air, with the sides of the specimens having a weld joint geometry closely conforming to that of the panel. One specimen was placed in the EB chamber and pumped down to the vacuum level used in actual panel welding, and welded. The other specimen was pumped down to the same level and held overnight in vacuum.

An overnight increase in vacuum chamber pressure from .1 micron to 1000 microns was noted. The chamber was then pumped down for an additional two hours to .1 micron and welded. Both specimens exhibited no cracking although both contained heavy bluish-black discolorations identical to that witnessed on all of the panels welded. This discoloration was associated with the vaporization of a small portion of the tantalum during welding with the vapor being redeposited on the panel or specimen surface (as a very fine powder). This phenomenon is characteristic of E.B. welding. If this discoloration had been caused by contaminants it would seem that weld cracking would have resulted. Although the actual validity of this test may be questionable, it may be surmised that if contamination had occurred, it was not sufficient to produce weld cracking in the specimens. Residual stress due to restraint imposed on the weld as a result of panel design was considered as a possible factor in the cracking problem. The configuration used in the edge closure is one generally considered to be practical for welding. The tube sealing welds, however, being circular, present a severe stress condition. Cracking occurred in both regions, but was far more prevalent in the edge closure. The majority of the tube welds were completed without cracks. Since the least favorable portions of the configuration were more successfully welded, it was concluded that weld restraint in itself was not a determining factor. Some level of residual stress certainly exists in the welded joints, and in combination with contamination and/or brittleness of the base metal could result in cracking.

Joint preparation, filing to produce equal flange height, obtaining a good flange surface finish, and cleaning were also considered critical. While cleaning of the joint could easily be accomplished with suitable organic solvents such as alcohol, MEK, etc., minute foreign particles entrapped in the joint would be extremely difficult to remove. During the progress of this activity, special effort was applied to control these factors, but technique improvements did not eliminate the welding problem.

Several variations in E. B. welding techniques were tried in an effort to reduce or possibly eliminate weld cracking. A continuous travel technique was found to be neither economical nor technically possible. The precise joint-following capability necessary for the heat shield configuration and gage was not available. In addition, joint fitup consistency was not sufficient to permit the same welding schedules to be used all around a given

panel. Although continuous energy input offers some theoretical advantages regarding crack sensitive materials over pulsed energy input, it is doubtful that the former technique would have prevented or even reduced cracking in this case. Consequently, pulsed energy input was considered more suitable for the panels in question. This technique allowed the joint configuration to be easily followed by manipulating the work table within the E.B. chamber. In addition, the pulsed technique permitted the weld schedules to be tailored to suit the changing joint condition. The various weld schedules employed during actual panel welding are given below.

<u>VOLTAGE</u> <u>(KV)</u>	<u>CURRENT</u> <u>(MA)</u>	<u>FOCUS</u>	<u>TRAVEL</u>	<u>DECAY</u>	<u>PULSE</u> <u>WIDTH</u>	<u>PULSE</u> <u>FREQ.</u>	<u>VACUUM</u> <u>LEVEL (MM)</u>
80	3.5	.010"	Slow &	80%	10	3.3	2×10^{-4}
to	to	to	Inter-				to
100	6.0	.020"	rupted				8×10^{-5}

Direct visual monitoring during E. B. welding, and examination of the resulting panel welds resulted in the following observations:

1. Certain phenomena were localized - welding might proceed for several inches along an edge closure with good control and stable performance. Then a region would be encountered where sparking appeared, sometimes accompanied by expulsion, erratic melting and agglomeration of the molten metal
2. In some cases melt-through occurred, requiring later repair attempts. The regions exhibiting these reactions were at random locations and of random extent. Once past such a spot, weld control was again effective. Examination of the resulting joint always showed cracking associated with the above condition. Repair welding was extremely difficult, and often unsuccessful, due to the apparent contamination existing.

During the bonding cycle the full periphery of the panel was vented by galleries and perforations in the tooling items in the envelope. Any contaminations existing inside the envelope could flow equally to the entire periphery. Under these conditions, severely localized contamination in regions along the panel edges is improbable. If contamination occurred during the bonding cycle, it would more likely be common to all parts of the panel which were later welded. A possibility exists that atmospheric gases could have been ingested during exposure to the atmosphere prior to welding. The honeycomb cells were bonded to the facings in a vacuum, at elevated temperature. On cooling and exposure to air, a differential would exist tending to drive atmospheric gases through any microscopic opening which might exist into the interior of the honeycomb cells. The panels were exposed to air for several days before welding.

This observation was strengthened by results on the last panel welded. In bonding this panel, the procedure was changed to include a 14 hour (overnight) period immediately following the thermal cycle during which the assembly was held in argon at atmospheric pressure. This was done by argon backfilling the protective envelope used in the bonding cycle. The intent was to allow argon gas to infiltrate through any opening that may have existed in the joints. A very good fit-up was accomplished on this panel, also, and no filler strips were used, thus making possible a lower energy input to achieve flange fusion. Improved results were achieved, with completely crack-free sealing of all tube ends, and only four microscopic cracks on the entire panel periphery.

In conclusion, the weld cracking experienced in attempting to fulfill the weld requirement of the heat shield panels was probably due to a combination of factors rather than to any single one. It is the actual identification of these factors, and their interactions which could not be determined with any degree of certainty although interstitial contamination was considered the chief suspect.

Density

Weight determinations made on the flat heat shield panels yielded a density of 2.3 lbs/ft² for the .391x12x12 inch panel.

IX OXIDATION PROTECTIVE COATING SELECTION AND APPLICATION

In order to provide the necessary protection from oxidation during elevated temperature testing, a suitable coating had to be applied to the panels. An initial survey of several of the more promising coating systems for refractory alloys was made in order to select one which could adequately perform this function. In the selection of a coating for the Ta-8W-2Hf alloy, the following coating systems were considered:

- A. Modified chromium-titanium-silicide.
- B. Fused silicides.
- C. Aluminum-Tin-Molybdenum
- D. Duplex deposited tungsten-silicide.

The modified chromium-titanium-silicon coating was reported to be less protective in the range of 1800F to 3200F on tantalum than on columbium alloy substrates. Coating failures were attributed to:

- 1) depletion of titanium and/or chromium from matrix solid solution rendering the tantalum susceptible to oxidation
- 2) insufficient modification of the silicide to affect temperature upgrading of the refractory properties of the silicide.

The straight silicide coatings showed rapid oxidation behavior at 1800F, 2500F, and 2700F. The 1800F and 2500F affects were attributed to a typical silicide "pest" type failure in this range. The straight and modified silicide coatings also produced severe substrate embrittlement after 3000F exposure. Another problem with the straight silicide is the effect of thermal mismatch between coating and substrate at elevated temperatures which normally produces premature coating failure.

The two most promising coatings considered for tantalum alloys were found to be the Al-Sn-Mo and duplex tungsten-silicide coating.

The Al-Sn-Mo coating produced by Sylvania Electric Products affords good protection of the substrate to 2800F, the limiting design temperature of the structural panel manufactured in this program. Above this temperature, however, appreciable surface recession of the tantalum alloy substrate results due to coating diffusion and liquid alloy attack, although oxidation protection is still afforded. The Al-Sn-Mo slurry coating can be applied simply, is relatively inexpensive, and repairing of the coating in localized areas is easily accomplished. Under simulated service conditions, i.e., mass flow, reduced pressures, and high shear loads, the coating has been reported to be less than desirable in performance. However, in the current program, the structural panels were to be tested to destruction, encompassing a time exposure at test temperatures of only 15 minutes. Consequently, no evaluation or analysis of the coating could be considered during the course of performing these structural tests on the panels. The main objective of the testing program was to determine the structural integrity of the panels only. Therefore, it was decided that the Al-Sn-Mo coating would satisfactorily provide the necessary protection to the panel, with little or no effect on the panel

itself, for the times and temperatures to be employed during structural evaluation.

Four flat structural panels and four curved structural panels were coated with the Al-Sn-Mo coating by Sylvania Electric Products, Hicksville, New York. The panels, with the coating applied, are shown in Figures 76 and 77. The manufacturing procedure used in applying the coating consisted basically of the following steps:

1. Check all edges to ensure no cracks or other defects in the edge welds of the panels.
2. Sandblast the panels; this constituted the only cleaning procedure used.
3. Mix the appropriate powders with a suitable lacquer vehicle to form the coating slurry.
4. Coat panels by dipping into slurry bath.
5. Bake panels at 1900F for 1/2 to 1 hour.
6. Sandblast coating to ensure required adhesion of coating to panel.

Inspection of the panels after coating revealed generally good coverage at corners and radii, which are usually the most difficult areas to coat. Several panels did exhibit some defects on the panel edges consisting of small cracks and chipping. These defects are shown in Figures 78 and 79. However, this proved to be of little consequence as these particular panels were later selected for testing at room temperature. The panels exhibiting good coating coverage all over were used in testing at elevated temperatures. The only inspection which could be performed on the coating was visual, as the coating surface was very granular in appearance due to the molybdenum addition. The molybdenum forms angular particles within the coating which effectively reduces run-off during dipping and baking. Consequently, very minute defects such as micro-cracks could very well go undetected.

MOLYBDENUM AND TUNGSTEN DISILICIDE COATINGS

The heat shield panels fabricated during this program, being designed for service temperatures of 3000F-3500F with no structural loading requirements, required a more durable coating at these higher temperatures than could be provided by the Al-Sn-Mo coating. In addition, unlike the structural panels, these panels would encompass more of a test of the coating than of the panel itself, since panel failure would more than likely result from coating performance. Consequently, two types of coatings were considered; one a tungsten disilicide, the other a molybdenum disilicide. These coatings are, in effect, duplex coating systems as the coating process consists essentially of the initial application of a metallic pre-coat on the substrate followed by the diffusion of silicon into the metallic pre-coat to form the silicide coating. Several methods are currently being investigated for applying the tungsten pre-coat to the substrate, some of which are: 1) chemical vapor deposition 2) electrophoretic deposition, and 3) slurry. The chief problem encountered with the first two methods has been non-uniformity of coating thickness.

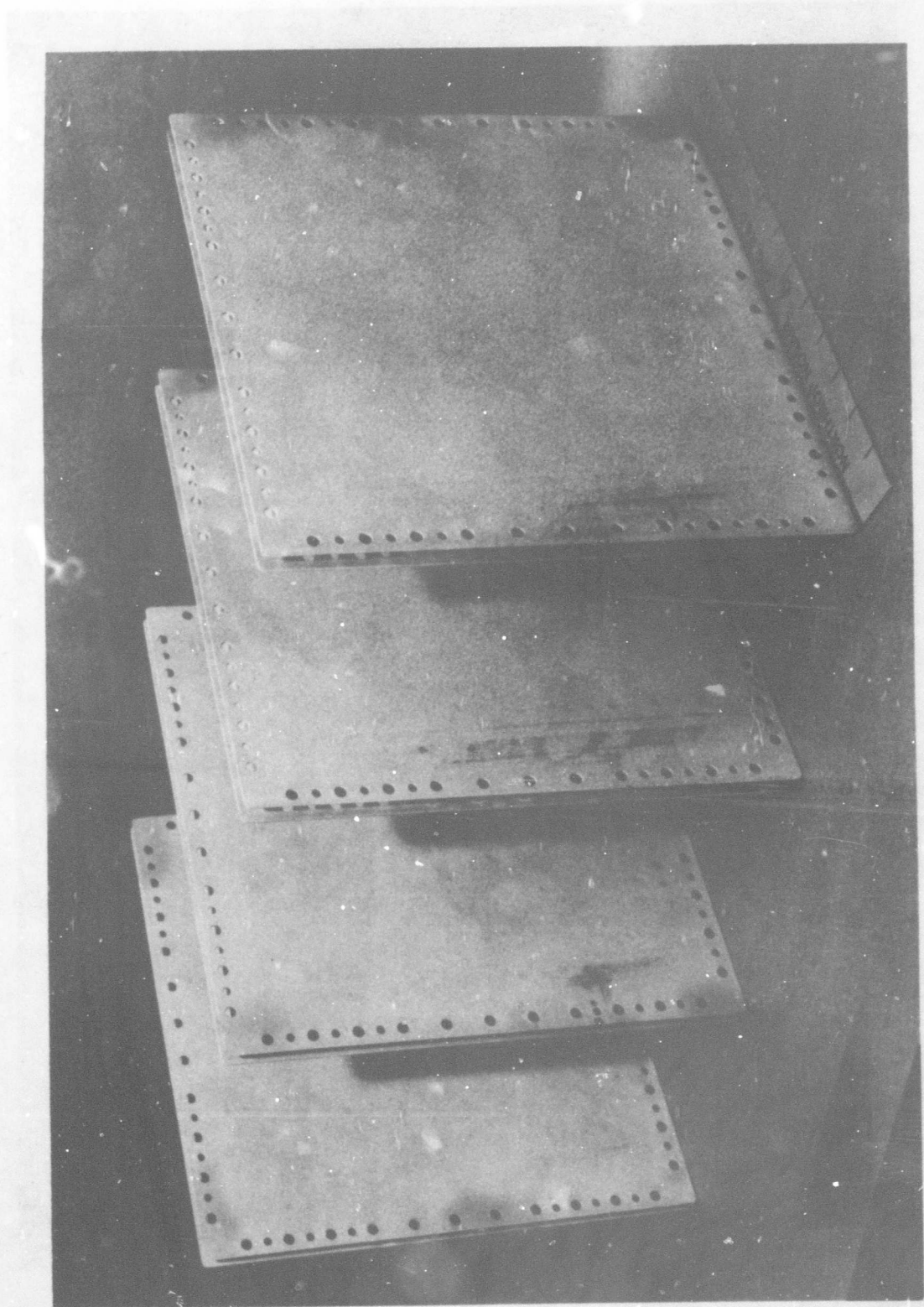


FIGURE 76 FOUR FLAT STRUCTURAL PANELS COATED WITH SYLVANIA
R505F AL-Sn-Mo COATING

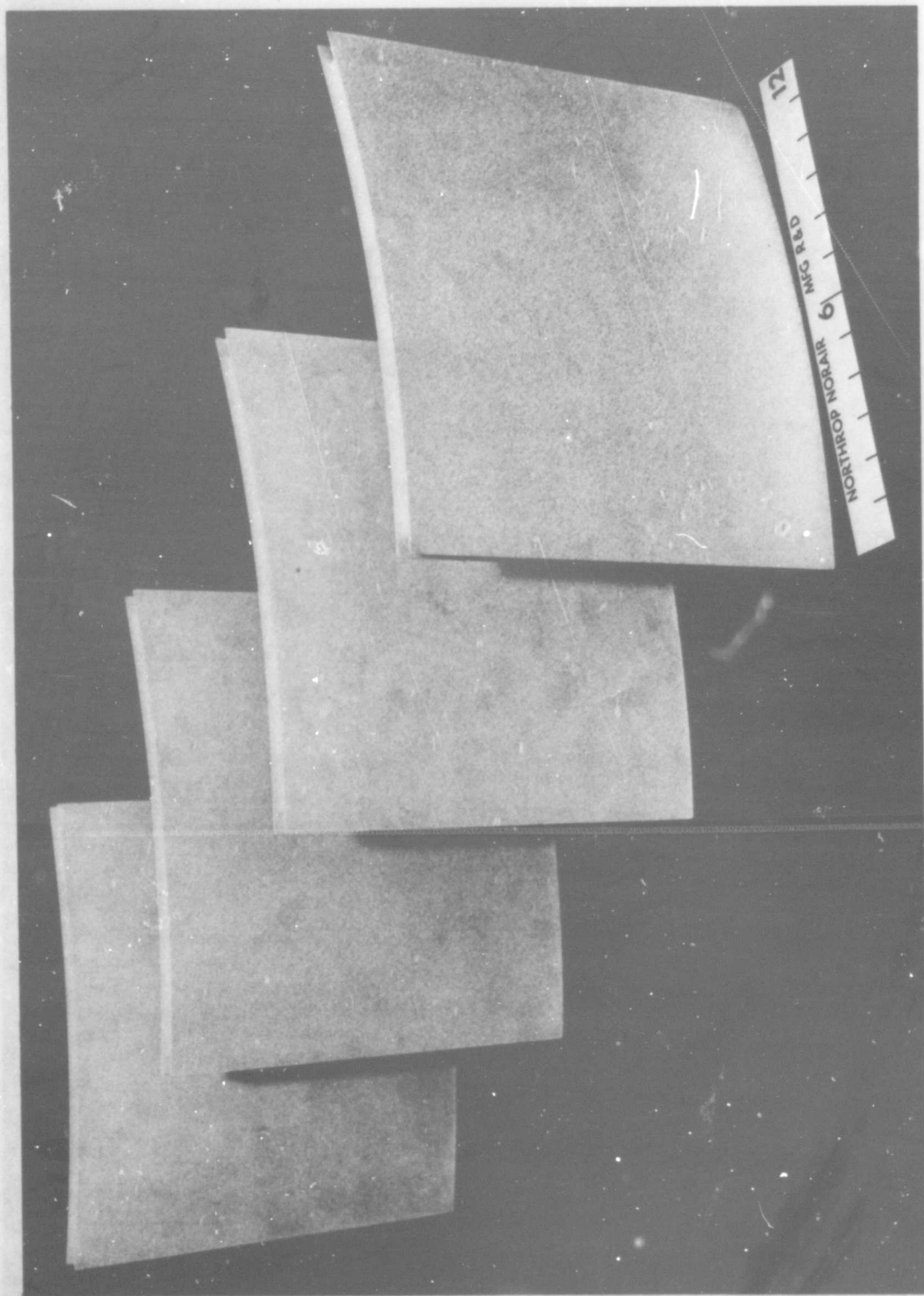


FIGURE 77 FOUR CURVED STRUCTURAL PANELS COATED WITH SYLVANIA
R505F Al-Sr-Mo OXIDATION PREVENTATIVE COATING

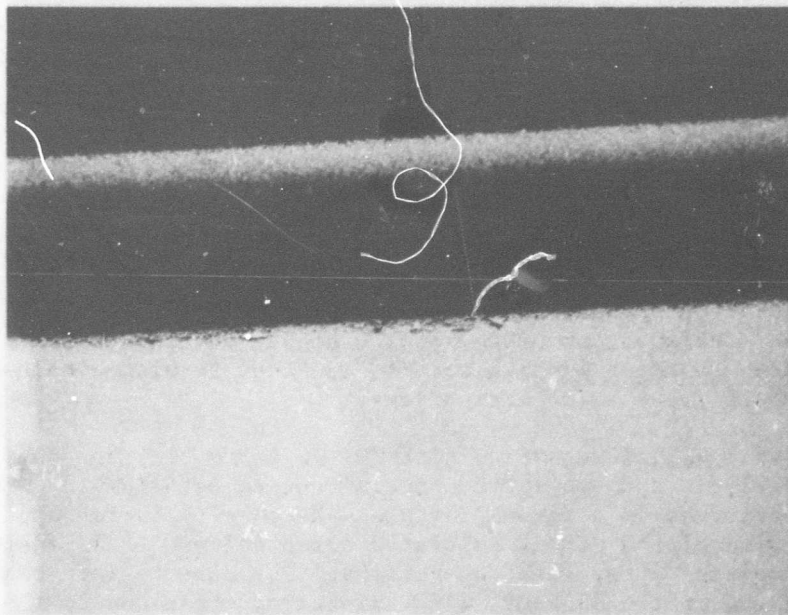


FIGURE 78 CLOSE-UP OF COATED PANEL EDGE
SHOWING CRACKS IN Al-Sn-Mo COATING

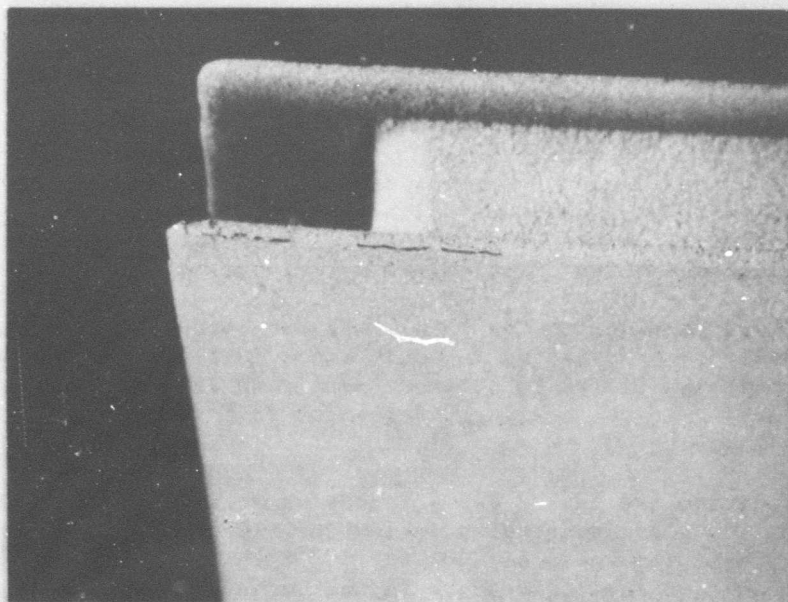


FIGURE 79 CLOSE-UP OF COATED PANEL CORNER SHOWING
CRACKING AND CHIPPING OF Al-Sn-Mo COATING

The more recent technique of application being investigated is by slurry. The slurry approach appears to offer more consistent uniformity of coating thickness and simpler, more reliable application procedures. Chiefly for this reason, and the fact that the tungsten and molybdenum silicides are the most promising coatings developed to date for service temperature above 3000F, the heat shield panels were coated by Solar Division of International Harvester, San Diego, California. Since both WSi_2 and $MoSi_2$ (actual compositions: (95W-5Ti) Si_2 and (95Mo-5Ti) Si_2) exhibited comparable results at the proposed test temperatures, it was decided to coat one panel with $MoSi_2$ and three panels with the WSi_2 , thereby gaining a comparison of the two coatings under almost identical test conditions. The $MoSi_2$ does have a decided weight advantage over the WSi_2 coating and also reportedly exhibited improved adherence to the substrate. However, the WSi_2 shows a higher melting point (3930F) than the $MoSi_2$ (3685F). Table XVI shows some of the test results obtained with the WSi_2 coating during previous investigations.

The two flat panels (one coated with TNV-12 (95Mo-5Ti) and one coated with TNV-13 (95W-5Ti), and two curved panels (coated with TNV-13) were processed in separate runs in a vacuum furnace. Neither the spray application, drying or sintering of the panels presented any problems. All panels were in excellent condition after these operations. The core to face sheet bond appeared unimpaired by the 15 hour, 2760F sintering cycle and to the vacuum environment. All liquids and gases were either excluded from inside the panel or were removed in the 3-hour vacuum bake-out at temperatures to 800F.

The two flat and two curved panels were pack silicided in separate runs. Horizontal placement was used because of available retorts. After the 2150F siliciding run on the two flat panels, the TNV-13 coated panel was in excellent condition; whereas the TNV-12 coated panel had a number of small cracks (Figure 80) indicating shear fracture of the coating from the substrate. The down side of both panels was mottled (Figure 81) after siliciding indicating some movement of the silicon pack away from the surface. A test specimen included with the pack did not show the mottled surface to contain less silicon than the top surface. Siliciding in a vertical position should correct this appearance. The upside of the panels shown in Figure 82 exhibited a much superior appearance to the downside. Too high a silicon weight gain appeared to be responsible for the cracking in the TNV-12 panel. (Recommended silicon is 25 to 30 mg/cm²-34 mg/cm² was obtained).

The two curved panels with the TNV-13 modifier were excellent after siliciding, exhibiting no cracking and only minor mottling on the down side. The silicon deposit was decreased on these panels to 26.5 mg/cm² to avoid any possible cracking in the coating. Facesheet to core bond appeared excellent after siliciding.

The final step in the TNV-12 and -13 coating process was impregnation with a finely milled glass suspension in a water vehicle. This slip was applied by spraying a thickness of .001 to .002 inch, hot air drying and brushing off the bisque leaving residue in the pores only. Since the TNV-12

TABLE XVI
9SUMMARY OF VERY HIGH TEMPERATURE TESTING ON SOLAR WSi_2 COATING (1)

Testing Organization	Substrate Alloy	Test Technique	Test Cycle	LIFE-HOURS				
				1600F	2000F	3100F	3500F	3600F
McDonnell-Douglas TRW	T111	Furnace	60 min.	20+, 20+ 20+	---	20+, 7, 10+	5.5, 5.5, 2.5	1.75, 0.5, .25
			30 min.					
			15 min.					
	T222	Furnace or Induction	.8 to 3 hrs	---	39.5 39.5 14.5	86.0(2) 86.0(2) 93.0(2)	0.5 2.0 8.5	.08(3) .08(3) .08(3)

		Torch (localized) heating) Plasma arc	.5 to 1.0 " "	---	---	2.0 2.25 3.0	2.0 2.25 3.0	1.16(4) 1.88(4)

		$\text{O}_2\text{-C}_2\text{H}_2$.5 to 1.0 " "	---	---	6.5 12.0 13.0		

(1) (95W-5Ti)-S1 (2) Support failure (3) Optical temperature, uncorrected
 (4) Uncorrected optical reading of 3150 F, melted at optical reading of 3300F.

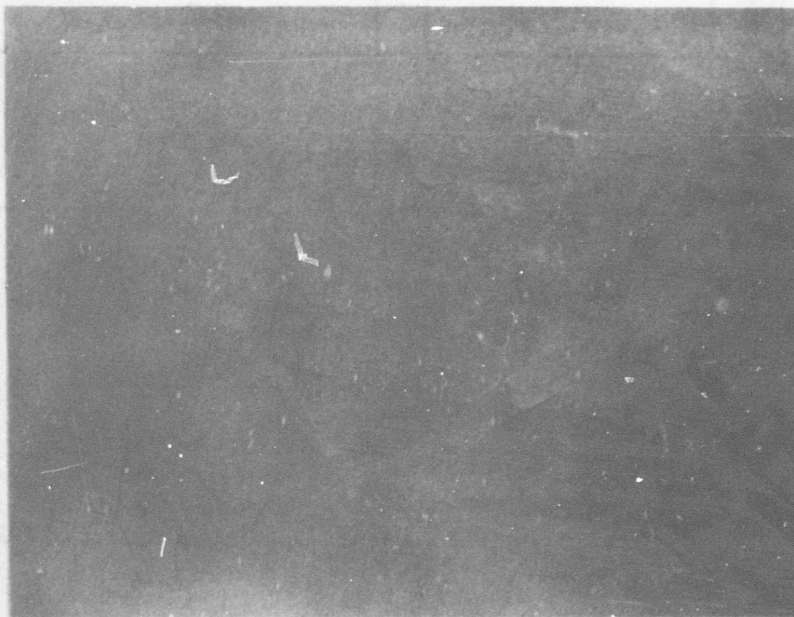


FIGURE 80 CLOSE-UP OF FLAT HEAT SHIELD PANEL COATED WITH MoSi_2 (TNV-12) SHOWING CRACKS IN COATING

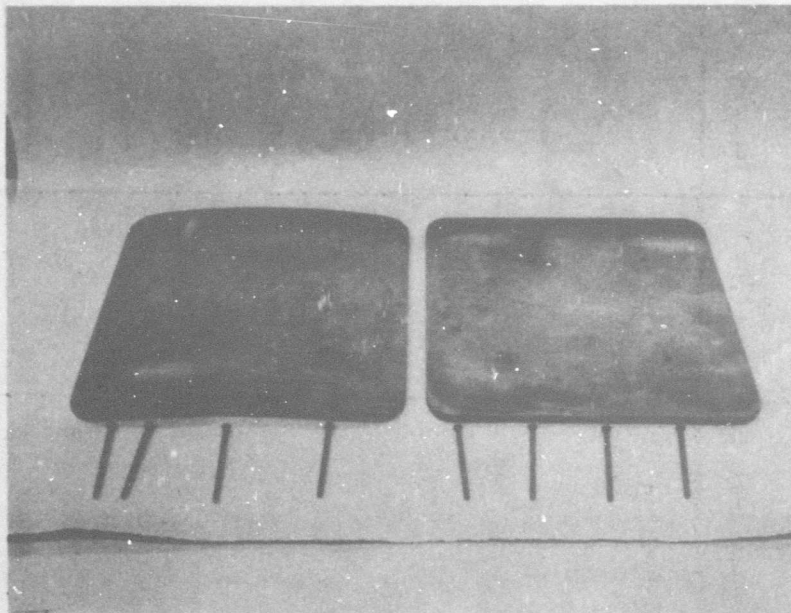


FIGURE 81 DOWNSIDE OF HEAT SHIELD PANELS COATED WITH WSi_2 (LEFT) AND MoSi_2 (RIGHT) SHOWING MOTTLED APPEARANCE OF COATING INCLUDED ARE COLUMBIUM (D36) BOLTS COATED WITH WSi_2 TO BE USED FOR ATTACHMENT OF PANEL TO TEST FIXTURE

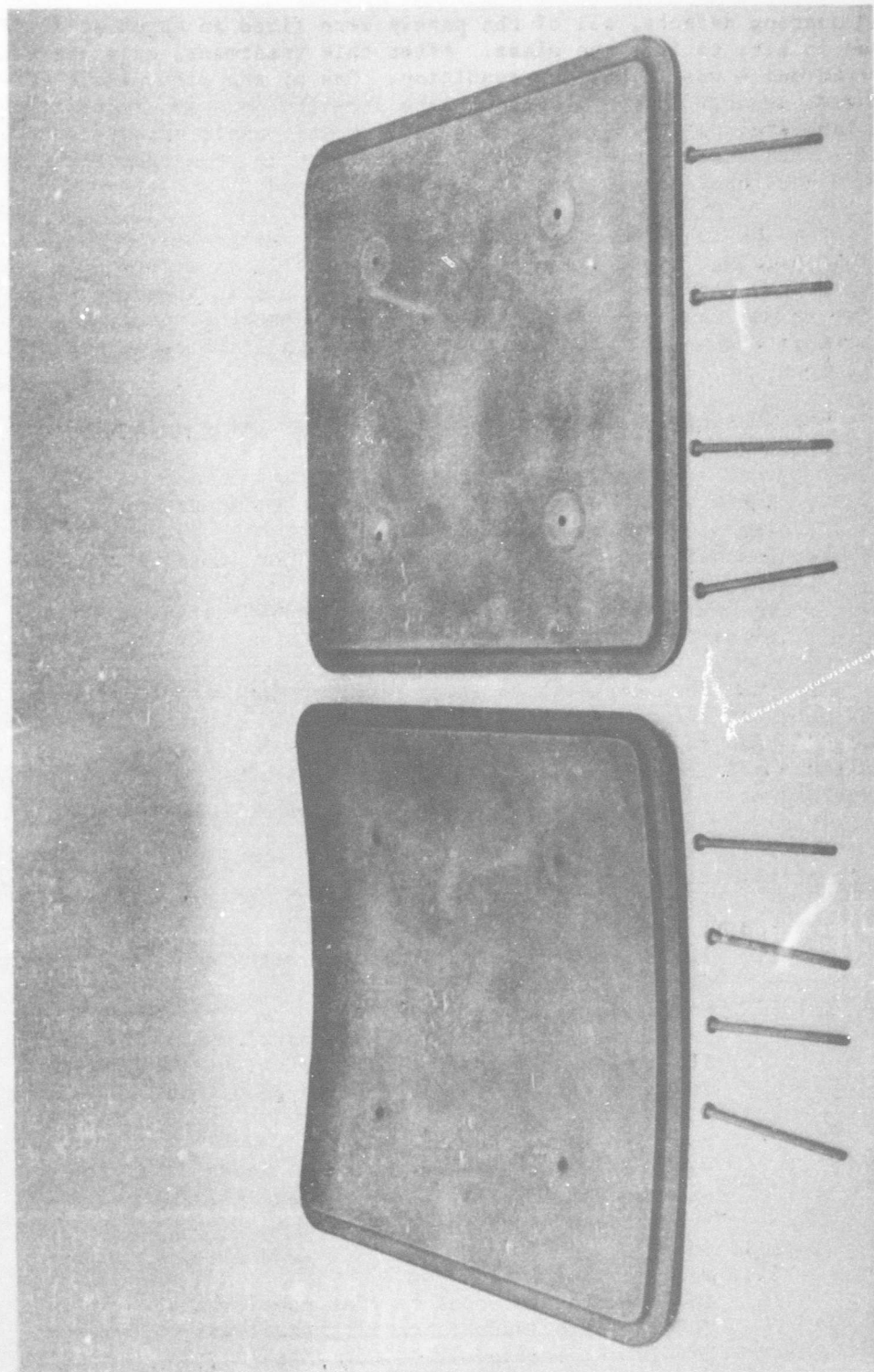


FIGURE 82 UPSIDE OF HEAT SHIELD PANELS COATED WITH WS12 (LEFT) AND MoSi2 (RIGHT) SHOWING A SOMEWHAT IMPROVED SURFACE APPEARANCE WS12 COATED COLUMBIUM ATTACH BOLTS ARE SHOWN IN FOREGROUND

had coating defects, all of the panels were fired in argon at 1800F, rather than in air, to fuse the glass. After this treatment, only one panel - a curved one - was in perfect condition. One of the flat panels (TNV-13) expanded, separating the two facesheets from the core and separating the welds at the panel access holes. One of the curved panels separated in a localized area. The other flat panel (TNV-12) revealed no core-face sheet failure, but had a poor quality coating, as previously noted.

The TNV-13 coating appeared to be quite applicable to the honeycomb heat shield panels. Application of modifier and silicon afforded no problems. Wetting the panels with the glass impregnation slip appeared to be undesirable. Moisture may have penetrated the panel face sheet, probably through micro cracks in the welds. Heating of the panels to 1800F cause separation of the core from the face sheet.

Three changes in technique could probably yield a higher percentage of good panels:

1. Improvement in welding techniques to eliminate micro cracking in the panel welds.
2. Use of a dry, finely powdered glass for impregnation rather than the water vehicle.
3. Vacuum outgassing at temperatures to 800F after application of the glass impregnation slip.

The fact that no burst failures occurred in the initial 2760F sintering treatment for the modifier indicated that 1) the panel contained no micro cracks (which is doubtful) or 2) the organic vehicle used to suspend the modifier was outgassed in the preliminary three hour outgassing treatment at temperatures to 800F.

The following process outline summarizes the procedures used in coating the heat shield panels.

1. Modifier application (Mo and W)
 - 1.1 Surface degreased with trichloroethylene. Lightly sandblasted with 80 grit garnet.
 - 1.2 Modifier applied by spraying.
TNV-13 weight deposit on flat panel was 141.0 mg/cm²
TNV-12 weight deposit on flat panel was 69.0 mg/cm²
TNV-13 weight deposit on curved panel was 130.0 mg/cm²
 - 1.3 Air dry
 - 1.4 Modifier vacuum furnace fired
Heat up and out gassed three (3) hours
At temperature (2760F) for fifteen (15) hours
Parts cooled in furnace
2. Silicide
 - 2.1 Pack flushed with argon
TNV-13 weight deposit on flat panel was 33.0 mg/cm²
TNV-12 weight deposit on flat panel was 34.0 mg/cm²
TNV-13 weight deposit on curved panel was 26.5 mg/cm²

- 2.2 Fired in preheated furnace
 - Flat panels were run at 2150F for ten (10) hours
 - Curved panels were run at 2150F for six (6) hours
- 2.3 Post cleaning consisted only of brushing off loose silicon
- 3. Glass Impregnation
 - 3.1 Water based ceramic coating used
 - 3.2 No surface preparation was necessary
 - 3.3 Applied by spraying
 - Weight deposit was 0.4 to 1.0 mg/cm²
 - 3.4 Dried at 200F in circulating air
 - 3.5 Fired in preheated furnace with purge box at 1800F for twenty (20) minutes and cooled in the purge box
 - 3.6 No post cleaning

The application of the MoSi₂ coating proved unsuccessful as numerous cracks in the coating resulted. (Figure 80) It was surmised that the MoSi₂ coating could not tolerate the high silicon (34.0 mg/cm²) content as could the WSi₂ coating. As a result, Solar is not recommending this coating for further use. Two panels did not survive the coating cycle as bulging of the face skins occurred during the 1800F glass impregnation step. It could only be deduced that during the spraying of the water based ceramic coating some of the spray managed to enter the panel through possible defects in the welds around the panel access holes. Upon heating to 1800F vaporization and subsequent pressure build up severed the bond and bulged the face skins. One curved panel was coated successfully with WSi₂. The panel appeared to exhibit good coverage as no defects were seen to exist. Since no testing was performed on the panel, its actual performance at elevated temperature was not determined.

X STRUCTURAL TESTING AND ANALYSIS

Curved and flat structural panels were tested at room and elevated temperatures to determine the strength and producibility of the diffusion bonded honeycomb sandwich constructions. The flat panels were tested in edgewise shear while the curved panels were tested in edgewise compression as illustrated in Figure 83. Upon completion of structural testing, specimens were sectioned from undamaged portions of the panels and tested in flatwise tension, flatwise compression, and edgewise compression at both room and elevated temperature.

The structural panels were analyzed for both general and local instability type failures at room and elevated temperatures. The analysis is presented in the form of generalized formulae and design charts for evaluating sandwich honeycomb panels fabricated from Tantalum alloy T-111 loaded in shear or compression. Every effort has been made to describe the cause and mechanism of failure of the panel and panel components. Due to the limited number of panels available for testing and evaluation, it was not possible to test for the cumulative effects of combined aerodynamic and thermal loading environments.

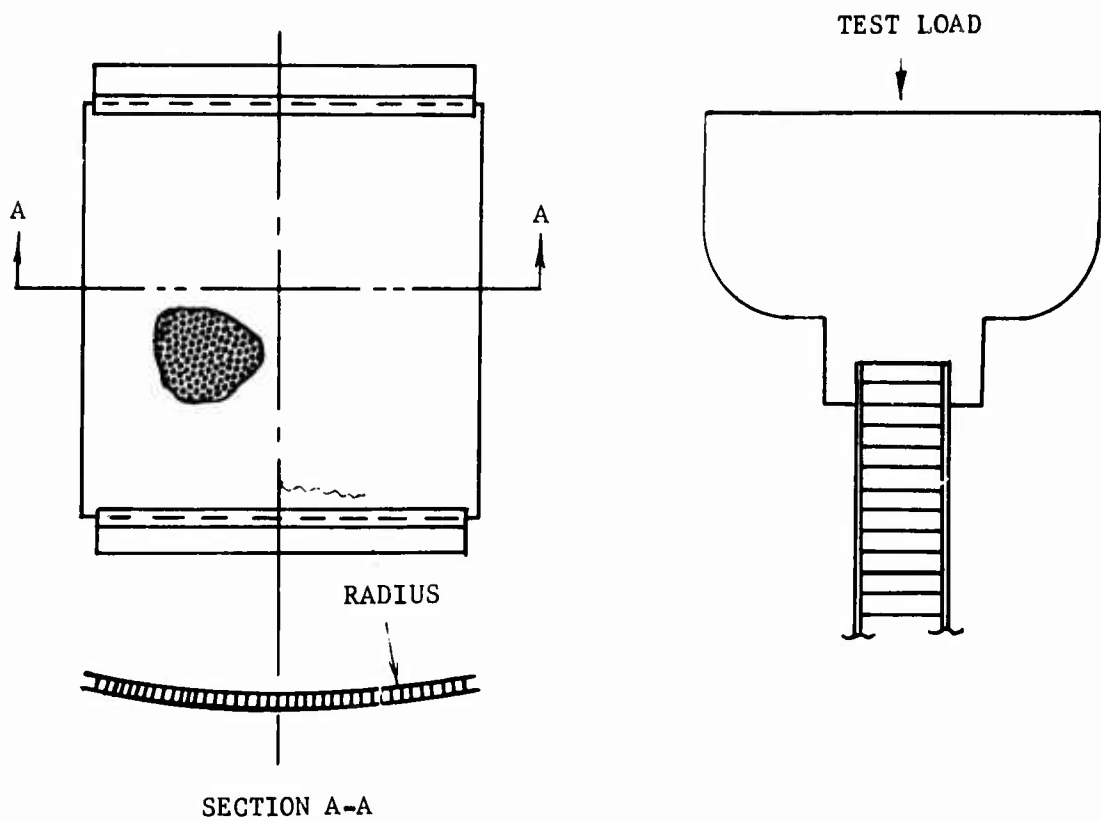
The objective of testing small specimens taken from structural panels was to characterize the diffusion bonding achieved from panel to panel and obtain a correlation between specimen data and full-scale panel data. The existence of such a correlation allows interpolation of the limited amount of structural panel data to range over temperatures corresponding to those applied in specimen tests. Further, a qualitative indication of the amount of degradation of panel properties caused by testing may be observed.

Due to the problems that developed in the manufacture of the heat shield panels, testing and analysis of these panels was not accomplished in the contract period.

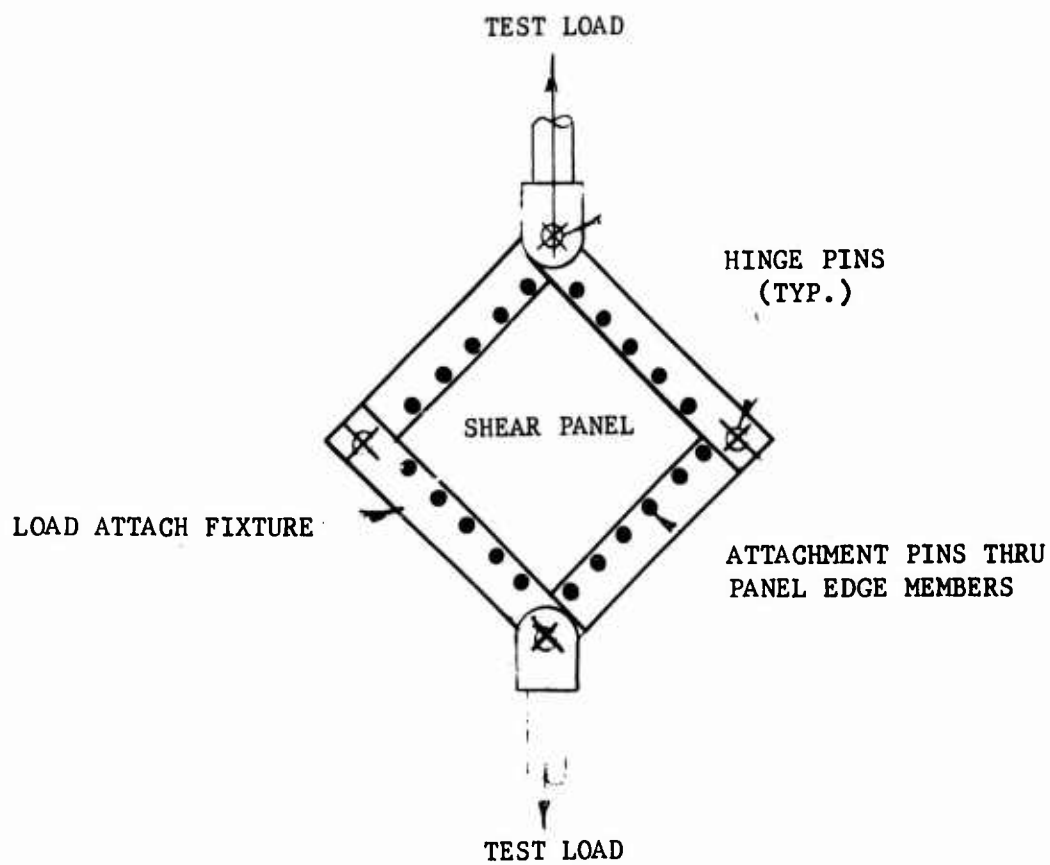
STRUCTURAL AND SPECIMEN TESTING PROCEDURE

Panel Test Fixturing

The curved panels were tested in axial compression by applying the load uniformly to the curved edgemembers of the panel. The primary objective in the design of the fixturing was to uniformly transmit the predicted ultimate load of the panel into the thin (.012 inch) facings of the panel. Thus, the end fixtures of the panel consisted of two load transfer bars fabricated from L605 nickel-base alloy machined with parallel surfaces, and a channel to accommodate the curved edge of the panel to a depth of .340 inch. Figure 84 shows the room temperature test setup for edgewise compression testing. Stainless steel shims were utilized as filler within the channelled edgemember to prevent premature failure in this area during loading (Figure 85). No support was given the vertical or unloaded edgemembers. Edgewise compression tests at elevated temperatures utilized the same fixtures and test setup, except that glassrock insulation was employed to prevent excessive heating of the fixtures. Installation of the panel in the loading machine with radiant heating unit is shown in Figure 86.



EDGEWISE COMPRESSION



EDGEWISE SHEAR

FIGURE 83 MODES OF LOADING USED IN DETERMINING THE STRUCTURAL INTEGRITY OF TANTALUM HONEYCOMB PANELS

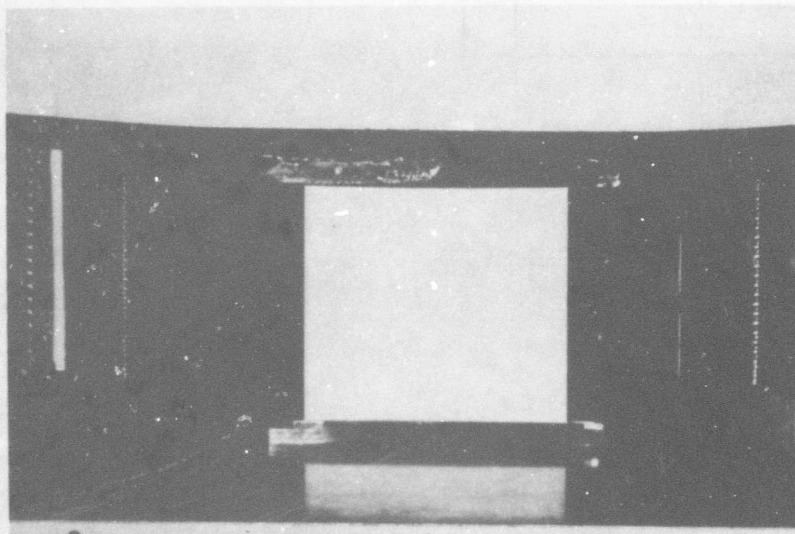


FIGURE 84 TEST SETUP FOR ROOM TEMPERATURE EDGEWISE COMPRESSION TESTING OF CURVED STRUCTURAL PANEL

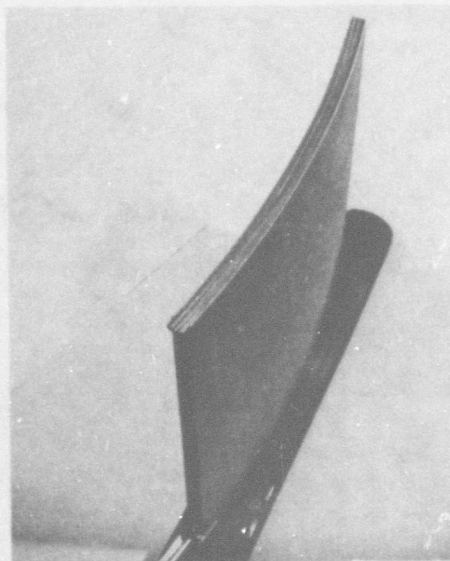


FIGURE 85 CURVED PANEL EDGEMEMBER WITH STAINLESS STEEL SHIMS TO PREVENT COLLAPSE OF THIS AREA DURING LOADING

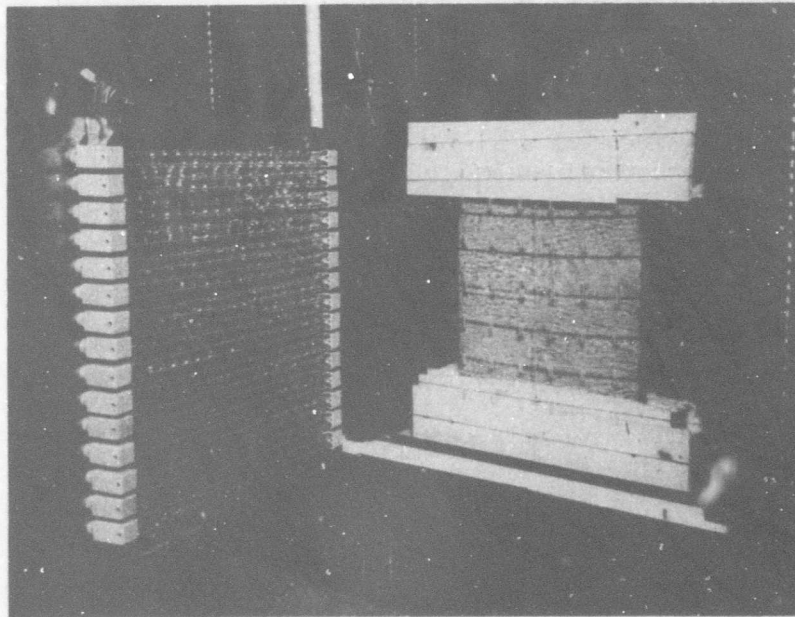


FIGURE 86 TEST SETUP OF PANEL AND QUARTZ LAMP RADIANT HEATING FIXTURE FOR EDGEWISE COMPRESSION TESTING OF CURVED STRUCTURAL PANEL AT ELEVATED TEMPERATURES

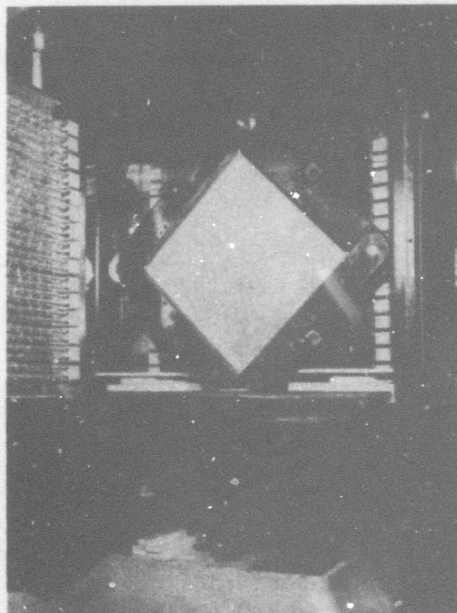


FIGURE 87 TEST SETUP OF PANEL AND HEATING UNIT FOR EDGEWISE SHEAR TESTING OF FLAT STRUCTURAL PANEL AT ELEVATED TEMPERATURES

The flat panels were loaded in edgewise shear by using a "picture frame" type loading fixture. The test panel was attached to the shear fixture through the edgemembers of the panel with machined pins. The fixtures and pins were fabricated from L605 material allowing the fixtures to be employed for both room and elevated temperature testing. The panel edgemembers were fitted with spacers to prevent premature buckling of the U-channels. The panel and fixtures with loading and heating systems are shown in Figure 87. Panel loading was accomplished by means of a Tinius-Olsen Universal Testing machine. This is a four-screw electromechanical-drive system capable of applying compression and tension loads up to 200,000 pounds using manual or automatic modes of operation. The system may be operated in load ranges of 2,000, 10,000, 50,000, and 200,000 pounds with an accuracy of $\pm .2$ percent of the full-load range being used and is also provided with stress and strain recording equipment. The system with a panel installed for testing is shown in Figure 88.

Furnace Design and Instrumentation

Test temperatures were attained by means of the Quartz lamp radiant heat fixture shown in Figures 86 and 87. This unit was of a design similar to that used earlier in the program during panel manufacture. The side reflectors were gold-fired and water-cooled. Air was circulated through the electrical conduits to allow cooling of the lamp end-seals. Vycor windows were placed between the panel and lamps to diffuse the radiation from the lamps producing a more even distribution of heat. In addition, the vycor windows allowed the use of an air plenum between the windows and lamps providing cooling for both components without affecting the panel temperature. Each side of the panel was heated with 30 T3-3200 watt lamps located on 1/2 inch centers yielding a power density of 400 watts/in² at a lamp-rated voltage of 300V. A power input of 384 volts was actually used in attaining a 2800F test temperature.

Power to the heating fixture was supplied by six Research Incorporated 384 KVA power units and regulated from a six-channel control console capable of either manual or automatic operation. Six Research Incorporated function generators were employed to control temperature cycles. Test temperatures were recorded on six dual-point Bristol strip-chart recorders. Fixture temperatures were recorded on a Leeds and Northrup 20-channel multipoint recorder.

Temperature Control

Panel temperatures were monitored utilizing platinum-rhodium thermocouple probes with the hot junction protected with boron nitride caps to prevent interaction between the thermocouple and panel coating. Attempts to attach the thermocouples directly to the panel would have resulted in numerous problems involving the coating of the panels. The thermocouple lead-in wires were sheathed in porcelain insulators. Fixture temperatures were monitored with chromel-alumel thermocouples spot welded to the fixtures. The platinum-rhodium thermocouples were located through holes in the radiant heater reflectors and positioned such that contact was made directly on the panel surface and maintained by spring loaded thermocouple holders as shown in Figure 89.

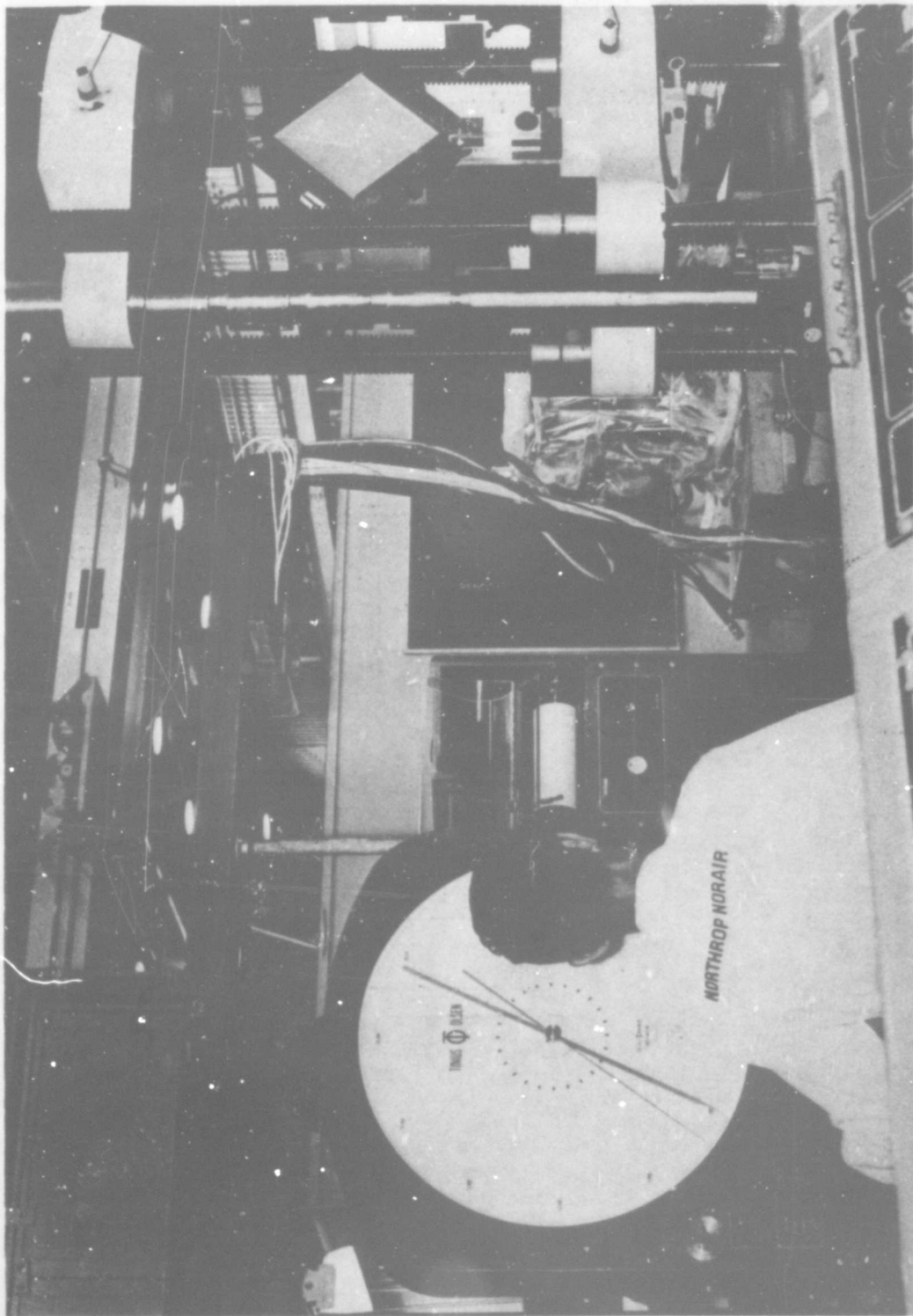


FIGURE 88 TEST SETUP FOR ROOM TEMPERATURE EDGEWISE
SHEAR TESTING OF FLAT STRUCTURAL PANELS

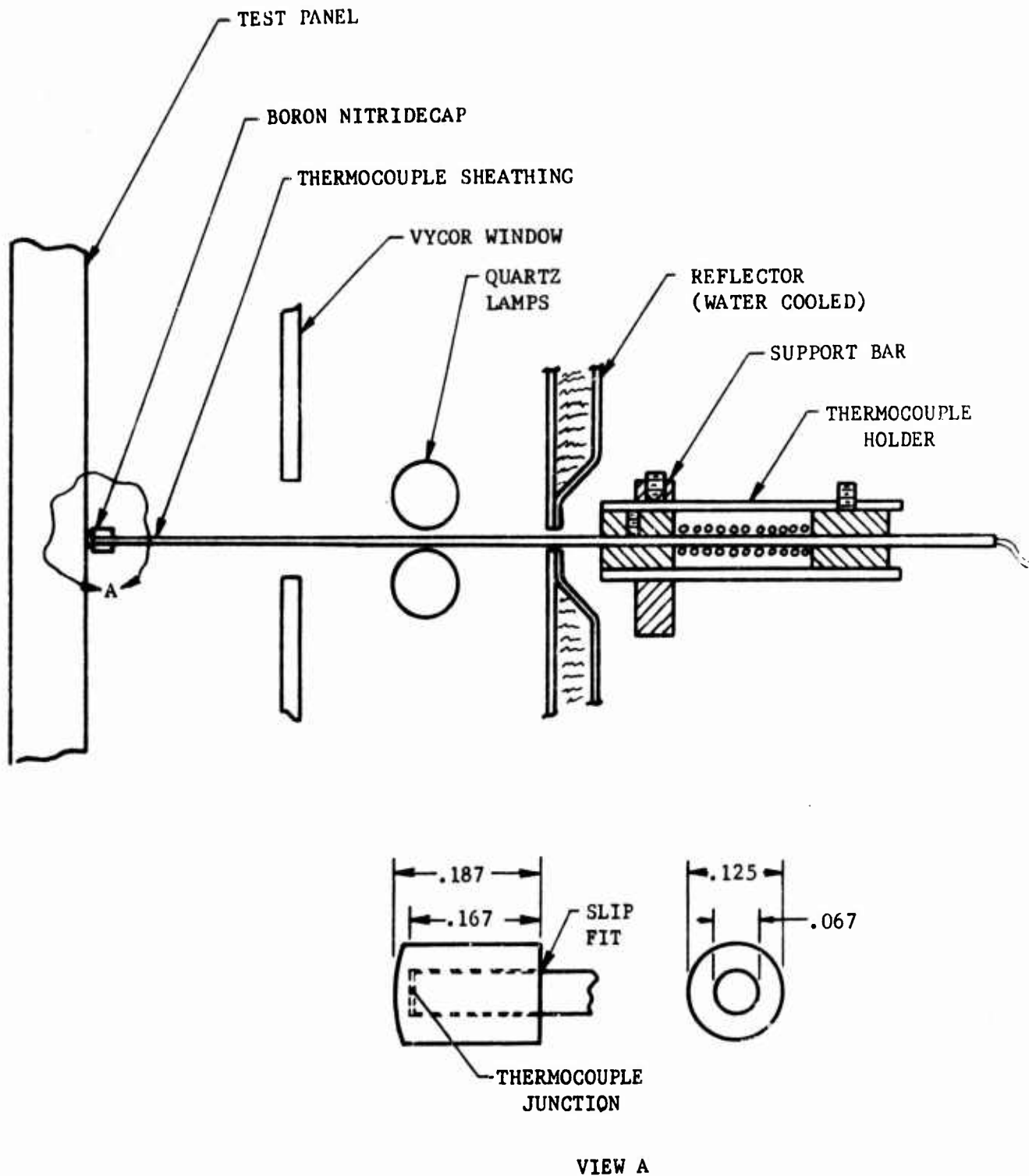


FIGURE 89 THERMOCOUPLE INSTALLATION TECHNIQUE

Since it was recognized that both a delay in thermal response and the insulating properties of the boron nitride caps would result in a significant variation in temperatures recorded to actual panel temperatures, a calibration was performed to determine the actual extent of this discrepancy. Three chromel-alumel thermocouples were spot welded to the surface of a .125 inch thick 410 stainless steel sheet and three platinum-rhodium capped thermocouples were placed just touching the surface of the sheet as would be the case during actual panel testing. With the chromel-alumel thermocouples as standards, a comparison was made between the two temperature recording systems during heating of the sheet. A plot of this data is shown in Figure 90 and indicates a temperature differential of approximately 100F existing between thermocouples welded to the metal and the capped thermocouples. This correction factor was used in reporting test temperatures.

To minimize thermal stresses at elevated temperatures, the panel and loading fixtures were free to expand in the testing machine prior to load application. When the desired test temperature was achieved, the loading rig was activated placing the panel in a rigid, load-carrying condition.

To minimize thermal stresses due to the difference in expansion characteristics between the panel and fixture materials during panel edgewise shear tests, the fixture temperature was monitored to assure that the temperature rise of the panel and fixture was compatible with the curve in Figure 91.

Small Specimen Testing Procedure

Eleven diffusion bonded panels were sectioned into small test specimens. A summary of the panel conditions studied is given in Table XVII. Specimens were tested in the as-fabricated condition to obtain base-line data and after structural testing to determine bond strength retention. Modes of testing included edgewise compression, flatwise tension, and flatwise compression over a range of temperatures from room temperature to 2800F. The specimen configurations are shown in Figure 92. In addition to the panel specimen tests, tensile tests were run on .040 inch Ta-8W-2Hf to obtain facesheet properties for structural analysis. Metallographic and electron microprobe analyses were performed to study the various bonded joints and to investigate the protective qualities and effects of the coating on the substrate properties.

The panels were rough-cut into specimens on a bandsaw and finished to final dimensions by grinding. Protective coatings were removed prior to testing to prevent contamination of the inert furnace atmosphere and insure adhesion of flatwise compression tension specimens to test fixtures. A chemical solution of 50 NaOH-50HCL was used on panels 1 and 4 to remove the coating. This solution badly embrittled the core of Panel 1 and no specimens were obtained. To prevent this from happening to Panel 4, the core was coated with Turco 4472 for protection against acid attack. However, it was felt that some embrittlement of the core still occurred. Therefore, coating removal procedures on subsequent panels consisted of sandblasting using light pressure (approximately 80 psi) prior to sectioning. This technique for coating removal proved satisfactory.

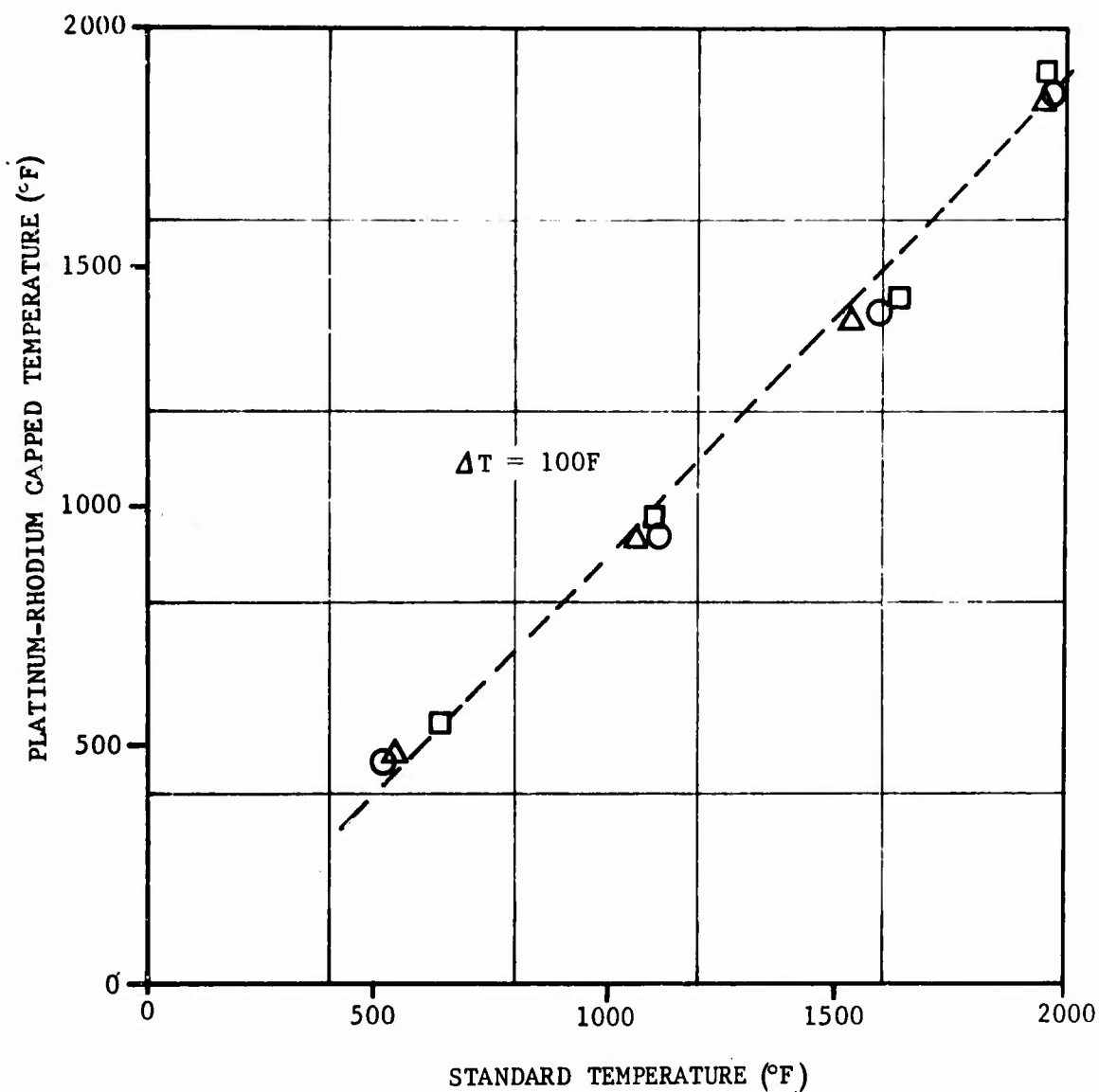


FIGURE 90 COMPARISON OF TEMPERATURE MEASUREMENTS BETWEEN PLATINUM-RHODIUM THERMOCOUPLES WITH BORON NITRIDE CAPS AND CHROMEL-ALUMEL THERMOCOUPLES

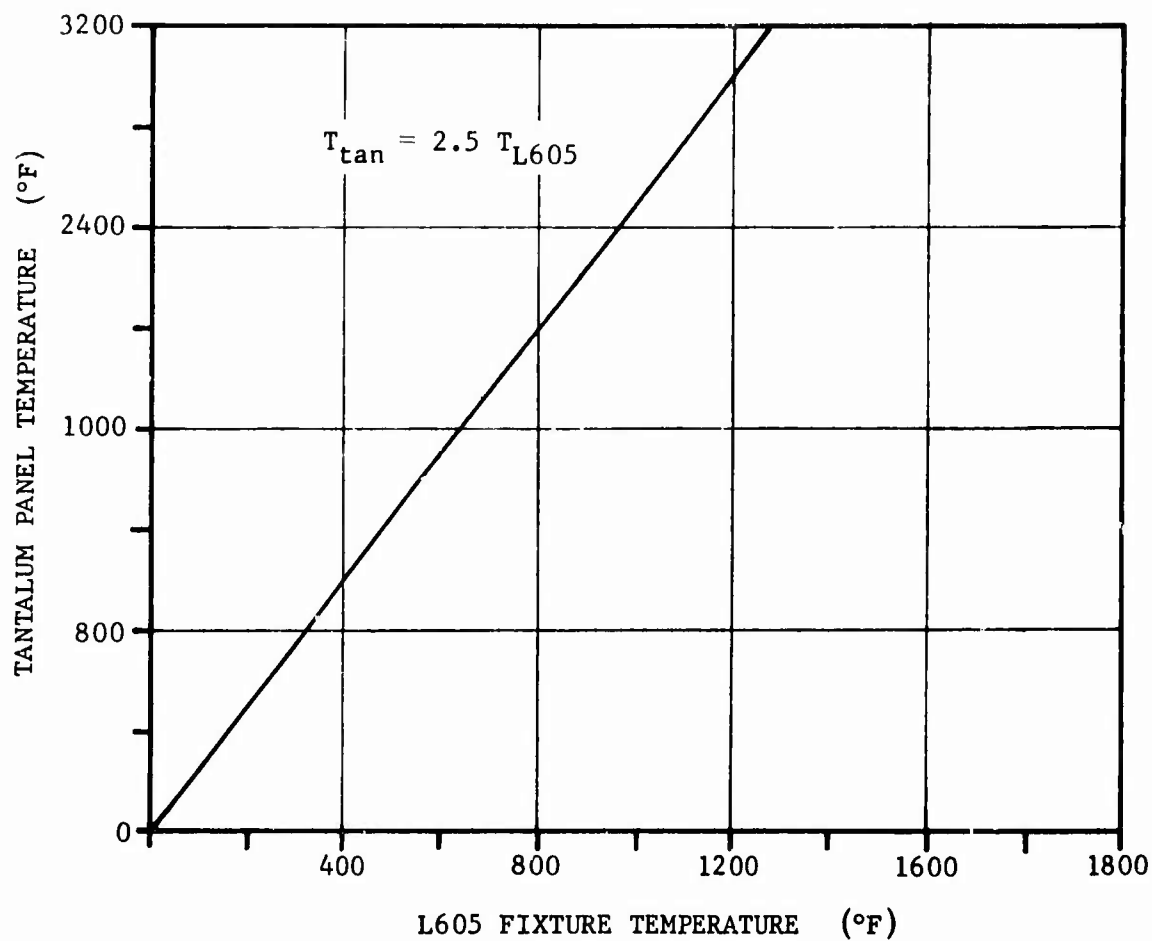


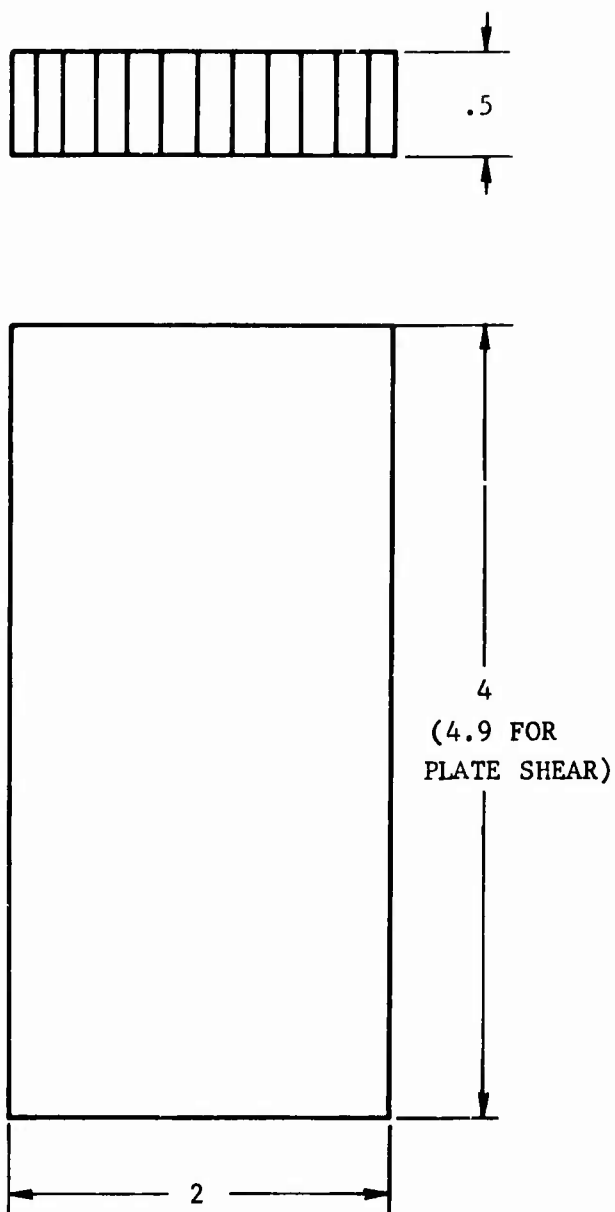
FIGURE 91 TEMPERATURE COMPATIBILITY CURVE USED TO ALLOW FOR THE DIFFERENCE IN THERMAL EXPANSION BETWEEN THE TANTALUM PANEL AND L605 TEST FIXTURE DURING TESTING

TABLE XVII

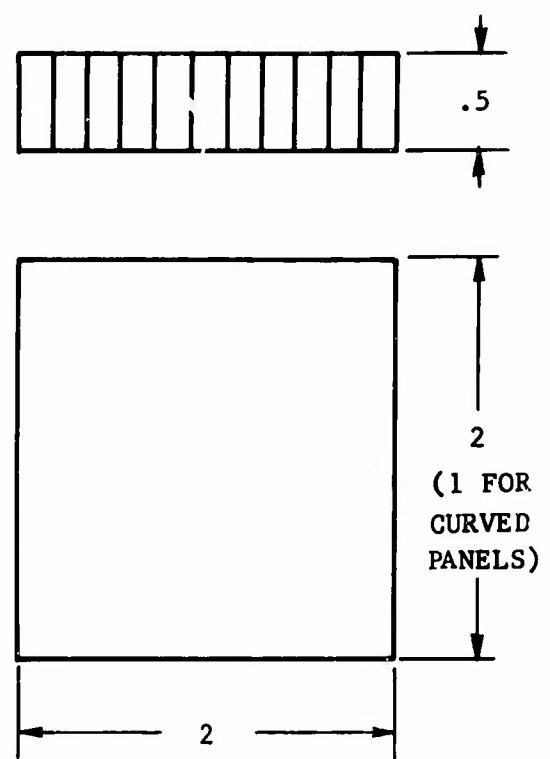
SUMMARY OF PANEL CONFIGURATIONS AND VARIOUS CONDITIONS ANALYZED

PANEL NUMBER	TYPE OF PANEL	PANEL SHAPE	COATED WITH Al-Sn-Mo	HISTORY BEFORE SECTION-ING FOR SPECIMEN TESTING
1 ^a	Structural	Curved	Yes	Failed in edgewise compression at R.T.
2	Structural	Curved	Yes	Failed in edgewise compression at 2800F
3 ^b	Structural	Curved	Yes	Failed in edgewise compression at 2900F
4	Structural	Curved	Yes	Failed in edgewise compression at R.T.
5	Structural	Flat	No	As fabricated
6 ^c	Heat Shield	Flat	No	As fabricated
7	Structural	Flat	Yes	Failed in shear at R.T.
8 ^d	Structural	Flat	Yes	Failed in shear at R.T.
9	Structural	Flat	Yes	Failed in shear at 2100F
10	Structural	Flat	Yes	Failed in shear at 2650F
11	Structural	Flat	No	As fabricated

- (a) Core embrittled by chemical used to remove coating; no mechanical test specimens obtained.
- (b) Due to coating failure and subsequent oxidation at 2800F, no mechanical test specimens were obtained.
- (c) No mechanical test specimens were obtained as bandsaw cutting damaged the panel.
- (d) No mechanical test specimens obtained due to overpressure during sand-blasting for coating removal.



(a) EDGEWISE COMPRESSION
OR PLATE SHEAR



(b) FLATWISE TENSION
OR COMPRESSION

FIGURE 92 CONFIGURATIONS FOR HONEYCOMB SPECIMEN TESTING

The edgewise compression specimen tests were conducted in a Brew high-temperature furnace with an Instron tensile unit employed to obtain failure loads. Tantalum tooling was used throughout the testing. The set-up with a specimen readied for testing is shown in Figure 93.

Flatwise tension and compression specimen tests were run in a similar manner as shown in Figure 94. With the Instron tensile unit used to obtain failure loads, load versus crosshead movement measurements were obtained in the case of flatwise compression tests. For the flatwise tension tests at room temperature, the specimens were bonded to steel test blocks (1.5x2x2 inches) using epoxy resin adhesive EC-1614. The specimens were brazed to tantalum blocks (.075x2x2 inches) using titanium alloy foil (B120VCA) for the high temperature flatwise tension tests. Brazing parameters were 2950F for 5 minutes in vacuum.

Optical metallography was conducted on a Leitz MM5 metallographic unit with electron microprobe analyses being performed on an A.R.L. EMX electron microprobe unit.

PANEL SPECIMEN TEST RESULTS AND DISCUSSION

The panel specimen test results, and properties of the T-111 sheet used in the manufacture of the panels, were employed in determining the diffusion bonded joint strength and in developing sandwich structural design criteria. Because of the difficulty in obtaining some experimental data, particularly at elevated temperature, some data was derived from other sources. However, the majority of the data used in subsequent analyses were taken from tests performed at Northrop so as to obtain a true representation of the material used in panel construction.

The mechanical properties listed herein, by no means imply design allowances for tantalum sandwich constructions, but merely represent the structural integrity of the panels manufactured in this program. The mechanical properties presented here should be used as guidelines for actual material behavior. Lines drawn between test points are not statistical in nature, but represent trends in properties only.

Mechanical properties at temperature are short time, i.e., the effects of creep and other time-dependent effects are neglected in the analysis. However, as evident from tensile property data, strain rate, for example, does have a significant effect upon the structural behavior of the sandwich composites. Unfortunately, the limited number of panels available for testing in the program precluded investigation or inclusion of these property effects in the analysis.

Face Sheet Properties

Representative yield and ultimate strengths of the face-sheet material as a function of temperature are shown in Figure 95. These test were conducted on the uncoated T-111 material used in the program. Unfortunately,

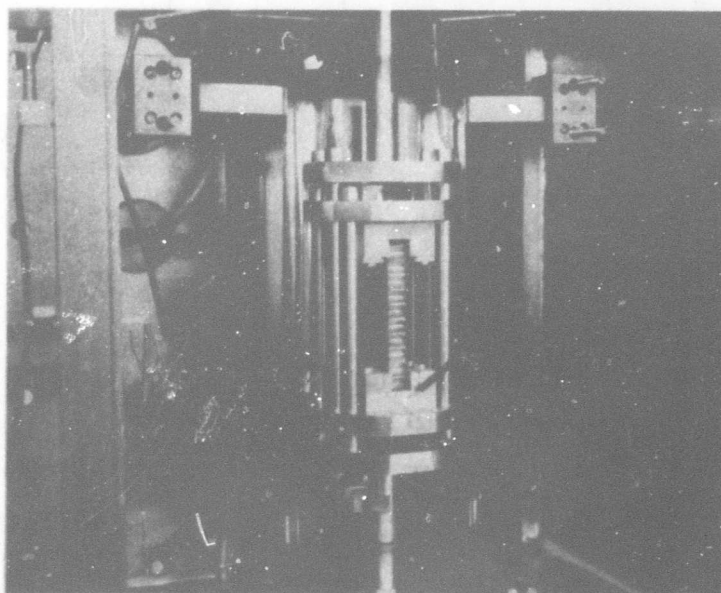


FIGURE 93 EDGEWISE COMPRESSION TEST SET-UP

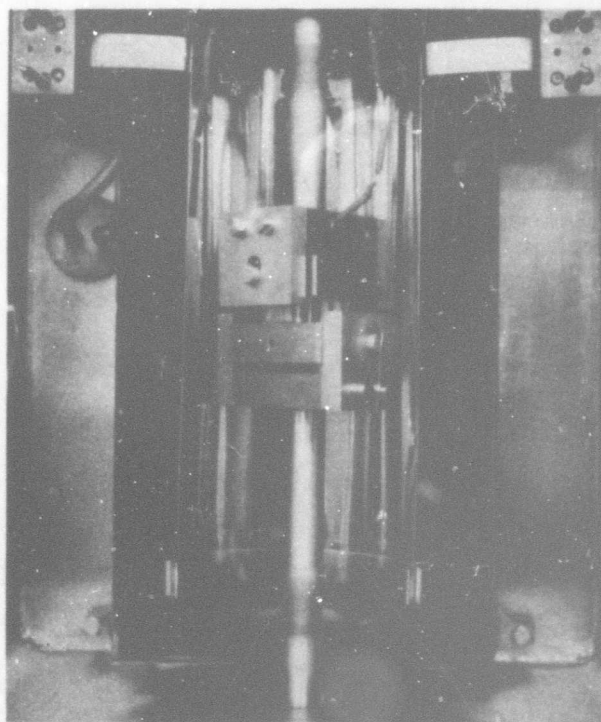


FIGURE 94 FLATWISE TENSION TEST SET-UP

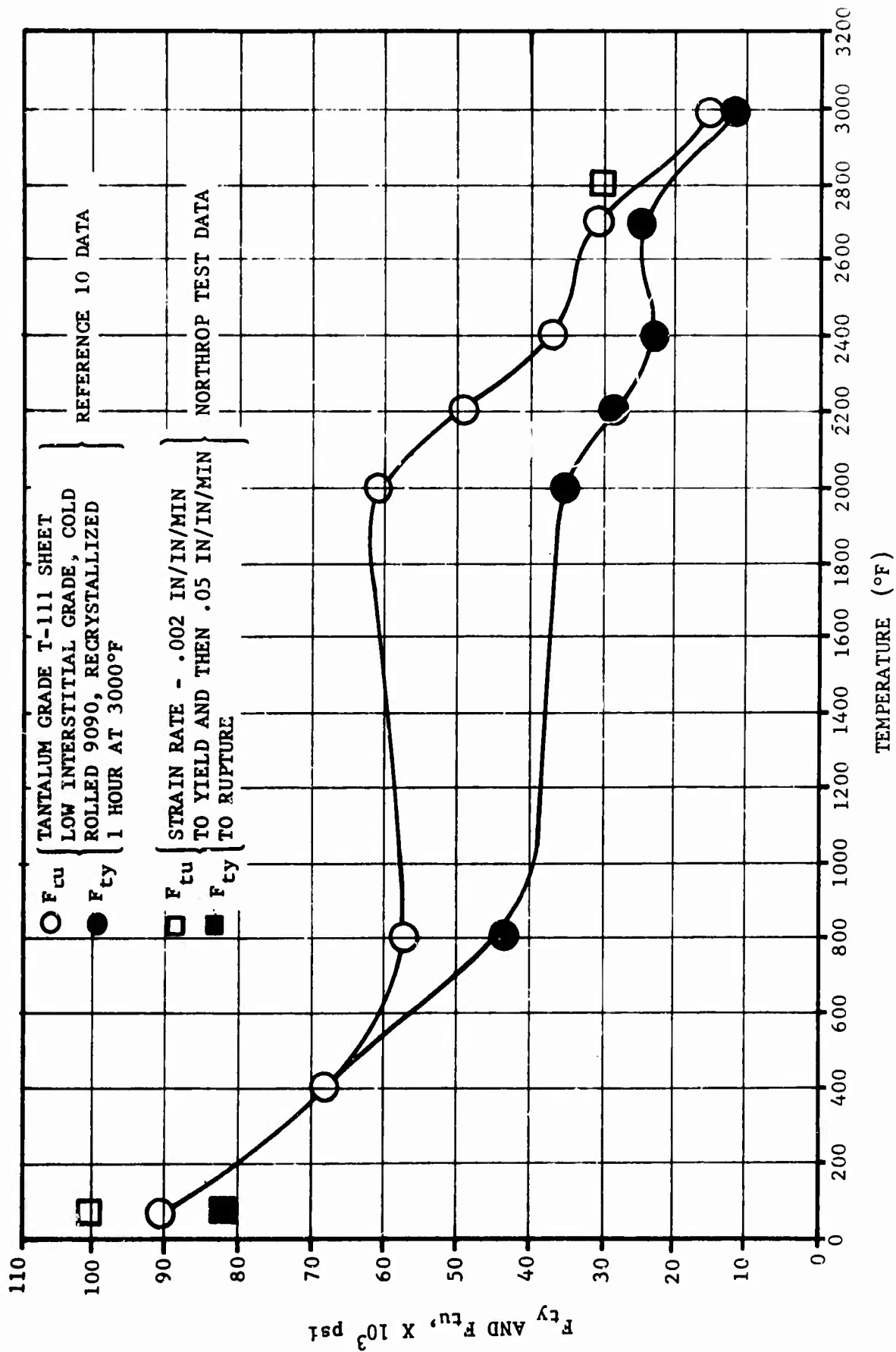


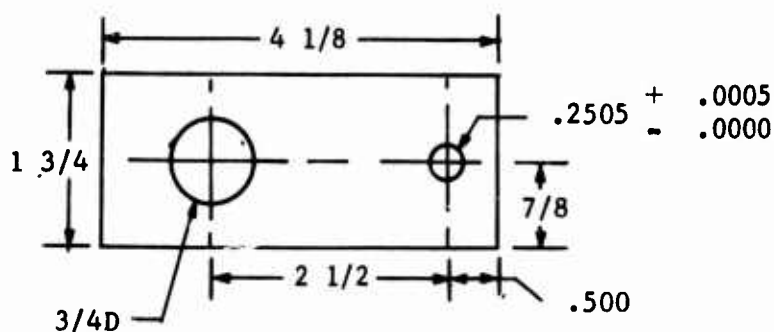
FIGURE 95 FACE SHEET TENSILE PROPERTIES AS A FUNCTION OF TEMPERATURE

some of the tensile coupons exhibited some surface contamination upon conclusion of the testing resulting in somewhat higher strength values. The questionable data was subsequently discarded with the exception of some modulus values. Modulus of elasticity values of some of the tensile specimens versus data obtained from Reference 4 are plotted in Figure 96. A stress-strain and tangent modulus curve of the facing material at room temperature and 2800F is shown in Figure 97.

To insure failures in the panel rather than at the attachment holes, bearing strength properties of the .012 inch T-111 facing were obtained for use in test fixture design. These tests were conducted at room temperature and are presented in the following table along with the standard bearing specimen used in their determination. A bearing stress-strain curve is shown in Figure 98.

BEARING SHEAR STRENGTH OF .012 INCH TANTALUM T-111 FACING SHEET MATERIAL			
Specimen Number	e/D^*	F_{bry} (ksi)	F_{bru} (ksi)
1	2.0	156.0	226.1
2	2.0	160.5	231.1

e = Distance from hole center to edge of sheet
 D = Hole diameter



THICKNESS = .013 & .014

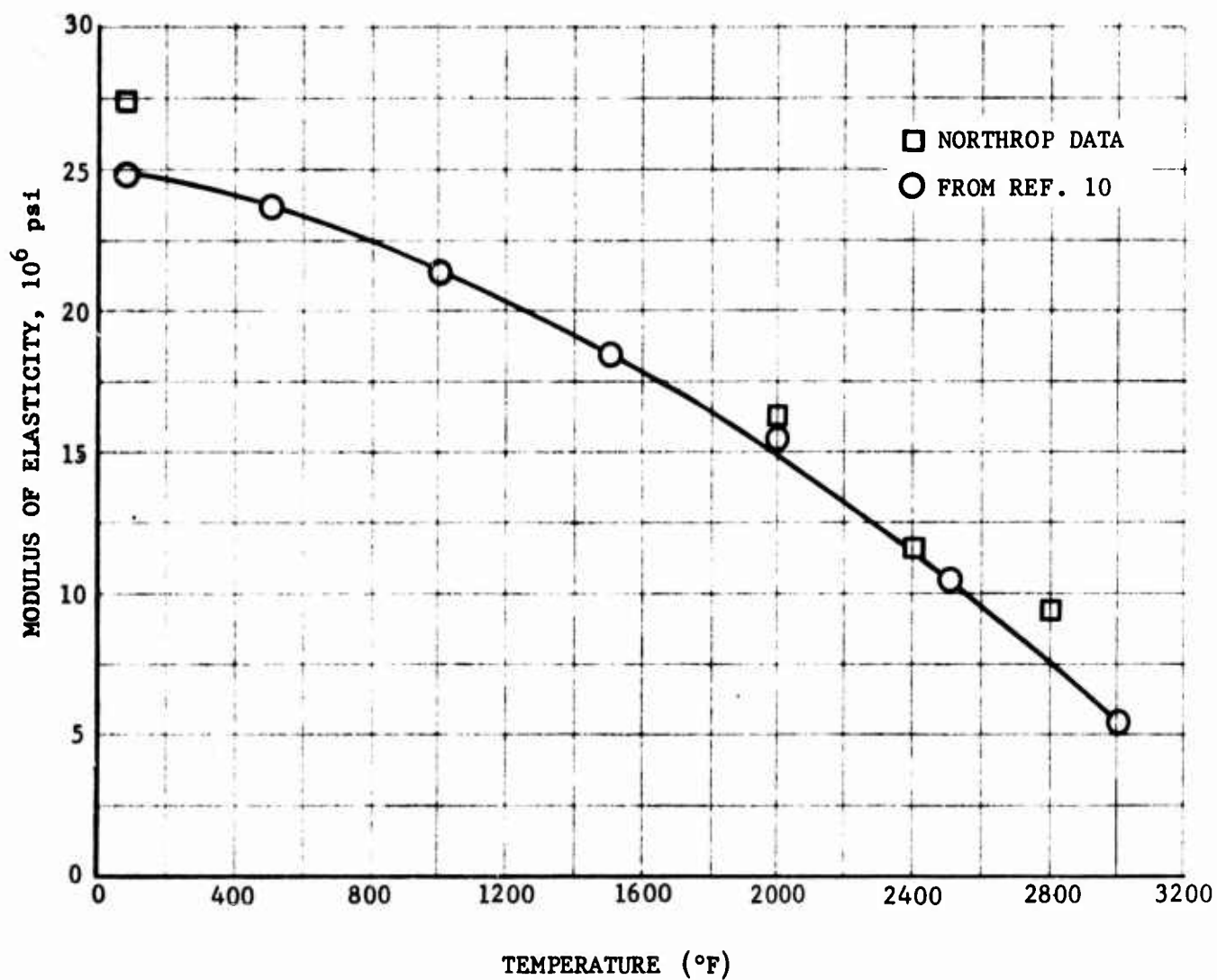


FIGURE 96 MODULUS OF ELASTICITY OF FACE SHEET MATERIAL AS A FUNCTION OF TEMPERATURE

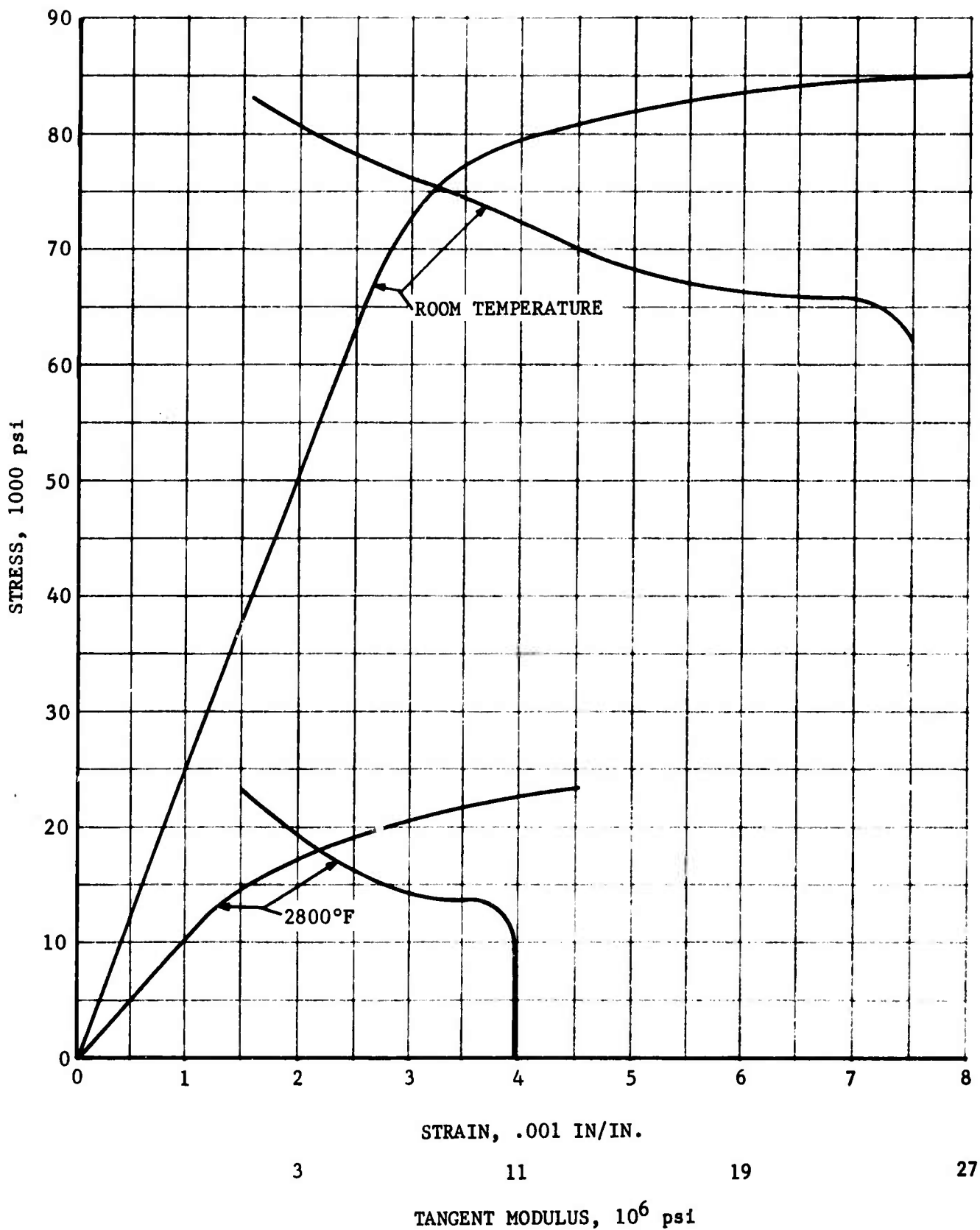


FIGURE 97 STRESS-STRAIN AND TANGENT MODULUS CURVES AT ROOM TEMPERATURE AND 2800F

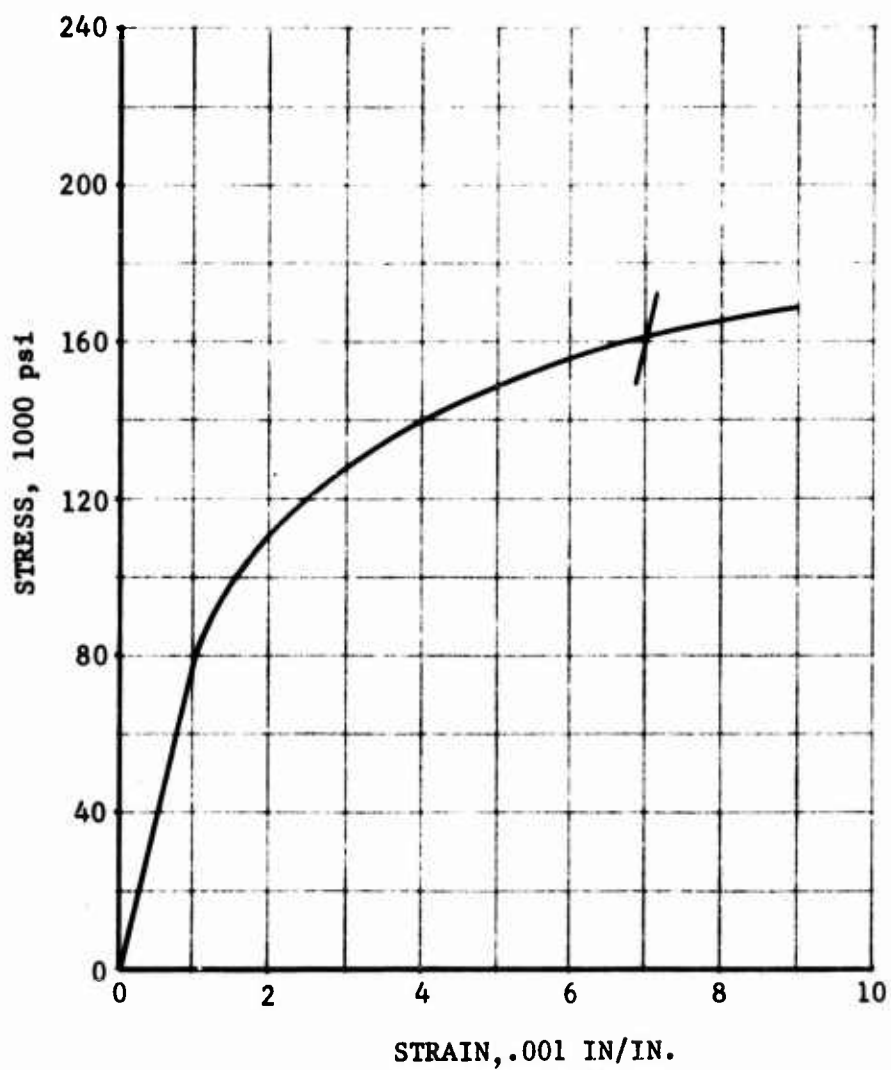


FIGURE 98 BEARING STRESS-STRAIN CURVE OF THE FACING MATERIAL ($e/D=2.0$)

Core Foil Properties

The .0022 inch foil utilized in the manufacture of the honeycomb core for this program was rolled under Air Force Contract AF33(657)-8912 with the following tensile properties in the fully recrystallized condition being reported:

<u>Temp of</u>	<u>Gain Direction</u>	<u>F_{tu} (ksi)</u>	<u>F_{ty} (ksi)</u>	<u>E %</u>
RT	Longitudinal	128.9	107.7	15.8
	Transverse	128.0	104.8	14.4
2800	Longitudinal	26.0	22.2	26.6
	Transverse	24.4	20.8	4.3

Flatwise Compression Properties

Flatwise compression tests were performed to determine core properties. These test results were obtained on Panel 11 and Table XVIII and Figure 99 show the compressive failure stress results at various temperatures from room temperature to 2800F. Figure 100 represents the flatwise compression modulus of the core material. Also included is a stress-strain curve of core specimens in flatwise compression at room temperature and 2800F (Figure 101).

In addition, one test was conducted to determine the core shear modulus of rigidity.

Flatwise Tension Properties

Flatwise tension tests are standard criteria for determining bond strengths of composite structures. To determine the strength of the solid-state bond attained during panel manufacture and the affect of stress and temperature on these bonded joints, flatwise tension tests were performed on several panels. Table XIX and Figure 102 show these results at various temperatures for each of four flat panels representing as-fabricated and post-structural test conditions.

Bond strength (especially at the higher test temperatures) is directly related to the amount of diffusion attained in the joint during panel fabrication. With the bond parameters used in panel bonding a center-of-joint concentration of approximately 60Ta-40Ti was expected according to the bond parameter study performed during Phase I of the program. Later analysis, however, revealed an actual joint concentration approximating 50Ta-50Ti. With the former concentration level, (60-40), a joint remelt temperature of about 3650F would have resulted. With the latter concentration (50-50) an actual joint remelt temperature of 3450F was experienced. This in part would account for lower joint strengths at 2800F than were expected. Higher elevated temperature bond strengths can be attained by merely adjusting the bonding parameters of temperature and time to reflect this discrepancy between theoretical and actual diffusion bonding conditions.

TABLE XVIII
SPECIMEN FLATWISE COMPRESSION TEST RESULTS

PANEL NO.	SPECIMEN NO.	FAILURE STRESS (psi)	TEST TEMP. (F)
11 (Flat, as fabricated)	1	1840	R.T.
	2	1730	R.T.
	3	734	2000
	4	825	2000
	5	750	2200
	6	588	2400
	7	431	2600
	8	336	2800

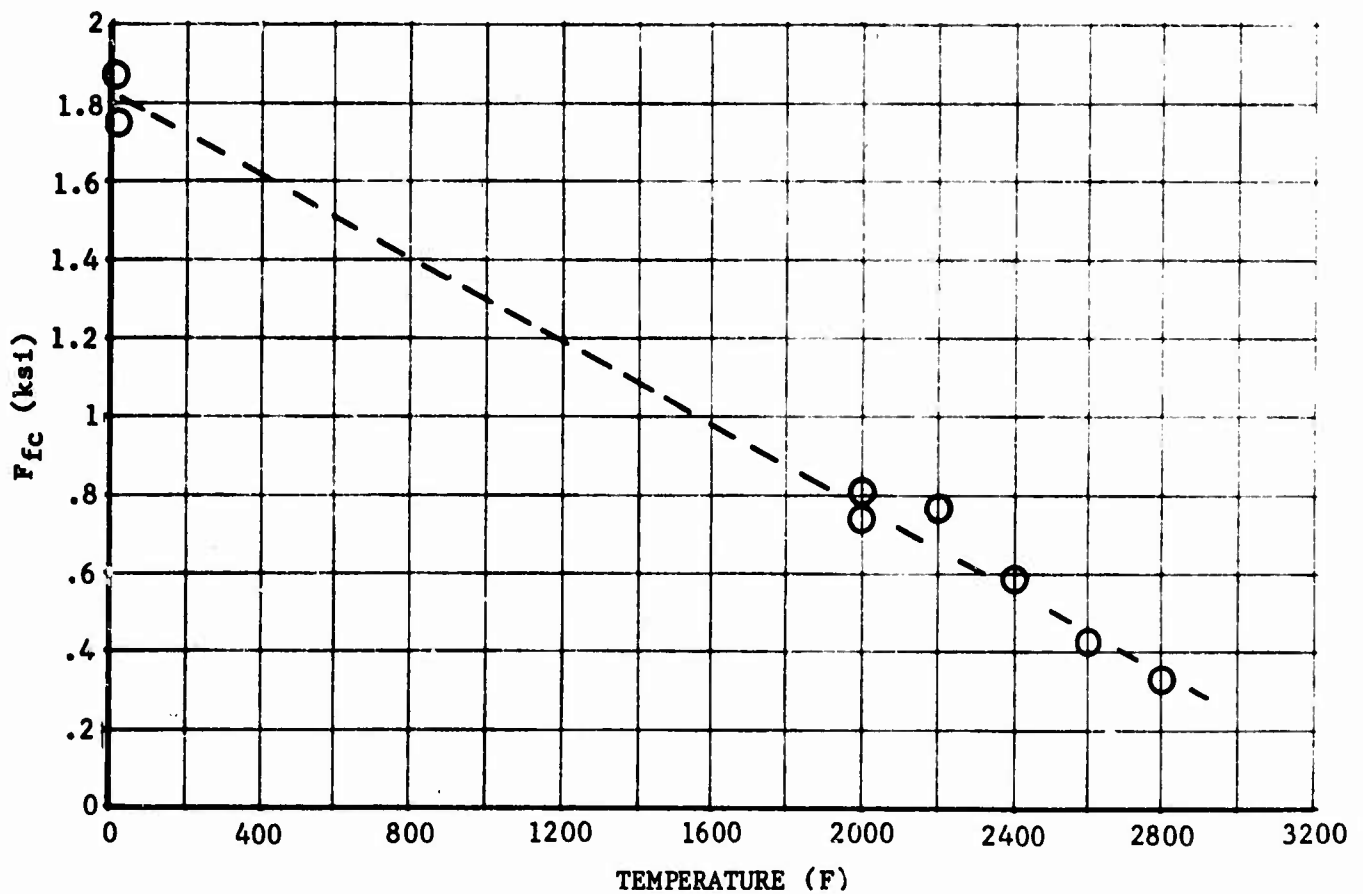


FIGURE 99 FLATWISE COMPRESSION STRENGTH AT ROOM AND ELEVATED TEMPERATURES FROM SPECIMENS TAKEN FROM PANEL 11

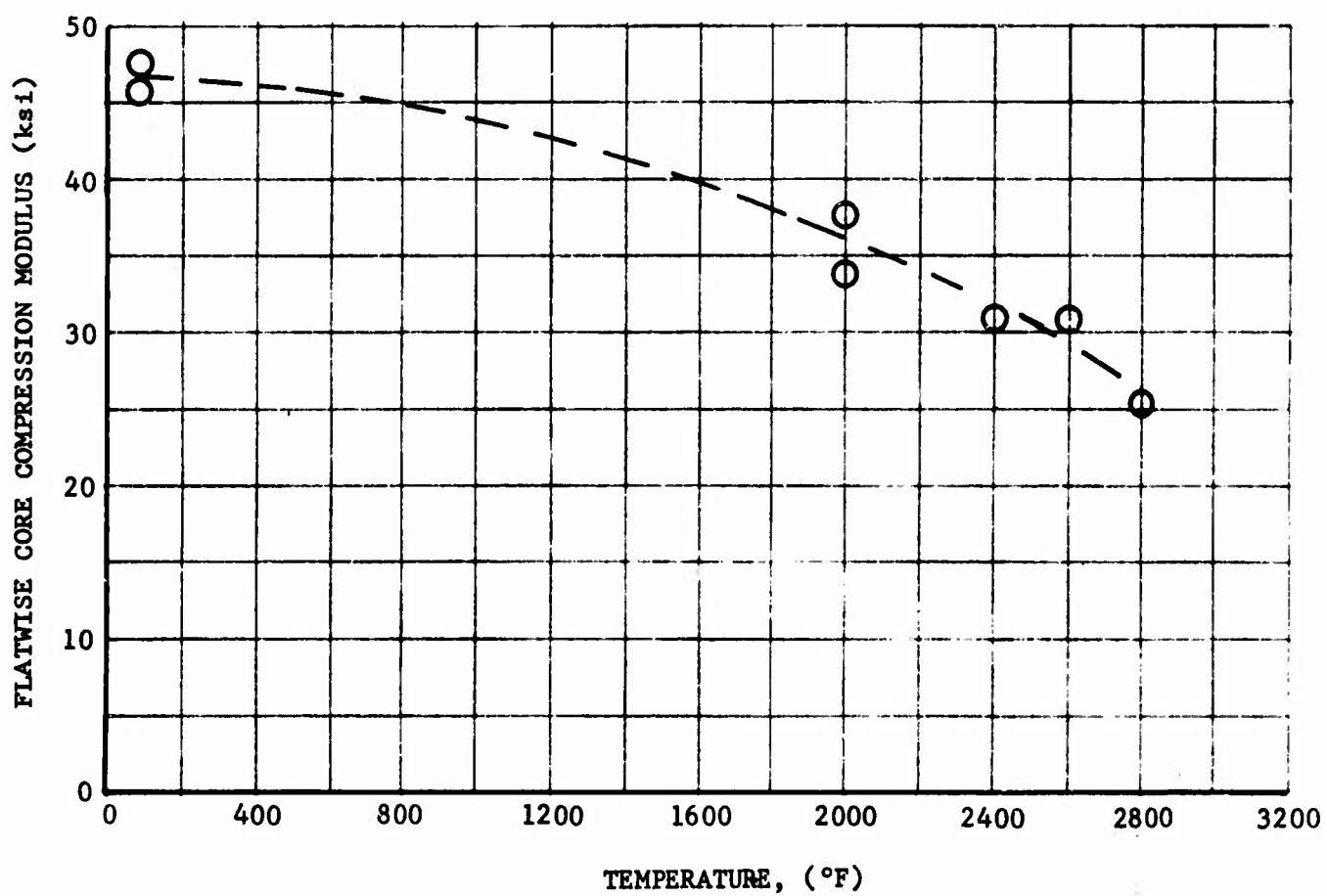


FIGURE 100 FLATWISE COMPRESSIVE MODULUS OF ELASTICITY OF THE CORE AT ROOM AND ELEVATED TEMPERATURES

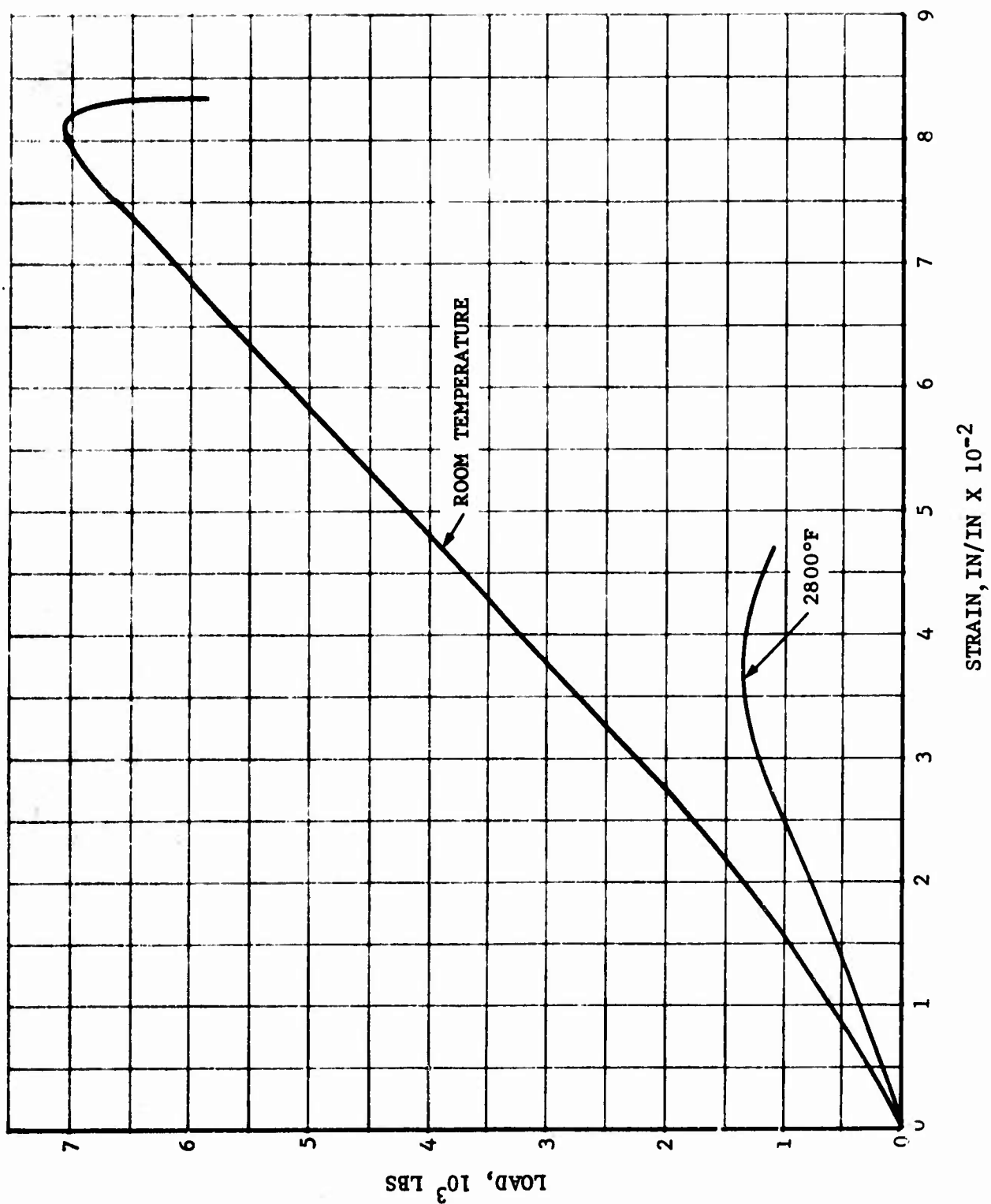


FIGURE 101 FLATWISE COMPRESSION STRESS-STRAIN CURVE AT ROOM TEMPERATURE AND 2800F

TABLE XIX
SPECIMEN FLATWISE TENSION TEST RESULTS

PANEL NO.	SPECIMEN NO.	FAILURE STRESS (psi)	TEST TEMP. (F)
5 (As-Fabricated)	1	1450 ⁽¹⁾	R.T.
	2	590	2000
	3	373	2200
	4	274	2400
	5	251	2600
	6	220	2800
7 (Tested in Shear at R.T.)	1	1160	R.T.
	2	662	2000
	3	375	2200
	4	395	2400
	5	305	2600
	6	240	2800
9 (Tested in Shear at 2100F)	1	1150 ⁽¹⁾	R.T.
	2	525	2000
	3	102	2800
10 (Tested in Shear at 2650F)	1	1375 ⁽¹⁾	R.T.
	2	420	2000
	3	78	2800

(1) Failure occurred at the adhesive bond between specimen and fixture.

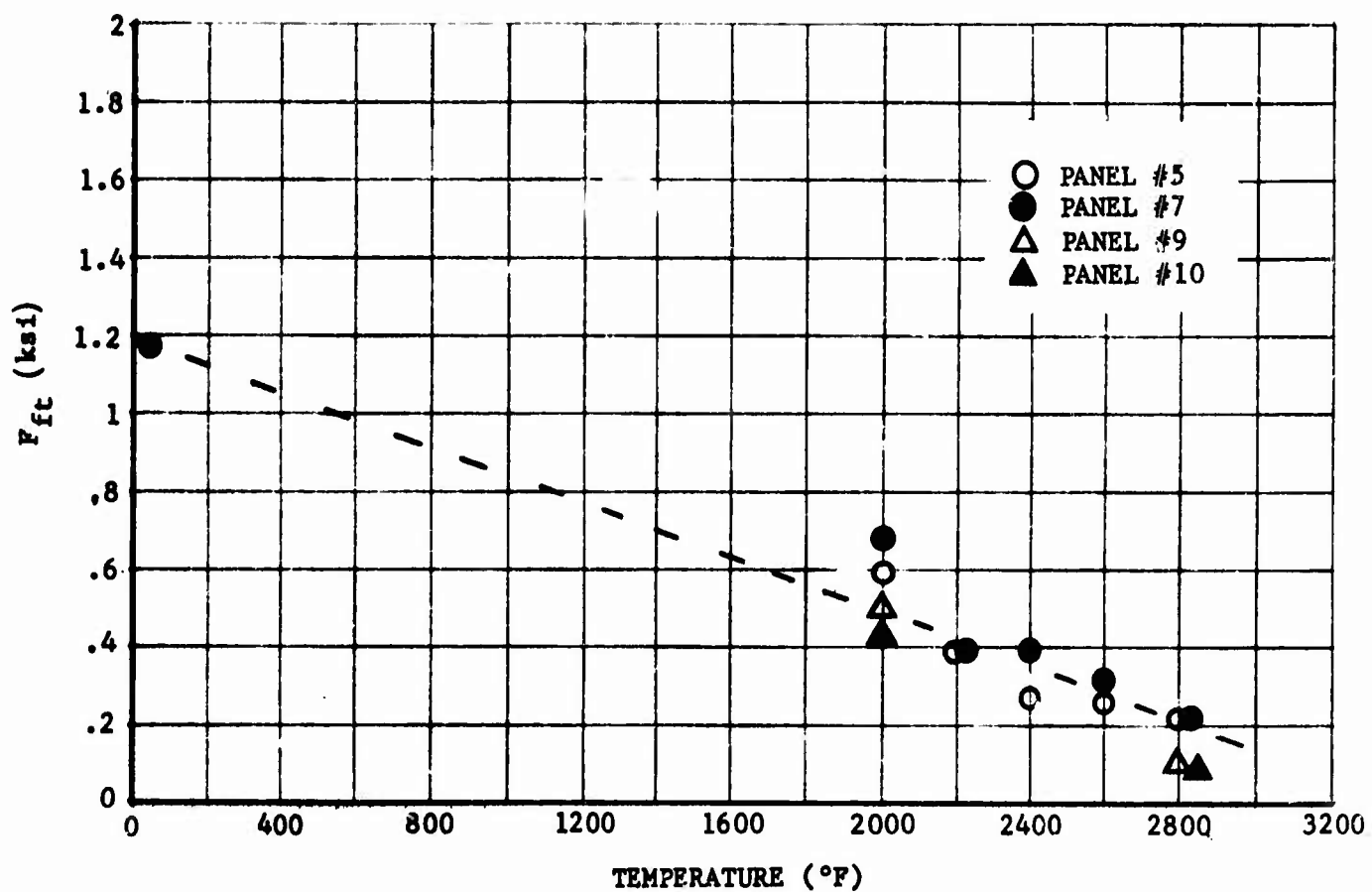


FIGURE 102 FLATWISE TENSION STRENGTH OF SPECIMENS TAKEN FROM AS FABRICATED AND STRUCTURALLY TESTED PANELS AT ROOM AND ELEVATED TEMPERATURES

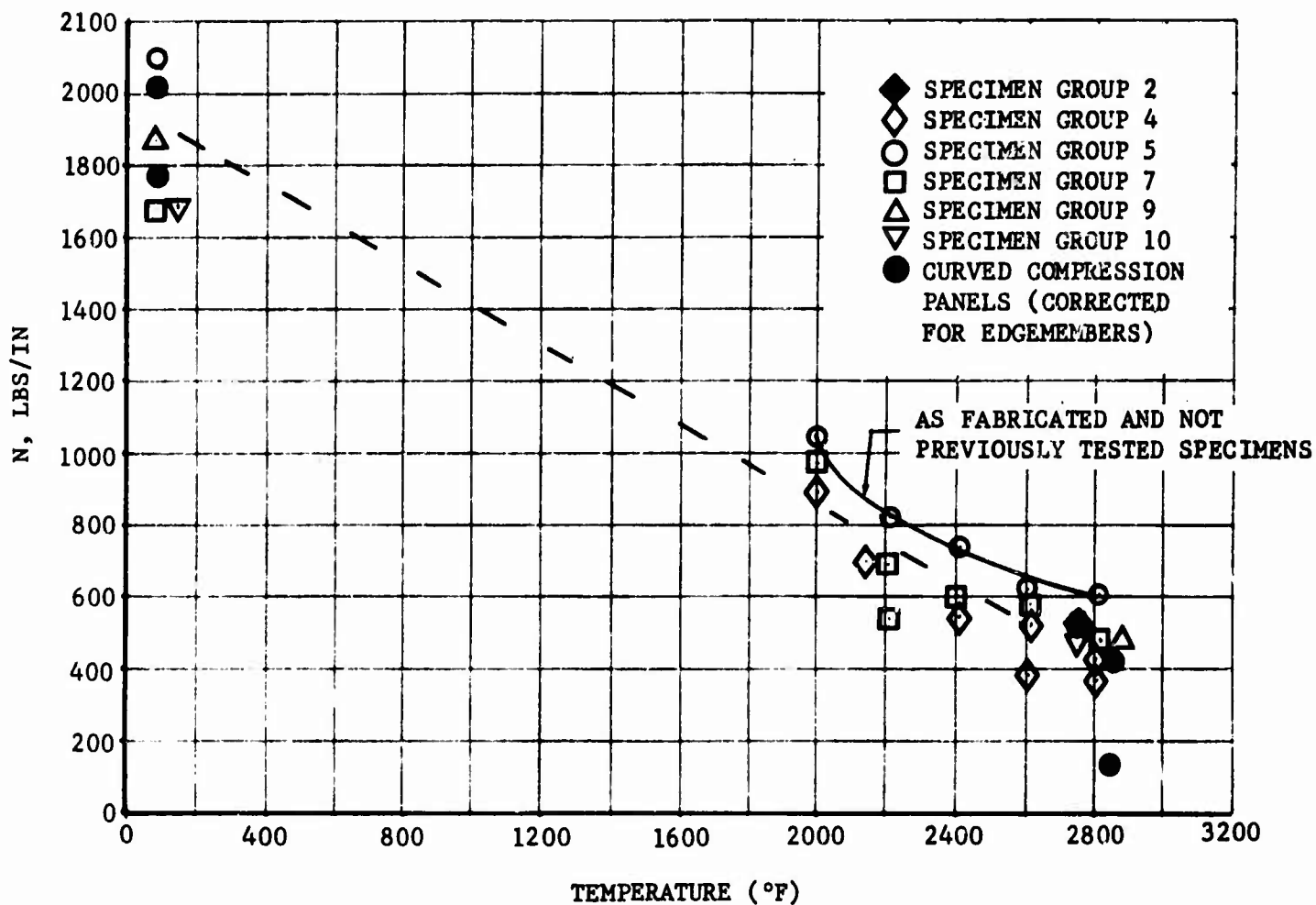


FIGURE 103 EDGEWISE COMPRESSION STRENGTH AS A FUNCTION OF TEMPERATURE OF SPECIMENS TAKEN FROM AS-FABRICATED AND STRUCTURALLY TESTED PANELS. FULL SIZE PANEL EDGEWISE COMPRESSION TEST RESULTS ARE INCLUDED FOR CORRELATIVE PURPOSES

Edgewise Compression Properties

Edgewise compression specimens were taken from both as-fabricated and the compression and shear tested structural panels. Table XX is a tabulation of the results of these tests with a plot of the edgewise compression strength shown in Figure 103. Included in the plot is the corrected* edgewise compression strength of the curved structural compression panels. Only a limited number of specimens were obtained from the curved structural panels.

Although the core of curved panel 4 was weakened by the solution used in removing the panel coating, specimens tested still exhibited good edgewise compression strength. Figure 103 graphically shows the loss in strength exhibited by the edgewise compression specimens taken from prior tested shear and compression structural panels.

The general mode of failure of the edgewise compression specimens is illustrated in Figure 104. The majority of the specimens failed at the mid length with intercell buckling followed by a sharp wrinkle of the face sheet across the width of the specimen on both sides.

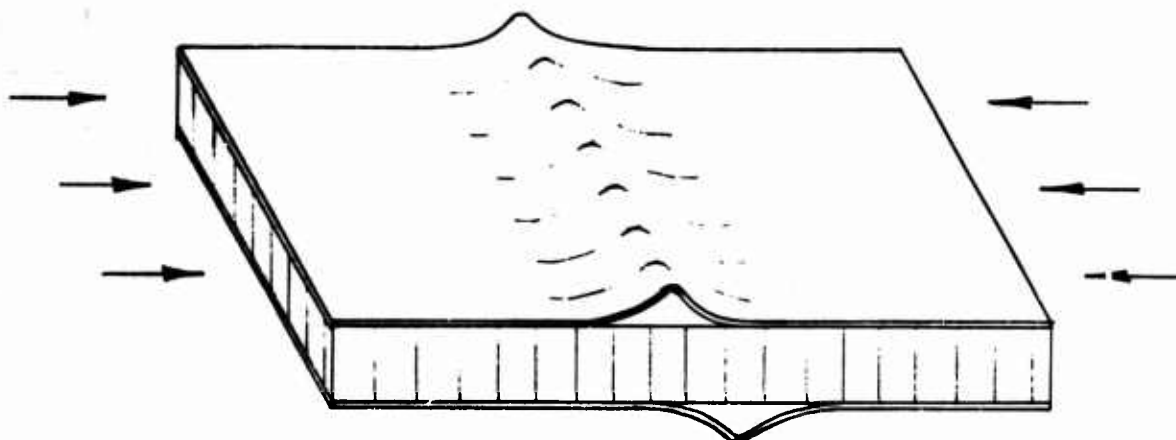


FIGURE 104 FAILURE MODE OF EDGEWISE COMPRESSION SPECIMENS.

*Panel length is increased proportional to the load carrying area of the edgemembers.

TABLE XX

SPECIMEN EDGEWISE COMPRESSION TEST RESULTS

PANEL NO.	SPECIMEN NO.	FAILURE STRESS (psi)	TEST TEMP. (F)
2 (Curved panel tested in compression at 2800F)	1	19,600	2800
	1	36,900	2000
4 (Curved panel tested in compression at room temperature)	2	29,500	2200
	3	23,500	2400
	4	23,100	2600
	5	16,000	2600
	6	15,100	2800
	7	17,900	2800
5 (Flat panel As-fabricated)	1	87,300	R.T.
	2	42,200	2000
	3	33,800	2200
	4	31,800	2400
	5	26,100	2600
	6	25,500	2800
7 (Flat panel Tested in shear at room temperature)	1	82,100	R.T.
	2	39,600	2000
	3	21,800	2200
	4	28,000	2200
	5	24,100	2400
	6	24,100	2600
	7	20,100	2800
9 (Flat panel Tested in shear at 2100F)	1	78,500	R.T.
	2	20,300	2800
10 (Flat panel tested in shear at 2650)	1	70,500	R.T.
	2	19,100	2800

This mode of failure differed from subsequent edgewise compression panel failures. No separation of the facing from the core was observed during testing of the complete panel assemblies.

Metallographic Analysis

Metallographic analysis was used merely to check the reproducibility of joints between panels during this final phase of effort on the program. Core-to-face sheet joints of an as-fabricated panel are shown in Figure 105. The upper photomicrograph shows a section through a node in the honeycomb core. Note the columbium intermediate used for solid-state diffusion-bonding of the core and the titanium intermediate (martensitic structure) used to form the solid-state bonded joint between the honeycomb core and face sheet. The lower photomicrograph shows a typical section through a cell-wall-to-face-sheet joint. The joint in Figure 106 was obtained from a deformed area of a panel tested in edgewise compression at 75F. Although some cracks have appeared in the tantalum foil, the joint remained intact.

Summary of Specimen Test Results

The integrity of the honeycomb-to-face sheet bonded joints from point to point within a given panel and from panel-to-panel were consistently good. This indicates that the fabrication procedures were such that good reproducibility was achieved. An increase in temperature from 75F to 2800F caused a 60 percent decrease in specimen mechanical properties which is in good agreement with published data for the T-111 base material. Structural panel testing prior to specimen testing caused an additional loss of not more than 15 percent, depending on the severity of the panel test. Panel design can be further optimized to take advantage of the method of construction. Bond strength could be improved by adjusting the bonding parameters to effect greater diffusion in the bonded joint thus yielding a higher center-of-joint concentration of tantalum.

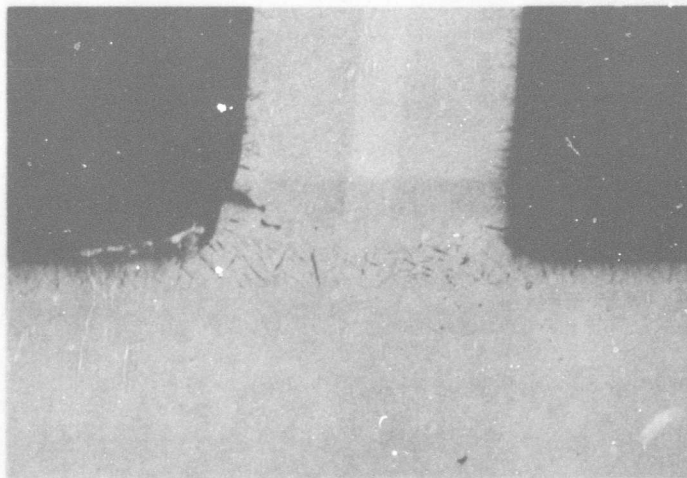
A summary of basic applicable mechanical properties derived from the diffusion-bonded panels and the tantalum construction materials is presented in Table XXI.

EDGEWISE COMPRESSION STRUCTURAL TEST RESULTS

Room Temperature Tests

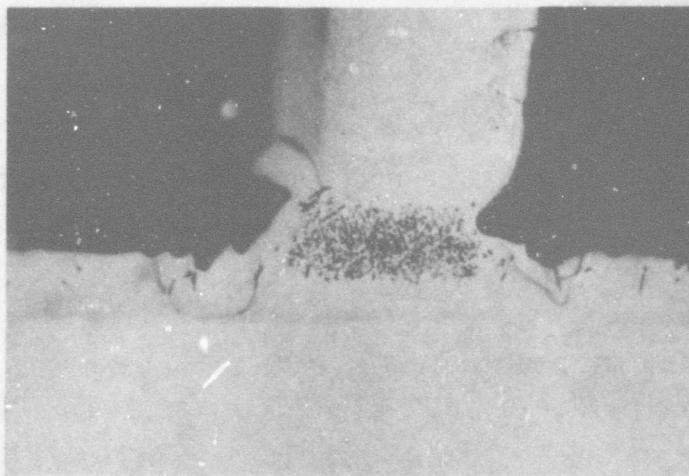
Strengths of the two curved structural panels tested at room temperature in edgewise compression were as follows:

<u>PANEL NO.</u>	<u>FAILURE LOAD (Lbs)</u>	<u>PANEL FAILURE STRESS (ksi)</u>
1	35,500	91.7
4	27,700	71.6



ETCHANT: 50 NH_4F + 50 HF
MAGNIFICATION: 250X

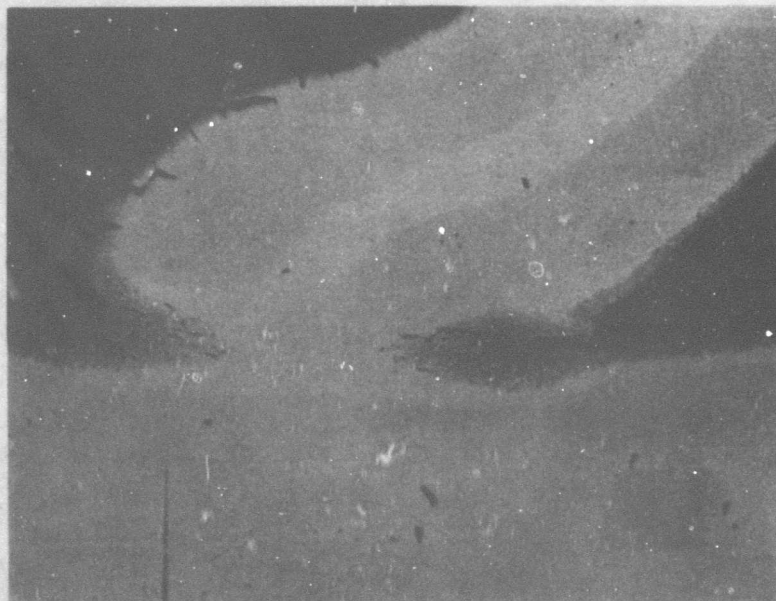
a. MICROSTRUCTURE OF A NODE/FACESHEET JOINT



ETCHANT: 50 NH_4F + 50 HF
MAGNIFICATION: 500X

b. MICROSTRUCTURE OF A CELL-WALL/FACESHEET JOINT

FIGURE 105 MICROSTRUCTURE OF TYPICAL HONEYCOMB/FACESHEET JOINTS



ETCHANT: 50 NH_4F + 50 HF
MAGNIFICATION: 250X

FIGURE 106 PHOTOMICROGRAPH SHOWING DEFORMATION ABSORBED
BY A HONEYCOMB/FACESHEET JOINT

TABLE XXI

TYPICAL MECHANICAL PROPERTIES OF THE TANTALUM
SANDWICH CONSTRUCTION COMPONENTS

FACINGS				FOIL			
	R.T.	2000F	2600F	2800F		R.T.	2800F
F_{tu} , ksi	99.0	62.0(1)	34.0(1)	31.0(1)	F_{tu} , ksi	128.5(1)	23.4(1)
F_{ty} , ksi	83.0	35.0(1)	25.0(1)	21.0(1)	F_{ty} , ksi	105.3(1)	23.3(1)
F_{su} , ksi	57.0(2)	36.0(2)	20.0(2)	18.0(2)			
E , 10^6 psi	25.0(1)	15.0(1)	9.5(1)	7.5(1)	CORE		
G , 10^6 psi	9.3				R.T.	2000F	2600F
F_{bru} , ksi ($e/D=2$)	229.0	144.0(3)	80.0(3)	73.0(3)	E_c , 10^3 psi	47.0	30.0
F_{bry} , ksi ($e/D=2$)	158.0	67.0(3)	48.0(3)	40.0(3)	G_c , 10^3 psi	68.5	52.0(3)
DENSITY, lbs/in ³	.608				F_{fc} , ksi	1.82	.78
					F_{ft} , ksi	1.16	.50
					Density, lbs/in ³	.0097(2)	.20

(1) Source other than Northrop

(2) Calculated

(3) Extrapolated

The loading rate used in testing both panels was 83 pounds per second with vertical deflection measurements taken every 5,000 pounds. Data plots of load rate and panel deflection are given in Figures 107 and 108 for Panels 1 and 4, respectively.

Panel 4 failed at the predicted failure stress whereas Panel 1 exceeded predicted values. Both failures occurred at the edgemember-core transition as shown in Figures 109 and 110 resulting in a shear crimp type failure mode. No evidence of defective bonding was noted in any portion of the panels. The difference in strength between the two panels was attributed to the degree of alignment in the vertical and horizontal plane during testing.

Elevated Temperature Tests

Two curved panels were tested at 2800F and 2900F. Strengths of the two edgewise compression tests at elevated temperatures were as follows:

<u>PANEL NO.</u>	<u>TEST TEMPERATURE (F)</u>	<u>FAILURE LOAD (Lbs.)</u>	<u>PANEL FAILURE STRESS (ksi)</u>
2	2,800	6,640	17.2
3	2,900	2,000	5.2

Panel 2 was tested with the convex side of the panel at 2800F and the loaded edgemember at 1025F due to the heat sink affect of the fixtures. The concave side of the panel measured 50F to 100F higher in temperature than the convex side. The actual temperature distribution on the panel is shown in Figure 111. During this test, a power supply malfunction occurred as the panel temperature reached 2600F, which shut down the quartz lamp radiant heater prior to the application of the compressive load. The panel was recycled and tested to failure. Figure 112 shows the time temperature cycle used on Panel 2. This severe thermal shock may have accounted for the vertical crack (both facings) shown in Figure 113. Vertical deflection measurements of the panel during loading are given in Figure 114. Panel 2 failed slightly below the predicted failure stress. Crippling occurred along the horizontal plane in a uniform manner. Some evidence of intercell buckling was noted adjacent to the crippled area.

Panel 3 was tested with the main portion of the panel, both sides, at 2900F, with the central portion of the edgemember at 1525F to 1700F. The temperature distribution across the panel is shown in Figure 115, with the temperature and loading cycle shown in Figure 116. No vertical deflection measurements were obtained during loading due to a recorder malfunction. Panel 3 apparently failed due to premature failure of the protective coating. From the examination of the panel (Figures 117 and 118) it was apparent that a minute defect in the coating may have allowed oxidation of the tantalum substrate during the heating cycle and stabilization time at temperature. This would have weakened the panel sufficiently to cause premature failure when the load was applied. In addition, the panel exhibited a non-uniform failure mode, as failure for the most part occurred on one-half of the panel whereas the failure of Panel 2 was uniformly distributed across the width of the panel. The arrow in Figure 118 indicates the initiation point of failure.

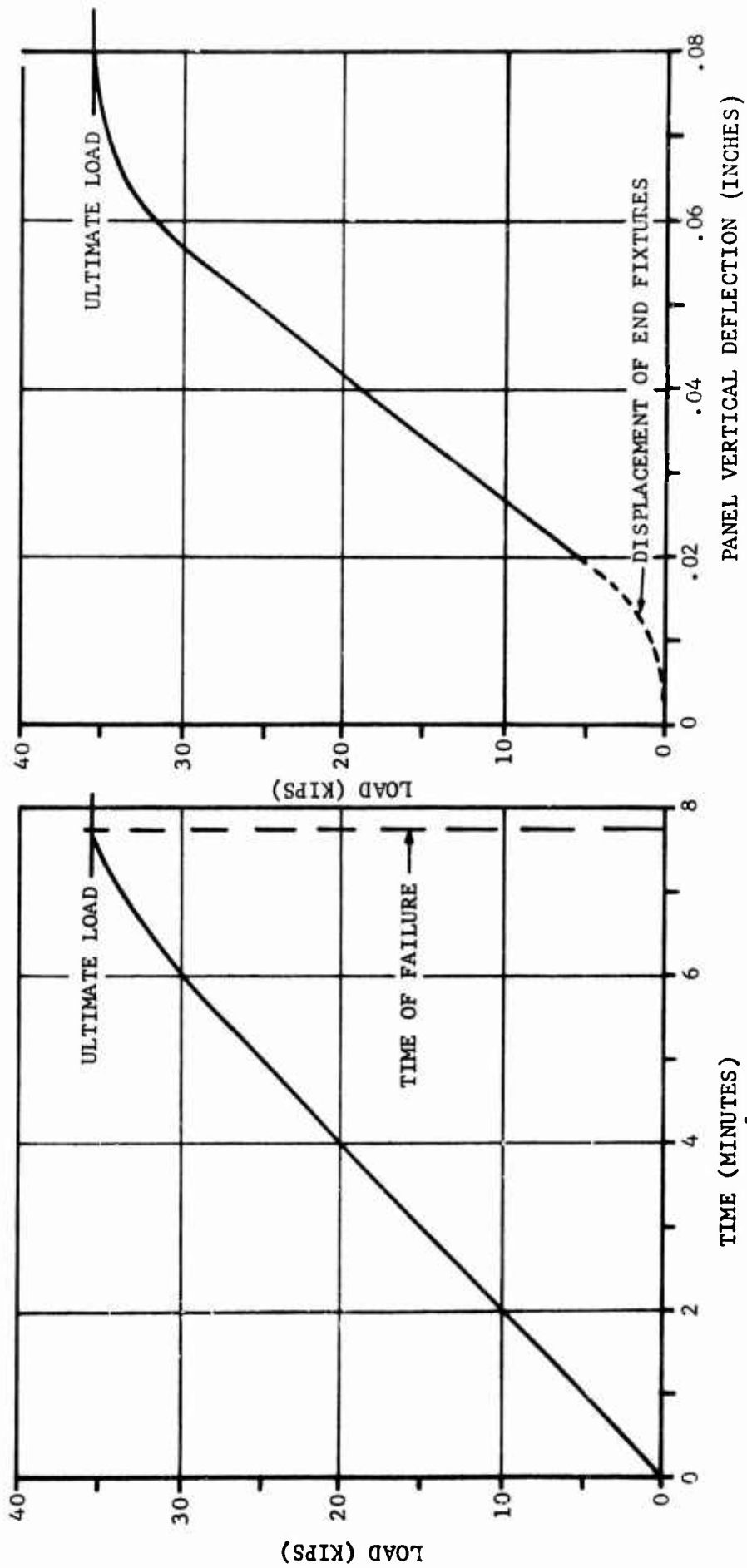


FIGURE 107 LOAD CYCLE AND DEFLECTION OF PANEL 1 TESTED IN EDGEWISE COMPRESSION AT ROOM TEMPERATURE

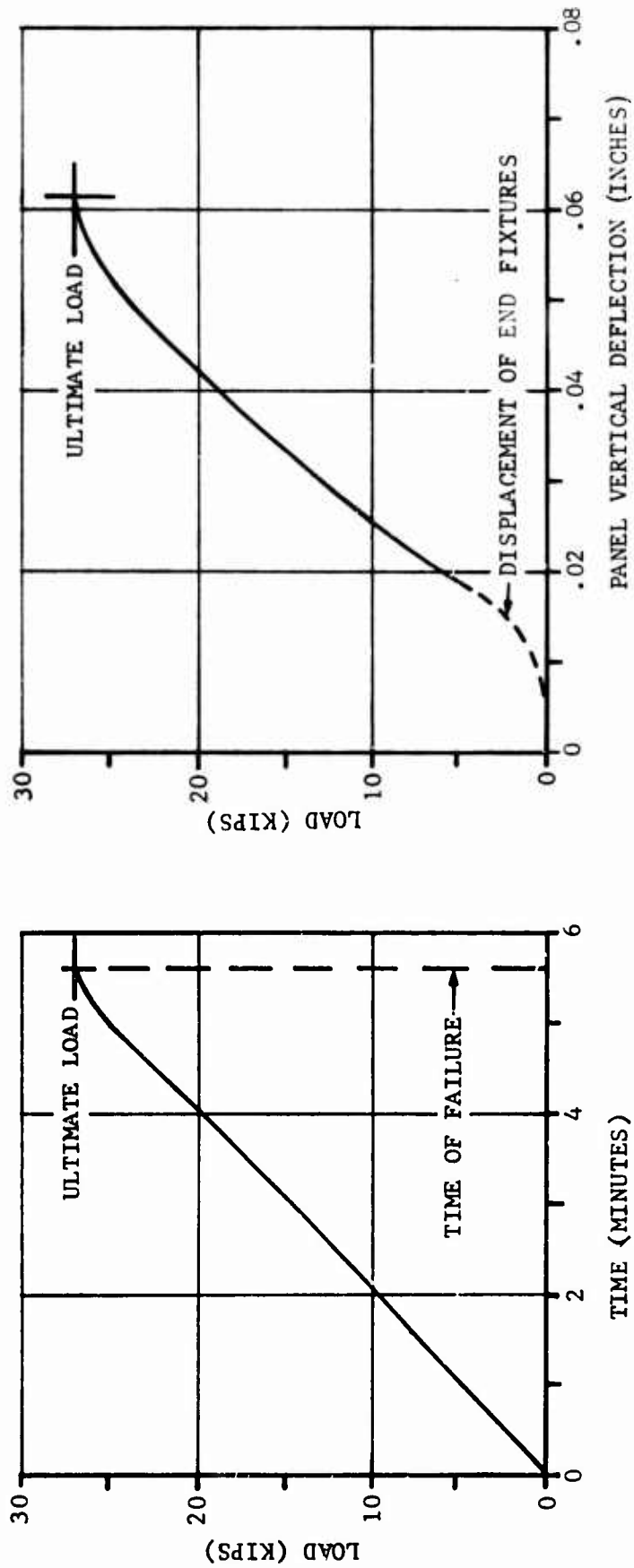


FIGURE 108 LOAD CYCLE AND DEFLECTION OF PANEL 4 TESTED IN EDGEWISE COMPRESSION AT ROOM TEMPERATURE

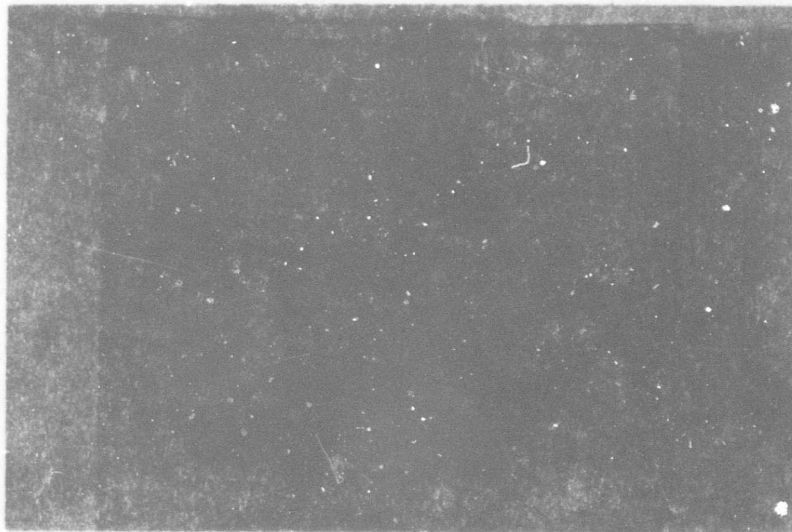


FIGURE 109 MODE OF FAILURE OF PANEL 1 TESTED IN EDGEWISE COMPRESSION AT ROOM TEMPERATURE. FAILURE WAS MAINLY AT THE EDGEMEMBER - CORE TRANSITION PLANE

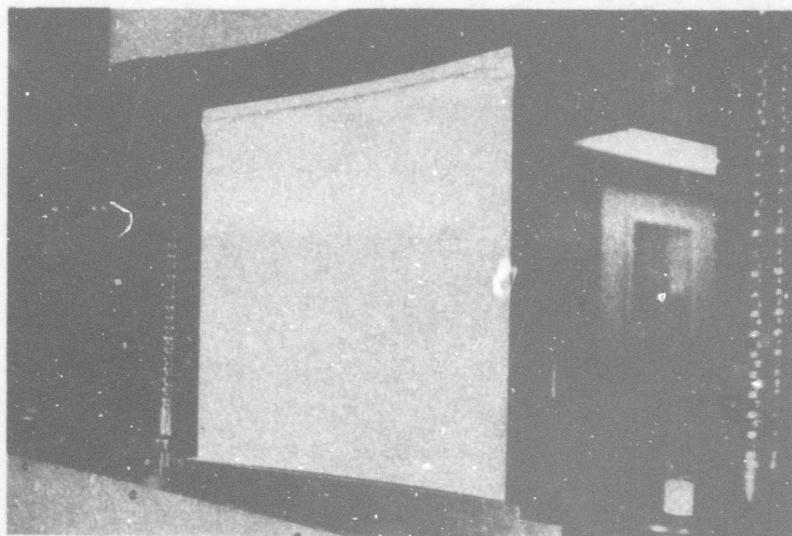


FIGURE 110 MODE OF FAILURE OF PANEL 4 TESTED IN EDGEWISE COMPRESSION AT ROOM TEMPERATURE. FAILURE WAS SHEAR CRIMPING AT THE EDGEMEMBER - CORE TRANSITION PLANE

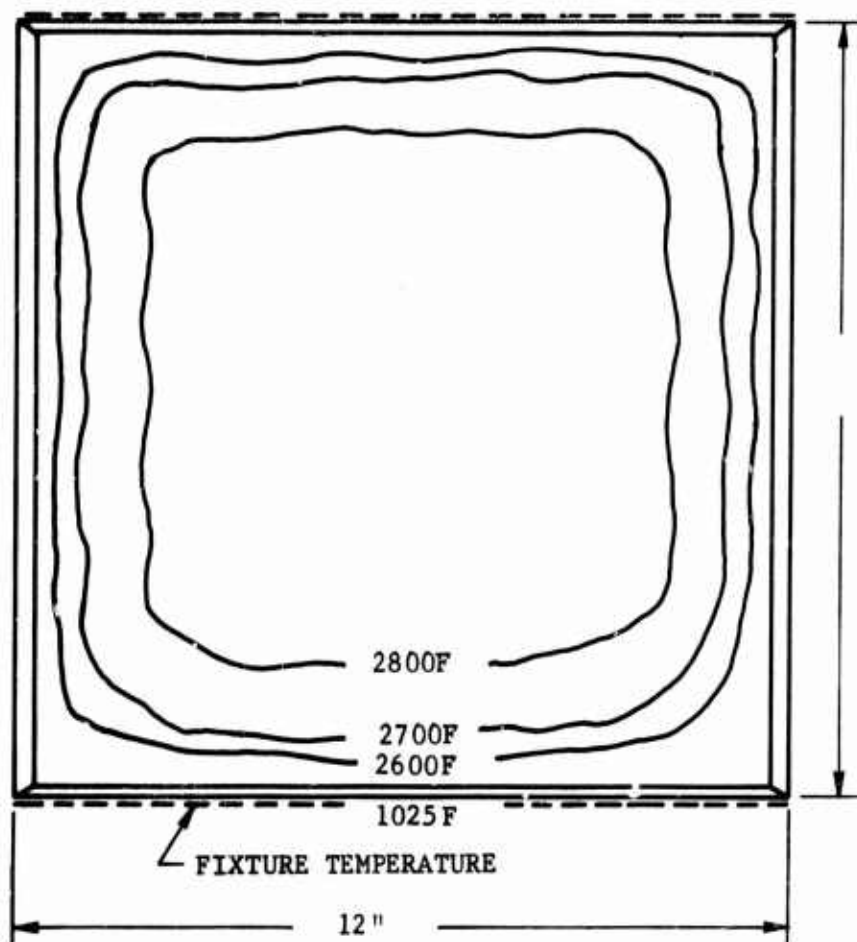


FIGURE 111 VARIATION OF TEMPERATURE ON CONVEX SIDE OF PANEL 2
TESTED IN EDGEWISE COMPRESSION AT 2800F

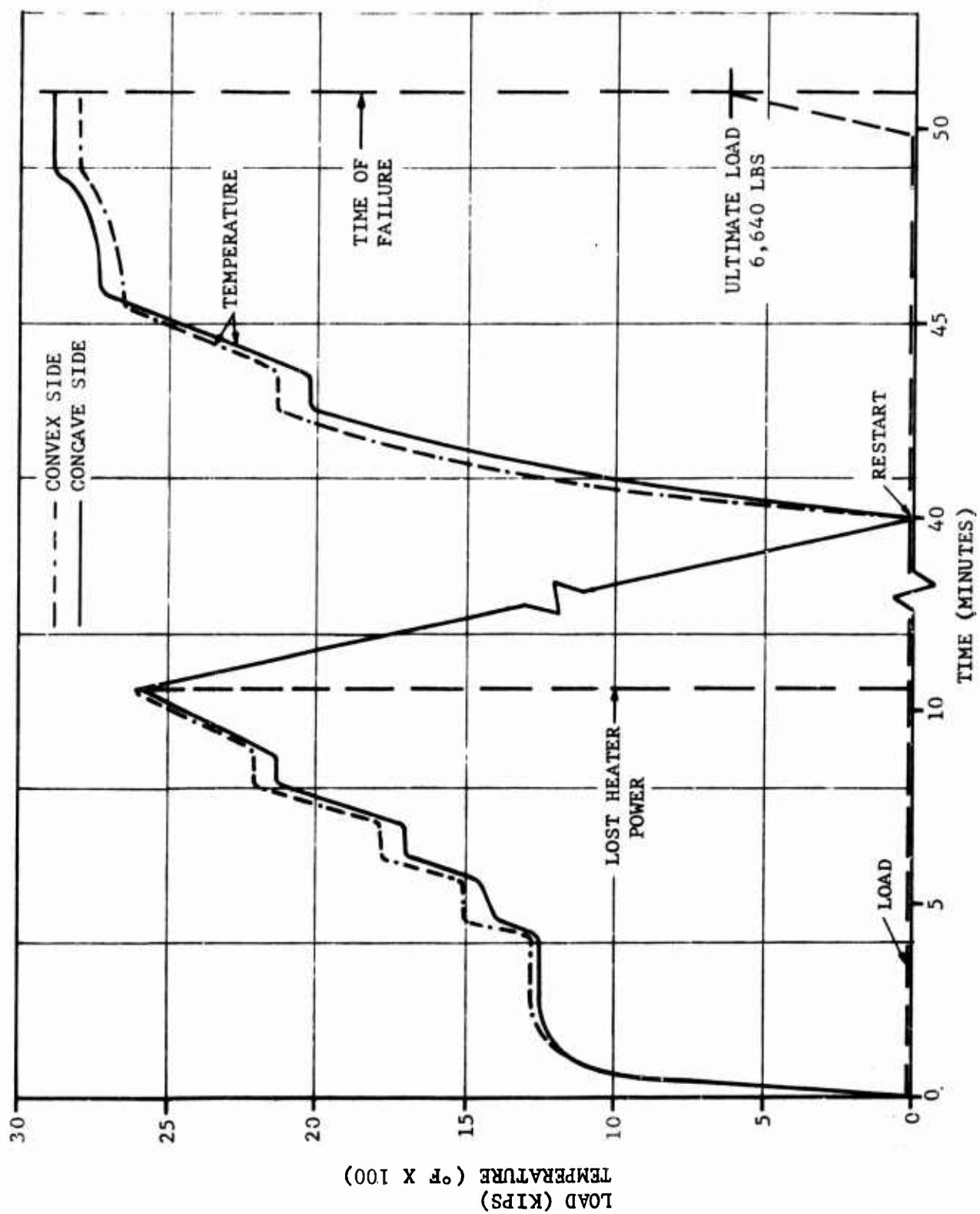


FIGURE 112 LOAD AND TEMPERATURE CYCLE FOR PANEL 2 TESTED IN EDGEWISE COMPRESSION AT 2800F

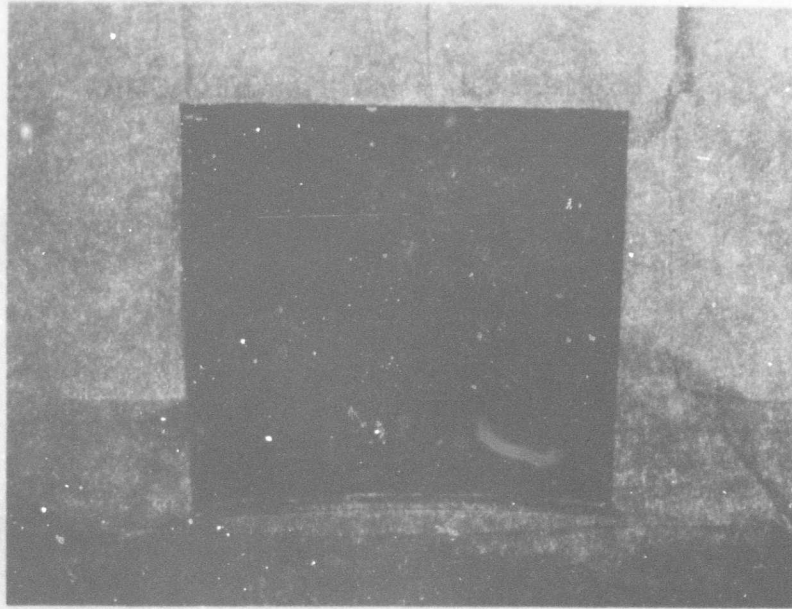


FIGURE 113 PANEL 2 TESTED IN EDGEWISE COMPRESSION AT 2800F SHOWING MODE OF FAILURE. NOTE SAGGING OF COATING AT BOTTOM OF PANEL DUE TO TIN RUN-OFF. WHITE SPOTS ON PANEL ARE THERMOCOUPLE CONTACT POINTS

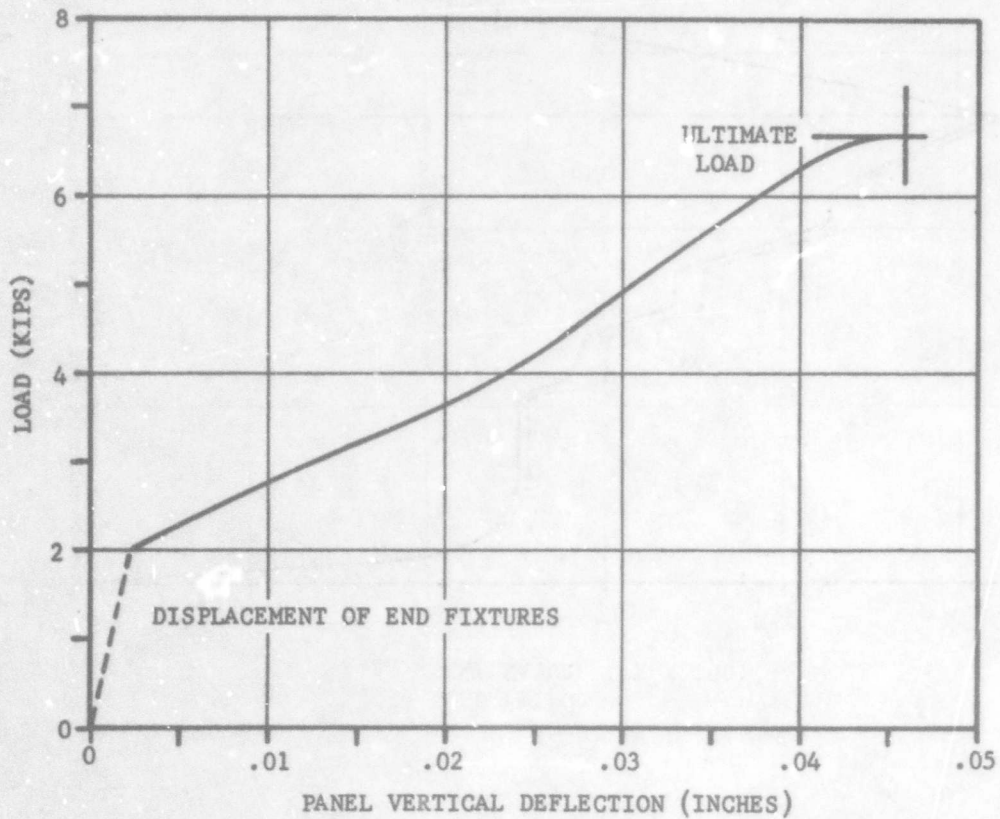


FIGURE 114 LOAD-DEFLECTION CURVE FOR PANEL 2 TESTED IN EDGEWISE COMPRESSION AT 2800F

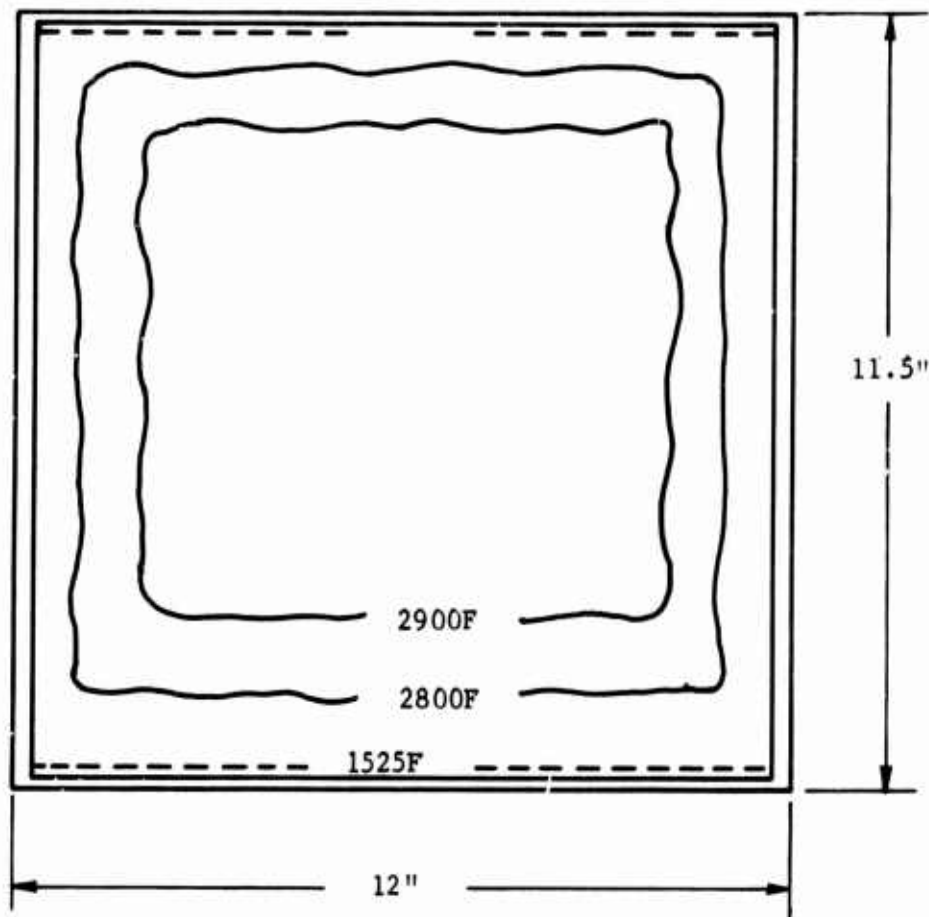


FIGURE 115 TEMPERATURE DISTRIBUTION OF BOTH SIDES OF PANEL 3
TESTED IN EDGEWISE COMPRESSION AT 2900F

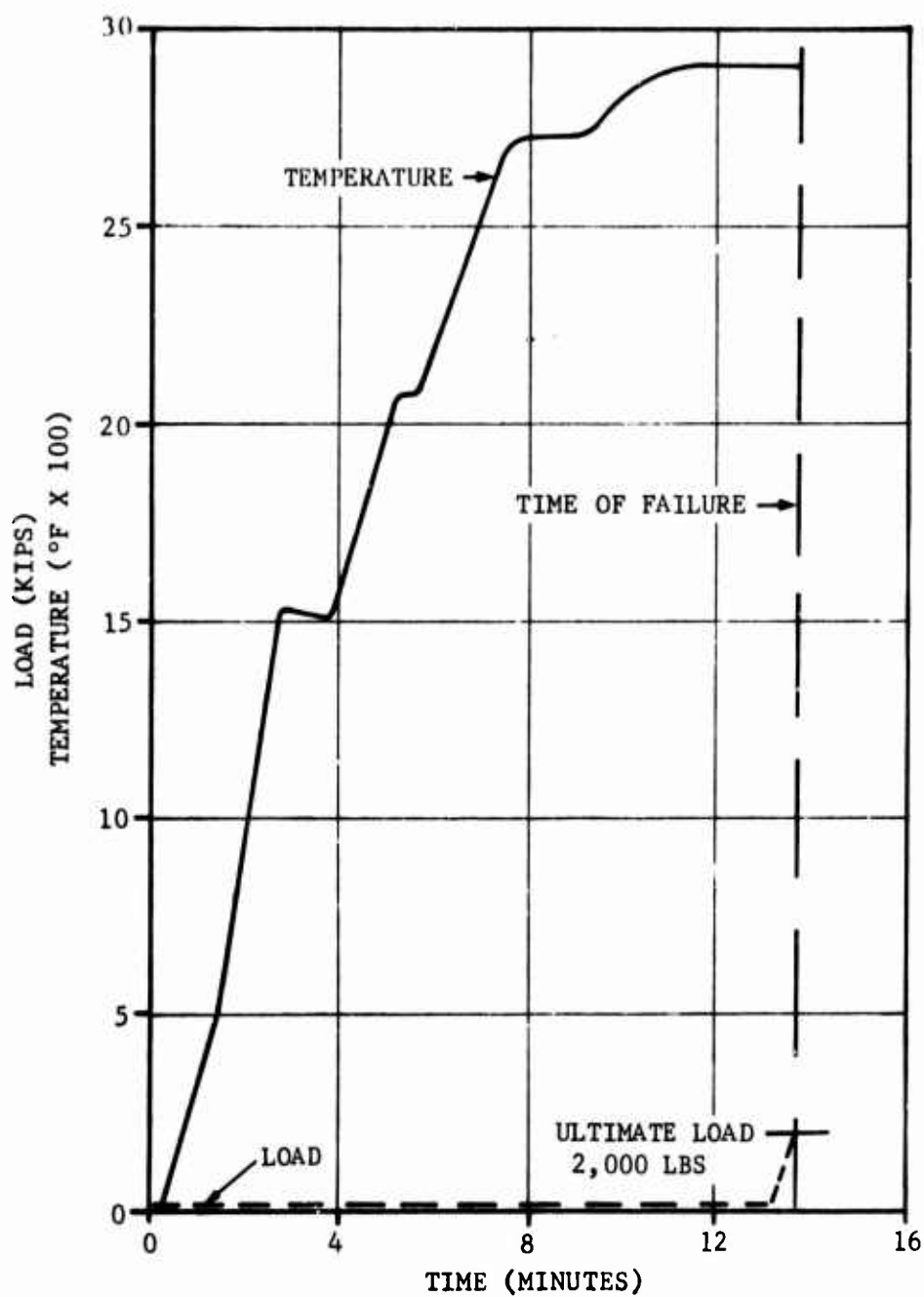


FIGURE 116 LOAD-TEMPERATURE CYCLE FOR PANEL 3 TESTED IN EDGEWISE COMPRESSION AT 2900F

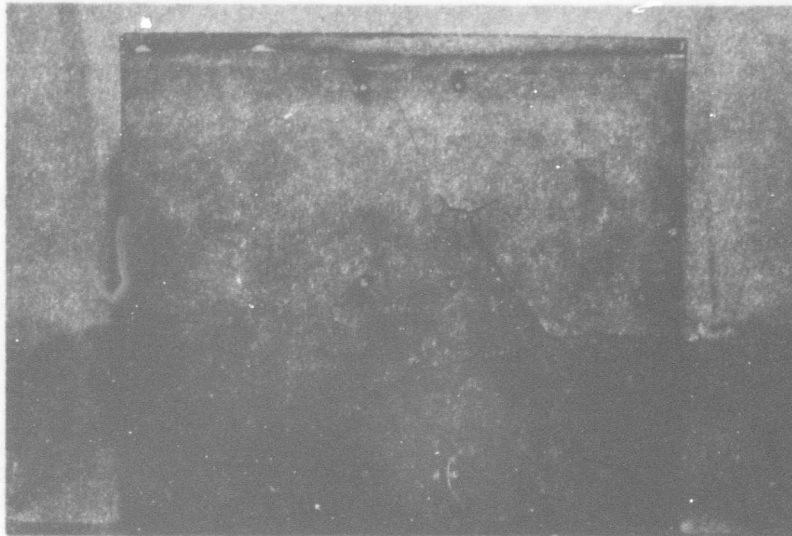


FIGURE 117 PANEL 3 FAILURE MODE AT 2900F. NOTE MOST OF FAILURE ON ONE SIDE AND THE OVERLAP OF FAILED SKIN SURFACES

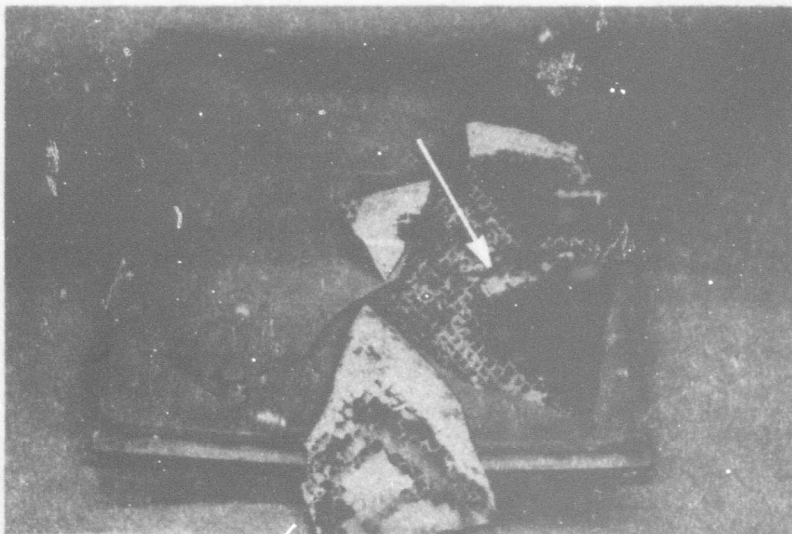


FIGURE 118 PANEL 3 AFTER 2900F STRUCTURAL TEST WITH FACE SHEET PULLED AWAY. NOTE HEAVY WHITE AREAS OF TANTALUM OXIDE. ARROW DESIGNATES PROBABLE START OF FAILURE AS CORE WAS COMPLETELY OXIDIZED IN THIS AREA

Specimens for electron microprobe analysis were obtained from Panel 3 adjacent to the oxidized area. Electron back-scatter photographs are shown in Figure 119. Examination of these pictures shows diffusion of the tantalum into the coating, a homogeneous dispersion of the aluminum in the coating, normal segregation of tin to the surface, and some tin segregates at the interface. Note that some of the tin segregates are situated at the interface between the coating and the face sheet of the panel. A continuous stringer of tin from the surface of the coating to the interface with the face sheet could act as a liquid diffusion path for oxygen during heating to 2800F, thus leading to erosion of the panel. A specimen from Panel 3 is shown in the photomicrographs in Figure 120. The cracks in the coating may have been present before the thermal cycle to 2800F or they may have been caused by the thermal cycle. If they were present before exposure to 2800F, they would have definitely contributed to oxidation of the substrate prior to loading. The lower photomicrograph shows the extent to which the tin on the surface wets and flows into the honeycomb when coating failure and subsequent panel erosion occurs. Consequently, it appeared that the test results obtained did not represent a true evaluation of the panel itself.

Of the two curved structural panels tested at elevated temperature, one failed at a load slightly below that predicted (possibly due to a prior thermal mishap) while the other panel failed prematurely due to defective protective coating.

EDGEWISE SHEAR STRUCTURAL TEST RESULTS

Room Temperature Tests

Panels 7 and 8 were edgewise shear tested at room temperature utilizing a load rate of 215 lbs/sec. Loading rate and vertical panel deflection are plotted in Figures 121 and 122 for Panels 7 and 8, respectively. Failure loads for the two panels were as follows:

<u>PANEL NO.</u>	<u>FAILURE LOAD (Lbs)</u>	<u>FACE SHEET SHEAR STRESS (ksi)</u>
7	32,700	74.5
8	35,880	81.5

The facing stresses in shear for this particular shear loading fixture is expressed by

$$\tau = P/A \quad \text{where} \quad A = 2\sqrt{2} t_f b$$

P = applied load in lbs.

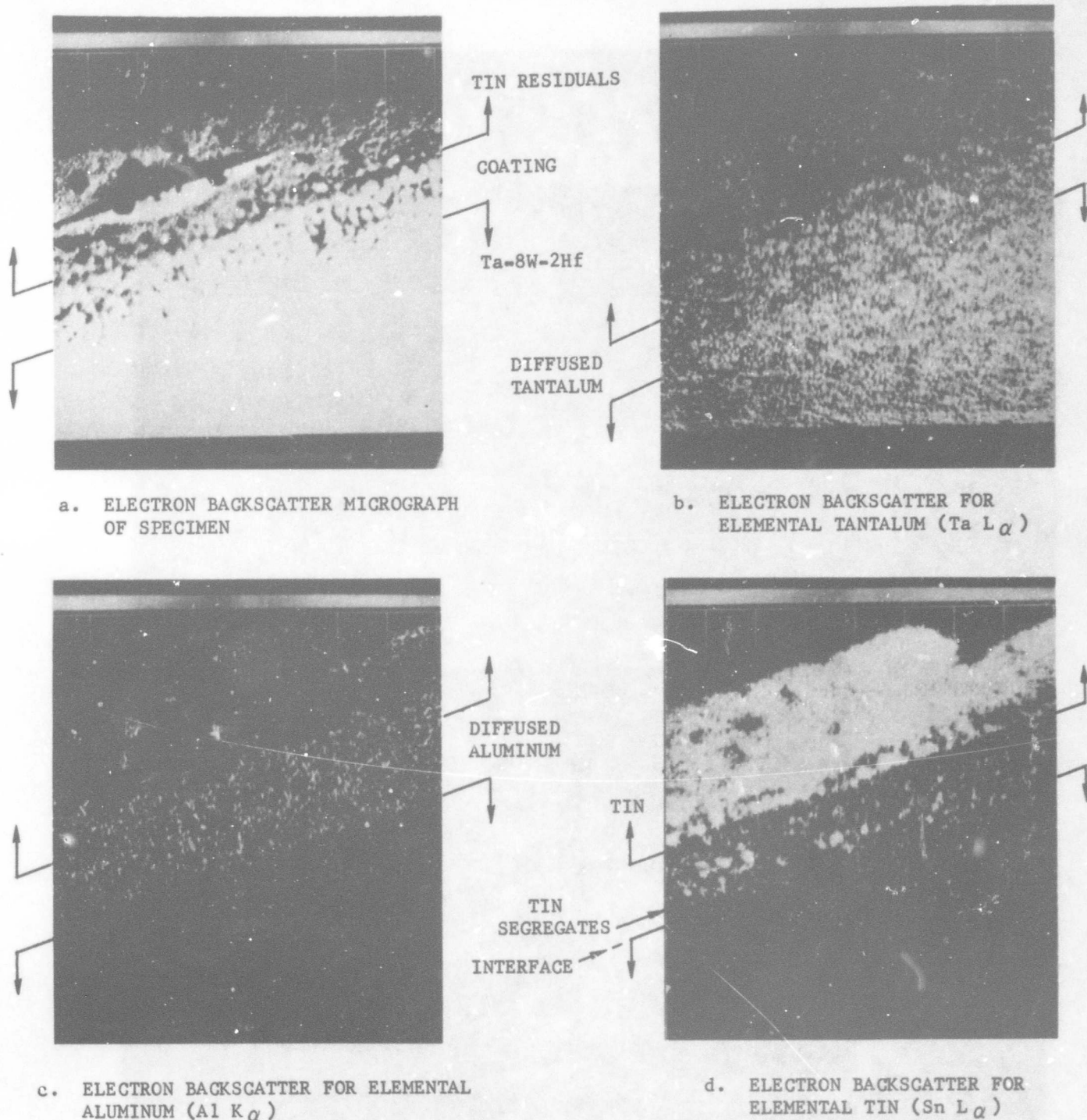
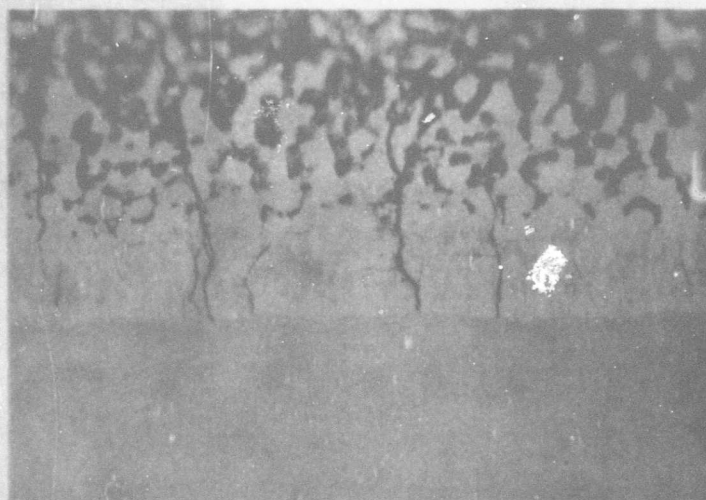


FIGURE 119 ELECTRON BACKSCATTER MICROGRAPHS OBTAINED FOR COATING ANALYSIS USING ELECTRON MICROPROBE TECHNIQUE

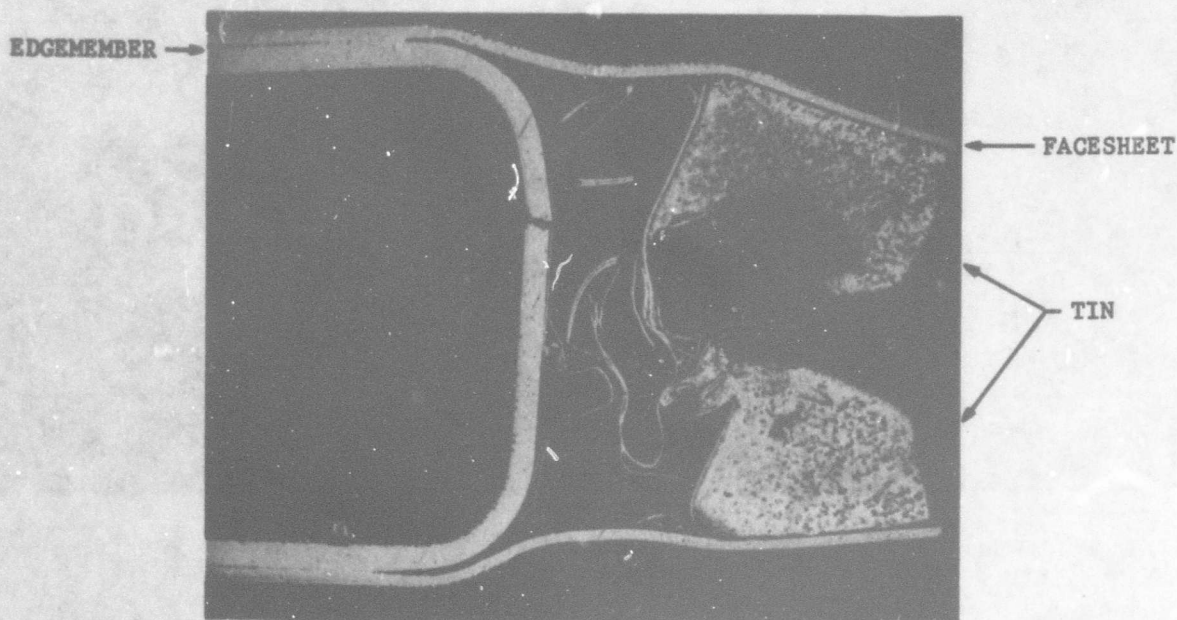


S_n -Al-M
Coating

Ta-8W-2Hf

ETCHANT: 50 NH_4F + 50 HF
MAGNIFICATION: 250X

a. PHOTOMICROGRAPH SHOWING CRACKS IN COATING



UNETCHED
MAGNIFICATION: 6X

b. PHOTOMICROGRAPH SHOWING TIN FLOW INTO HONEYCOMB

FIGURE 120 PHOTOMICROGRAPHS OF SPECIMENS OBTAINED FROM PANELS
FAILED IN EDGEWISE COMPRESSION AT 2800F

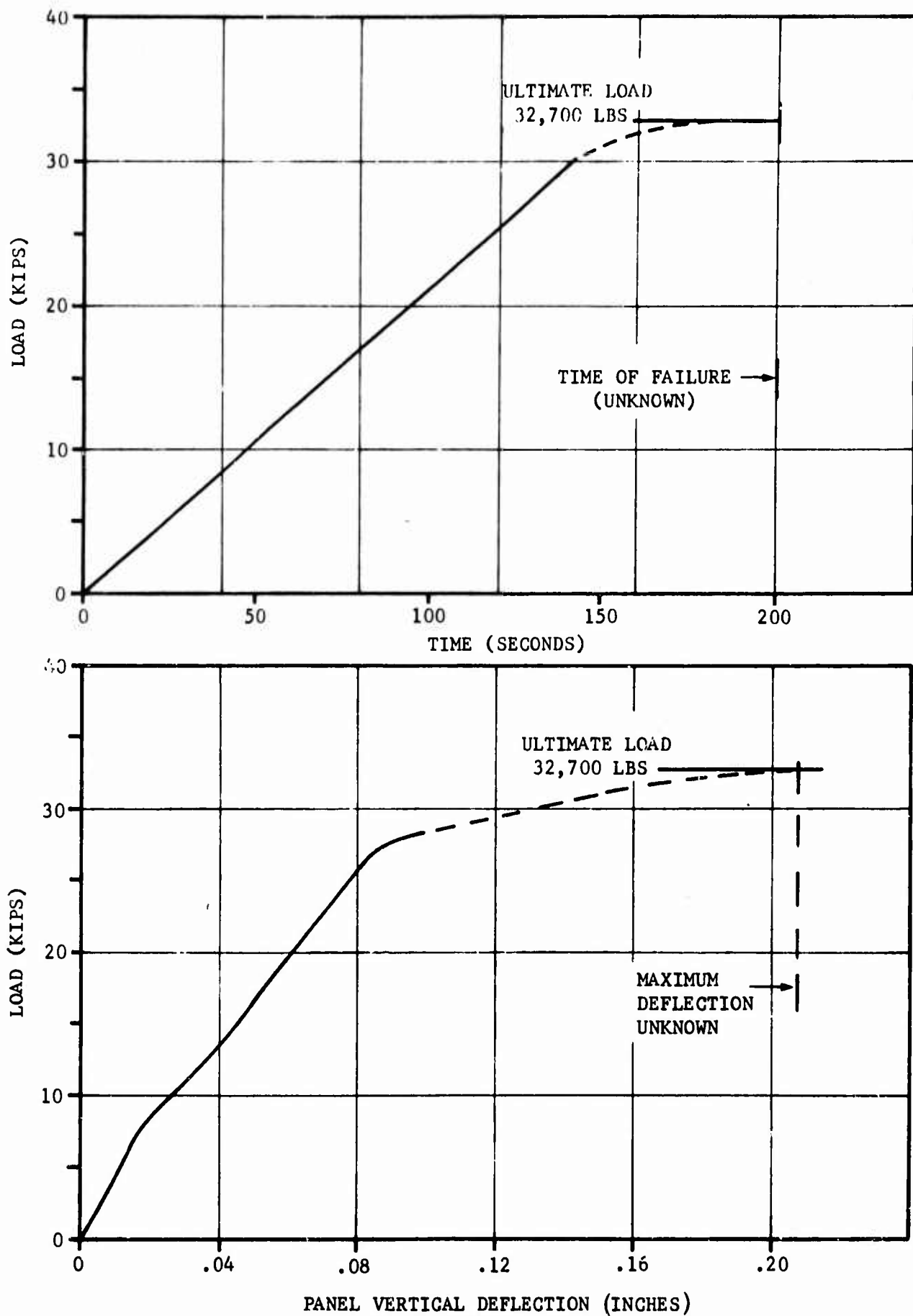


FIGURE 121 LOAD CYCLE AND LOAD-DEFLECTION CURVES FOR PANEL 7
TESTED IN EDGEWISE SHEAR AT ROOM TEMPERATURE

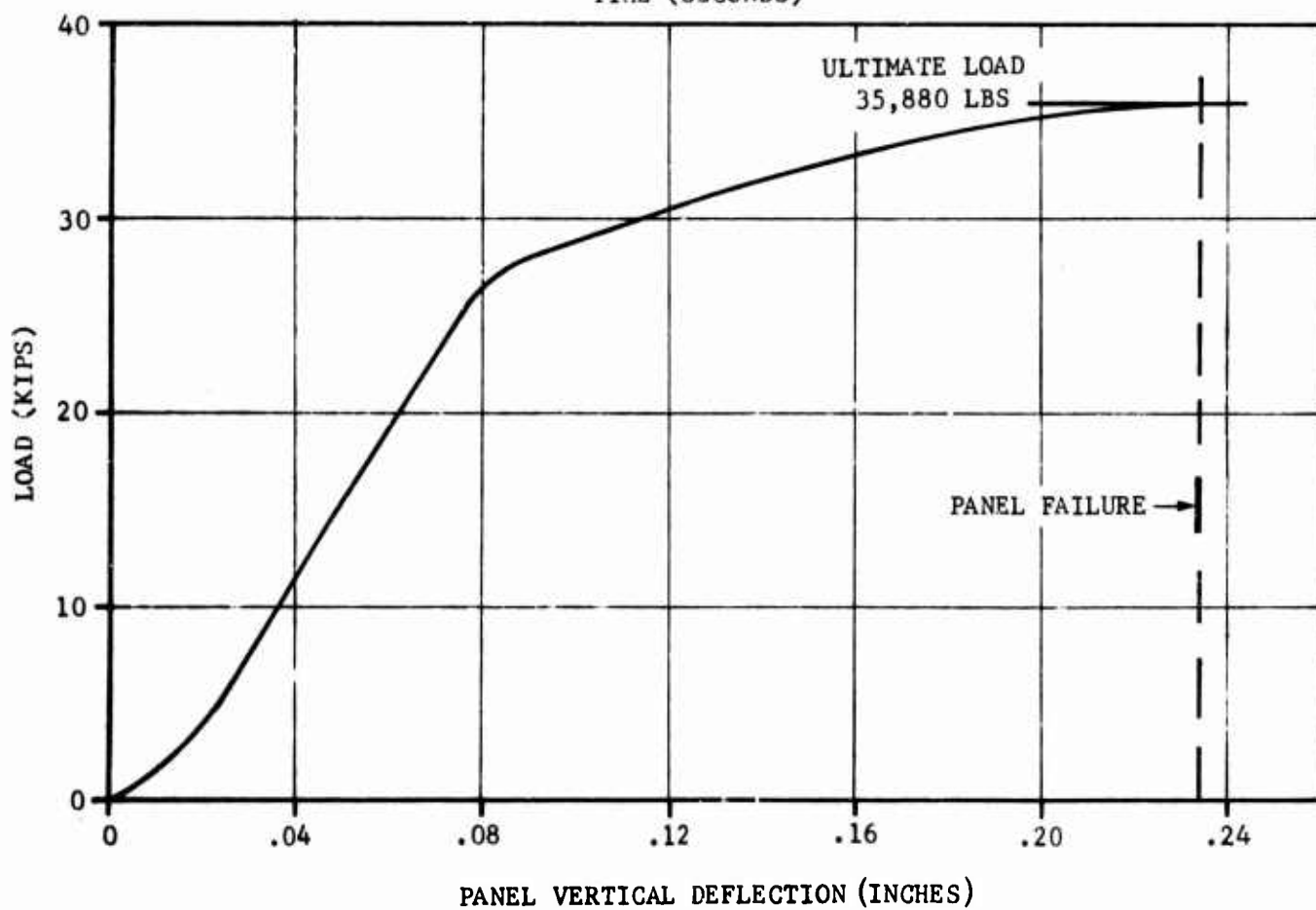
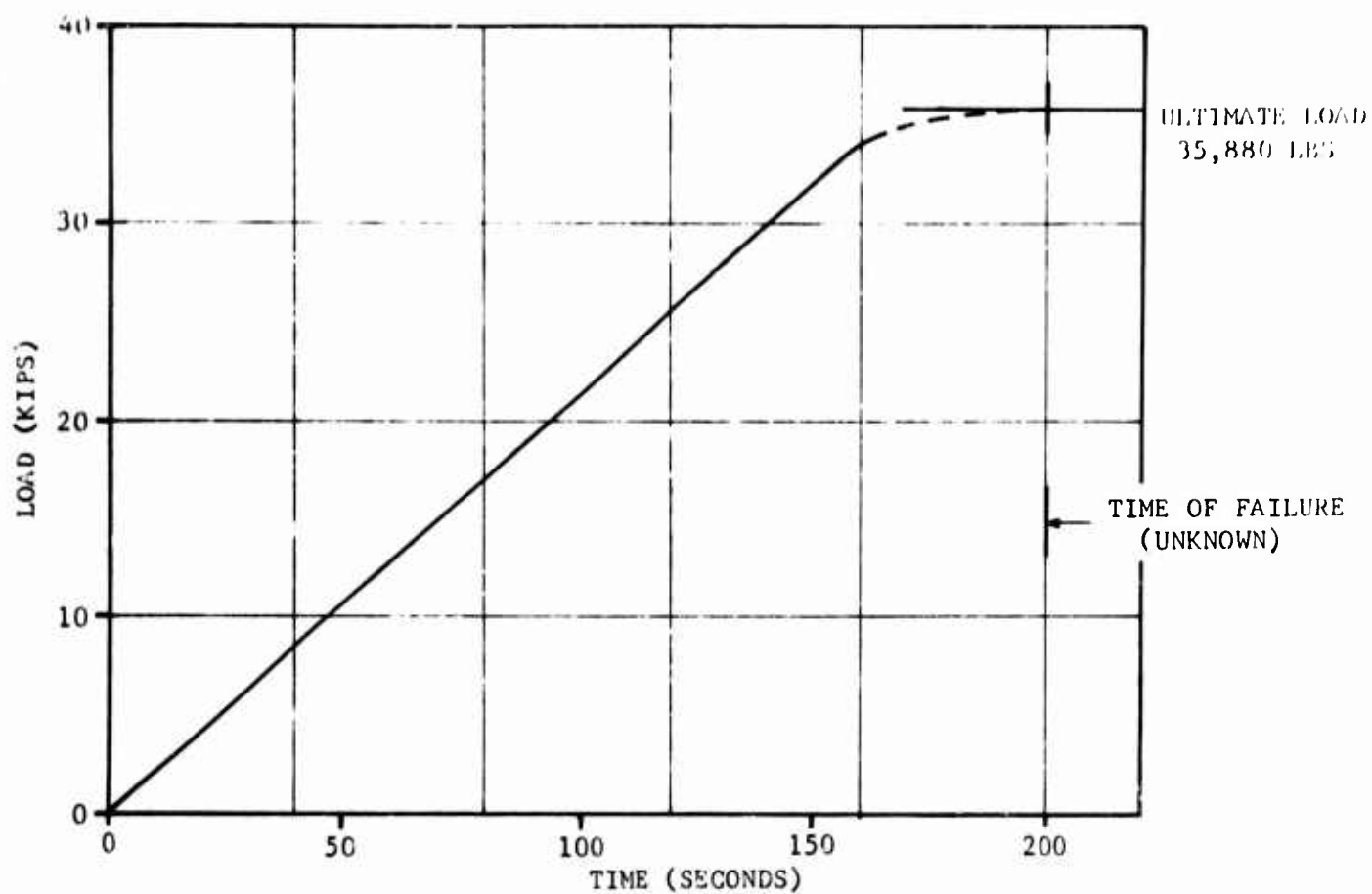


FIGURE 122 LOAD CYCLE AND LOAD-DEFLECTION CURVES FOR PANEL 8
TESTED IN EDGEWISE SHEAR AT ROOM TEMPERATURE

Examination of the panels revealed both to fail by the same mode of failure, buckling or wrinkling of the facing in the compression corners and shear slippage of the facing from the edgemembers in the tension corners. Both panels exhibited excellent ductility with near uniform deformation throughout the failed panels. Cracking around the periphery of the panel adjacent to the attachment holes occurred in the protective coating only. Figures 123 and 124 show the failure modes of both panels with Figure 125 showing a closeup of the failure at one corner.

Elevated Temperature Tests

Structural Panel 9 was tested with the main portion of the panel at 2100F and the fixture at 900F. The temperature distribution on the panel is shown in Figure 126. Temperature and load cycle and the vertical deflection of the panel during loading is shown in Figure 127.

Panel 10 was tested at 2650F with an overall temperature distribution as shown in Figure 128. Temperature and load cycle with vertical displacement measurements for this panel are shown in Figure 129. Failure loads for both panels were as follows:

<u>PANEL NO.</u>	<u>TEST TEMPERATURE (°F)</u>	<u>FAILURE LOAD (Lbs)</u>	<u>FACING SHEAR STRESS (ksi)</u>
9	2100	15,100	33.4
10	2650	5,900	13.4

Both panels approached their theoretical load limit. Failure mode was somewhat different from the room temperature panels. Panel 9 exhibited cracks initiating from two corners as shown in Figure 130 and wrinkling occurring in the adjacent corners with evidence of intercell buckling. Panel 10 exhibited a catastrophic failure attributed to the rapid oxidation rate of the tantalum substrate when the coating failed after overload as shown in Figure 131. Figure 132 is a graphic presentation of shear-panel strengths versus temperature.

PANEL STRUCTURAL ANALYSIS

The curved and flat structural panels were analyzed in compression and shear, respectively, utilizing formulae and charts presented in terms of general parameters of panel dimensions and material properties. The analysis includes the effects of elevated temperature on facings, honeycomb core, and diffusion bonded joint strength. The panels were analyzed for both general instability and local instability due to intercell buckling, shear crimping, and face wrinkling. Whenever possible, the analysis has been presented in the form of design charts applicable to honeycomb sandwich panels manufactured from tantalum core and facing material used in this program.

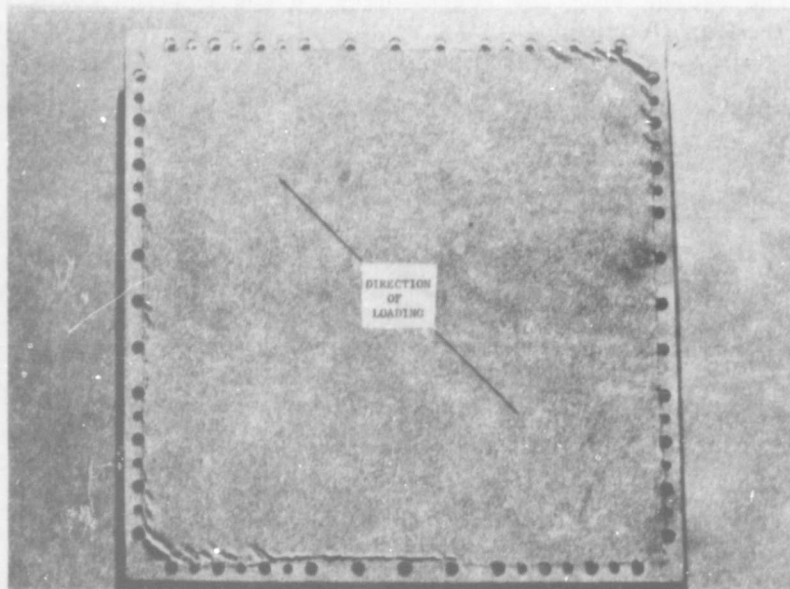


FIGURE 123 PANEL 7 TESTED IN EDGEWISE SHEAR AT ROOM TEMPERATURE. CRACK AROUND PERIPHERY OF THE PANEL AT THE LOAD HOLES IS IN COATING ONLY

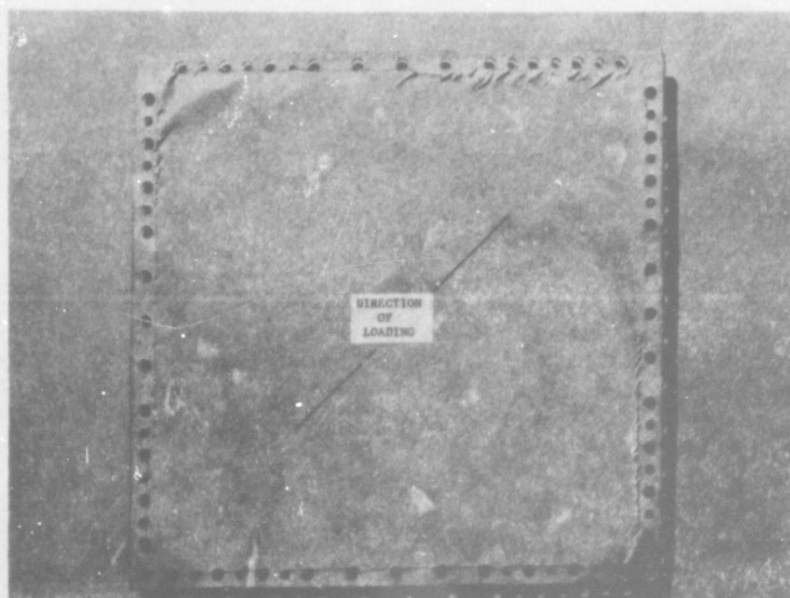


FIGURE 124 PANEL 8 TESTED IN EDGEWISE SHEAR AT ROOM TEMPERATURE



FIGURE 125 CLOSE UP OF FAILURE AT CORNER OF PANEL 8. CRACKING WAS ASSOCIATED WITH COATING ONLY AS PANEL EXHIBITED A DUCTILE TYPE FAILURE

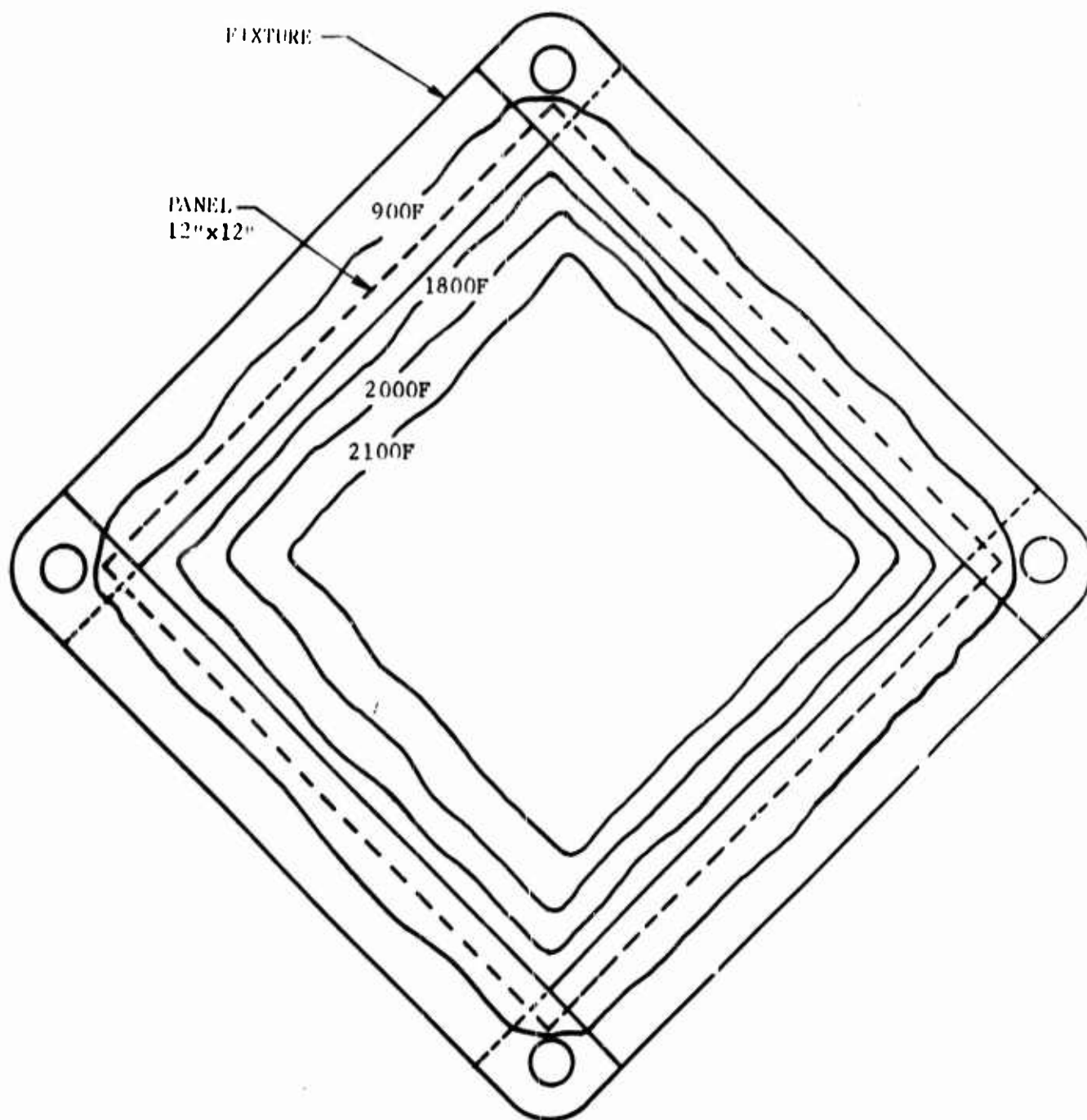


FIGURE 126 TEMPERATURE DISTRIBUTION ON PANEL 9
TESTED IN EIGEWISE SHEAR AT 2100F

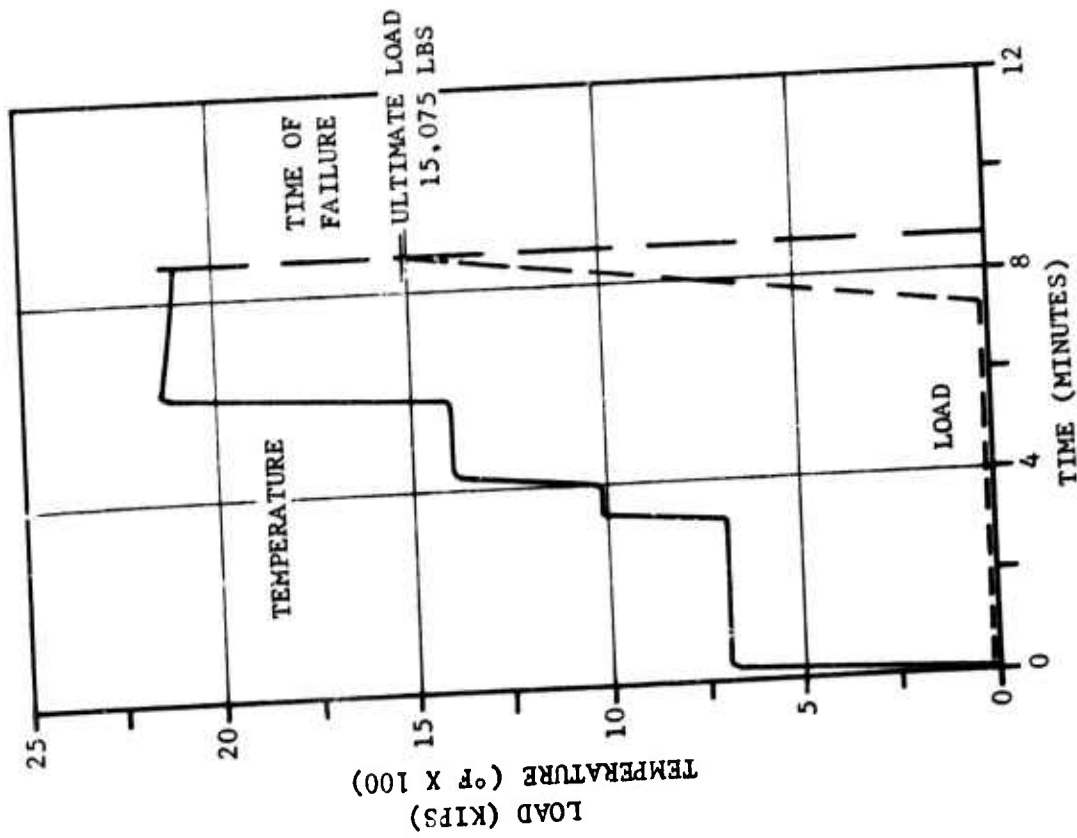
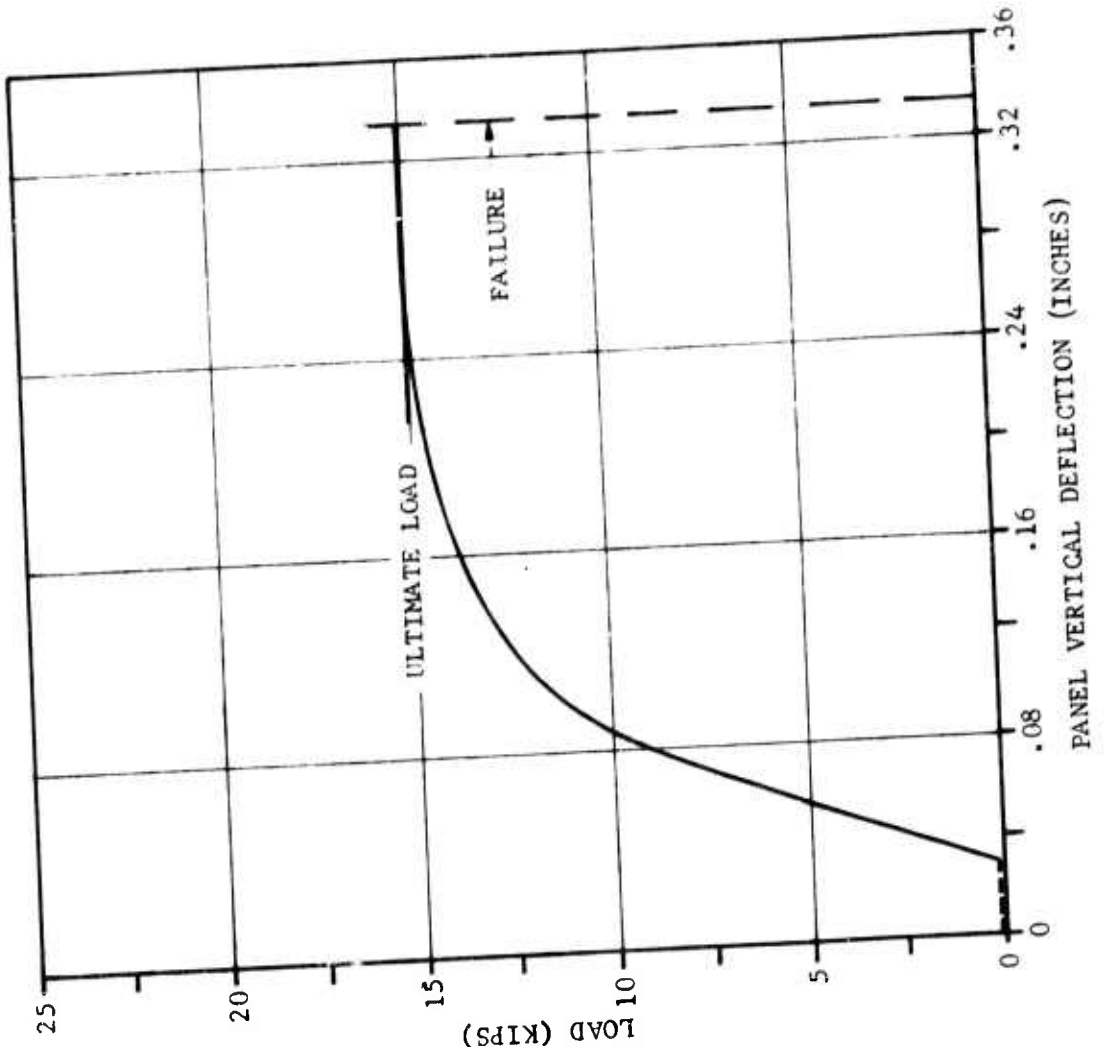


FIGURE 127 LOAD CYCLE AND LOAD-DEFLECTION CURVES FOR PANEL 9 TESTED IN EDGEWISE SHEAR AT 2100F

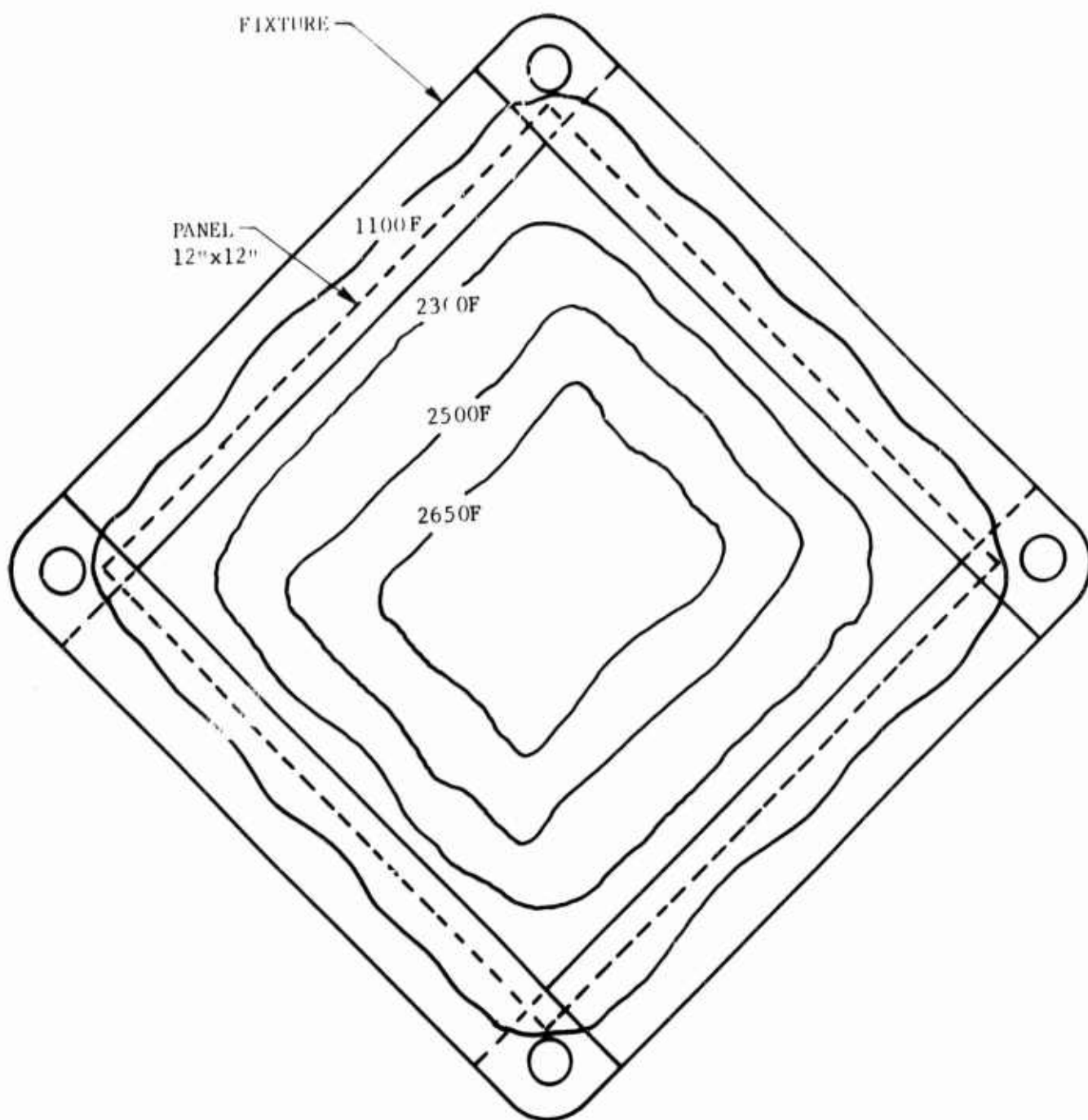


FIGURE 128 TEMPERATURE DISTRIBUTION ON PANEL 10
TESTED IN EDGEWISE SHEAR AT 2650F

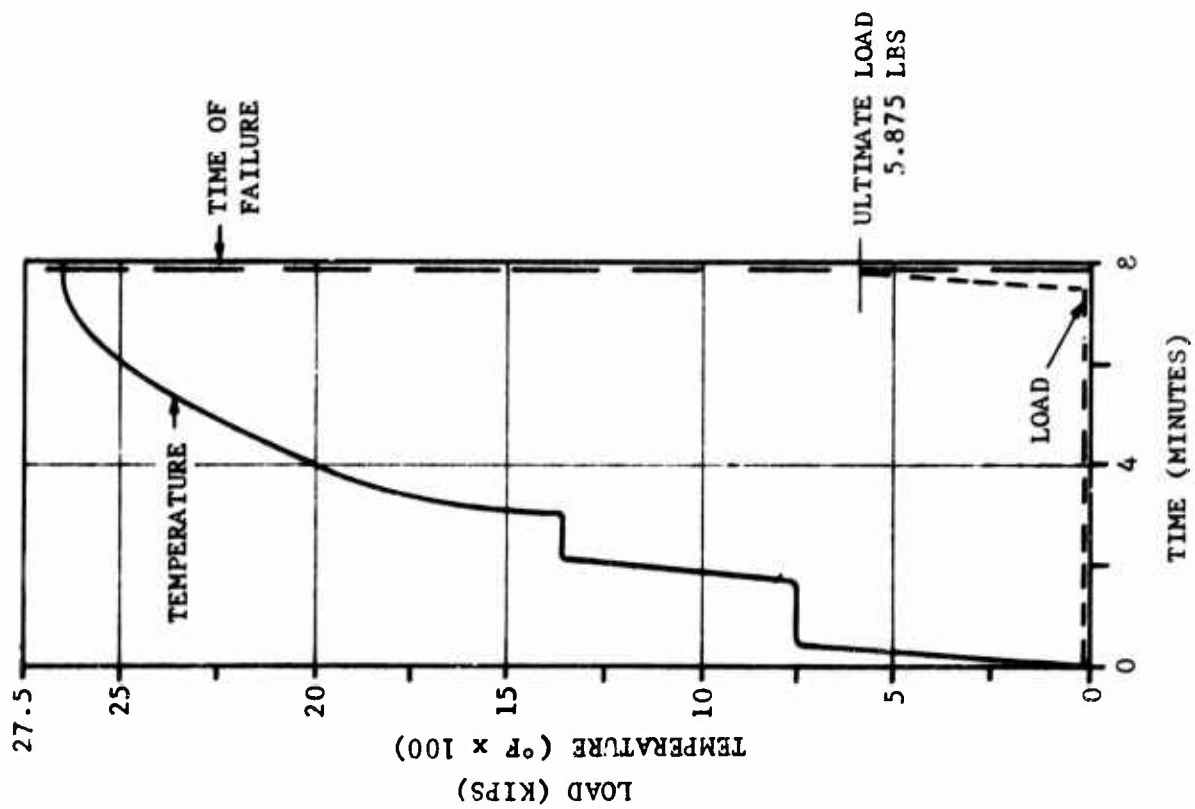


FIGURE 129 LOAD CYCLE AND LOAD-DEFLECTION CURVES FOR
PANEL 10 TESTED IN EDGEWISE SHEAR AT 2650F

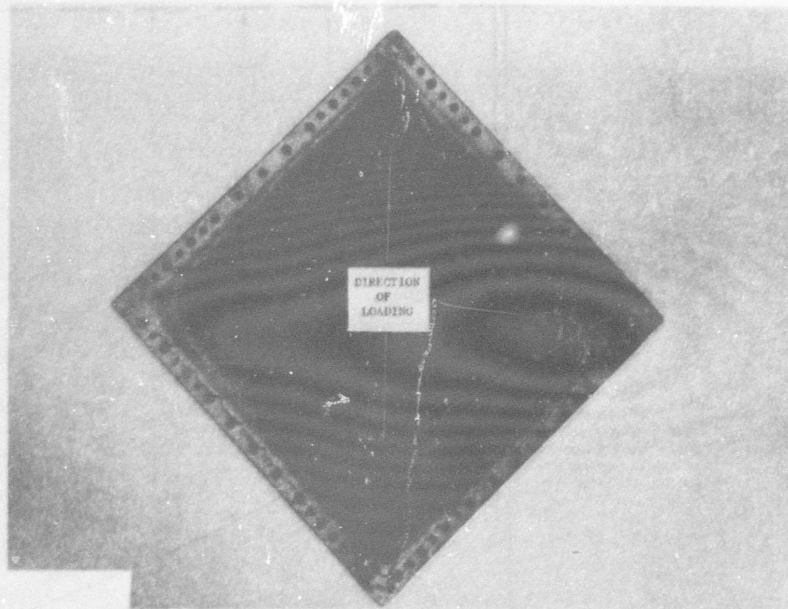


FIGURE 130 PANEL 9 TESTED IN EDGEWISE SHEAR AT 2100F

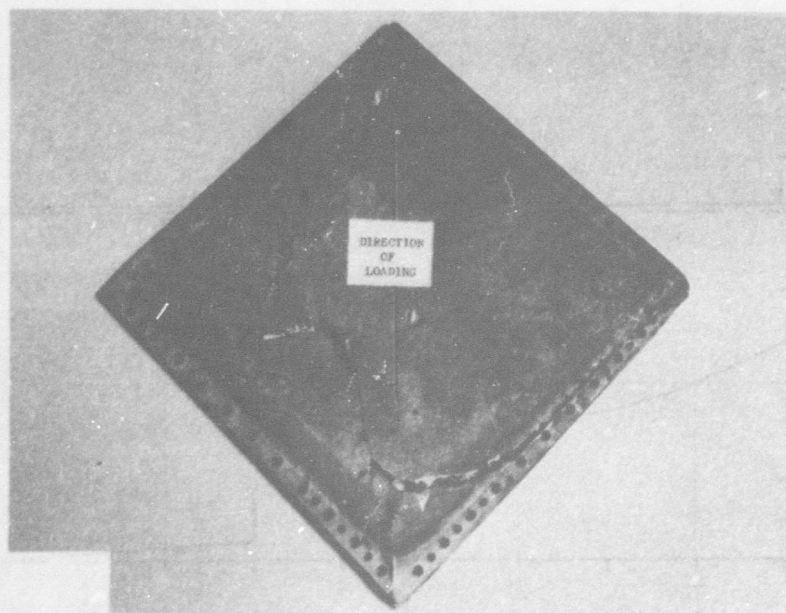


FIGURE 131 PANEL 10 TESTED IN EDGEWISE SHEAR AT 2650F

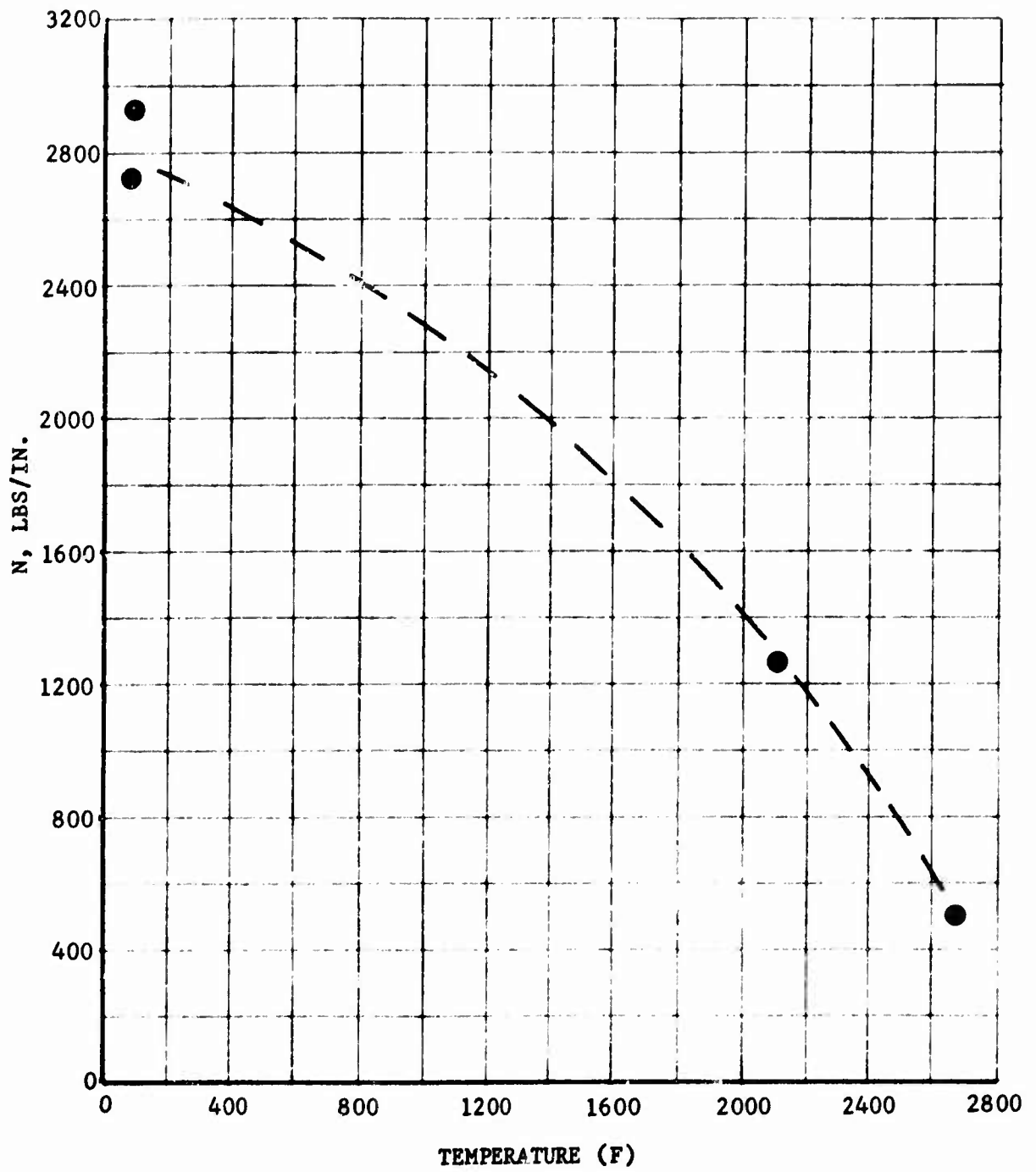


FIGURE 132 STRENGTH OF SHEAR PANELS AT ROOM AND ELEVATED TEMPERATURES

General Instability

The curved panels were considered to be a short, wide, curved column unsupported on the unloaded edges with a fixity on the loaded edges somewhere between simply supported and clamped. For the purpose of this analysis, the fixity coefficient \bar{c} was assumed to be 2.0 and the analysis was directed toward correlating the strength of tantalum sandwich constructions with standard analytical procedures. The Engesser formula for the strength of a flat or large curvature honeycomb sandwich column loaded in compression may be presented in parametric form as follows:

$$P_{cr} = \frac{P_E}{1 + \frac{P_E}{t_c G_c}} \quad \text{where} \quad P_E = \frac{\bar{c} \pi^2 EI}{L^2}$$

The ultimate facing stress reduces to the following parameters.

$$F_{cr} = \frac{P_{cr}}{2t_f} = \frac{\frac{P_E}{2t_f}}{1 + \frac{P_E}{t_c G_c}} = \frac{\frac{\bar{c} \pi^2 EI}{2t_f L^2}}{1 + \frac{\bar{c} \pi^2 EI}{L^2 t_c G_c}}$$

$$\text{Let } I = \frac{t_f (t_c + t_f)^2}{2}$$

Thus

$$F_{cr} = \frac{\frac{\pi^2 E}{\left[\frac{L}{\left(\frac{t_c + t_f}{2} \right) \sqrt{\bar{c}}} \right]^2}}{1 + \frac{\pi^2 E}{\left[\frac{L}{\left(\frac{t_c + t_f}{2} \right) \sqrt{\bar{c}}} \right]^2} \left(\frac{t_c}{t_f} \right) \left(\frac{G_c}{2} \right)}$$

$$\text{Let } \theta_o = \frac{\pi^2 E_t}{\left[\frac{L}{\left(\frac{t_c + t_f}{2} \right) \sqrt{c}} \right]^2} = \frac{\pi^2 E_t}{(l'/\rho)^2} \quad \text{where } l' = \frac{L}{\sqrt{c}}$$

$$\text{and } \rho = \frac{t_c + t_f}{2}$$

$$\text{and } Q = \frac{1}{1 + \frac{2\theta_o}{\left(\frac{t_c}{t_f} \right) G_c}} = \frac{1}{1 + \frac{2R}{\left(t_c/t_f \right)}} \quad \text{where } R = \frac{\theta_o}{G_c}$$

$$\text{thus } F_{cr} = \theta_o Q$$

The parameter Q is a measure of the reduction in column allowable due to finite core shear rigidity versus infinite core shear rigidity. The parameter θ_o is a measure of panel dimensional and material properties. Substitution of the panel material properties E_t and G_c results in the design curves shown in Figures 133 and 134. Data for the panel configuration as tested is also plotted.

Local Instability

Possible local failures of the sandwich construction under edgewise compression loads are as follows:

Intercell Dimpling

The equation for intercell dimpling and buckling was taken from Reference 11 where the stress direction is parallel to the cell diagonal

$$F_{cr} = 2.5 E_t (t/d)^2$$

The equation uses an empirical constant of 2.5 which is slightly higher than that given in Reference 12. A plot of this equation is shown in Figure 135. Data for the panel configuration as tested is also plotted.

Shear Crimping

Shear crimping failure is a form of general instability where the wave length of the buckle becomes very small due to low core shear modulus. This failure occurs suddenly and causes the core to fail in crimping as illustrated in Figure 136. The equation for shear crimping, Reference 13, is

$$F_{cr} = G_c \left(\frac{t_c + 2t_f}{2t_f} \right)$$

and is plotted in Figure 137. Data for the panel configuration as tested is included.

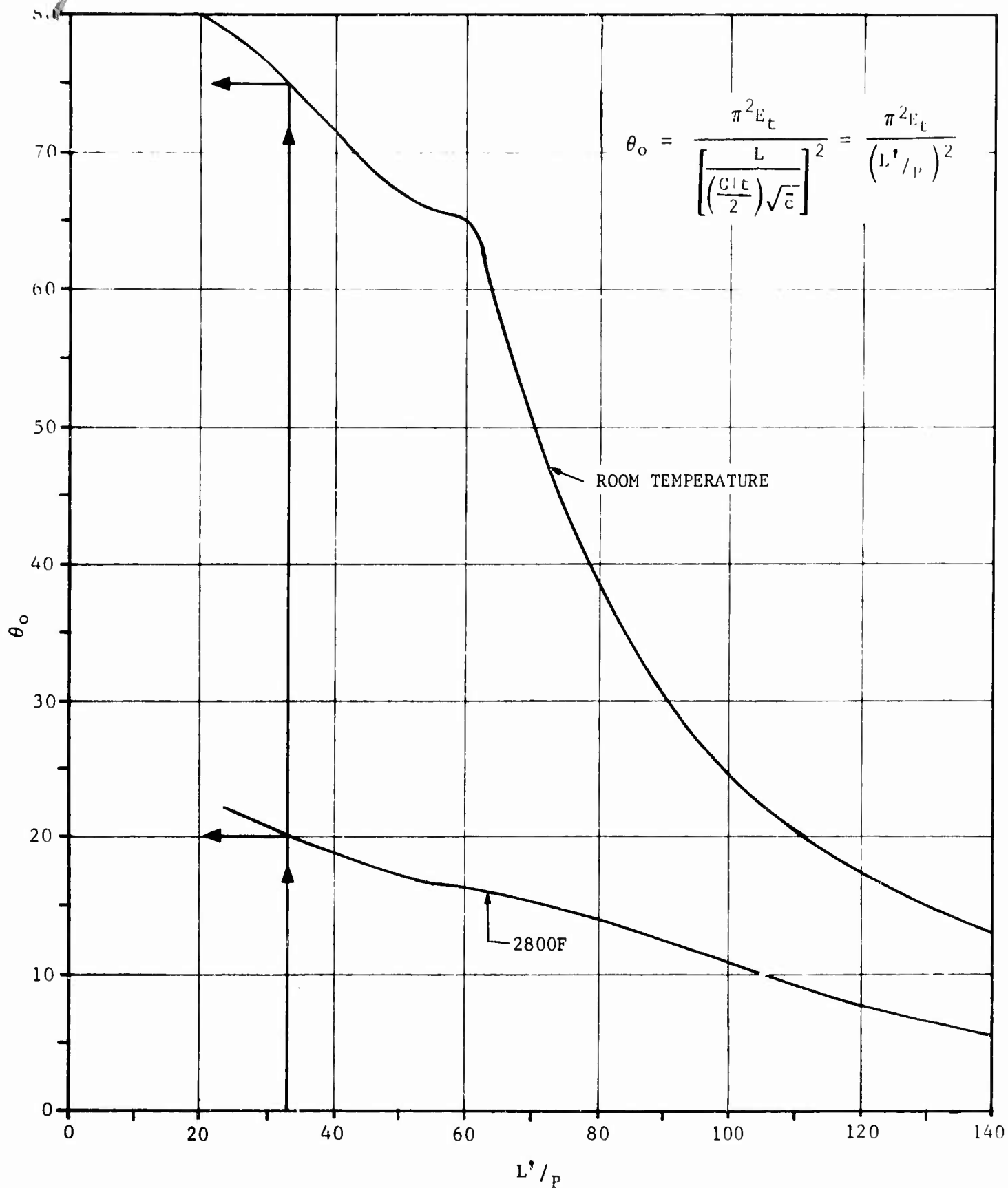


FIGURE 133 BUCKLING PARAMETER FOR TANTALUM T-111 SANDWICH PANELS

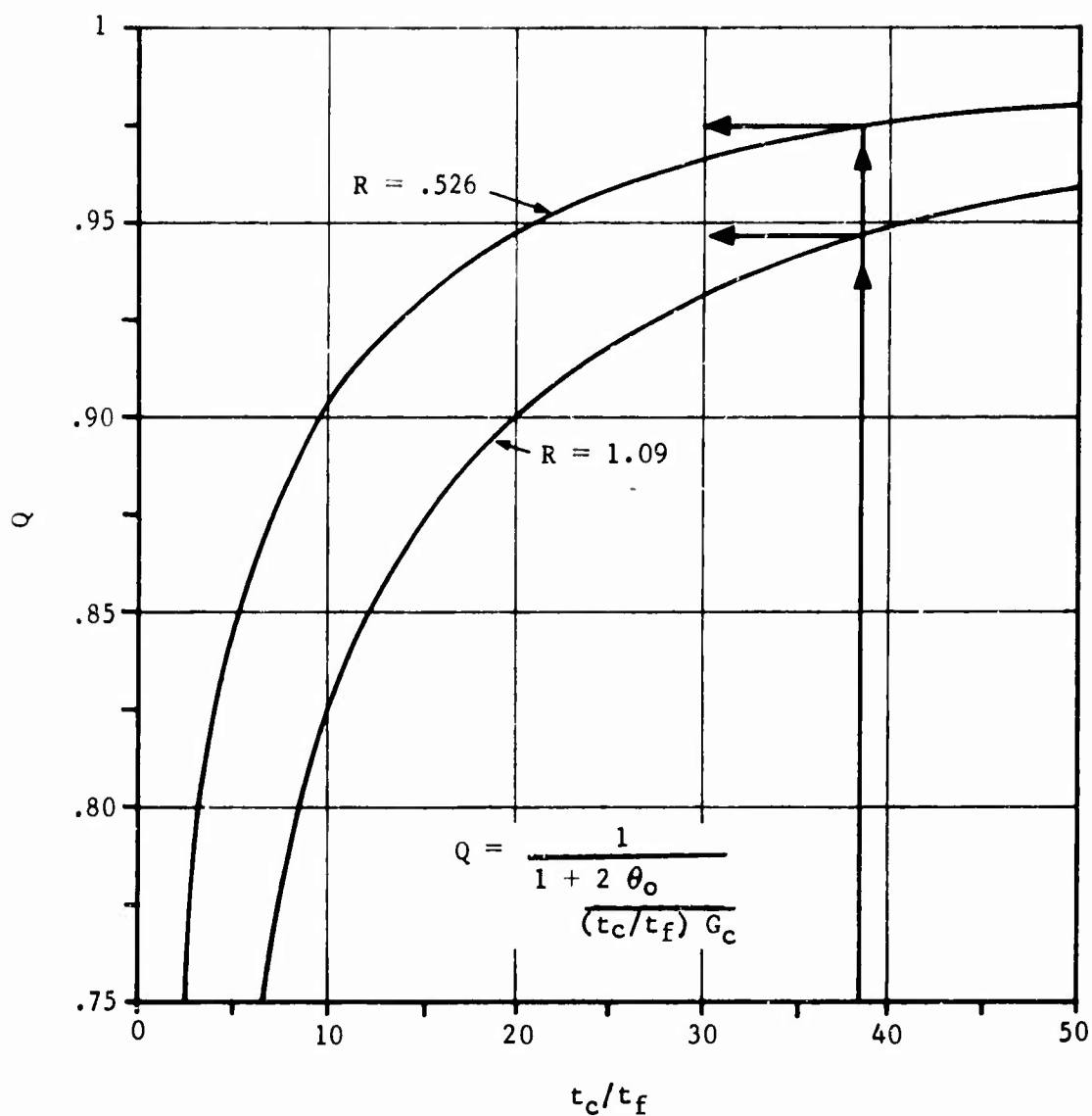


FIGURE 134 CORE SHEAR PARAMETER FOR DETERMINING THE BUCKLING STRENGTH OF TANTALUM HONEYCOMB PANELS

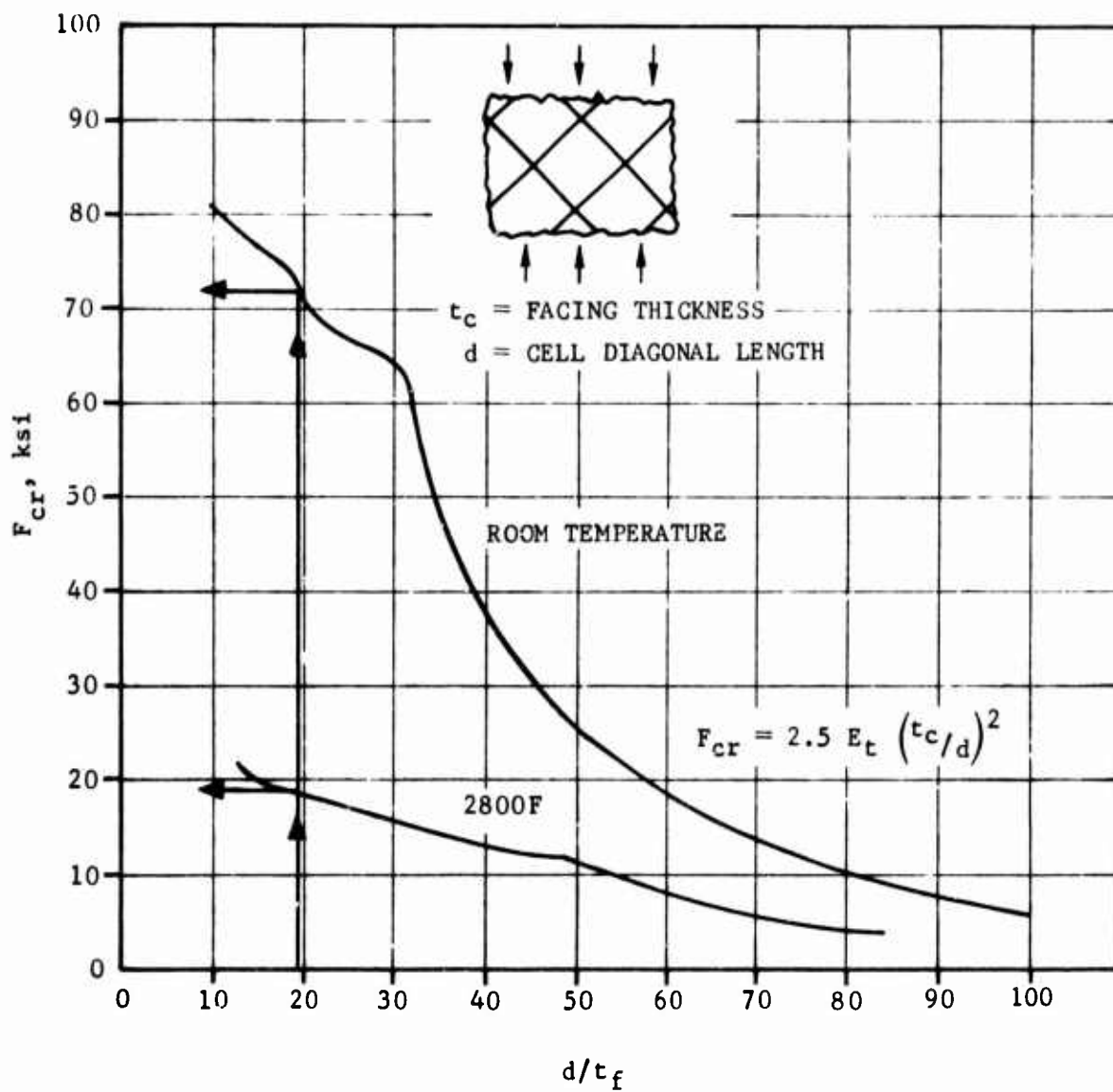
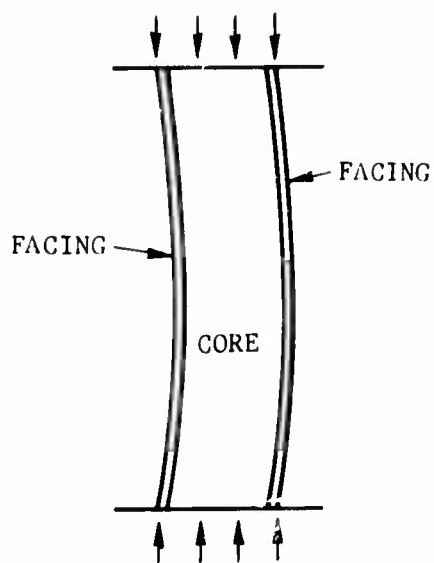
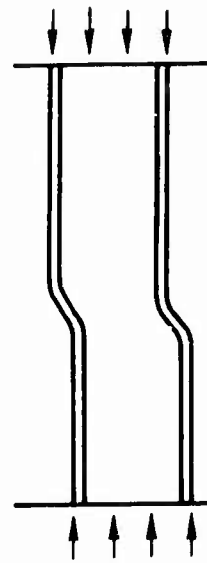


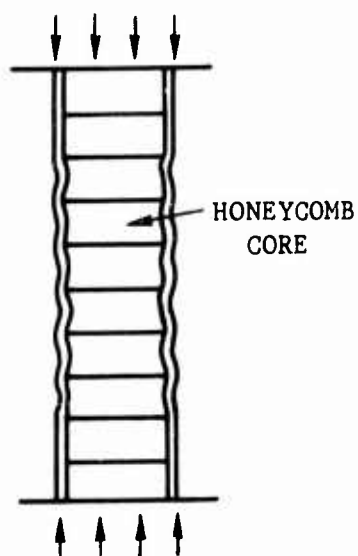
FIGURE 135 CHART FOR DETERMINING THE INTERCELL DIMPLING STRENGTH OF TANTALUM HONEYCOMB PANELS



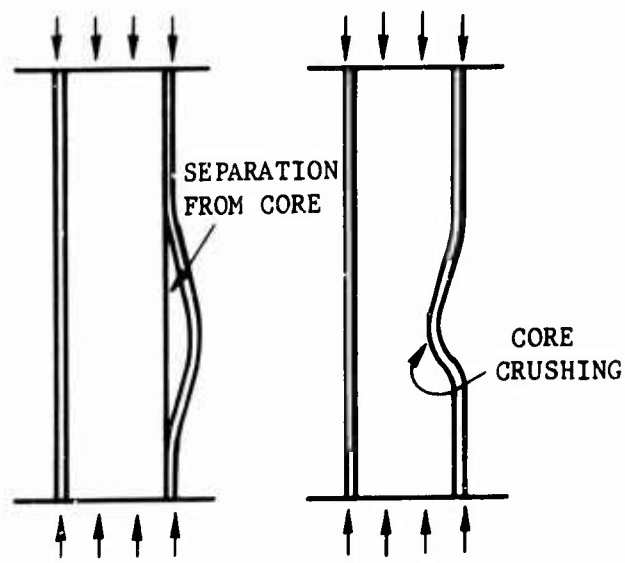
(a) GENERAL BUCKLING



(b) SHEAR CRIMPING



(c) DIMPLING OF FACINGS



(d) WRINKLING OF FACINGS

FIGURE 136 POSSIBLE MODES OF FAILURE OF SANDWICH COMPOSITE UNDER EDGEWISE LOADS: GENERAL BUCKLING, SHEAR CRIMPING, DIMPLING OF FACINGS, AND WRINKLING OF FACINGS EITHER AWAY FROM OR INTO THE CORE. (REFERENCE 12)

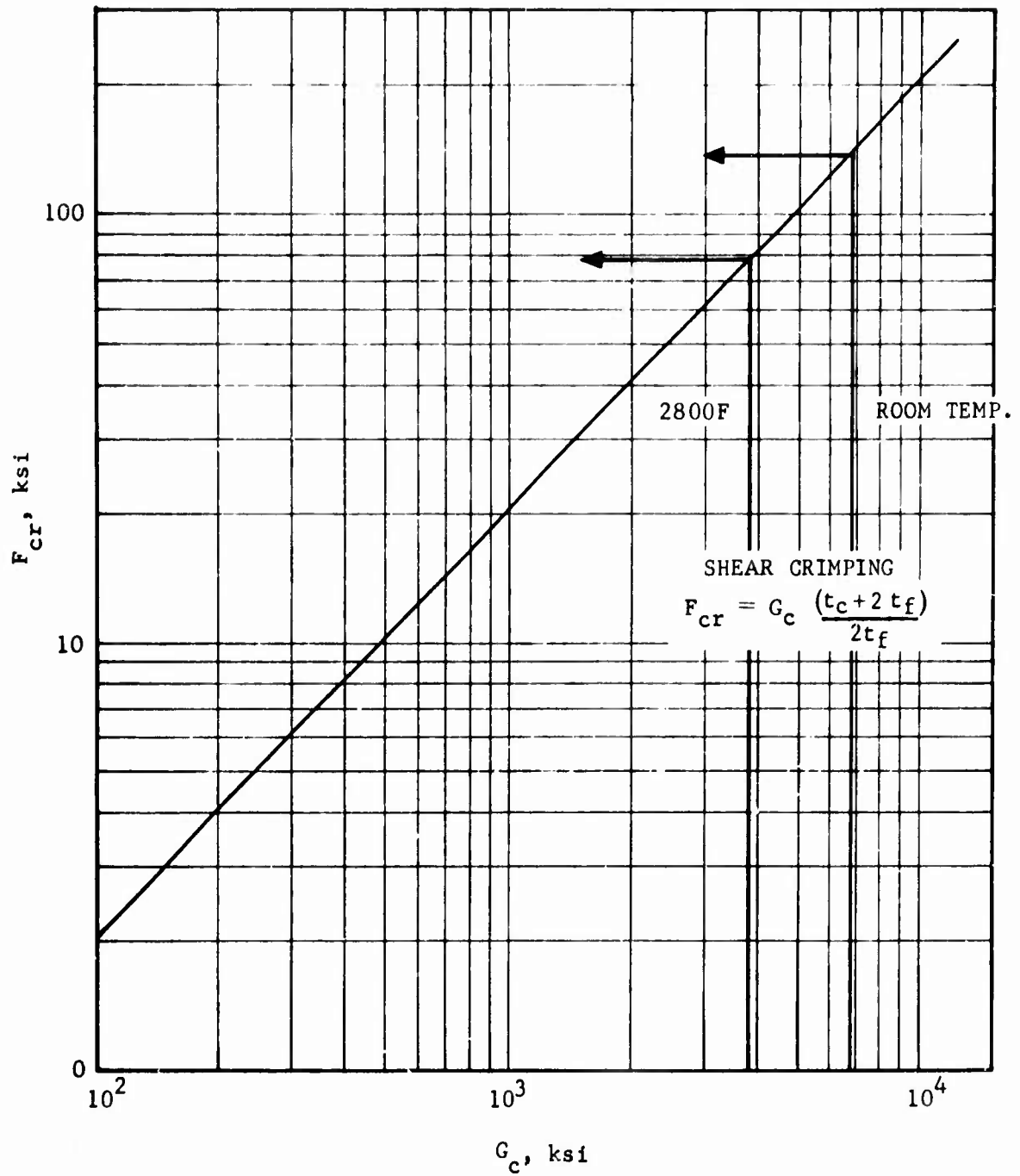


FIGURE 137 CHART FOR DETERMINING THE SHEAR CRIMPING STRENGTH OF TANTALUM T-111 HONEYCOMB PANELS

Face Wrinkling

The wrinkling criteria given in Reference 12 is for the design of sandwich constructions to insure that the facings do not wrinkle under design loads. Face wrinkling for honeycomb sandwich constructions is governed by the equation,

$$F_w = \frac{.82 \left(\frac{E_c t_f}{E' t_c} \right)^{\frac{1}{2}} E'}{1 + 0.64K} \quad \text{where} \quad K = \frac{8E_c}{t_c F_{fc}}$$

A plot of this equation is shown in Figure 138, including data for the panel configuration as tested.

Edgewise Shear Modes of Failure

The flat structural panels were analyzed for both general and local instability at both room and elevated temperatures. The general expression for determining the load carrying capability of a flat rectangular sandwich panel under edgewise shear loading is expressed by the following equation from Reference 12.

$$\frac{F_s}{\eta} = \frac{\pi^2 K}{4} \left(\frac{t_c + t_f}{b} \right)^2 \frac{E}{\lambda}$$

where K is a theoretical constant depending upon panel geometry and stiffness. Values of K are presented in chart form in the above reference. Edge fixity of the shear panels was assumed to be clamped considering the method of attachment and support employed during testing.

Intercell buckling criteria was taken from reference 13 where

$$\frac{F_s}{\eta} = 0.6E \left(\frac{t_f}{s} \right)^{3/2}$$

$$\text{and} \quad \eta = \frac{E_{sec}}{E} \quad \text{and} \quad F_{s \max} = \frac{F_{tu}}{\sqrt{3}}$$

Figure 139 is a chart of F_s/η versus F_s for the facing material at room temperature.

Summary of Structural Testing and Analysis

Table XXII summarizes the actual and predicted results of the diffusion bonded honeycomb panels tested in compression and shear at room and elevated temperatures. The analysis as shown by design charts and formulae revealed that both the compression and shear panels would fail by either a general

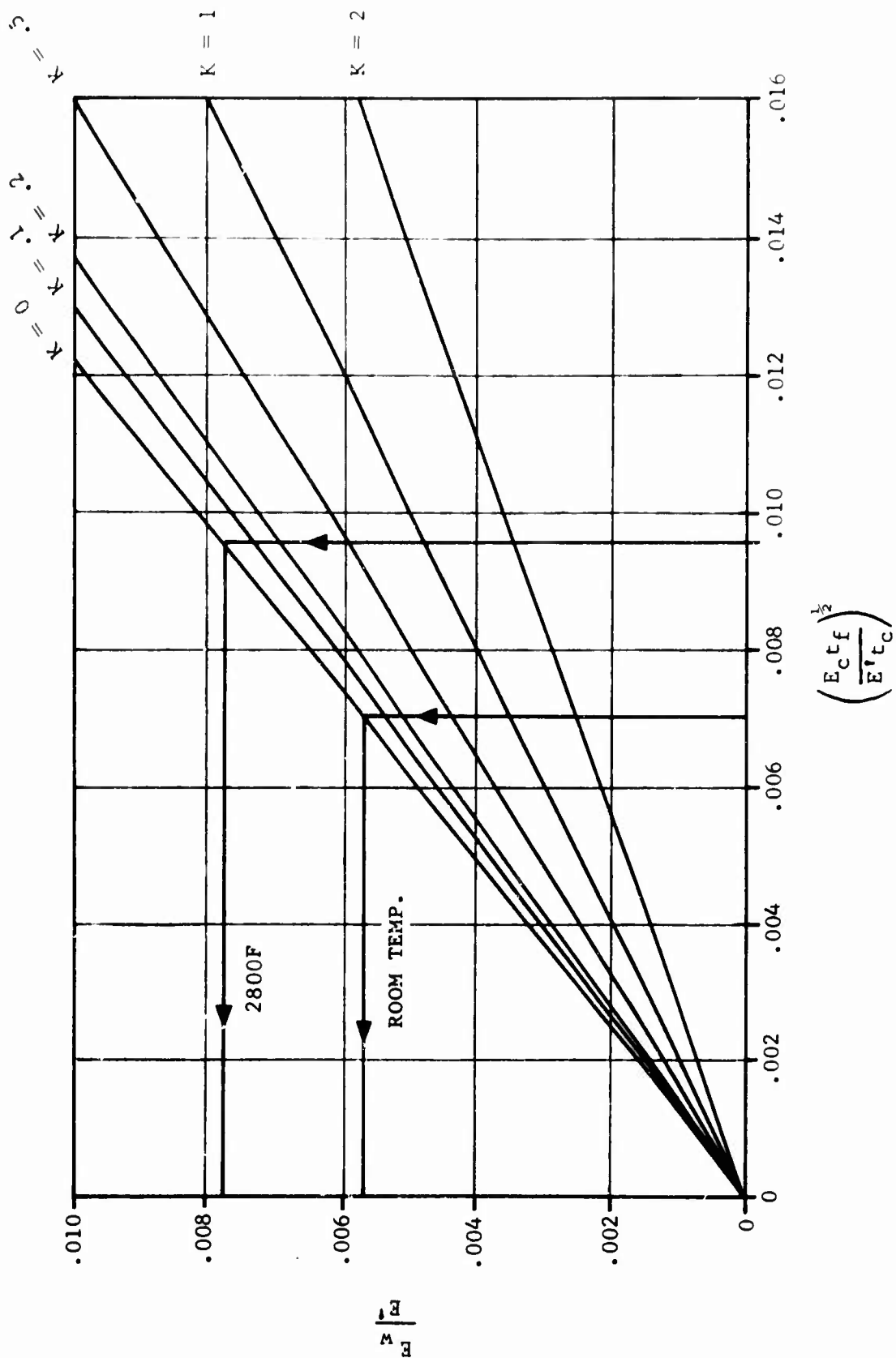


FIGURE 138 GRAPH OF FORMULA FOR THE WRINKLING STRESS OF FACINGS OF HONEYCOMB SANDWICH PANELS (REFERENCE 11)

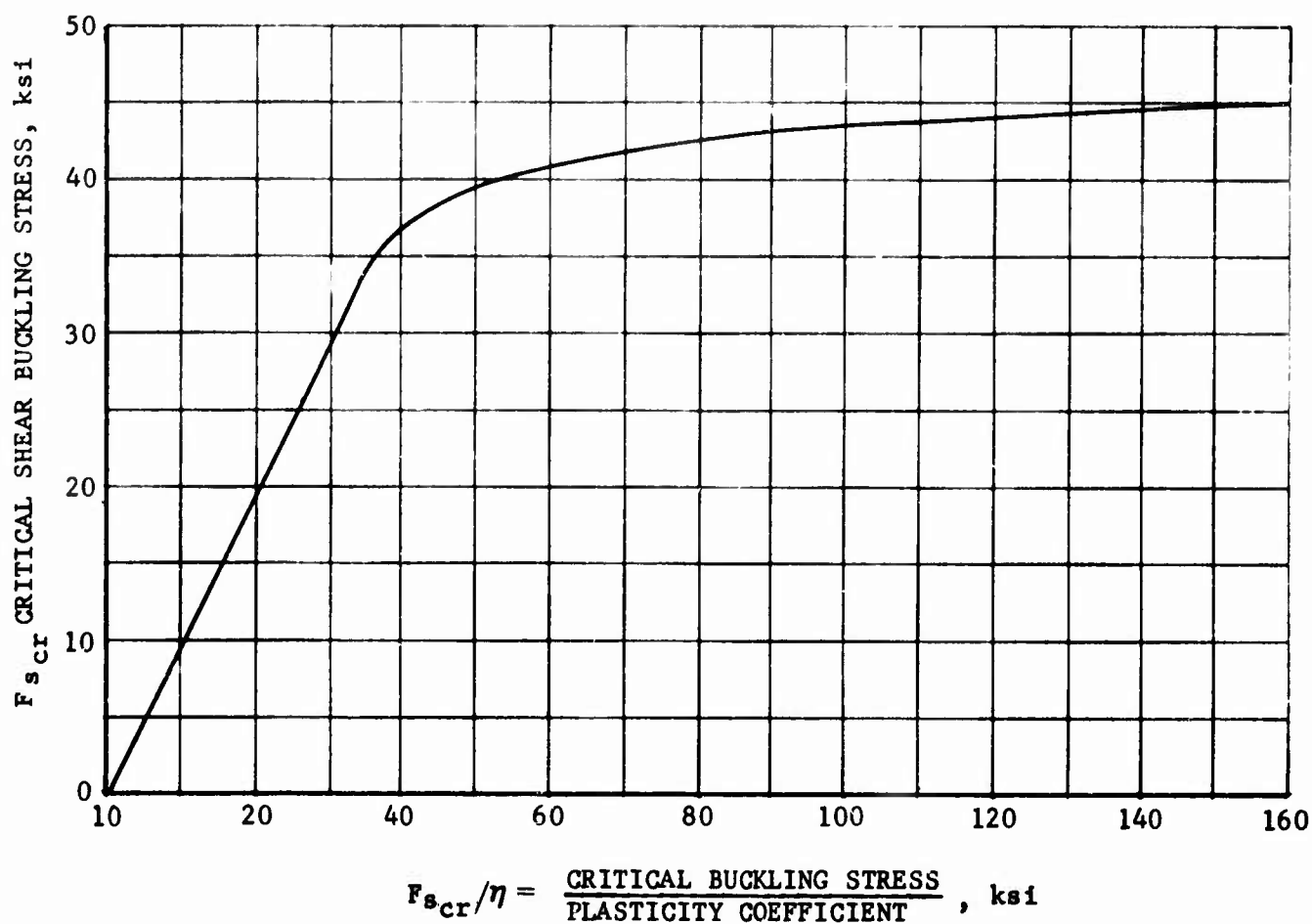


FIGURE 139 SHEAR BUCKLING CURVE FOR TANTALUM T-111 HONEYCOMB PANELS

TABLE XXII
SUMMARY OF RESULTS OBTAINED ON TANTALUM T-111 HONEYCOMB PANELS

PANEL NO.	PANEL TYPE	LOADING MODE	TEST TEMPERATURE (F)	FAILURE STRESS, F_c OR F_{su} (psi)	PREDICTED (2) FAILURE STRESS (psi)
1	Curved	Edgewise Compression	R.T.	91,700	71,000
2	Curved	Edgewise Compression	2800F	17,200	19,500
3	Curved	Edgewise Compression	2900F	5,200 ⁽¹⁾	19,500
4	Curved	Edgewise Compression	R.T.	71,600	71,000
7	Flat	Edgewise Shear	R.T.	74,500	45,000
8	Flat	Edgewise Shear	R.T.	81,500	45,000
9	Flat	Edgewise Shear	2100F	33,400	19,000
10	Flat	Edgewise Shear	2650F	13,400	13,500

(1) Coating Failure - Considered no test

(2) Predicted intercell dimpling stress is approximately the same as predicted F_c and F_{su}

and/or local failure mechanism at a stress above the yield strength of the tantalum T-111 material from which the panels were manufactured provided the diffusion bonded joint strengths and testing techniques were adequate. The flat structural panels tested in shear did not exhibit a completely shear type failure mode normally associated with this type test. This was due in part to the inherently high stiffness and rigidity of the panels resulting in either elongating or wrinkling of the facings, depending on local stress conditions on the panel. The room temperature test panels exhibited an unusual amount of plastic deformation without cracking. The tendency of the elevated temperature panels to crack was probably due to the unavoidable thermal gradients encountered at the panel edges in contact with the load fixtures.

All panels failed at or above the predicted failure stress with the exception of compression panels 2 and 3. The premature failure of Panel 2 was attributed to an unfortunate testing mishap whereas Panel 3 experienced a protective coating failure. The higher-than-expected failure loads encountered on the room temperature shear panels was attributed to a change in the shear stress distribution on the panel once appreciable deformation had taken place. Hence, the failure load was dependent upon the T-111 facing compression and tension strength. It was assumed that the same state of stress existed in the elevated temperature tests. However, thermal gradients coupled with stress concentrations (load fixture attachment holes) probably led to cracking.

No evidence of fixture deformation or binding of the linkage was observed after the tests. In general, all failures were due to overload.

XI CONCLUSIONS AND RECOMMENDATIONS

Two panel designs were manufactured in the program, structural and heat shield. The structural panels were designed to sustain structural loads at temperatures to 2800F. The heat shield panels were designed for thermal protection to 3500F with no load carrying capabilities other than normal aerodynamic surface loading.

The structural panels met all program requirements as evidenced by the results obtained during structural testing. As a result, a high degree of confidence in the techniques and procedures employed in the manufacture of these panels has been obtained. With a suitable oxidation protective coating, these panels would provide integrity and long service life in actual aerospace environments. The efficiency of these panels could be further improved through the following steps:

1. Increased elevated temperature strength by substituting the higher strength T222 alloy for the T111 alloy used in this program.
2. Higher service temperatures by employing other techniques such as vapor deposition to apply the titanium intermediate, and the use of higher bonding temperatures and/or longer bonding times to effect a higher joint remelt temperature.
3. Optimize panel design from the results obtained in the current program.

These recommendations for further improving the capabilities of the panels produced in this program would not present any unusual difficulties.

The heat shield panels manufactured in this program were somewhat less than desirable. Greater complexity of design as well as increased service temperature demands resulted in problems which could not be fully corrected within program limitations. They can only be defined for future reference.

These difficulties with recommended remedial courses of action are outlined below:

1. Panel design should be altered to accommodate welding and panel attachment requirements. The panel access holes should be eliminated, thus reducing panel complexity during manufacture as well as to eliminate possible hot-spots on the panel surface during service. One of the more difficult aspects of panel manufacture encountered in the program was the achievement of crack-free welds. Either a panel design change or further welding investigations should be considered.
2. To eliminate possible embrittlement at temperatures above approximately 2800F, techniques such as vapor deposition for applying the titanium intermediate, or, another intermediate material, should be established. The former action is recommended as a first step since titanium has been shown to produce high-strength joints as well as simplicity and consistency in manufacturing operations.

3. The limited number of panels manufactured in the current program precluded a complete evaluation of coating processes as well as service integrity. Consequently, no firm conclusions could be fully deduced in this area. Further coating investigations on actual parts are mandatory.
4. While the manufacturing techniques and procedures employed in the fabrication of these panels proved highly satisfactory, the incorporation of a strongback within the tooling design is necessary in order to obtain improved dimensional control. This should pose no unusual problems based on past experience in brazing high-temperature structures.

The implementation of the above recommendations would be highly desirable, and, in many cases, mandatory in order to realize the full potential of tantalum composite structures for aerospace applications.

REFERENCES

1. Refractory Alloy Foil Rolling Development Program, AF33(657)-8912, E. I. duPont de Nemours and Company, Inc., Baltimore, Maryland.
2. Patton, W. L., and Symonds, J; Final Report on Refractory Alloy Foil Rolling Development Program, AFML-TR-65-43, Air Force Materials Laboratory, Wright-Patterson Air Force Base, Ohio.
3. Freedman, A. H., Stone, L. H., and Mikus, E. G., Tantalum and Molybdenum Brazing Techniques, ML-TDR-64-270, Air Force Materials Laboratory, Wright-Patterson Air Force Base, Ohio, September 1964.
4. Freedman, A. H., Stone, L. H., and Mikus, E. B., Tantalum and Molybdenum Brazing Techniques, ML-TDR-64-270, Part II. Air Force Materials Laboratory, Wright-Patterson Air Force Base, Ohio.
5. Freedman, A. H., Stone, L. H., Mikus, E. B., Research on Tantalum and Molybdenum Brazing Techniques, Final Report ML-TDR-64-270, Air Force Materials Laboratory, Wright-Patterson Air Force Base, Ohio, June 1964, AF33(657)-11227, (Northrop Norair, Hawthorne, California).
6. Research on Tantalum and Molybdenum Brazing Techniques, Monthly Letter Report No. 10, September 1964, AF33(657)-11227, (Northrop Norair, Hawthorne, California).
7. "A Submicron Sectioning Technique for Analyzing Diffusion Specimens of Tantalum and Niobium", R. E. Pawel and R. S. Lundy; Vol. 35, February 1964, Journal of Applied Physics.
8. Birks, L. S., "Calculation of X-ray Intensities from Electron Probe Specimens", U. S. Naval Research Laboratory, Washington, D. C.
9. Wimber, R. T., Stetson, A. R., Development of Coatings for Tantalum Alloy Nozzle Vanes, Final Report NASA CR-54529, July 1967, Contract NAS 3-7276, (Solar Division International Harvester, San Diego, California).
10. Schmidt, F. F., and Ogden, H. R., "The Engineering Properties of Tantalum and Tantalum Alloys:", Battelle Memorial Institute, DMIC Report 14 (September 1963).
11. Plantema, F. J., Sandwich Construction, John Wiley and Sons, Inc. New York, 1966.
12. "Composite Construction for Flight Vehicles", Part III: Design Procedures. MIL-HDBK-23; Part III and Minutes of the Working Committee. U. S. Government Printing Office, Washington, D. C.
13. Bruhn, E. G., "Analysis and Design of Flight Vehicles Structures," Tri-State Offset Co., Cincinnati, Ohio, 1965.

Unclassified

Security Classification

DOCUMENT CONTROL DATA - R&D		
(Security classification of title, body of abstract and indexing annotation must be entered when the overall report is classified)		
1 ORIGINATING ACTIVITY (Corporate author) Northrop Corporation - Norair Division 3901 W. Broadway Hawthorne, California 90250		2a REPORT SECURITY CLASSIFICATION Unclassified
		2b GROUP
3 REPORT TITLE SOLID STATE DIFFUSION BONDED TANTALUM ALLOY HONEYCOMB PANELS		
4 DESCRIPTIVE NOTES (Type of report and inclusive dates) Final Technical Report 1 June 1965 to 30 November 1967		
5 AUTHOR(S) (Last name, first name, initial) Hugill, D. B. Shabarack, J.		
6. REPORT DATE March 1968	7a. TOTAL NO. OF PAGES 201	7b. NO. OF REFS 13
8a. CONTRACT OR GRANT NO. AF 33(615)-2777 ✓ b. PROJECT NO. MMP #8-214 c. d.	9a. ORIGINATOR'S REPORT NUMBER(S) NOR 67-292 9b. OTHER REPORT NO(S) (Any other numbers that may be assigned this report) AFML-TR-68-42	
10. AVAILABILITY/LIMITATION NOTICES The distribution of this report is limited because the report contains technology identifiable with items on the strategic embargo lists.		
11. SUPPLEMENTARY NOTES	12. SPONSORING MILITARY ACTIVITY AIR FORCE MATERIALS LAB. AFSC, WRIGHT-PATTERSON AIR FORCE BASE, OHIO	
13. ABSTRACT A program is described for the development of solid state diffusion bonding technology for production of tantalum alloy (T11) honeycomb panels suitable for either hot structural or heat shield applications in aerospace environments. The investigation and selection of appropriate intermediate materials to effect joining at relatively low temperatures and pressures suitable to the panel configurations is discussed. Emphasis was placed on methods suitable for reasonably low-cost processing. A method for determining optimum bonding parameters for a given binary alloy system is described. This technique was implemented in the current program to establish bonding parameters conducive to the fabrication of tantalum honeycomb panels. Selection of bonding parameters was further complicated by the manufacturing problems arising when bonding at the time and temperatures required to obtain a satisfactory bond of tantalum honeycomb structures. Consideration of these manufacturing problems and possible remedies are discussed. Program materials, equipment, and tooling utilized in panel manufacture, as well as processing procedures are described. Specific manufacturing problem areas encountered, such as forming, welding, and intermediate application, are discussed. Heating, atmosphere control, and pressure application requirements are described and actions taken to satisfy these requirements are reported. A survey of oxidation protective coatings for tantalum alloys is presented with the actual coatings and procedures used in the program being discussed. Structural testing techniques used in evaluating the integrity of the manufactured honeycomb panels are described. Standard analytical procedures employed in determining failure modes and predicted failure stresses are presented.()		

Unclassified

Security Classification

14	KEY WORDS	LINK A		LINK B		LINK C	
		ROLE	WT	ROLE	WT	ROLE	WT
TANTALUM DIFFUSION BONDING HONEYCOMB STRUCTURES							

INSTRUCTIONS

1. **ORIGINATING ACTIVITY:** Enter the name and address of the contractor, subcontractor, grantee, Department of Defense activity or other organization (*corporate author*) issuing the report.

2a. **REPORT SECURITY CLASSIFICATION:** Enter the overall security classification of the report. Indicate whether "Restricted Data" is included. Marking is to be in accordance with appropriate security regulations.

2b. **GROUP:** Automatic downgrading is specified in DoD Directive 5200.10 and Armed Forces Industrial Manual. Enter the group number. Also, when applicable, show that optional markings have been used for Group 3 and Group 4 as authorized.

3. **REPORT TITLE:** Enter the complete report title in all capital letters. Titles in all cases should be unclassified. If a meaningful title cannot be selected without classification, show title classification in all capitals in parenthesis immediately following the title.

4. **DESCRIPTIVE NOTES:** If appropriate, enter the type of report, e.g., interim, progress, summary, annual, or final. Give the inclusive dates when a specific reporting period is covered.

5. **AUTHOR(S):** Enter the name(s) of author(s) as shown on or in the report. Enter last name, first name, middle initial. If military, show rank and branch of service. The name of the principal author is an absolute minimum requirement.

6. **REPORT DATE:** Enter the date of the report as day, month, year, or month, year. If more than one date appears on the report, use date of publication.

7a. **TOTAL NUMBER OF PAGES:** The total page count should follow normal pagination procedures, i.e., enter the number of pages containing information.

7b. **NUMBER OF REFERENCES:** Enter the total number of references cited in the report.

8a. **CONTRACT OR GRANT NUMBER:** If appropriate, enter the applicable number of the contract or grant under which the report was written.

8b, 8c, & 8d. **PROJECT NUMBER:** Enter the appropriate military department identification, such as project number, subproject number, system numbers, task number, etc.

9a. **ORIGINATOR'S REPORT NUMBER(S):** Enter the official report number by which the document will be identified and controlled by the originating activity. This number must be unique to this report.

9b. **OTHER REPORT NUMBER(S):** If the report has been assigned any other report numbers (*either by the originator or by the sponsor*), also enter this number(s).

10. **AVAILABILITY/LIMITATION NOTICES:** Enter any limitations on further dissemination of the report, other than those

imposed by security classification, using standard statements such as:

- (1) "Qualified requesters may obtain copies of this report from DDC."
- (2) "Foreign announcement and dissemination of this report by DDC is not authorized."
- (3) "U. S. Government agencies may obtain copies of this report directly from DDC. Other qualified DDC users shall request through _____."
- (4) "U. S. military agencies may obtain copies of this report directly from DDC. Other qualified users shall request through _____."
- (5) "All distribution of this report is controlled. Qualified DDC users shall request through _____."

If the report has been furnished to the Office of Technical Services, Department of Commerce, for sale to the public, indicate this fact and enter the price, if known.

11. **SUPPLEMENTARY NOTES:** Use for additional explanatory notes.

12. **SPONSORING MILITARY ACTIVITY:** Enter the name of the departmental project office or laboratory sponsoring (*paying for*) the research and development. Include address.

13. **ABSTRACT:** Enter an abstract giving a brief and factual summary of the document indicative of the report, even though it may also appear elsewhere in the body of the technical report. If additional space is required, a continuation sheet shall be attached.

It is highly desirable that the abstract of classified reports be unclassified. Each paragraph of the abstract shall end with an indication of the military security classification of the information in the paragraph, represented as (TS), (S), (C), or (U).

There is no limitation on the length of the abstract. However, the suggested length is from 150 to 225 words.

14. **KEY WORDS:** Key words are technically meaningful terms or short phrases that characterize a report and may be used as index entries for cataloging the report. Key words must be selected so that no security classification is required. Identifiers, such as equipment model designation, trade name, military project code name, geographic location, may be used as key words but will be followed by an indication of technical context. The assignment of links, rules, and weights is optional.